ENERGY STATES AND INTERMOLECULAR INTERACTIONS IN MOLECULAR AGGREGATES--CRYSTALLINE NAPHTHALENE

Thesis by
David M. Hanson

In Partial Fulfillment of the Requirements

For the Degree of
Doctor of Philosophy

California Institute of Technology
Pasadena, California
1969
(Submitted August 9, 1968)

for

Colleen

ACKNOWLEDGMENTS

I am indebted to my research adviser, Professor G. Wilse Robinson, for his ideas that led to this research, for his uniquely critical advice that improved it, and for the creative environment he provided in terms of people and equipment that made it possible and exciting. Professor Raoul Kopelman is equally acknowledged for his advice, creativity, encouragement, and enthusiasm.

Some of the experimental work was done in collaboration with S. D. Colson and A. R. Gee. My education as an experimentalist is due in part to their example as my scientific education is due to the contentious discussions of the group.

The transcendent secretarial skills and interest of Mrs. Adria D. Larson made answering correspondence, writing papers and, most important, preparing this thesis enjoyable and efficient. I am indeed grateful.

ABSTRACT

The stationary states of condensed systems such as crystals are characterized by energy bands. These energy bands are described by a dispersion relation and a density function. Within the Frenkel tight-binding method, the physical quantities that determine the band structure are the intermolecular resonance interactions.

The density functions for the first excited singlet states of crystalline benzene and naphthalene are determined experimentally from spectral data involving band ⟷band transitions. The experimental results are not in complete agreement with a transition octopole model for the intermolecular interactions.

Mixed molecular crystals provide theoretically and experimentally tractable systems for studying the properties of molecular aggregates. This knowledge is basic to understanding the liquid and biological states and may in the future be of significant technological importance. Spectroscopic observations on isotopic mixed crystals of naphthalene are made to determine the energy of the crystal states that correlate with the $^1B_{2u}$ state of the free naphthalene molecule. The spectral data for the dilute crystals are interpreted in terms of

a one-particle Green's function and are consistent with the band structure as observed in band ⟷ band transitions. The transition energies of guest levels disagree with a model involving configuration interaction with charge transfer states. New theoretical models are suggested, and the data available for evaluating these models are outlined.

Very high resolution spectra at 4.2 °K reveal fine structure in the $^1B_{2u} \leftarrow {}^1A_g$ and $^3B_{1u} \rightarrow {}^1A_g$ electronic transitions of the naphthalene mixed crystals. Some of the structure corresponds to the resonance splitting of pairs of guest molecules in the host lattice. In the Frenkel tight-binding approximation, this structure gives directly the intermolecular excitation transfer matrix elements responsible for the exciton mobilities and the energy band structures.

Optical spectra of $^{13}CC_5H_6$-C_6H_6 mixed crystals show that the shallow impurity $^{13}CC_5H_6$ shifts the $^1B_{2u}$ factor group components by 2 cm^{-1} and increases the linewidth by 5 cm^{-1} in going from 6% to 50% $^{13}CC_5H_6$. The effect is explained qualitatively by an extension of the Frenkel exciton theory to the mixed crystal system.

Exciton structure in the two lowest ungerade triplet states of crystalline naphthalene is reported. For the lowest state the calculated splitting of 40 cm^{-1} is in good agreement with the experimental result.

The Raman scattering tensor for each vibrational mode is determined by polarized Raman scattering from oriented single crystals. The experimental data when compared with the

phosphorescence spectrum of the $C_{10}H_8$ - $C_{10}D_8$ mixed crystal allow unambiguous vibrational assignments to be made and provide a measure of the intermolecular interactions in the crystal. It is found that the crystal effects on the gerade vibrations are small. Frequency shifts are 2-4 cm^{-1}; exciton splittings are less than 1 cm^{-1}; and intensities are described qualitatively by the oriented gas model.

TABLE OF CONTENTS

PART I

Direct Observation of the Entire Exciton Band of the First Excited Singlet States of Crystalline Benzene and Naphthalene

I. INTRODUCTION

The stationary states of condensed systems such as crystals are characterized by energy bands. The individual states within these bands for periodic systems are designated by $\underset{\sim}{k}$, the reduced wave number vector.[1] The standard spectroscopic data concerning the low energy electronic states of molecular crystals consist of a few lines (Davydov components) corresponding to some or all of the $\underset{\sim}{k} = \underset{\sim}{0}$ levels. Only these levels are observed in transitions from the crystal ground state ($\underset{\sim}{k} = \underset{\sim}{0}$) because of the selection rule[2] $\Delta\underset{\sim}{k} = \underset{\sim}{0}$. In certain cases even some $\underset{\sim}{k} = \underset{\sim}{0}$ levels cannot be observed because of additional selection rules, e.g., the restrictions of factor group symmetry in the benzene crystal.

Within the framework of the Frenkel approach, the physical quantities that determine the band structure are the intermolecular resonance interactions. If all of the Davydov components were spectroscopically allowed, one could determine directly the magnitudes and relative signs of the interactions between interchange equivalent molecules. From these data alone nothing could be said about the interactions between translationally equivalent molecules. The latter may, in principle, be the dominant interactions responsible for the band structure.

An indication of the magnitude of the translationally equivalent interactions has been obtained recently from isotopic mixed crystal experiments.[3,4] A more direct approach is given in the present work and utilizes exciton band $\rightarrow$ exciton band spectroscopic transitions in

neat crystals (we use the word neat to mean unadulterated crystals, as distinguished from the word pure used in reference to the chemical purity of the crystal).

This technique allows all $\underset{\sim}{k}$ states to be observed since the initial state is no longer restricted to $\underset{\sim}{k} = \underset{\sim}{0}$. The method was first proposed by Rashba;[5] however, its practical and detailed utilization depends upon a knowledge of selection rules for $\underset{\sim}{k} \neq \underset{\sim}{0}$ transitions, and the use of extremely pure, high quality crystals. In a certain restricted Frenkel exciton limit, where the interactions are extremely short range and which we believe to be applicable to the low lying excited electronic states of benzene and naphthalene crystals, the selection rules are particularly simple;[6] and techniques for obtaining high purity are known for these crystals.[7] For these cases therefore it is possible to find the density of states in the electronic exciton band as well as the total band width, quantities that depend in principle upon all of the intermolecular interactions in the crystal.

Even though the complete exciton band structure in molecular crystals has been the object of several calculations,[8] it has not up to now been presented experimentally. It is of interest to compare experiment and theory, especially concerning the applicability of multipole expansions, the assumption of pairwise interactions, the location of ion-pair states,[9] and the quality of the available atomic and molecular eigenfunctions.[3,9]

II. GENERAL DISCUSSION

A. Band-to-Band Transitions

Exciton band ⟶ exciton band transitions involving the first excited singlet states of crystalline benzene and naphthalene are observed in both absorption and emission. Benzene and naphthalene crystals are good candidates for such an investigation for several reasons.

(1) These systems are of general interest since the electronic and vibrational states have been extensively studied experimentally and theoretically in the molecule as well as in the crystal.

(2) Naphthalene is a case where the extremes of the electronic exciton band are approximately known, while benzene is an intriguing case where the extent of the exciton band is unknown. The predicted locations of the forbidden Davydov component in benzene have ranged from the bottom to the top of the band.[3,10,11]

(3) Benzene and naphthalene are some of the few compounds that have been purified to the degree necessary for such experiments.

The transitions shown schematically in Fig. 1 are exciton band ⟶ exciton band transitions. In absorption, this method relies upon the thermal population of <u>all</u> the $\underset{\sim}{k}$ levels of a ground state <u>vibrational</u> exciton band. The absorption process, then, involves all these levels as initial states and all the $\underset{\sim}{k}$ levels of the electronic exciton band as final states. In emission, the initial states are the thermally populated[12] $\underset{\sim}{k}$ states of the electronic exciton band while the $\underset{\sim}{k}$ states of the vibrational exciton band serve as the final states. The intensity distributions in both the absorption and emission bands are proportional,

except for appropriate Boltzmann factors, to the density of $\underset{\wedge}{k}$ levels in the electronic exciton band provided (1) the width of the vibrational exciton band is negligible, (2) an equilibrium population of the levels in the electronic exciton band is attained in a time fast compared with the emission lifetime, (3) intensity contributions from phonon transitions are negligible, (4) the transition probability is $\underset{\wedge}{k}$ independent, (5) the $\Delta\underset{\wedge}{k} = 0$ selection rule is valid, and (6) the differences in branch-to-branch[13] transition probability do not alter this intensity distribution.

The width of vibrational exciton bands in molecular crystals is known[14] to be approximately 1-10 cm^{-1}. The vibrational exciton band of benzene that is utilized in the present experiment is that corresponding to the ν_6'' (e_{2g}) vibration (606 cm^{-1}), which is known to have an exciton splitting[15] of ~ 5 cm^{-1}. This finite width could introduce an uncertainty in the density function $\rho(E)$. However, the maximum of the density function determined from ν_6'' coincides with that determined from ν_1'' (a_{1g}) for which no exciton splitting has been observed.[15] Unfortunately, the band $\longrightarrow$ band transition involving ν_1'' is not intense enough to give the entire density function accurately. For naphthalene, the nearly degenerate vibrational exciton bands at 510 and 514 cm^{-1} are used. The total width of these two bands[16] is less than 6 cm^{-1}, which is small compared to the 160 cm^{-1} exciton splitting in the electronic state. The finite width of the vibrational exciton band also results in a Boltzmann population distribution of the $\underset{\wedge}{k}$ levels in the lower state; however, for a 500 cm^{-1} vibration at liquid nitrogen temperature, ignoring the population difference between the highest and lowest $\underset{\wedge}{k}$ states in a band $\longrightarrow$ band absorption experiment will probably cause an error in $\rho(E)$ of no more than 10%.

Boltzmann statistics closely describe the population of the energy levels provided there is sufficient time for equilibrium to be attained. The fact that relaxation within the manifold of $\underset{\sim}{k}$ levels is fast relative to the fluorescence lifetime is shown by the temperature dependence of the fluorescence lineshapes (vide infra).

Optical transitions involving lattice vibrations or phonons are expected to contribute to the shape and width of the observed band $\rightarrow$ band transitions. The magnitude of this contribution can be estimated from the temperature dependence of the fluorescence spectra and the comparison of it with the absorption spectra (vide infra). It should be emphasized that we use the term phonons synonymously with lattice vibrations as distinguished from the internal vibrations of the molecule.

B. Selection Rules

The electric dipole transition moments involved in a band $\rightarrow$ band transition have been shown[6] to be independent of $\underset{\sim}{k}$, the reduced wave number vector, provided certain long-range interactions can be neglected. Within the limit of applicability of this approximate Hamiltonian, it has also been shown that the factor group selection rules[6] as well as the $\Delta\underset{\sim}{k} = \underset{\sim}{0}$ selection rule are valid for all $\underset{\sim}{k}$. The validity of the $\underline{g} \rightarrow \underline{u}$ selection rule in centrosymmetric crystals for all $\underset{\sim}{k}$ has also been proved in this limit and is of special interest. For, if a breakdown of this selection rule was seen to occur, the approximations leading to the restricted Frenkel selection rules would be known to be invalid, causing the interpretation

of the intensity distribution in the band ⟷ band transition to be no longer straightforward. Unfortunately, not observing such a breakdown cannot be considered a justification for using this limit. Since, in this restricted limit, the factor group selection rules are valid for all $\underset{\sim}{k}$, it can easily be shown, assuming an oriented site[17] model, that the transition probability from any single branch to all bands is a constant. For benzene the factor group selection rules show that only the following transitions are allowed: $A \longleftrightarrow B_1$, $A \longleftrightarrow B_2$, $A \longleftrightarrow B_3$, $B_1 \longleftrightarrow B_2$, $B_1 \longleftrightarrow B_3$, $B_2 \longleftrightarrow B_3$. Thus, in a band-to-band transition involving crystal states that correlate with non-degenerate molecular states, there are three distinct transitions originating from each of the four branches. For the case where all branches of the vibrational band are isoenergetic, three of the twelve possible transitions occur at the same energy for each value of $\underset{\sim}{k}$. The sum of the intensities of these three is independent of the symmetry classification of the initial branch in emission or the final branch in absorption. No additional complications arise when the vibrational exciton band corresponds to a degenerate molecular state as long as the site and exciton splittings are negligible relative to the width of the electronic exciton band. Thus, the intensity distribution of the band-to-band transition gives the density of states in the electronic exciton band within the other limitations cited above.

C. Density-of-States Function

It is of interest now to consider how the density-of-states function is determined by the intermolecular interactions in the crystal. This derivation is straightforward within the formalism of first-order perturbation theory using one-site basis functions. This first-order theory has formed the basis for the development and application of the Frenkel approach by Davydov and others.[19] Although a higher-order formalism has been suggested,[9] there exists no experimental evidence demonstrating the failure of the first-order approach as far as the lowest excited states of benzene and naphthalene are concerned. On the other hand a disagreement between the higher-order theory and experiments on crystalline naphthalene may exist. Sarti-Fantoni[20a] first pointed out an apparent discrepancy. His criticism has recently been discussed by Silbey, et al.[20b] As Craig and Philpott,[8b] and Sarti-Fantoni[20a] have pointed out, it is unfortunate that the complete band structure has not been calculated using higher-order theory. It would be of interest to compare such results with those of the octopole model and with the present experimental results. However, it should be remembered that when higher-order terms are considered the transition probability may be $\underset{\sim}{k}$ dependent. This possibility must be considered before comparison with the present experiments can be made.

Because of its apparent accuracy, we treat the exciton band structure for the $^1B_{2u}$ states of benzene and naphthalene within the framework of the simple first-order theory.[21] The density function $\rho(E)$, which gives the number of exciton or $\underset{\sim}{k}$ states per unit of energy, can be determined from the dispersion relation. In the restricted Frenkel limit,[6] the dispersion relation $L^{f\alpha}(\underset{\sim}{k})$ that gives the energy of the state with wave number vector $\underset{\sim}{k}$ has an especially simple form,

$$L^{f\alpha}(\underset{\sim}{k}) = \sum_{q=1}^{m} a_q^{\alpha} L_{Iq}^{f}(\underset{\sim}{k}) \tag{1}$$

The zero of energy for this equation is the algebraic mean of the exciton band; or, equivalently, the energy of the corresponding transition in a hypothetical crystal in which all resonance interactions are zero.[22] Here, m is the number of molecules per primitive unit cell, a_q^{α} are the coefficients corresponding to the α^{th} representation of the interchange group,[23] and the $L_{Iq}^{f}(\underset{\sim}{k})$ are the $\underset{\sim}{k}$-dependent sums of excitation exchange matrix elements for the f^{th} excited state:[21]

$$L_{qq'}^{f}(\underset{\sim}{k}) = \sum_{n'=1}^{n/m} \exp i\underset{\sim}{k}\cdot(\underset{\sim}{\tau}_{q'} - \underset{\sim}{\tau}_{q}) \exp i\underset{\sim}{k}\cdot(\underset{\sim}{r}_{n'} - \underset{\sim}{r}_{n}) \times \int \phi_{nq}^{f*} H \phi_{n'q'}^{f} dR \; (1 - \delta_{nn'}\delta_{qq'}), \tag{2}$$

where $\underset{\sim}{r}_n$ defines the origin of the n^{th} unit cell, $\underset{\sim}{\tau}_q$ is a vector from that origin to the q^{th} molecule in that unit cell, and ϕ_{nq}^{f} is the localized excitation function[24] representing the molecule at the nq^{th} site in its f^{th} excited state.

The density of states in the exciton band corresponding to the f^{th} excited state of the molecule is obtained by computing $L^{f\alpha}(\underset{\sim}{k})$ for all α and tabulating the number of states per energy interval. Such a computation requires evaluation of the pairwise excitation exchange integrals ($\mathscr{M}_{ij}$). These can be evaluated theoretically or empirically and compared with experiments. For this comparison, the density-of-states functions are normalized so that the areas under each curve are equal. The value of the normalized density function gives the fraction of states at a particular energy. The Davydov splittings place restrictions on the possible values of the interchange equivalent interactions since these splittings depend upon sums of the $\mathscr{M}_{ij}$ over the entire lattice.[21] Note that we reserve

the term Davydov splitting for the exciton splitting at $\underset{\sim}{k} = \underset{\sim}{0}$. Data from the spectra of isotopic mixed crystals provide similar information about the sums of translationally equivalent interactions.[3,4] In contrast, the density function depends upon $\underset{\sim}{k}$-dependent sums of all these interactions and thus provides an independent measure of the intermolecular resonance interactions.

For weak transitions, such as the lowest singlet states of benzene and naphthalene, the lattice sums are expected to converge rapidly. By considering just the interactions with the nearest translationally and interchange equivalent molecules, $\mathcal{M}_a$, $\mathcal{M}_b$, $\mathcal{M}_c$, $\mathcal{M}_{I\,II}$, $\mathcal{M}_{I\,III}$, $\mathcal{M}_{I\,IV}$, it can easily be shown that for benzene,

$$\begin{aligned} L^{f\alpha}(\underset{\sim}{k}) = {} & 2\mathcal{M}_a \cos(k_a a) + 2\mathcal{M}_b \cos(k_b b) + 2\mathcal{M}_c \cos(k_c c) \\ & + 4 a_{II}^{\alpha} \mathcal{M}_{I\,II} \cos\left(k_a \tfrac{a}{2}\right) \cos\left(k_b \tfrac{b}{2}\right) \\ & + 4 a_{III}^{\alpha} \mathcal{M}_{I\,III} \cos\left(k_b \tfrac{b}{2}\right) \cos\left(k_c \tfrac{c}{2}\right) \\ & + 4 a_{IV}^{\alpha} \mathcal{M}_{I\,IV} \cos\left(k_a \tfrac{a}{2}\right) \cos\left(k_c \tfrac{c}{2}\right) \end{aligned} \tag{3}$$

where $\mathcal{M}_{Iq} = \int \phi_I^{f*} |H'| \phi_q^f dR$. $\mathcal{M}_{a,b,c}$ represent the interaction of molecule I with its translationally equivalent nearest neighbors along the $\underset{\sim}{a}$, $\underset{\sim}{b}$, and $\underset{\sim}{c}$ axes, respectively, and

$$\underset{\sim}{k} = \underset{\sim}{k}_a + \underset{\sim}{k}_b + \underset{\sim}{k}_c$$

$$\underset{\sim}{k}_a = \frac{\pi n_a}{N_a} \underset{\sim}{t}_a, \qquad -N_a < n_a \leq N_a$$

$$\underset{\sim}{t}_a \equiv \frac{\underset{\sim}{b} \times \underset{\sim}{c}}{\underset{\sim}{a} \cdot \underset{\sim}{b} \times \underset{\sim}{c}}$$

etc.

The number of values of $\underset{\sim}{k}_a$ is equal to the number of primitive unit

cells ($2N_a$) along the $\underset{\sim}{a}$ crystal axis, since n_a takes all integral values between the limits specified. The values of the coefficients a^{α}_{II}, a^{α}_{III}, a^{α}_{IV} are respectively +1, +1, +1 for $\alpha = A$; +1, -1, -1 for $\alpha = B_1$; -1, +1, -1 for $\alpha = B_2$; and -1, -1, +1 for $\alpha = B_3$.

Naphthalene is an example of a crystal with two molecules per unit cell. The dispersion relation for such crystals has been considered in detail by Davydov[25] and Knox.[26] Here we shall assume that only certain near-neighbor interactions contribute; namely, $\mathcal{M}_a$, $\mathcal{M}_b$, $\mathcal{M}_c$; $\mathcal{M}_{I\,II}$, and $\mathcal{M}_{I\,II'}$, where $\mathcal{M}_{I\,II'}$ is the next nearest interchange equivalent interaction. The following dispersion relation is then obtained for the two branches of the lowest singlet exciton band of naphthalene:

$$\begin{aligned} L^{\pm}(\underset{\sim}{k}) = {} & 2\mathcal{M}_a \cos(k_a a) + 2\mathcal{M}_b \cos(k_b b) + 2\mathcal{M}_c \cos(k_c c) \\ & \pm 4\mathcal{M}_{I\,II} \cos(k_a \tfrac{a}{2}) \cos(k_b \tfrac{b}{2}) \\ & \pm 4\mathcal{M}_{I\,II'} \cos(k_c c) \cos(k_a \tfrac{a}{2}) \cos(k_b \tfrac{b}{2}) \\ & \mp 4\mathcal{M}_{I\,II'} \sin(k_c c) \sin(k_a \tfrac{a}{2}) \cos(k_b \tfrac{b}{2}), \end{aligned} \tag{4}$$

where, for the $\underset{\sim}{C_2}$ interchange group, the plus sign of $L^{\pm}$ refers to $L^{A_u}(\underset{\sim}{k})$ and the minus sign to $L^{B_u}(\underset{\sim}{k})$. The superscript f of $L^{f\alpha}(\underset{\sim}{k})$ has been omitted.

III. EXPERIMENTAL TECHNIQUES

As already mentioned, these experiments are made possible by the recent advancements in purification techniques for benzene and naphthalene.[27,28] For the band → band absorption studies, purified crystals 1 to 5 cm long were grown from the melt by slowly lowering the cells through a sharp temperature gradient directly into a liquid nitrogen cooled chamber. Using this technique, one obtains crystals with few or no cracks at 77 °K that can be cooled to 4.2 °K with little or no additional

cracking. As the resultant crystal is in an evacuated container, several hours are required from the time the container is immersed in liquid helium until the crystal cools to 4.2 °K. The hot band absorption was monitored during this period, and while no significant change in the structure of this absorption was observed upon cooling, the intensity gradually decreased until no residual absorption could be detected at liquid helium temperature.

The 0, 0 absorptions in thin crystals were also observed at 77 °K, 27 °K (the temperature of boiling neon; benzene only), and 4.2 °K. The spectra were taken utilizing a 150 W Xe arc lamp and the third order of a 600 line/mm Bausch and Lomb grating (212 × 157 mm) in a 2 m Czerny-Turner mount. Tracings of the photographic plates were taken on a Joyce and Loebel Model E12 MK III microdensitometer and a Jarrell-Ash Model 23-500 microphotometer.

The fluorescence spectra of benzene and naphthalene were observed at 77 °K, 27 °K (benzene only), and 4.2 °K on the above two-meter photographic instrument. The intensity distribution of the 0 - "606" fluorescence band in benzene and the 0 - "512" fluorescence band in naphthalene was determined at 77 °K and 20.4 °K (the temperature of boiling hydrogen) using the third order of a 600 line/mm grating (102 × 102 mm) in a 1.83 M Jarrell-Ash Ebert photoelectric spectrometer. Both the photoelectric and photographic line positions were determined by reference to an iron-neon standard.

The thin crystals (20μ to 2 mm) used for the 0, 0 absorption and all fluorescence studies were grown in a manner similar to that used for the band – band absorption spectra. For the fluorescence studies it was necessary to open the crystal cell, exposing the crystal to the cryogenic liquid, in order to prevent the excitation source from heating the sample.

IV. EXPERIMENTAL RESULTS

A. Band-Band Fluorescence

Figure 2 shows the microdensitometer tracings of the band → band fluorescence transition at temperatures of 77 °K, 27 °K, and 4.2 °K in benzene. Also included in Fig. 2 is the corresponding transition of a benzene guest in a deuterobenzene host at 4.2 °K. The isotopic mixed crystal spectrum demonstrates the sharpness of these transitions when they are not associated with exciton bands. Jarrell-Ash 1.83 M spectrometer tracings of the benzene and naphthalene band → band fluorescence are shown in Figs. 3, 4, and 5. Figure 4 includes the neat crystal and the isotopic mixed crystal transitions for naphthalene at 4.2 °K taken with a 300 line/mm grating (190 × 80 mm) in 18th order. The two accidentally degenerate vibrations (510 cm^{-1} and 514 cm^{-1}) are nearly resolved. These are easily resolved in mixed crystal phosphorescence.

The density functions for both benzene and naphthalene were derived from the fluorescence lines by assuming the lowest energy levels in the electronic exciton bands are coincident with the lowest Davydov component. This assumption is believed to be valid since the 0, 0 transitions are observed in fluorescence at 1.8 °K, and since fluorescence lines involving vibrational exciton bands are shifted only by the value of the ground-state vibrational quantum. For example, in benzene, the $0' \rightarrow \nu_6''$ (606 cm^{-1}) transition does not extend to the red of 38,003 - 606 cm^{-1}, where 38,003 cm^{-1} is the location of the lowest Davydov component above the ground state. Additional evidence has been presented for the case of naphthalene by experiments with isotopic mixed crystals.[29] With this assumption and the assumption of Boltzmann equilibrium within the band, the density function can be calculated from the fluorescence line shape by dividing the intensity at a

given energy by the appropriate Boltzmann factor. The plate optical density was converted to intensity before making the calculation for the 27 °K benzene fluorescence. These density functions are shown in Figs. 6, 7, and 8 for benzene and naphthalene. The "double-peaked" fluorescence band shape in the neighborhood of 20-27 °K for benzene, seen in both Figs. 2 and 3, is real. It is a result of a balance between exponentially decreasing Boltzmann factors and a density-of-states function that begins to increase more rapidly than exponentially in the energy range corresponding to $T \approx 20\text{-}27$ °K. This shape for the fluorescence band is exactly that predicted from the derived density functions.

It is of interest to note that one expects a decrease in 0, 0 fluorescence intensity with increasing temperature. This decrease occurs at elevated temperatures because the statistical weight of the $\underset{\sim}{k} = \underset{\sim}{0}$ level in the upper electronic state is very small relative to that of the rest of the $\underset{\sim}{k}$ levels. Thus most of the emission originates from within the band, where the $\Delta\underset{\sim}{k} = \underset{\sim}{0}$ selection rule[2c] prohibits the transition to the absolute ground state. Actually, this simple picture can be modified since $\underset{\sim}{k}$ can be conserved through various combinations of phonon, photon, and exciton momenta. Furthermore, as relaxation among the $\underset{\sim}{k}$ levels appears complete in a time short compared with the fluorescence lifetime, the exciton $\underset{\sim}{k}$ states cannot be pure and possibly a large number of states near the bottom of the band have some $\underset{\sim}{k} = \underset{\sim}{0}$ admixture. Alternately, in the presence of shallow traps, one might even expect the intensity of the 0, 0 transition to increase with temperature, at least initially. Rather qualitative experiments here show some decrease in the relative intensity of the 0, 0 transition of crystalline naphthalene over the temperature range studied. For benzene the decrease is more pronounced, no 0, 0 fluorescence being observed at 27 °K. These results are complicated by broadening (which can be construed as weakening),

self absorption, and the (unlikely) presence of residual traps. If there is a real difference between the benzene and naphthalene results, it could be caused by the difference in shape near the bottom of the band of the density functions for these two systems. The steeper density function for naphthalene could insure that more states near the bottom of the band are mixed with $\underset{\sim}{k} = \underset{\sim}{0}$ than in the case of benzene. Another difference, in the right direction, could arise because of the greater breadth of the naphthalene exciton band and the greater thermal inacessibility of the higher $\underset{\sim}{k}$ states. Obviously, further experiments are needed in order to clarify these points.

B. Band-Band Absorption

Microdensitometer tracings of the absorption band → band transitions in benzene and naphthalene are shown in Figs. 9 and 10. For the purpose of computing $\rho(E)$ from these data, the plate optical density has been converted to sample optical density by calibrating the plate. The sample optical density is linearly proportional to the density function $\rho(E)$. The $\rho(E)$ function found in this way for the $^1B_{2u}$ state of benzene is shown in Fig. 7, where a comparison is made with the $\rho(E)$ function derived from the fluorescence spectrum. The corresponding $\rho(E)$ function for naphthalene is shown in Fig. 11.

C. Phonon Contributions

The contribution of lattice vibrations or phonons to the experimentally derived density functions can be evaluated from the temperature dependence of these density functions, from the temperature dependence of the 0, 0 absorptions in thin crystals, and from a comparison of density functions derived from absorption and emission data at the same temperature. The 0, 0 absorptions shown in Figs. 10 and 12 have been discussed

previously by Maria,[30] Prikhot'ko and Soskin,[31] and Maria and Zahlan.[32] Phonons are expected to contribute to these experimental results in two ways. Transitions involving phonons in either the initial or final states may contribute to the observed intensities and line shapes. The electronic band structure itself may depend upon the motion of the molecules in the lattice.

A comparison of the benzene density functions at several temperatures (Figs. 6 and 7) shows that the temperature effect is not negligible. Relative to the density function at 20.4 °K, the maximum of the density function at 77 °K has shifted ~12 cm^{-1} to the red, its halfwidth has increased from 15 to 45 cm^{-1} and the wings are considerably extended. In contrast, the effect on $\rho(E)$ of changing the temperature from 20.4 ° to 27 °K is well within experimental accuracy and thus may indicate that the effects of thermal phonons can be neglected at these low temperatures. This suggestion is supported by the temperature dependence of the 0, 0 absorption spectrum as shown in Fig. 12. There, it can be seen that the change in linewidth between 1.8 ° and 27 °K is relatively small. The highest energy Davydov component broadens by about 4 cm^{-1} at 27 °K. This thermal broadening partially masks the middle Davydov component, which is clearly visible on the photographic plates as a shoulder but is poorly reproduced in Fig. 12. A broad absorption develops under the lowest energy Davydov component. However, no measurable change in the Davydov splitting occurs in this temperature range. On the other hand, at 77 °K the absorption is quite different. The linewidth of the Davydov components increases to 30-50 cm^{-1}, and their splitting appears to have decreased; the upper two components, now unresolved, being shifted toward lower energy. This decrease in splitting, however, may be only

apparent since the broad components are not clearly resolved.

These results are not at complete variance with the findings of Maria and Zahlan[32] (MZ) but they differ in several significant respects. (1) The linewidths of the Davydov components that we observe at low temperatures ($T < 27\,^{\circ}K$) are two to four times narrower than those reported by MZ at corresponding temperatures. Our results therefore agree in this regard with the findings of Broude.[33] (2) The change in these linewidths in going from 4.2 to 1.8 °K is not outside the normal crystal-to-crystal fluctuations ($\lesssim 1\ cm^{-1}$) in contrast to the "sudden 50% increase in bandwidth at temperatures below 4.2 °K" observed by MZ. Such an increase would make it impossible to resolve the splitting between the upper Davydov components at 1.8 °K, contrary to what is seen in Fig. 12. The broadness as well as the temperature dependence of the absorptions of MZ could easily be due to crystal imperfections and strains, since their crystals were obtained by pressing benzene between quartz plates.[34] (3) The relative intensities of the Davydov components and their intensity relative to that of the phonon addition bands appear to be very different from the findings of MZ. This, however, is felt merely to be an indication of the difficulty in making accurate intensity measurements of intrinsically very sharp, intense lines.[35] Little significance should therefore be attached to the apparent intensities of the sharp Davydov components relative to the intensities of the broad phonon bands. Likewise, the apparent relative intensities of the Davydov components can be misleading. See Fig. 12, for example.

There is considerable reason to believe that the 0, 0 transition in crystalline benzene is not primarily phonon induced. In the crystal, the

benzene molecule is at a site of C_i symmetry. The 0, 0 transition is therefore no longer forbidden provided there is an interaction between the molecule and its environment. These crystal interactions are sufficiently strong to induce all ten of the ungerade benzene vibrations in the infrared spectrum of the crystal[14] even though only four of these are allowed in the gas phase. The infrared crystal spectra are independent of temperature[21] between 4.2 and 77 °K indicating that the crystal perturbation is not dependent upon the occupation of phonon states.

For the case of benzene, then, it is felt that band → band transitions at temperatures below ~30 °K give a qualitatively accurate description of the density function associated with the $^1B_{2u}$ state. The low energy tail in fluorescence has a mirror image relationship with the broad absorptions on the short wavelength side of the Davydov components (Fig. 12). The absorption tails have been previously assigned as phonon addition bands by several other authors.[33a, 36] The fluorescence and the absorption tails can therefore be omitted from the density function.

Likewise for naphthalene, the spectroscopic transitions are not temperature independent. Unfortunately, because of the width of the naphthalene exciton band, the high energy portion of the density function cannot be determined accurately from fluorescence measurements at low temperatures where the phonon contribution is a minimum. Thus, the effects of phonons must be evaluated, at least qualitatively, in order to learn about the density function.

The 0, 0 absorption for naphthalene at 77 and 4.2 °K is shown in Fig. 10. This transition has been studied as a function of temperature by Maria,[30] and Prikhot'ko and Soskin.[31] It should be noted that Maria's

absorption bands (his Fig. 1) are much broader than ours or than those of Prikhot'ko and Soskin. The distortion of this spectrum, as pointed out by Prikhot'ko and Soskin, is caused by crystal strains and defects. Conclusions regarding the intensity, shape, and temperature dependence of such distorted and overlapping spectra must be made cautiously. The naphthalene data of Prikhot'ko and Soskin show, just as for the case of benzene, that the 0, 0 absorption of naphthalene is independent of temperature below ~ 30°K. The half-widths of the two Davydov components increase by 10 and 30 cm^{-1} respectively in going from 4° to 77°K. However, the spectra remain qualitatively the same over this temperature range and no change occurs in the Davydov splitting. This fact indicates the temperature independence of the band structure. In addition, Prikhot'ko and Soskin have shown, through good polarization measurements, that phonon addition bands analogous to those in benzene under the $\underset{\wedge}{b}$ polarized Davydov component. Their data indicate that these absorptions increase in intensity with increasing temperature.

From the above considerations of the phonon contribution to $\underset{\wedge}{k} = 0$ transitions in naphthalene, the phonon contribution to a band-band transition at 77°K can be estimated. It is expected that the transition involving each $\underset{\wedge}{k}$ state will be broadened roughly 25 cm^{-1}. There will also be an intensity contribution from the phonon addition bands. In absorption these transitions will contribute intensity roughly 70 cm^{-1} above the center of the exciton band just as they do in the 0, 0 transition. In fluorescence these phonon transitions will originate from all $\underset{\wedge}{k}$ states of the exciton band, and, modified by the Boltzmann factor, they will retrace the density function ~ 70 cm^{-1} to lower energy. The observed band — band fluorescence

and absorption line shapes in both benzene and naphthalene are consistent with these expectations. For the case of benzene (see Fig. 7), the density-of-states function determined from absorption is broadened to high energy relative to that from fluorescence. On the other hand, the density function determined from fluorescence (see Fig. 3) is broadened to low energy relative to that from absorption. The same behavior is observed for naphthalene but the low energy fluorescence tail is even more pronounced (compare Figs. 8 and 11).

For the above model, which is analogous to the weak coupling model[18] for vibronic transitions in molecular crystals, the phonon contribution is a minimum at the low energy edge of the band-band absorption and at the high energy edge of the 77 °K fluorescence. The composite density function for naphthalene calculated from these portions of the respective spectra is shown in Fig. 13. The lower Davydov component is taken as the bottom of the band. The 20.4 ° and 77 °K fluorescence spectra calculated from this density function are shown in Figs. 14 and 15. This phenomenological approach for subtracting phonon contributions accounts only for the temperature-dependent component of exciton-phonon coupling. Because the phonon frequencies are roughly equal to the exciton bandwidth, the electronic $\underset{\sim}{k}$ band may not be rigorously separable from the phonon $\underset{\sim}{k}$ bands. Such coupling may well be the source of the anomalous width of the naphthalene $\underset{\sim}{b}$-polarized Davydov component.

Figure 14(A) shows the experimental naphthalene fluorescence band at 20.4 °K. This band can be compared with that predicted by the octopole model [Fig. 14(B)] and by the composite density function [Fig. 14 (C)]. The fluorescence intensity is obtained from the density function through

multiplication by the appropriate Boltzmann factors. The disagreement between Fig. 14(A) and 14(C) may indicate that the density function rises even more rapidly to its maximum than the composite function shows.

Figure 15(A) shows the fluorescence band of naphthalene at 77 °K. The intensity below 30,963 cm^{-1} in both the 20.4 °K and 77 °K spectra is attributed to phonons. This contribution is not considered in the calculated line shapes, Figs. 15(B) and 15(C). Although the octopole model (see Fig. 18) disagrees with the experimental result at 77 °K, with respect to both the width and shape of the fluorescence line, this disagreement may be due only to the effect of phonons.

D. Previous Work on Band → Band Transitions

Band → band transitions of benzene have been observed and discussed by A. Zmerli,[36] and by V. N. Vatulev, N. I. Sheremet, and M. T. Shpak.[37] However, neither group attempted to interpret their results quantitatively in terms of the density-of-states function of the excited state. In fact, Zmerli interprets his spectra in terms of emission from $\underset{\sim}{k} = 0$ states only. Vatulev, et al., interpret their spectra in terms of emission from an exciton band containing two branches instead of four. The small difference between our fluorescence line shape at 20.4 °K and that of Vatulev, et al., could be caused by the presence of excitation traps (chemical impurities or benzene molecules at defect sites) in their samples. A considerable portion of their emitted intensity comes from defects and impurities as shown in their published spectra while no such emission is observed in our spectra.

Pröpstl and Wolf[38] measured the fluorescence of crystalline naphthalene between 2 ° and 100 °K. At low temperatures (4-20 °K) they observed fluorescence only from the lower (ac) Davydov component. At higher temperatures (50-90 °K) the 0-0 emission arises from both high (b) and low (ac) Davydov components while the 0-ν'' emissions seemed to originate from between the Davydov components. Although it was recognized by Pröpstl and Wolf that emission originates from the upper regions of the exciton band at high temperatures, they did not appreciate the exact role of the vibrational exciton band in explaining the difference between 0-0 and 0-ν'' emissions. It is precisely this difference that allows the phonon contribution to be estimated and the density function of the electronic band to be determined.

Following the theoretical development of Rashba,[5] several Russian researchers have discussed exciton band ⟷ exciton band transitions. Davydov[25] has summarized these results for the case of naphthalene and has applied Rashba's ideas to predict the emission curve from the absorption curve. However, in view of the temperature dependence of the band ⟷ band transitions in both benzene and naphthalene, Davydov's assumption that phonon contributions can be neglected is not completely justified. If the vibrational exciton bands are narrow, as they are in benzene and naphthalene, the low energy broadening of the fluorescence with increasing temperature cannot be explained using electronic exciton states alone. Therefore Davydov's calculation of the fluorescence line shape is not justified because such a calculation must use transitions originating at energies lower than the $\underset{\sim}{ac}$ polarized Davydov component, which is known experimentally to be the bottom of the naphthalene exciton band. Furthermore, Davydov's treatment assumed a $\underset{\sim}{k}$ dependence in the transition matrix element. It is the approximations discussed earlier that remove such $\underset{\sim}{k}$ dependence and allow the density function to be discussed directly and simply in terms of the band ⟷ band transitions. Davydov therefore did not attempt to relate directly the band ⟷ band spectra to the density function.

Recently Broude, Rashba, and Sheka[39] have interpreted the broad absorptions above the $^1B_{2u}$ 0,0 transition in crystalline naphthalene in terms of double exciton states. These states have been previously discussed in footnote 31 of Ref. 3. This interpretation requires a knowledge of $\sigma(E)$, which was approximated by absorption band ⟷ band transition spectra taken at 90°K. It is only in the limit discussed in the present

paper that this approximation is justified. It should be noted that the $1' \leftarrow 0''$ absorptions are about as broad as the $0' \leftarrow 1''$ absorptions because of these double exciton states.

V. DENSITY CALCULATIONS

The density-of-states functions for the first excited singlet states of benzene and naphthalene have been calculated using the first-order Frenkel theory described in Sec. II. Sets of $\mathscr{M}_{ij}$ have been chosen in accordance with restrictions set by the Davydov splittings. For benzene, the assignments of the Davydov components are in question. The most recent work of Broude[33a] at 20°K gives one line at 37,803 cm^{-1} polarized parallel to the $\underset{\sim}{a}$ crystal axis and three lines (37,839; 37,846; and 37,847 cm^{-1}) referred to in Broude's Table VI as being "$\underset{\sim}{c}$-polarized". One of the two high-frequency lines however appears weakly in the reproduction of the $\underset{\sim}{b}$-polarized spectrum shown in Fig. 10 of Broude's paper. But so apparently does the $\underset{\sim}{a}$-polarized component! On page 602 of the translation to this article, however, is stated that there is a variation of the relative intensities of the two high-frequency components for different lattice planes, and Broude therefore assumes one to be the $\underset{\sim}{b}$-polarized Davydov component. Broude's polarization results are consistent with the work of Zmerli,[36] who, however, was unable to resolve the splittings of the "$\underset{\sim}{c}$-polarized" lines. Even though our resolution is probably at least as good as that used by Broude, we have been unable to observe any additional splitting in the highest energy component,[40] observing lines only at 37,803 cm^{-1}, 37,842 cm^{-1}, and 37,847 cm^{-1}. Recently, Wolf[41] has been quoted[9b] as having observed the $\underset{\sim}{a}$ and $\underset{\sim}{c}$

polarizations to be reversed from the above findings. However as Wolf states, his assignment was taken to be in agreement with Broude's earlier work,[42] which Broude later revised in light of additional experimental results. In view of this discussion of the spectral data, we have assigned the polarizations of our lines as $\hat{a}$, $\hat{c}$, $\hat{b}$ in order of increasing energy; i.e., the Davydov components in order of increasing energy belong to the factor group representations B_{1u}, B_{3u}, B_{2u}, respectively. This is consistent with the choice of Nieman and Robinson and the finding of Claxton.[43] Obviously the situation is not terribly clear and more experiments are definitely needed on this point. The results of the density-of-states calculations, however, will be independent of the choice of polarizations, provided of course one of the higher energy components is indeed $\hat{b}$ polarized; the $\mathscr{M}_{ij}$ will not be uniquely related to a specific excitation exchange integral until the polarizations are clarified. The $\mathscr{M}_{ij}$ for the benzene calculation have been determined by choosing an energy for the dipole inactive A_u component, solving Eq. (18) of Ref. 21 for $M_{I\,II}$, $M_{I\,III}$, and $M_{I\,IV}$ and then assuming that only the nearest-neighbor interchange equivalent interactions contribute to the Davydov splitting, i.e., by assuming $M_{ij} \equiv \mathscr{M}_{ij}$.

The interaction among the translationally equivalent molecules shift all the Davydov components equally and thus have to be determined separately. Recent experiments in our laboratory[44] have shown that the interpretation of isotopic mixed crystal data by Nieman and Robinson[3] is subject to question as the energies of isotopic guests of higher energy than the host are not given by a normal extension of the mixed crystal theory. This merely indicates that their stated assumptions must be reevaluated. We, therefore, have no independent measure of the translationally equivalent interactions $\mathscr{m}_a$, $\mathscr{m}_b$, $\mathscr{m}_c$ and, as a result, they have been chosen to give the best fit to the experimental $\rho(E)$ for each choice of the energy of the A_u level. In order to account crudely for the different $\underset{\sim}{a}$, $\underset{\sim}{b}$, and $\hat{c}$ crystal axis lengths, the relative magnitudes of $\mathscr{m}_a$, $\mathscr{m}_b$, and $\mathscr{m}_c$ have been chosen to agree with the predictions of Nieman and Robinson based on an electron exchange model for the excitation exchange integrals, i.e., $\mathscr{m}_a : \mathscr{m}_b : \mathscr{m}_c = 1:0:3$.

The results of these calculations for a crystal of 32,000 molecules, for various values of the A_u level, are given in Fig. 16. Two choices of $\mathscr{m}_a$, $\mathscr{m}_b$, and $\mathscr{m}_c$ are given in Figs. 16(G and H) to illustrate the effect of such interactions. $\rho(E)$ is also calculated from the $\mathscr{m}_{ij}$ obtained from the isotopic mixed crystal data of Nieman and Robinson. See Fig. 17 where this $\rho(E)$ is compared to that obtained from the 20.4 °K fluorescence. The poor agreement with experiment is consistent with the complications mentioned above.[44] From these calculations it can be concluded that, if Frenkel theory is applicable, the A_u level most likely lies between 37,815 cm^{-1} and 37,875 cm^{-1}.

The density function of naphthalene has been calculated from Eq. (4) for several choices of the $\mathcal{M}$'s using a model crystal containing 128,000 molecules. The Davydov splitting ($\underset{\sim}{k} = 0$) is given by $8M_{I\,II'}$ where $M_{I\,II} = \mathcal{M}_{I\,II} + \mathcal{M}_{I\,II'} + \cdots$. The density function for the case where the translationally equivalent interactions are nearly zero is very sharply peaked as shown in Fig. 18.

The band structure of the octopole model has been presented by Craig and Philpott.[8b] We have recalculated it for 128,000 molecules using the $\mathcal{M}$'s provided by R. G. Body.[45] The result of this calculation is also shown in Fig. 18. Only five of the octopole excitation exchange integrals were used in our calculation. Although other terms are predicted to be finite by the octopole model, these do not affect the shape of the density function as can be seen by comparing our result with that of Craig and Philpott.[8b] The fluorescence line shapes at 77° and 20.4°K predicted from the above models are shown and compared with the experimental results in Figs. 14 and 15. Even though the octopole band structure is not in complete agreement with the experimental result (see Figs. 13, 14, 15, and 18), it cannot be eliminated due to the very qualitative estimate of the phonon contributions to the band ⟷ band transitions.

VI. CONCLUSIONS

The recent theoretical developments concerning band → band transitions in molecular crystals have been examined experimentally. The application of these theories has enabled us to evaluate approximately the density function for the lowest excited singlet states of crystalline benzene and naphthalene as well as the temperature dependence and nature of the exciton-phonon coupling.

A comparison of the experimental density function with that obtained from semi-empirical calculations has provided information concerning the detailed nature of the excitation exchange interactions. Since the density function for naphthalene lies primarily between the Davydov components, it is concluded that the sum of the translationally equivalent interactions is small. This conclusion has also been derived from spectra of isotopic mixed crystals.[46] The density function calculated when these terms are the same order of magnitude as the interchange equivalent interactions gives reasonable agreement with the experimental result, although this agreement is in no way unique. The experimental results are in qualitative agreement with the predictions of the octopole model; no comparison could be made with the model involving interaction with charge transfer states.

For benzene, a sharply peaked density function is found. Since there are four exciton branches, of which at least two lie close together, such a function is not inconsistent with some translationally equivalent and interchange equivalent interactions being the same size. However, excellent agreement with the experimental result is obtained when the translationally equivalent interactions are neglected.

Such a calculation places the forbidden A_u Davydov component above all three B_u components but not as far above as predicted by mixed crystal experiments.[3] No purely theoretical calculation of the density function for crystalline benzene is available for comparison with these experimental results.

These results are not in any sense final, but they do indicate the power of Rashba's proposal, the importance of $\underset{\sim}{k} \neq \underset{\sim}{0}$ selection rules, the necessity for the consideration of the entire band structure in theoretical calculations, and the need for an analysis of phonon effects in the spectra of aromatic molecular crystals. In addition, the application of this technique to the elucidation of the band structure of different molecular crystals, including triplet states, should prove of general interest in the study of intermolecular interactions in the organic solid state. Of particular interest are crystals with one molecule per unit cell, crystals with two or more physically inequivalent sites per unit cell, and crystals with more than one molecule per unit cell but no apparent Davydov splitting.

REFERENCES

1. (a) L. P. Bouckaert, R. Smoluchowski, and E. Wigner, Phys. Rev. 50, 58 (1956); (b) J. M. Ziman, Principles of the Theory of Solids (Cambridge University Press, Cambridge, 1964).

2. (a) H. Winston and R. S. Halford, J. Chem. Phys. 17, 607 (1949); (b) Jon Mathews and R. L. Walker, Mathematical Methods of Physics (W. A. Benjamin, Inc., New York, 1964), Sec. 4.1; (c) It should be noted that throughout our own papers, including this one, $\underset{\sim}{k} = 0$ is sometimes used loosely to mean $\underset{\sim}{k} = \underset{\sim}{q}$ where $\underset{\sim}{q}$ is the wave vector of the incident radiation. This terminology is quite common in the literature.

3. G. C. Nieman and G. W. Robinson, J. Chem. Phys. 39, 1298 (1963).

4. D. M. Hanson, R. Kopelman, and G. W. Robinson, manuscript in preparation .

5. E. I. Rashba, Fiz. Tver. Tela 5, 1040 (1963) [English transl: Soviet Phys.--Solid State 5, 757 (1963)].

6. S. D. Colson, R. Kopelman, and G. W. Robinson, J. Chem. Phys. 47, 27 (1967); 47, 0000 (1967).

7. See, for example, S. D. Colson and E. R. Bernstein, J. Chem. Phys. 43, 2661 (1965). It should be noted that a 4 cm benzene crystal containing 10^{-5} parts phenol would be nearly opaque in the region of the band -- band absorption to be studied here. Similarly β-methyl naphthalene absorbs in the region of the corresponding naphthalene transition.

8. (a) R. G. Body and I. G. Ross, Australian J. Chem. 19, 1 (1966); (b) D. P. Craig and M. R. Philpott, Proc. Roy. Soc. (London) 290A, 583 (1966); (c) J. Jortner, S. A. Rice and J. L. Katz, J. Chem. Phys. 42, 309 (1965); and (d) A. S. Davydov and E. F. Sheka, Physica Status Solidi, 11, 877 (1965).

9. (a) R. Silbey, J. Jortner, M. T. Vala, and S. A. Rice, J. Chem. Phys. 42, 2948 (1965); (b) R. Silbey, S. A. Rice, and J. Jortner, J. Chem. Phys. 43, 3336 (1965).

10. (a) D. Fox and O. Schnepp, J. Chem. Phys. 23, 767 (1955); (b) T. Thirunamachandran, Ph. D. thesis, University of London, 1961.

11. The results of the calculations including interactions with the ion-pair states of crystalline benzene (Ref. 9a) place the A_u Davydov component near the B_{3u} Davydov component. R. Silbey, private communication.

12. The electronic exciton states are optically pumped after which they come into thermal equilibrium with respect to the bottom of the band.

13. An exciton branch is composed of those $\underset{\sim}{k}$ states that correspond to one of the representations of the interchange group. There are as many branches as molecules in the primitive unit cell. This term is adopted from discussions of lattice waves in crystals.[16]

14. D. A. Dows, Physics and Chemistry of the Organic Solid State, D. Fox, M. M. Labes, and A. Weissberger, Eds. (Interscience Publishers, Inc., New York, 1963), Vol. I., Chap. 11.

15. A. R. Gee and G. W. Robinson, J. Chem. Phys. 46, 4847 (1967). For convenience we shall retain the molecular point group labels for electronic and vibrational states.

16. (a) D. P. Craig, J. M. Hollas, M. F. Redies, and S. C. Wait, Jr., Phil. Trans. Roy. Soc. London A253, 543 (1961); (b) D. P. Craig and J. M. Hollas, ibid., A253, 569 (1961); (c) D. P. Craig and H. C. Wolf, J. Chem. Phys. 40, 2057 (1964); (d) A. R. Gee and D. M. Hanson, unpublished results.

17. The oriented site model differs from the oriented gas model[18] in that the transition moments for a molecule distorted by the site are used to predict the crystal moments.

18. R. M. Hochstrasser, Molecular Aspects of Symmetry (W. A. Benjamin, Inc., New York, 1966).

19. (a) A. S. Davydov, Theory of Molecular Excitons (McGraw-Hill Book Co., New York, 1962); (b) D. P. Craig and S. H. Walmsley, Physics and Chemistry of the Organic Solid State, D. Fox, M. M. Labes, and A. Weissberger, Eds. (Interscience Publishers, Inc., New York, 1963), Vol. I, Chap. 10, p. 586, and references therein.

20. (a) P. Sarti-Fantoni, Molecular Crystals 1, 457 (1966); (b) R. S. Silbey, J. Jortner, M. Vala, and S. A. Rice, Molecular Crystals 2, 385 (1967).

21. E. R. Bernstein, S. D. Colson, R. Kopelman, and G. W. Robinson (Manuscript in preparation).

22. That is, the zero of energy is chosen at $\bar{\epsilon} + \Delta$. See Eq. (16), Ref. 21.

23. R. Kopelman, J. Chem. Phys. 47, 0000 (1967).

24. H. Winston, J. Chem. Phys. 19, 156 (1951).

25. A. S. Davydov, Usp. Fiz. Nauk 82, 393 (1964). [English transl.: Soviet Phys.--Usp. 7, 145 (1964)].

26. R. S. Knox, Theory of Excitons (Academic Press, New York, 1963).

27. S. D. Colson and E. R. Bernstein, J. Chem. Phys. 43, 2661 (1965).

28. D. M. Hanson and G. W. Robinson, J. Chem. Phys. 43, 4174 (1965).

29. V. L. Broude, E. I. Rashba, E. F. Sheka, Soviet Phys.--Doklady 6, 718 (1962).

30. H. Maria, J. Chem. Phys. 40, 551 (1964).

31. A. F. Prikhot'ko and M. S. Soskin, Opt. i Spektroskopiya 13, 522 (1962) [English transl.: Opt. Spectry. (USSR) 13, 291 (1962)].

32. H. Maria and A. Zahlan, J. Chem. Phys. 38, 941 (1963).

33. (a) V. L. Broude, Usp. Fiz. Nauk 74, 577 (1962) [English transl.: Soviet Phys.--Usp. 4, 584 (1962)]; (b) V. L. Broude and M. I. Onoprienko, Opt. i Spektroskopiya 8, 629 (1960) [English transl.: Opt. Spectry. (USSR) 8, 332 (1960)].

34. S. D. Colson, J. Chem. Phys. 45, 4746 (1966).

35. Different crystals at the same temperature give quite different values for the relative intensity of these transitions. In some crystals the peak height of the lowest energy component is about the same as that of the maximum of the phonon bands and, while the highest energy Davydov component always appears the most intense, its intensity relative to the other two seems to vary by as much as a factor of 2-3. These effects are probably a manifestation of the difficulty inherent in the measurement of the intensity of a very sharp absorption line. When an absorption line is narrow compared with the spectral resolution, the line appears weaker the narrower it is because of the difficulty of resolving it from the continuous background. On the other hand, relative intensities of very intense absorption lines, even when using adequate resolution, are difficult to measure accurately from percent transmission curves because of the extremely small values of I/I_0. Additional problems with relative intensity measurements arise in partially oriented crystals studied with unpolarized light. As the linewidth and energy of the Davydov components are very dependent upon crystal strains and stresses,[34] their apparent intensity could easily change from sample to sample.

36. A. Zmerli, J. Chim. Phys. 56, 387 (1959).

37. V. N. Vatulev, N. I. Sheremet, and M. R. Shpak, Opt. i Spektroskopiya 16, 577 (1964) [English transl.: Opt. Spectry. (USSR) 16, 315 (1964)].

38. A. Prőpstl and H. C. Wolf, Z. Naturforsch. 18a, 724 (1963).

39. V. L. Broude, E. I. Rashba, and E. F. Sheka, Physica Status Solidi 19, 395 (1967).

40. A fourth line might be expected to be observed near the center of the band because of the presence of 6% (natural abundance) $^{13}C^{12}C_5H_6$, which has recently been shown to have its 0, 0 shifted 3.7 cm^{-1} to the blue of C_6H_6 as shown in the experiments of E. R. Bernstein, S. D. Colson, and D. S. Tinti, manuscript in preparation.

41. H. C. Wolf, Solid State Physics 9, 1 (1959).

42. V. L. Broude, V. S. Medvedev, and A. F. Prikhot'ko, Opt. i Spektroskopiya 2, 317 (1957).

43. T. A. Claxton, Ph. D. thesis, University of London, 1961, as quoted by O. Schnepp, Annual Reviews of Physical Chemistry, Vol. 14, H. Eyring, Ed. (Annual Reviews, Inc., Palo Alto, Calif. 1963), p. 35.

44. S. D. Colson, manuscript in preparation.

45. R. G. Body, private communication; also see Ref. 8a. For $\mathcal{M}$ values used, see caption, Fig. 18.

46. D. M. Hanson, R. Kopelman, and G. W. Robinson, unpublished results.

Fig. 1. Schematic diagram of an exciton band → band transition in a linear crystal compared with a transition from the crystal ground state.

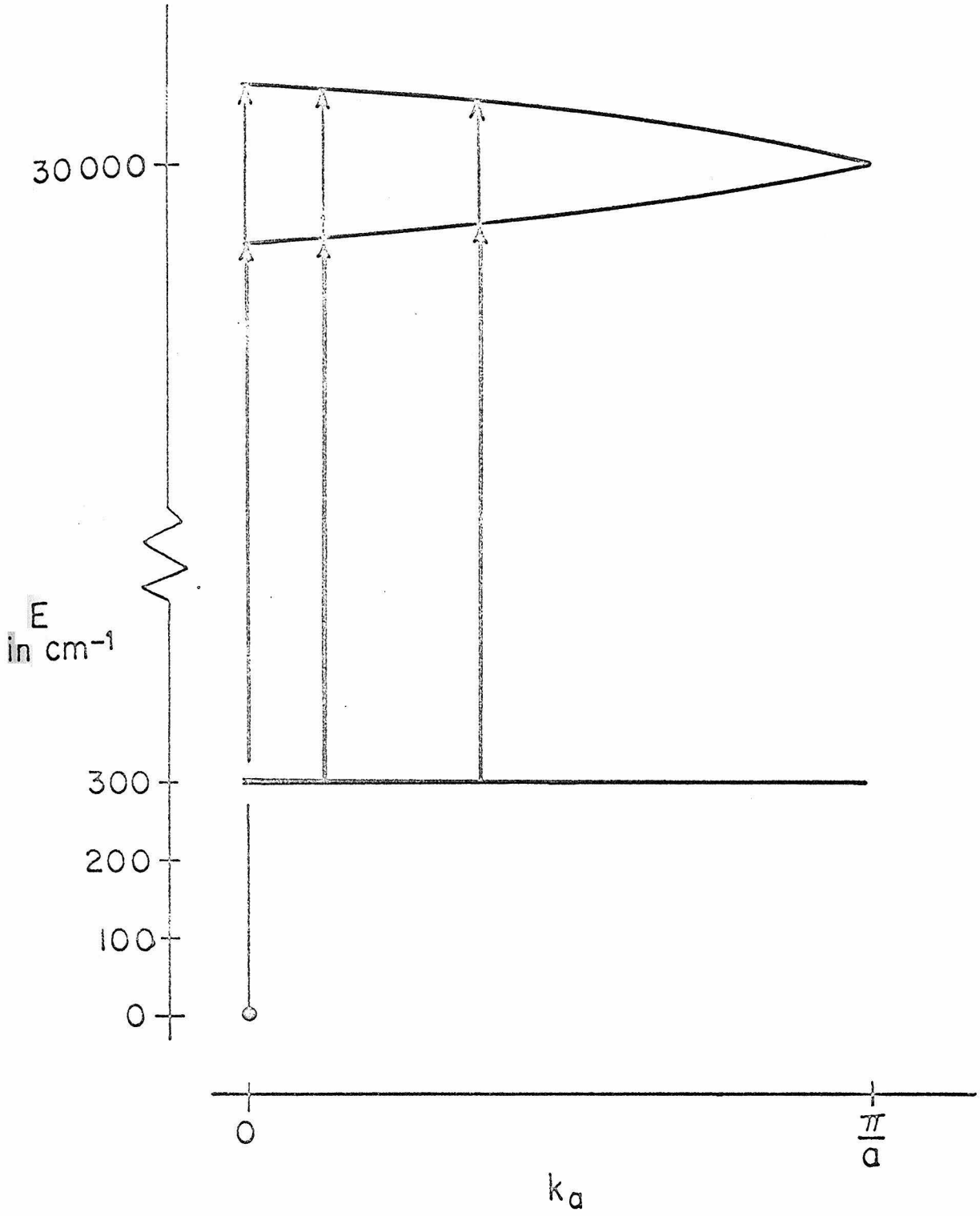
30 000
E
in cm⁻¹
300
200
100
0
0
π/a
k a

Fig. 2. Microdensitometer tracings of the $0 - \nu_6''$ fluorescence band – band transition of crystalline benzene at 77, 27, and 4.2 °K, illustrating the temperature dependence of the linewidth and shape. Also included is the corresponding transition for ~1% C_6H_6 in C_6D_6 showing the 3.1 cm^{-1} site splitting of the ground state $e_{2g}(\nu_6)$ vibration. The mixed crystal transition has been shifted 50 cm^{-1} to the red to account for the difference in the neat and mixed crystal origins.

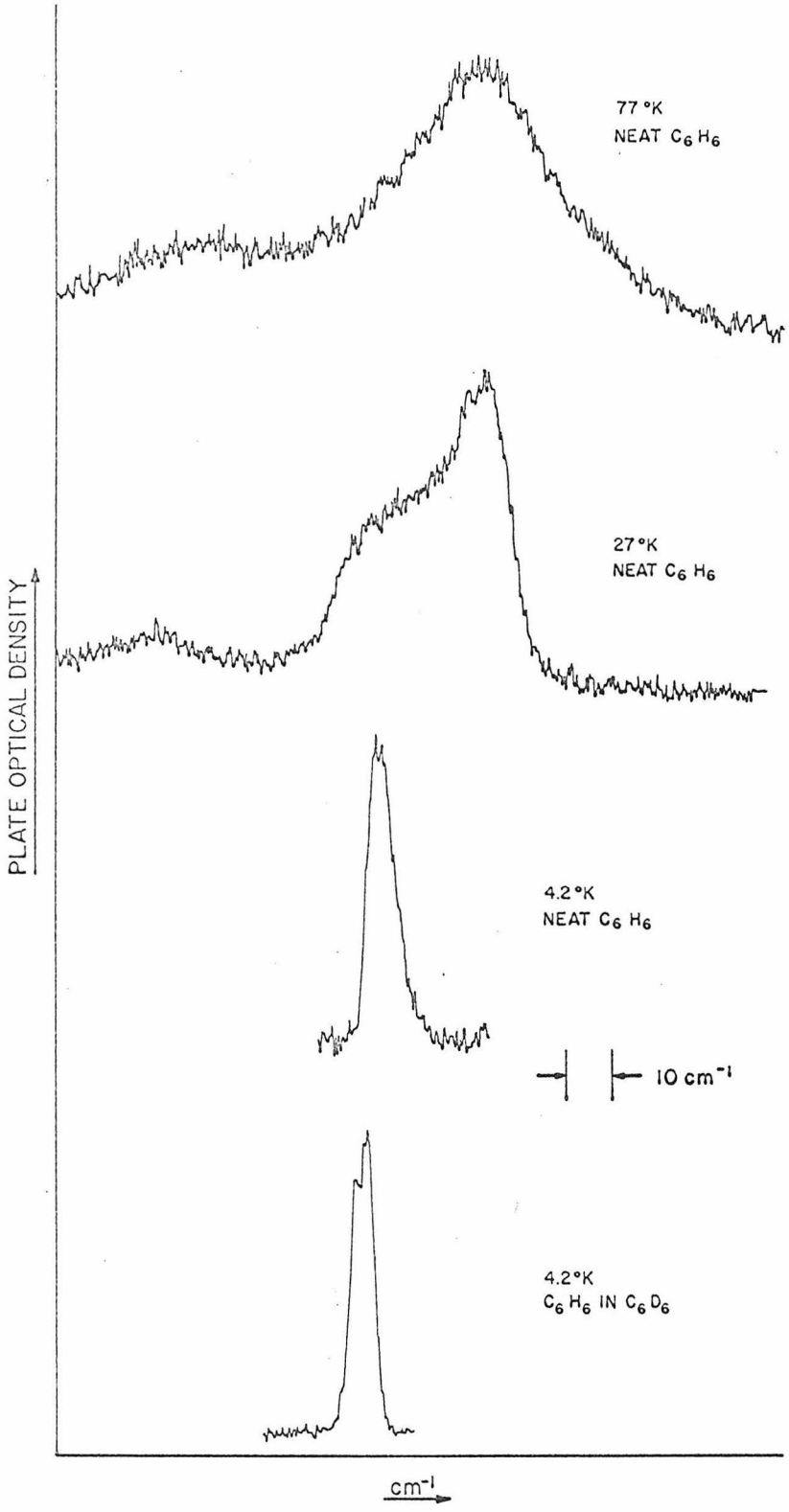
77 °K
NEAT C_6H_6
27 °K
NEAT C_6H_6
4.2 °K
NEAT C_6H_6
10 cm^{-1}
4.2 °K
C_6H_6 IN C_6D_6
PLATE OPTICAL DENSITY
cm^{-1}

Fig. 3. The $0 - \nu_6''$ fluorescence transition of crystalline benzene observed with the 1.83 M Jarrell-Ash spectrometer at 77 and 20.4 °K. The solid curves represent the average of the noise as determined by repeating the spectrum several times.

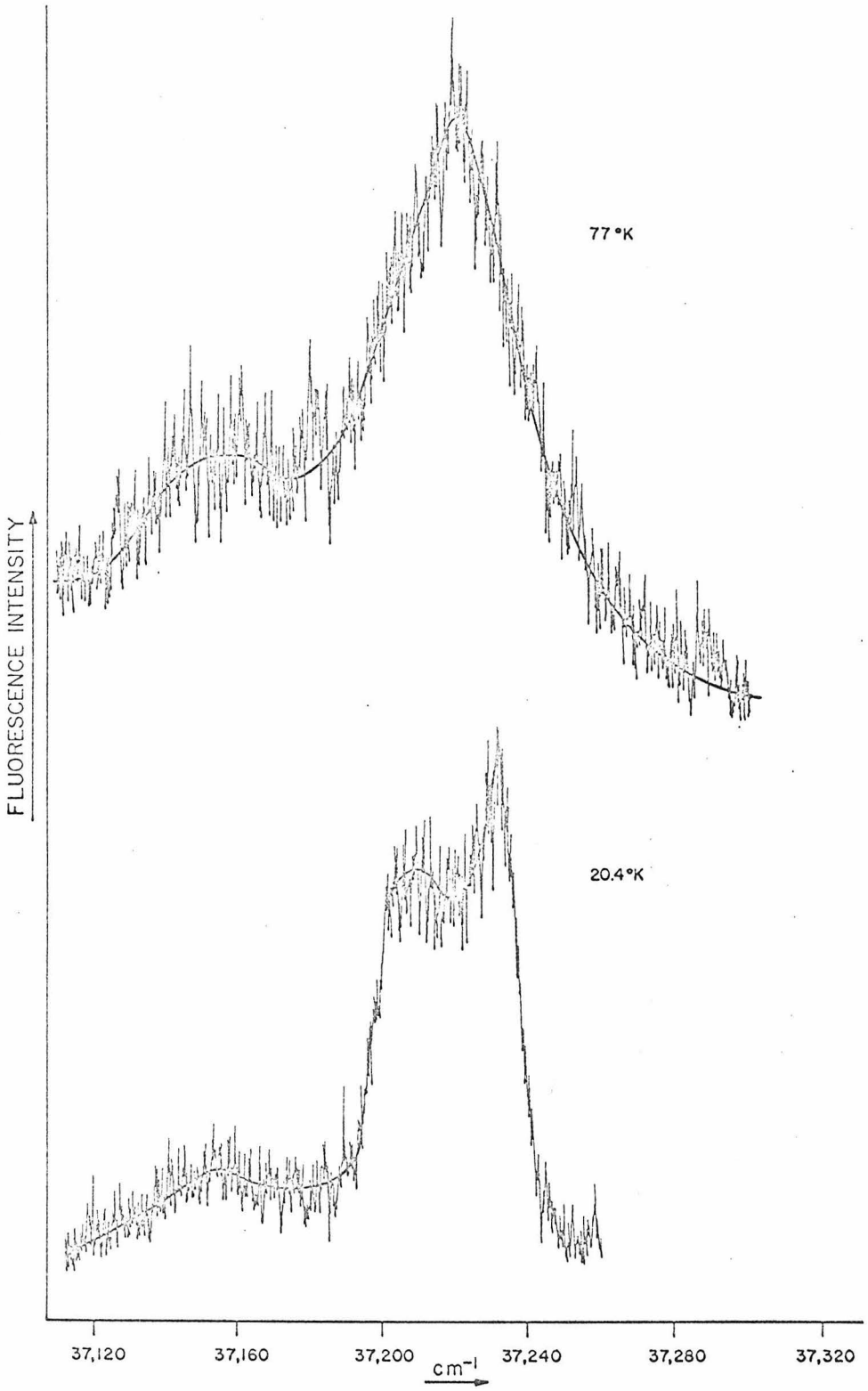
77 °K
20.4 °K
FLUORESCENCE INTENSITY
37,120
37,160
37,200
37,240
37,280
37,320
cm⁻¹

Fig. 4. The 0 - "512" fluorescence transition of crystalline naphthalene observed with the 1.83 M Jarrell-Ash spectrometer. The band at 20.4 °K was graphed from Fig. 5 in order to correct for the different recorder speed. The neat and mixed (1% $C_{10}H_8$ in 99% $C_{10}D_8$) crystal transitions at 4.2 °K were observed using the high-resolution grating in the 18th order. The 0, 0 fluorescence line in the neat crystal is even sharper than the vibronic transition in the mixed crystal. A comparison of these transitions illustrates the participation of $\underset{\sim}{k} \neq 0$ levels in the neat crystal vibronic transition, even at 4.2 °K.

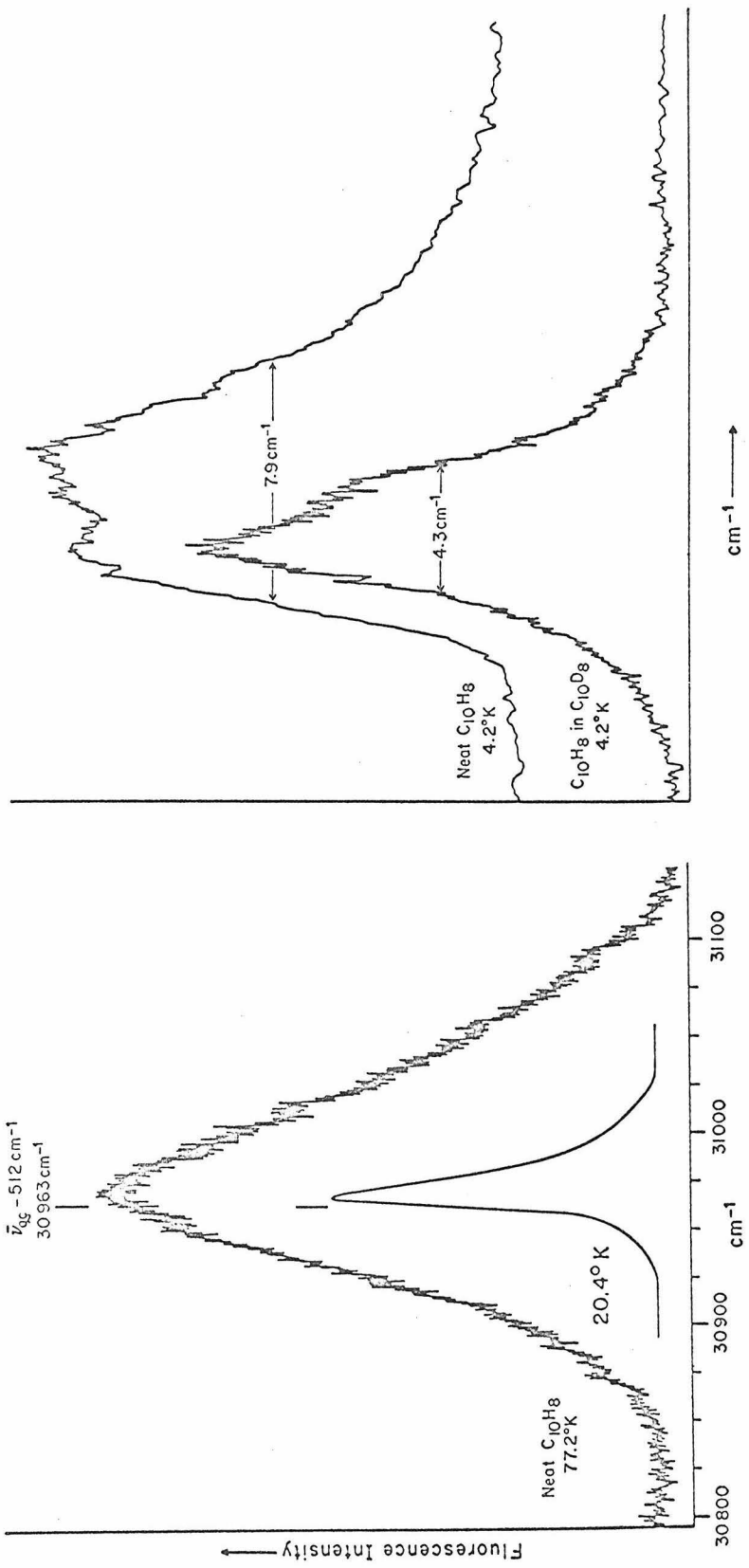
Fluorescence Intensity
Neat $C_{10}H_8$
77.2°K
20.4° K
$\bar{\nu}_{gs}$ - 512 cm^{-1}
30963 cm^{-1}
30800
30900
31000
31100
cm^{-1}
Neat $C_{10}H_8$
4.2°K
$C_{10}H_8$ in $C_{10}D_8$
4.2°K
7.9 cm^{-1}
4.3 cm^{-1}
cm^{-1}

Fig. 5. The 0 - "512" fluorescence transition in neat crystalline naphthalene at 20.4 °K.

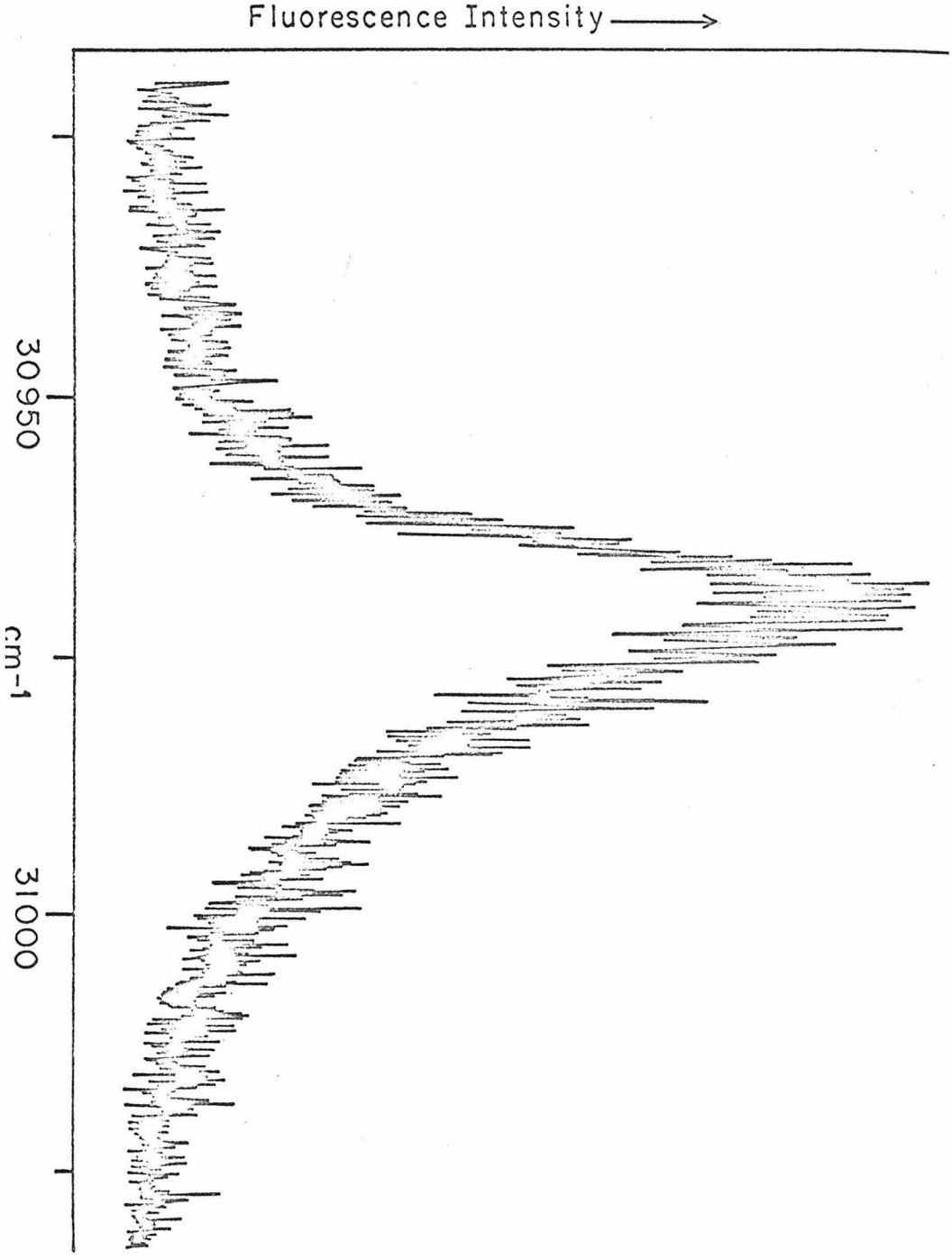
Fluorescence Intensity
30950
cm-1
31000

Fig. 6. Density-of-states function of the lowest singlet exciton band of crystalline benzene as determined from the 20.4 °K () and 27 °K () fluorescence shown in Figs. 2 and 3. The observed Davydov components are indicated symbolically and designated by their polarizations (see text).

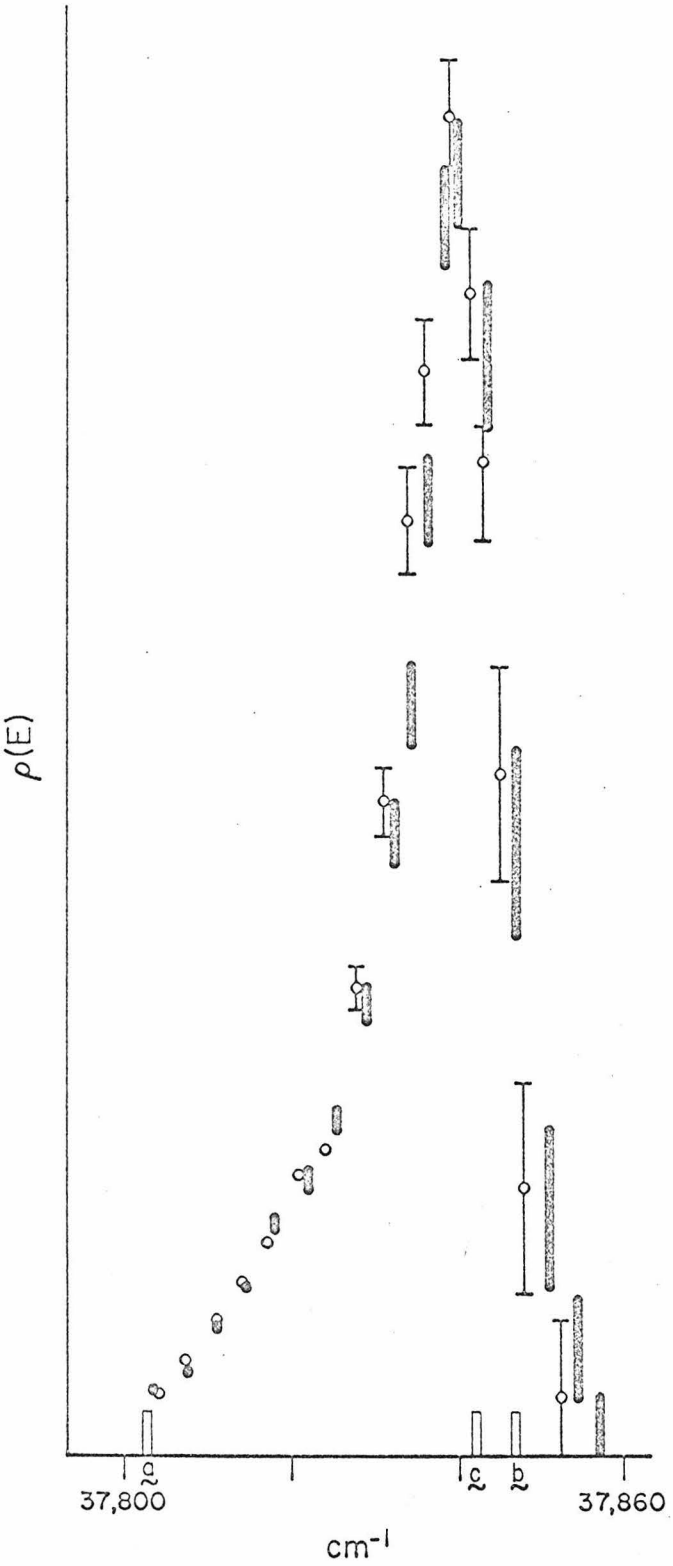
ρ(E)
a
c
b
37,800
37,860
cm⁻¹

Fig. 7. Density-of-states function of the $^1B_{2u}$ benzene exciton band as determined from the 77 °K fluorescence (▯) and the ~60 °K absorption (⊥○⊥) band ⟷ band transitions. The $\underset{\sim}{a}$ polarized Davydov component is taken as the bottom of the band and, thus, the fluorescence intensity to lower energy is attributed to phonons and is shown as a dashed line. The different roles of the addition phonons in absorption and emission can be clearly seen in the wings of the respective functions.

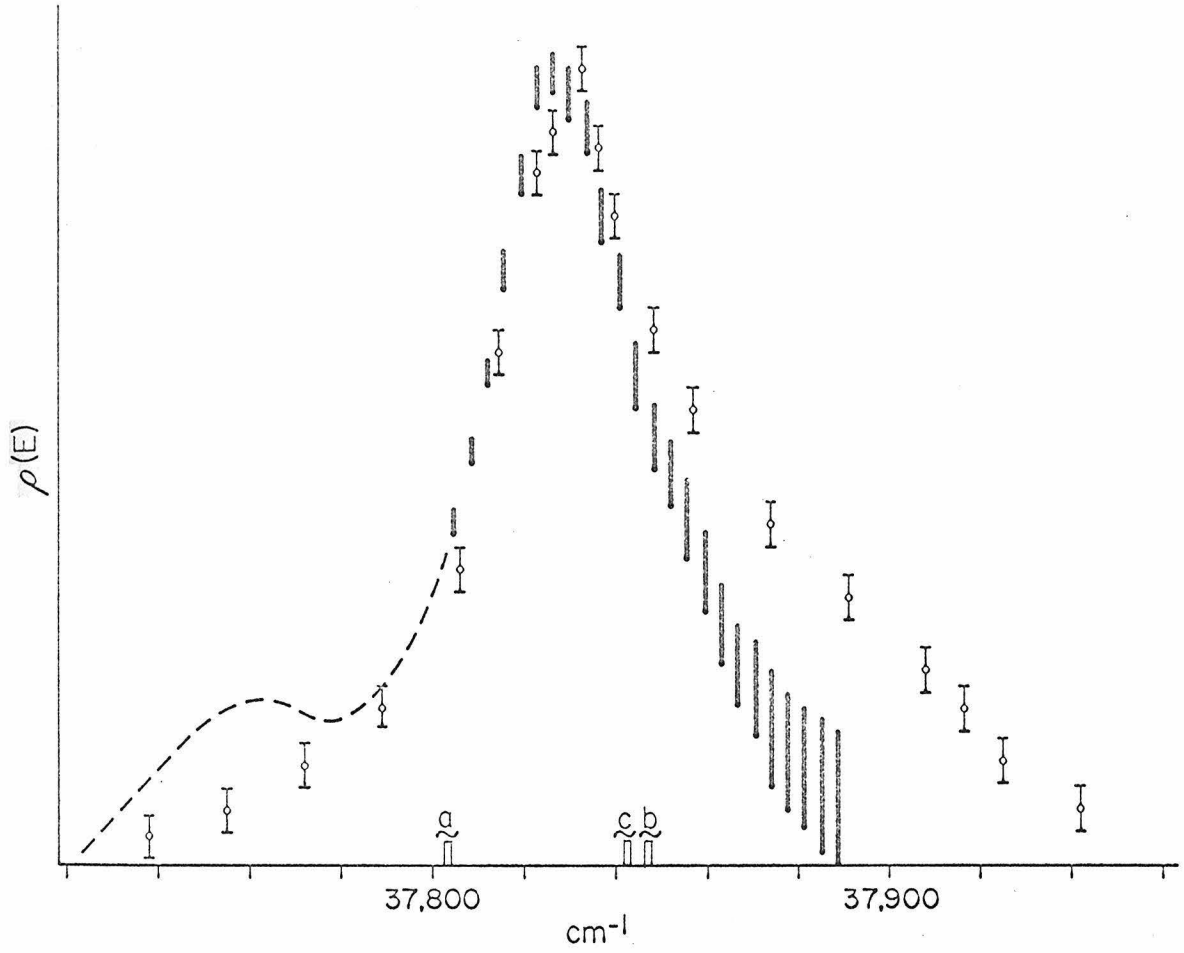
ρ(E)
a
c
b
37,800
37,900
cm-1

Fig. 8. Density-of-states function for the naphthalene exciton band derived from the 77 °K (▯) and 20.4 °K (⊺) fluorescence shown in Fig. 4. The Davydov components are indicated symbolically and designated by their polarizations. The ac component is assumed to be at the bottom of the exciton band, and intensity at lower energy is attributed to phonons and is shown with the dashed lines. The density function is obtained from the fluorescence intensity by dividing by the appropriate Boltzmann factor. This operation magnifies the experimental uncertainty in the fluorescence lines. The intensity below the ac Davydov component is not corrected for a thermal distribution.

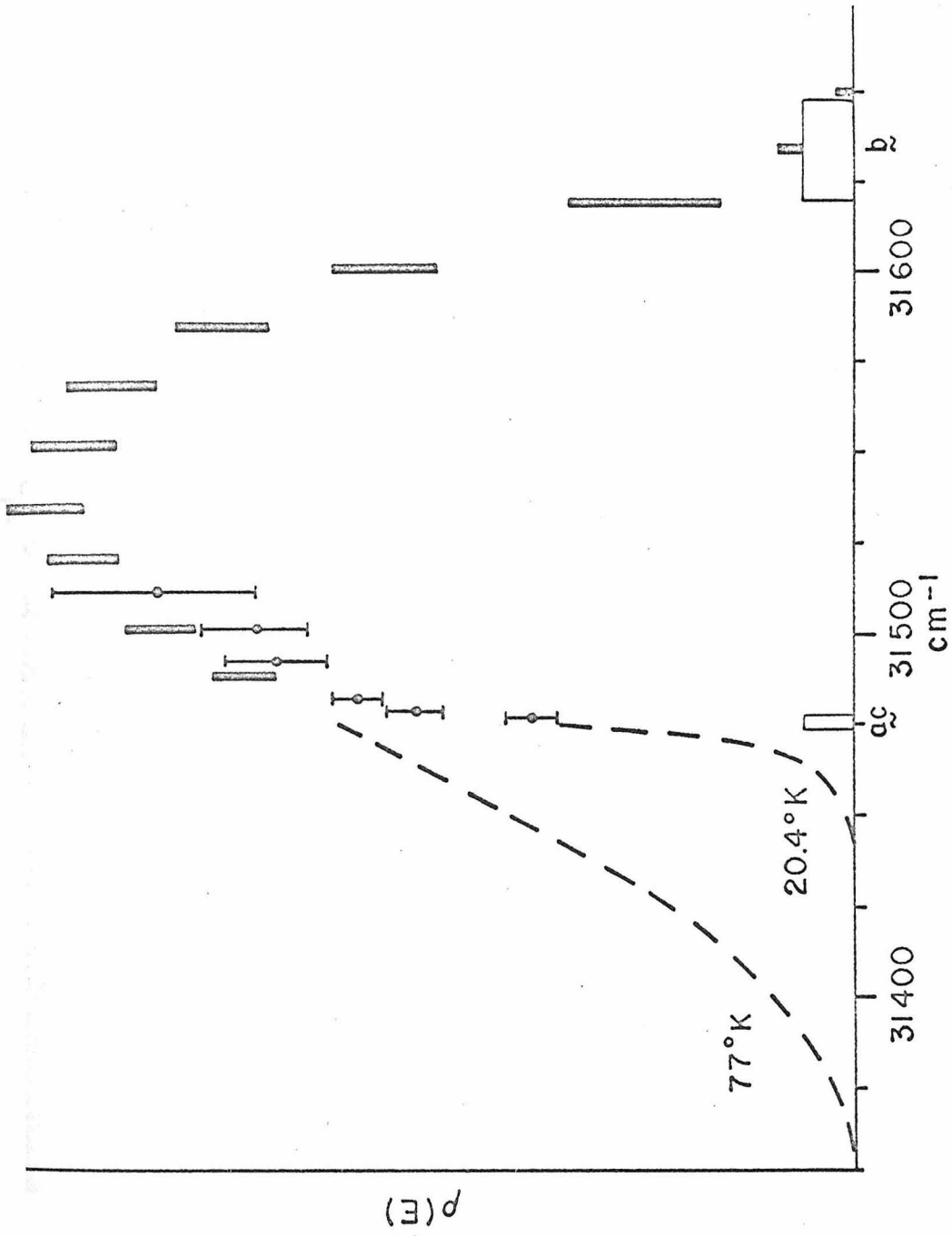
ρ(E)
77°K
20.4°K
a≳c
b≳
31400
31500
31600
cm⁻¹

Fig. 9. Microdensitometer tracings of the absorptions to the pure electronic $^1B_{2u}$ state of crystalline benzene from the 606 cm^{-1} vibrational band at ~60°K (top) and from the crystal ground state at 4.2°K (bottom). The origin of the band → band absorption has been shifted 606 cm^{-1} to higher energy in order to compare the two spectra. The broad, double-peaked absorption on the right of the three Davydov lines in the 4.2°K spectrum is due to phonons.

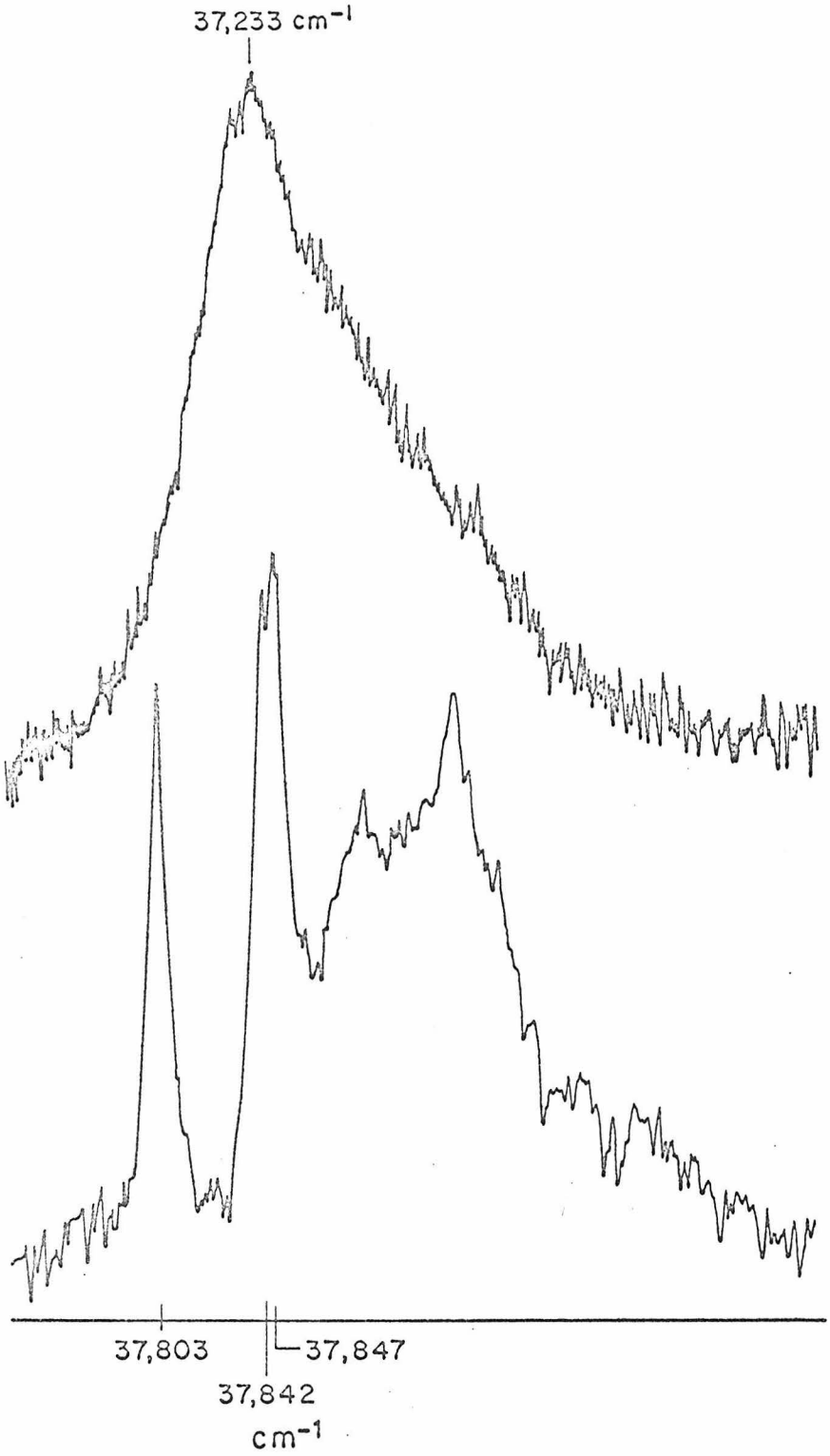
37,233 cm⁻¹
37,803
37,842
37,847
cm⁻¹

Fig. 10. Microdensitometer tracings of the 0, 0 absorption transition in crystalline naphthalene (i) at 4.2 °K and (ii) at 77 °K, and (iii) the exciton band – exciton band absorption transition observed in a 1 cm thick crystal at 77 °K. The latter tracing has been shifted to higher energy by the value of the vibrational quantum in order to compare it with the Davydov splitting. The rising background to high energy is caused by the onset of other vibronic transitions.

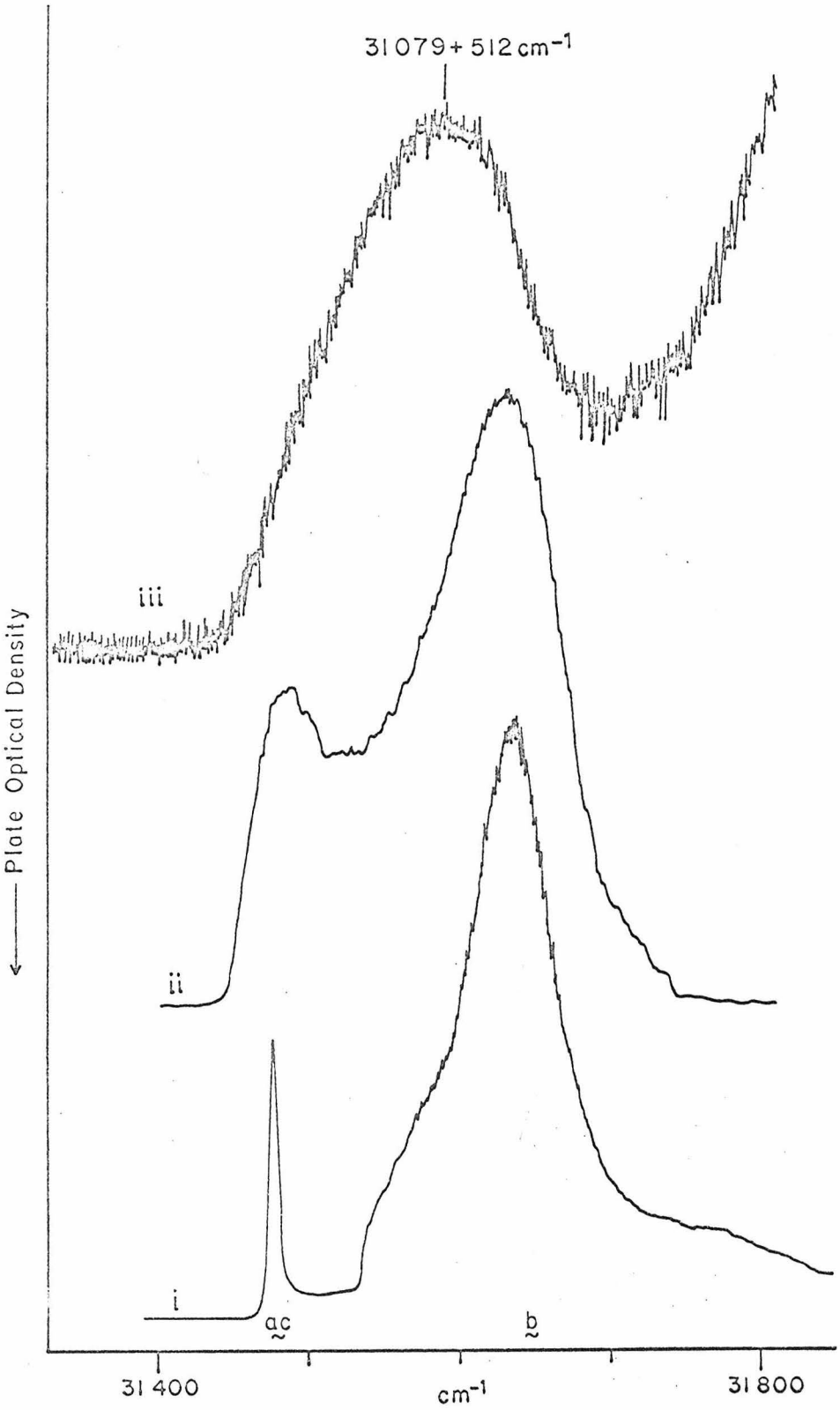
31 079 + 512 cm⁻¹
iii
ii
i
Plate Optical Density
a,c
b
31 400
cm⁻¹
31 800

Fig. 11. Sample optical density for the band – band transition of Fig. 10. A consideration of Lambert's law shows that the density function is linearly proportional to sample O. D. within the restrictions discussed in this paper. The background absorption on which the band – band transition is observed is accounted for as a change in I_0. The difficulty in determining I_0 is represented by the shading of the curve.

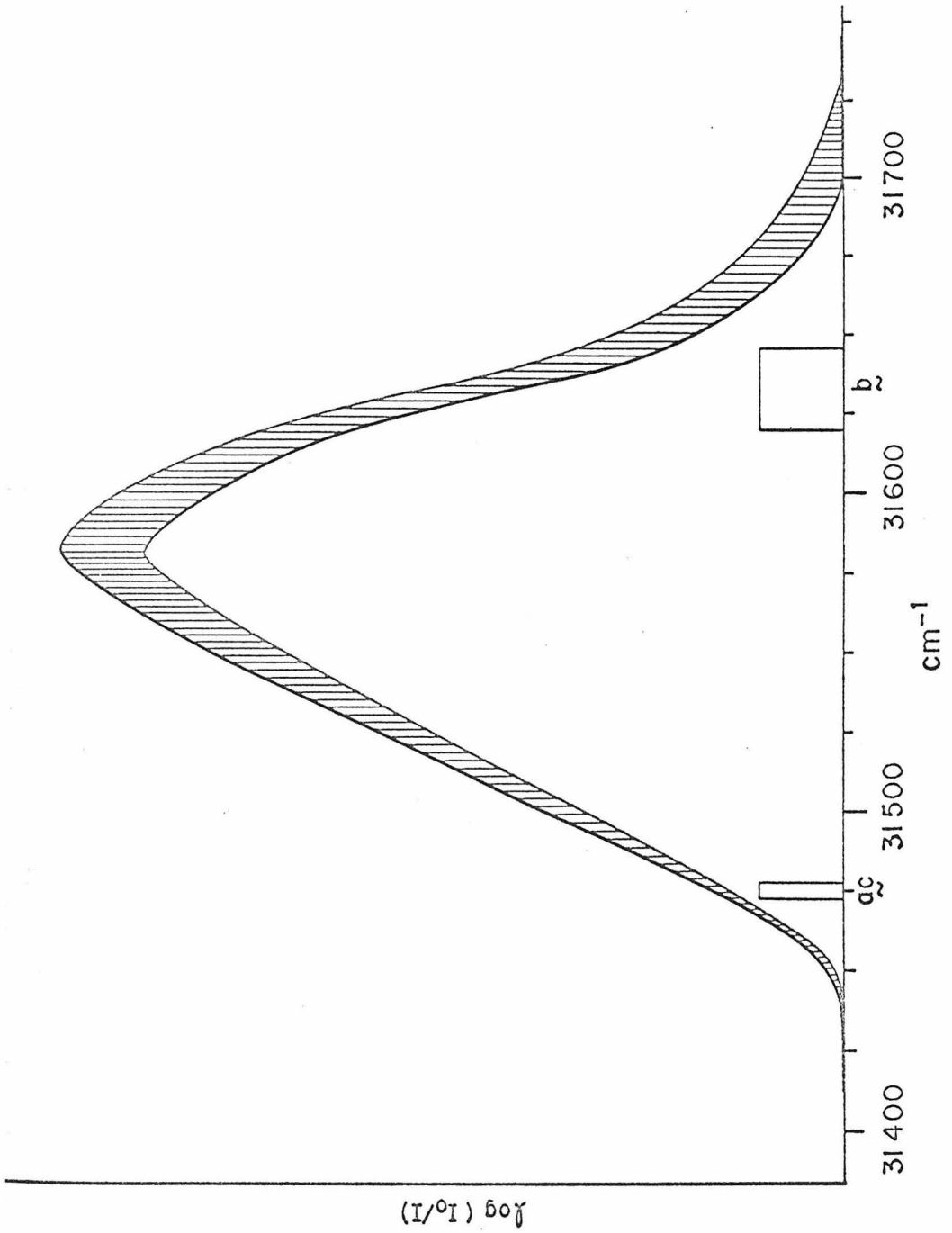
log (I₀/I)
31400
31500
31600
31700
cm⁻¹
a_c
b

Fig. 12. Microphotometer tracings of the 0, 0 $^1B_{2u} \leftarrow {}^1A_{1g}$ transition of crystalline benzene at 77, 27, 4.2 and 1.8 °K. The spectra were taken from different samples whose thicknesses ($\sim 20\,\mu$) were not accurately determined. The middle Davydov component at 27 °K can be seen on the photographic plate as a shoulder on the highest energy one. The energy scale is in an opposite direction from that of Fig. 9. Note the <u>apparent</u> increase in phonon contribution as the exciton absorptions become sharper.

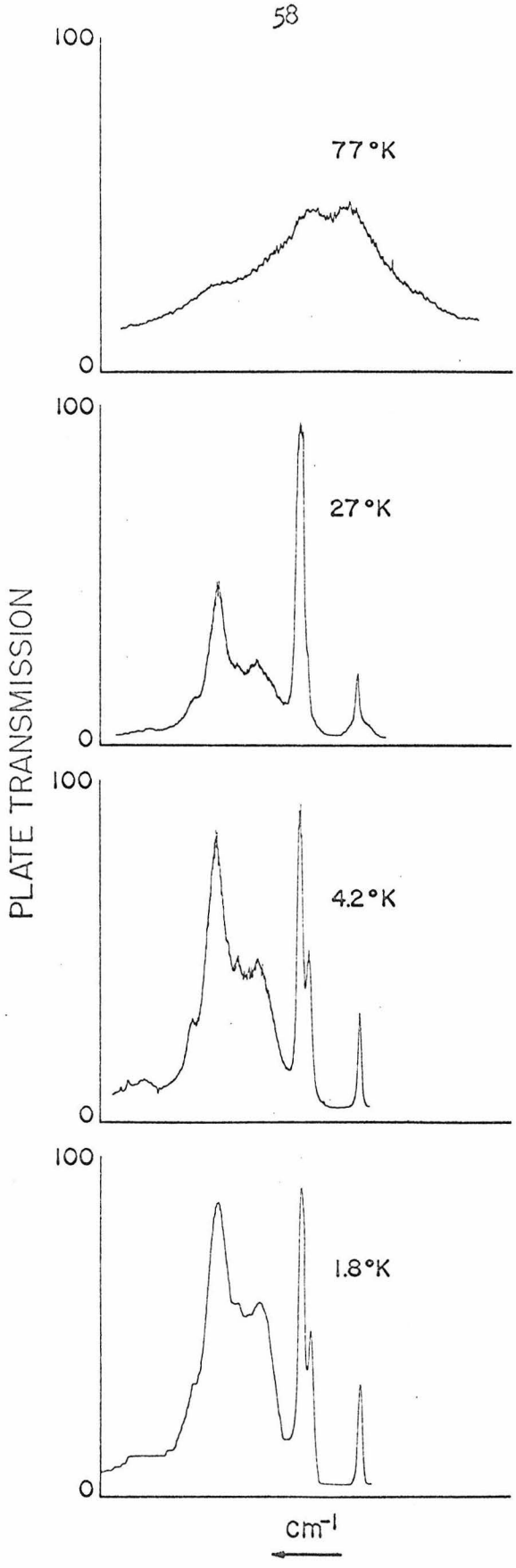
100
77°K
0
100
27°K
0
PLATE TRANSMISSION
100
4.2°K
0
100
1.8°K
0
cm⁻¹

Fig. 13. The composite density function for naphthalene, determined roughly from the high-energy edge of the band → band fluorescence and the low-energy edge of the band → band absorption: Figs. 8 and 11, respectively.

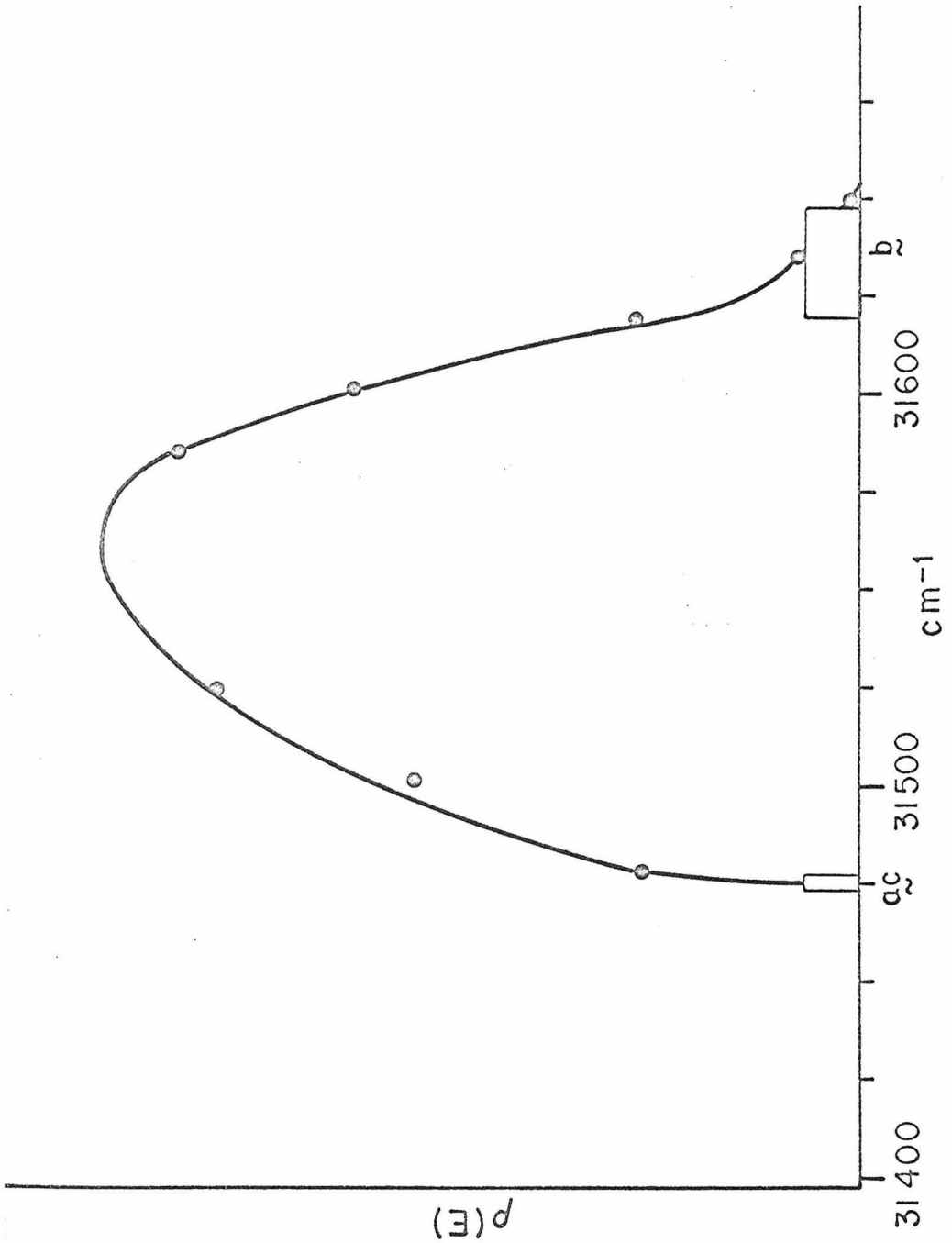
ρ(E)
31 400
a,c
31500
31600
b
cm-1

Fig. 14. (A) The experimental fluorescence band of naphthalene (0 - "512") at 20.4 °K. The half-width, neglecting the phonon contribution, is shown by the arrow and is 16 cm^{-1}. (B) This fluorescence band as predicted from the density function of the octopole model (see Fig. 18). The half-width equals 15 cm^{-1}. (C) This fluorescence band predicted from the composite density function, see Fig. 13. The half-width equals 24 cm^{-1}.

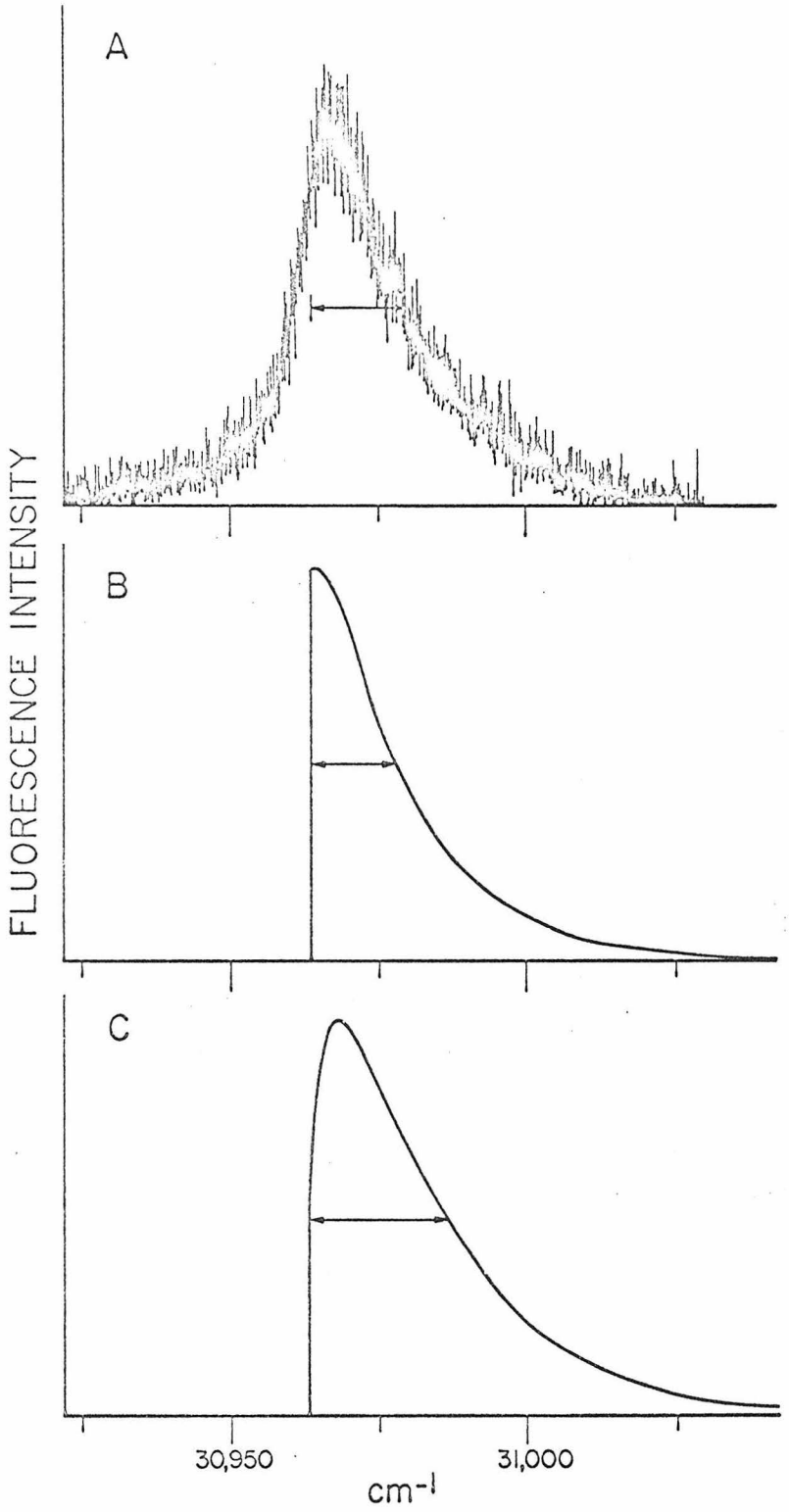
A
B
C
FLUORESCENCE INTENSITY
30,950
31,000
cm-1

Fig. 15. (A) The experimental fluorescence band of naphthalene at 77°K. (B) This fluorescence band as predicted from the octopole model, and (C) from the composite function.

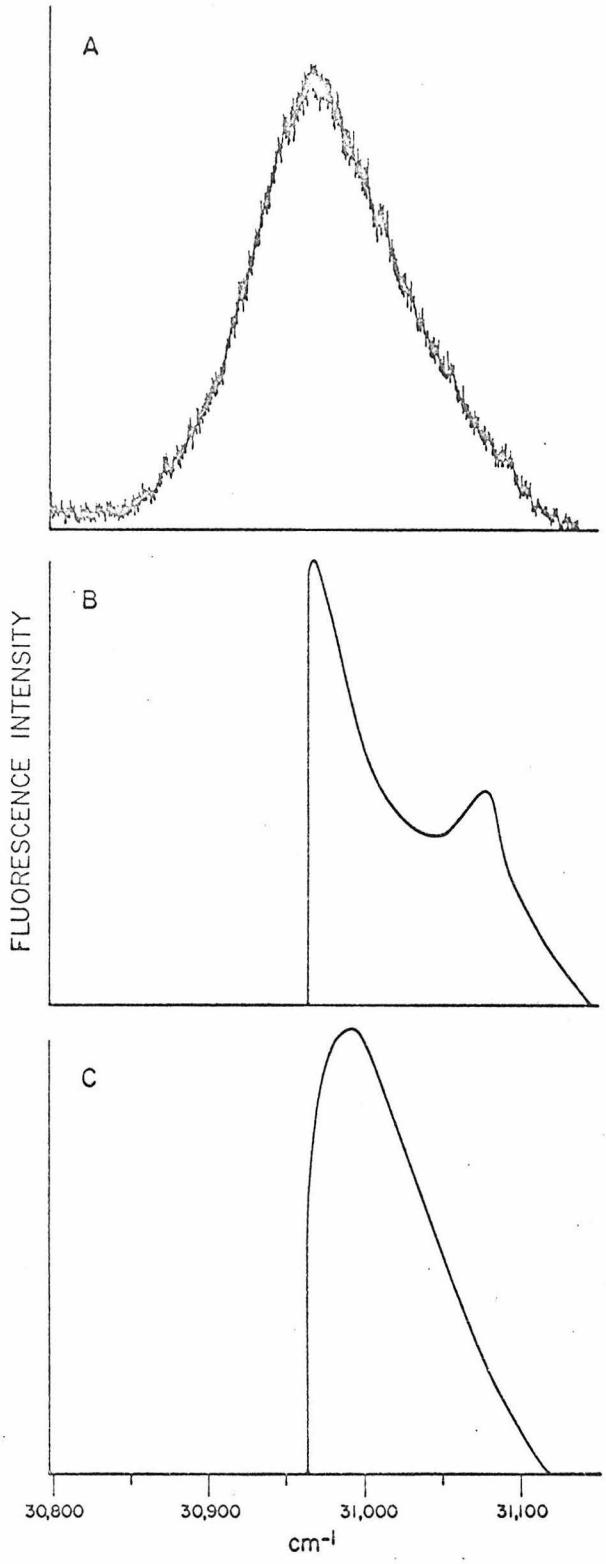
A
B
C
FLUORESCENCE INTENSITY
30,800
30,900
31,000
31,100
cm-1

Fig. 16. Density-of-states function for benzene giving the relative number of states per wavenumber interval as determined by the dispersion relation [Eq. (3)] for various values of the excitation exchange integrals. The positions of the allowed (▯) and forbidden (▯ plus arrow) Davydov components are indicated along the horizontal axis.

(A) $\mathscr{M}_{I\,II} = -0.90$, $\mathscr{M}_{I\,III} = 4.85$, $\mathscr{M}_{I\,IV} = 4.25$, and $\mathscr{M}_a = \mathscr{M}_b = \mathscr{M}_c = 0\ cm^{-1}$. (B) $\mathscr{M}_{I\,II} = -1.55$, $\mathscr{M}_{I\,III} = 3.93$, $\mathscr{M}_{I\,IV} = 3.28$, $\mathscr{M}_a = -0.25$, $\mathscr{M}_b = 0$, $\mathscr{M}_c = -0.75\ cm^{-1}$. (C) $\mathscr{M}_{I\,II} = -2.03$, $\mathscr{M}_{I\,III} = 3.45$, $\mathscr{M}_{I\,IV} = 2.80$, and $\mathscr{M}_a = \mathscr{M}_b = \mathscr{M}_c = 0\ cm^{-1}$. (D) $\mathscr{M}_{I\,II} = -2.96$, $\mathscr{M}_{I\,III} = 2.51$, $\mathscr{M}_{I\,IV} = 1.86$, $\mathscr{M}_a = -0.60$, $\mathscr{M}_b = 0$ and $\mathscr{M}_c = -1.80\ cm^{-1}$. (E) $\mathscr{M}_{I\,II} = -3.69$, $\mathscr{M}_{I\,III} = 1.89$, $\mathscr{M}_{I\,IV} = 1.24$, $\mathscr{M}_a = -0.75$, $\mathscr{M}_b = 0$, and $\mathscr{M}_c = -2.25\ cm^{-1}$. (F) $\mathscr{M}_{I\,II} = -4.22$, $\mathscr{M}_{I\,III} = 1.26$, $\mathscr{M}_{I\,IV} = 0.60$, $\mathscr{M}_a = -1.00$, $\mathscr{M}_b = 0$, and $\mathscr{M}_c = -3.00\ cm^{-1}$. (G) $\mathscr{M}_{I\,II} = -4.82$, $\mathscr{M}_{I\,III} = 0.65$, $\mathscr{M}_{I\,IV} = 0$, and $\mathscr{M}_a = \mathscr{M}_b = \mathscr{M}_c = 0$. (H) $\mathscr{M}_{I\,II} = -4.82$, $\mathscr{M}_{I\,III} = 0.65$, $\mathscr{M}_{I\,IV} = 0$, $\mathscr{M}_a = -1.00$, $\mathscr{M}_b = 0$, and $\mathscr{M}_c = -3.00\ cm^{-1}$.

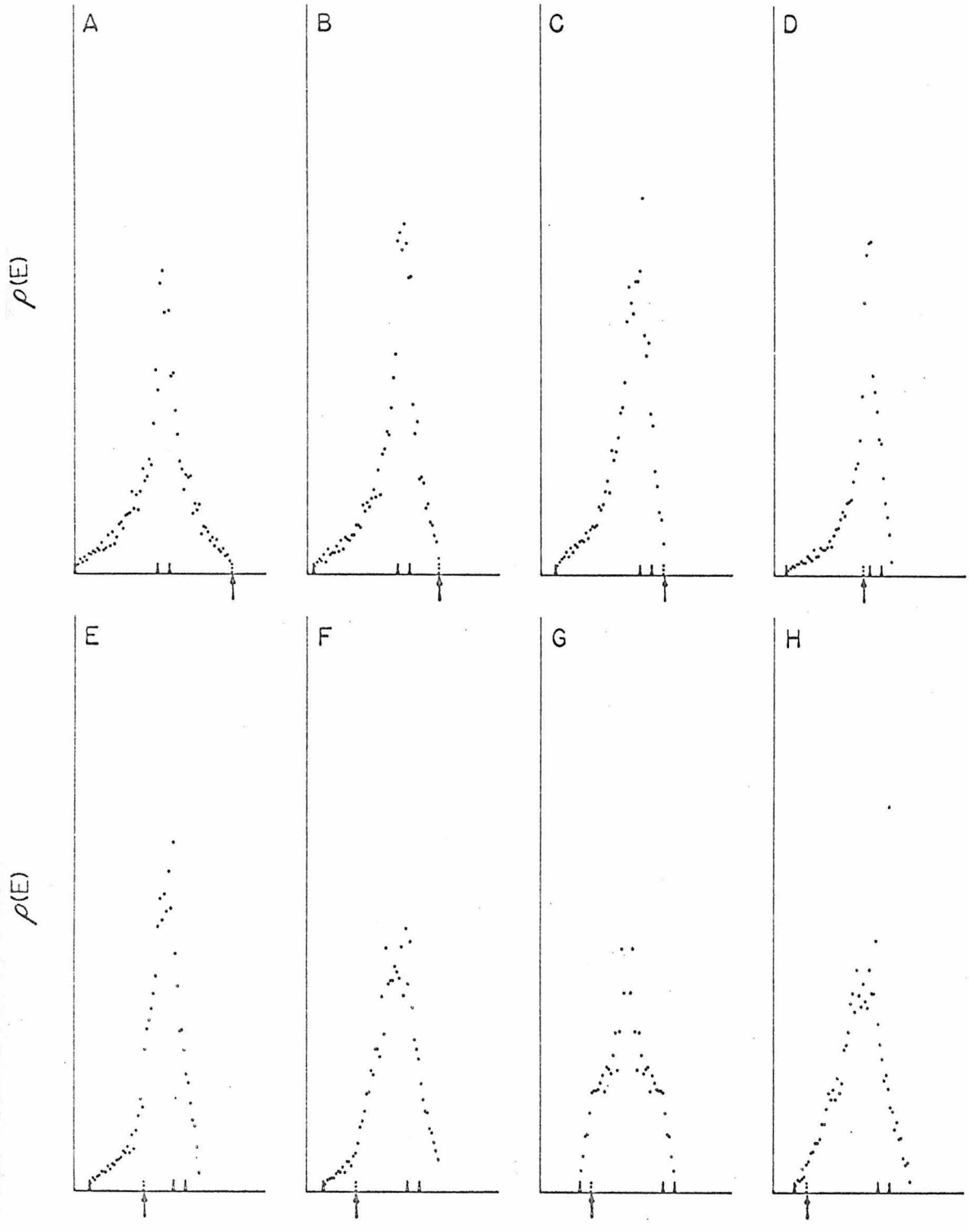
A
B
C
D
E
F
G
H
ρ(E)
ρ(E)

Fig. 17. Comparison of the 20.4 °K experimental (▯) density-of-states function with that calculated from the $\mathscr{m}_{ij}$ of Nieman and Robinson (•••) [$\mathscr{m}_{I\,II} = 6.90$, $\mathscr{m}_{I\,III} = 12.40$, $\mathscr{m}_{I\,IV} = 11.70$, $\mathscr{m}_a = 1.00$, $\mathscr{m}_b = 0$, and $\mathscr{m}_c = 3.00\ cm^{-1}$] and from a set of $\mathscr{m}_{ij}$ that approximately fit the experimental function (solid curve) [$\mathscr{m}_{I\,II} = -1.55$, $\mathscr{m}_{I\,III} = 3.93$, $\mathscr{m}_{I\,IV} = 3.28$, and $\mathscr{m}_a = \mathscr{m}_b = \mathscr{m}_c = 0\ cm^{-1}$]. The functions are normalized such that the area under each curve is the same.

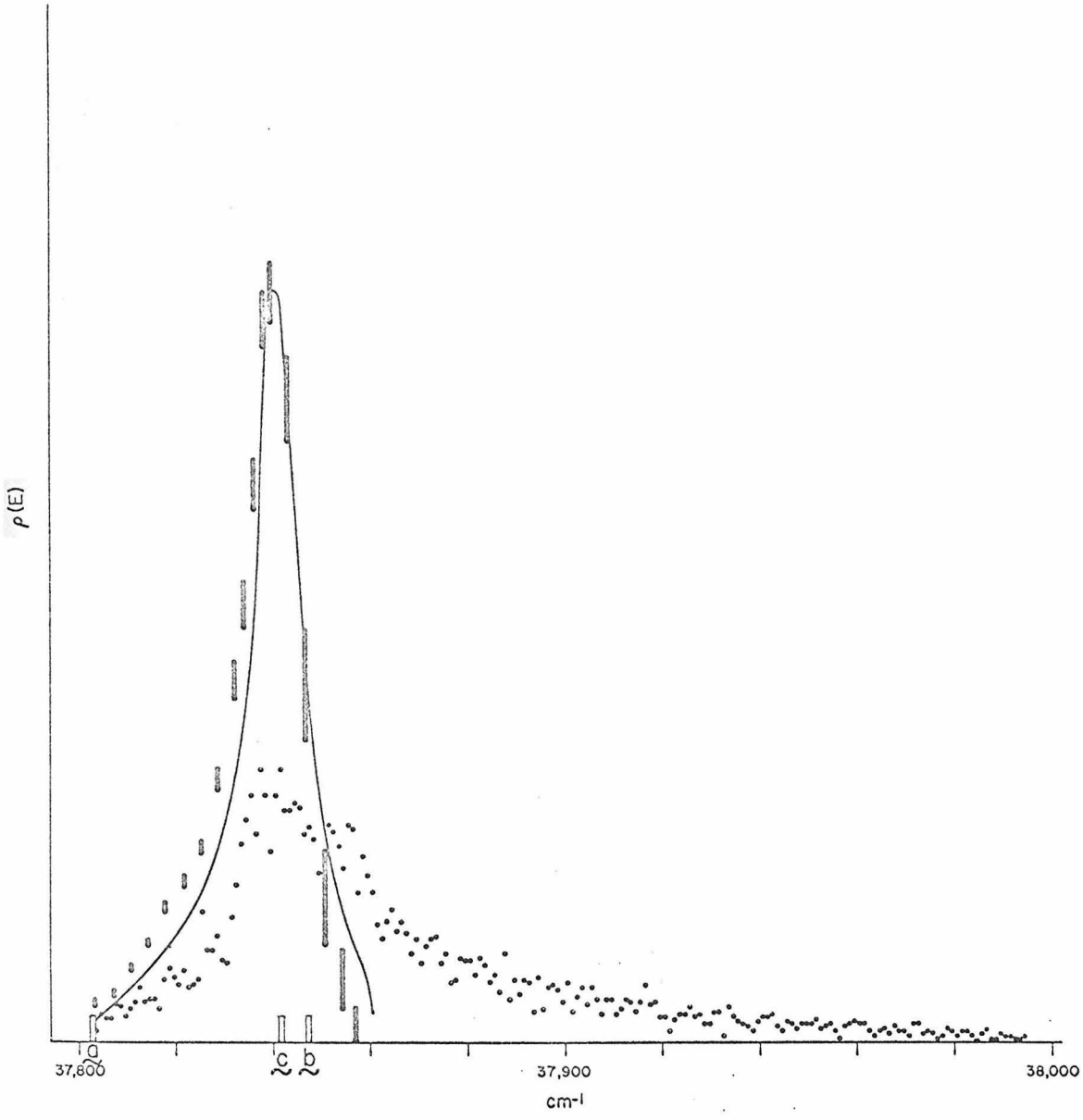
ρ(E)
a
c
b
37,800
37,900
38,000
cm-1

Fig. 18. Density functions for naphthalene giving the relative number of states per wavenumber as determined from the dispersion relation [Eq. (4)] for various values of the excitation exchange integrals. (A) The octopole model: ——————— $\mathscr{M}_a = -4.8$, $\mathscr{M}_b = -3.9$, $\mathscr{M}_c = -2.4$, $\mathscr{M}_{I\,II} = -21.1$, $\mathscr{M}_{I\,II'} = 1.6$ cm^{-1}. These were obtained from Ref. 45, also see Ref. 8 b. (B) $\mathscr{M}_a = 2$, $\mathscr{M}_b = -1$, $\mathscr{M}_c = -1$, $\mathscr{M}_{I\,II} = 22$, $\mathscr{M}_{I\,II'} = -2$ cm^{-1}. (C) $\mathscr{M}_a = 10$, $\mathscr{M}_b = -6$, $\mathscr{M}_c = -4$, $\mathscr{M}_{I\,II} = 22$, $\mathscr{M}_{I\,II'} = -2$ cm^{-1}. The latter two density functions show the effect of translationally equivalent interactions. As shown in (C), a broad density function, consistent with the experimental result, can be obtained within the framework of the simple Frenkel approach. Note that the ordinate scale changes at 300 units.

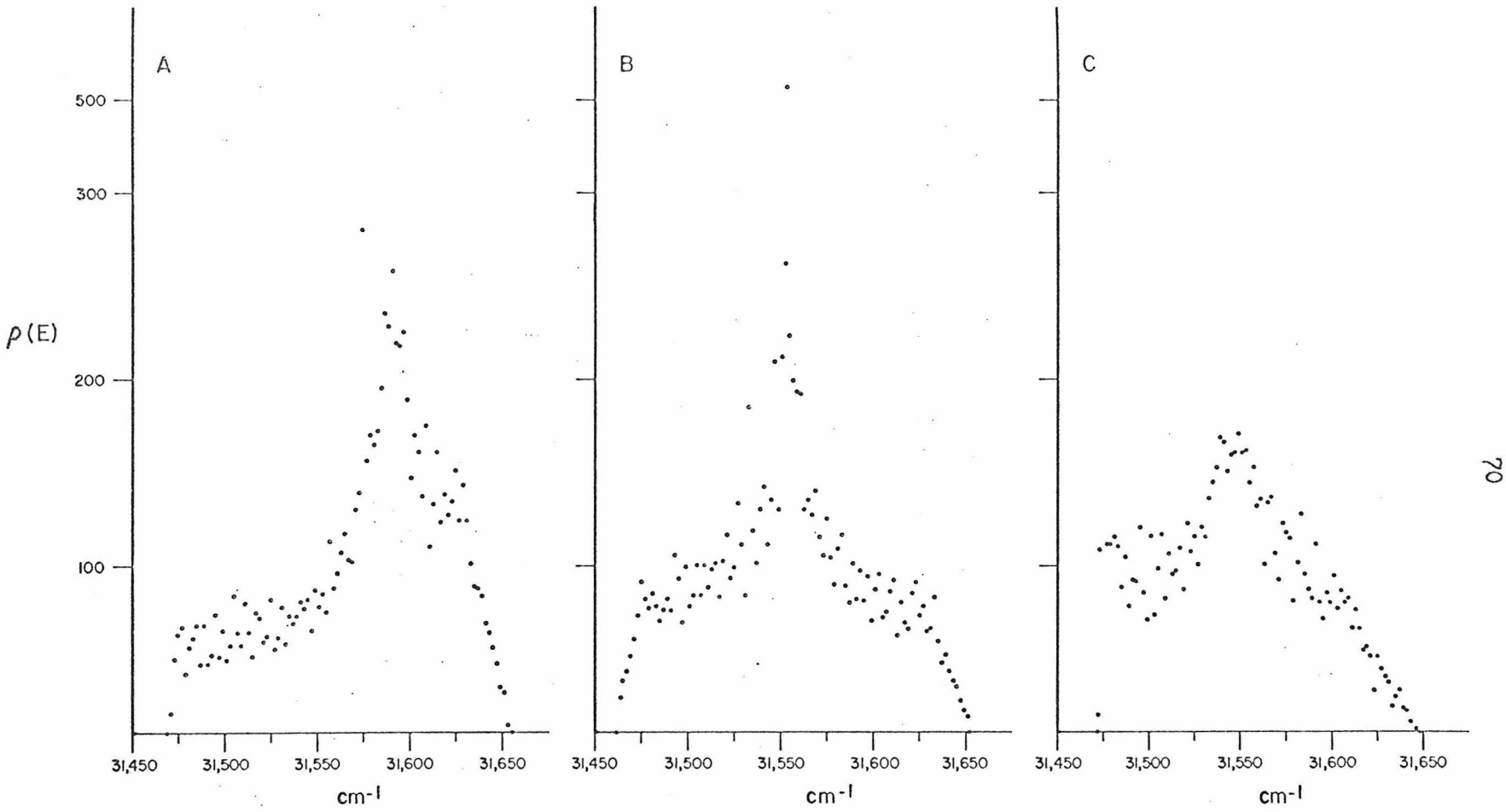
A
B
C
ρ(E)
500
300
200
100
31,450
31,500
31,550
31,600
31,650
cm-1

PART II

The Exciton Band Structure of the $^1B_{2u}$ State of Crystalline Naphthalene by the Variation of Energy Denominators Method Using Isotopic Substitution

I. INTRODUCTION

Mixed molecular crystals provide theoretically and experimentally tractable systems for studying the properties of molecular aggregates. Crystals made by isotopic substitution are of special interest because the intermolecular interactions or force fields often are invariant to the substitution. Consequently, observations made on these mixed crystal systems provide information not only about the interactions in the mixed crystal but also about those in the pure crystal.

The present work utilizes various deuterated naphthalenes in isotopic mixed crystal experiments. Spectroscopic observations are made to determine the energy of the crystal states that correlate with the $^1B_{2u}$ state of the free naphthalene molecule. The spectral data are interpreted in terms of a one-particle Green's function, and information is obtained about the gas-to-crystal energy shifts, the intermolecular interactions in the crystal, and the complete exciton band structure of the crystal. An independent experimental evaluation of the recently determined band structure therefore is provided. It is also of interest to compare these new results with theory, especially with respect to the applicability of multipole expansions, configuration interaction with charge transfer states, and the Green's function description of mixed crystals.

II. THEORY

A. Exciton Structure in Pure Molecular Crystals

Recent papers have summarized the application of group theory[1] and the development of Frenkel exciton theory[2] for molecular crystals. Most important for the present discussion are the role of individual excitation exchange interactions in the theory and the concept of "the ideal mixed crystal level".

The energy of the electronic transition from the crystal ground state to the $\underset{\sim}{k}^{\text{th}}$ component of the α^{th} branch of the f^{th} exciton band is given by[2]

$$E^{f\alpha}(\underset{\sim}{k}) = \bar{\epsilon} + \Delta + L^{f\alpha}(\underset{\sim}{k}) + w(k) , \qquad (1)$$

where $\bar{\epsilon}$ is the transition energy between the ground state and a given excited state (f) in the free molecule. The Δ term is called the site shift and includes all static interactions that lead to the gas-to-crystal shift in the transition energy. The resonance interactions and the exciton band structure are given by $L^{f\alpha}(\underset{\sim}{k}) + w(\underset{\sim}{k})$ where $\underset{\sim}{k}$ is the reduced wave number vector. Here $L^{f\alpha}(\underset{\sim}{k})$ is the first-order k-dependent energy and $w(\underset{\sim}{k})$ results from higher-order mixing of the $f\alpha^{\text{th}}$ exciton state with other exciton states. The transition energy in a hypothetical crystal with no excitation exchange interactions is therefore equal to $\bar{\epsilon} + \Delta$. This energy is the "center-of-gravity" of the exciton band and is termed the ideal mixed crystal level.

A number of theoretical papers[3] have attempted to describe the interactions responsible for exciton effects in molecular crystals. Silbey, et al.[3b] have shown that the splitting and polarizations of the Davydov components in naphthalene can be fit to a parameterized theory where only a higher-order charge-transfer contribution is taken to be non-zero. However, a wide range of exciton effects in the lowest singlet state of naphthalene, beyond the simple Davydov splitting, can be understood by assuming $w(\underset{\sim}{k})$ to be small and letting $L^{f\alpha}(\underset{\sim}{k})$ be the dominant $\underset{\sim}{k}$-dependent term in Eq. (1). In fact, except for the polarizations, which must arise from a second-order mixing of states, not necessarily related to the exciton splittings, it appears that the first singlet state of the naphthalene crystal can be considered an isolated Frenkel exciton state.

For the case of naphthalene, neglecting $w(\underset{\sim}{k})$ and translationally equivalent interactions skew to the crystallographic axes,[4] one has,

$$L^{f\alpha}(\underset{\sim}{k}) = L^{f}(\underset{\sim}{k}) + a_{II}^{\alpha} L^{f}_{I\,II}(\underset{\sim}{k}) , \qquad (2)$$

where $f = {}^1B_{2u}$; α = A, B, and $a_{II}^{\alpha} = +1, -1$ from the C_2 interchange group. The L's are sums of excitation exchange matrix elements $\mathcal{M}_{ij}$ modulated by $e^{i\underset{\sim}{k}\cdot\underset{\sim}{r}_{ij}}$, $\underset{\sim}{r}_{ij}$ being the vector from site $\underline{i}$ to site $\underline{j}$ in the crystal. $L^{f}(\underset{\sim}{k})$ contains $\mathcal{M}_{ij}$ for translationally equivalent $\underline{i}$ and $\underline{j}$, while $L^{f}_{I\,II}(\underset{\sim}{k})$ contains the $\mathcal{M}_{ij}$ for interchange equivalent $\underline{i}$ and $\underline{j}$. The magnitude of $L^{f}_{I\,II}(\underset{\sim}{k})$ determines the energy difference between the two branches of the exciton band. $L^{f}(\underset{\sim}{k})$ determines the displacement of the mean of

these branches from the ideal mixed crystal level. For example, in the case of $\underset{\sim}{k} = \underset{\sim}{0}$, the Davydov splitting is $2L^{f}_{I\,II}(\underset{\sim}{0})$ and the displacement of the mean of the Davydov components from the ideal mixed crystal level is $L^{f}(\underset{\sim}{0})$. This displacement at $\underset{\sim}{k} = \underset{\sim}{0}$ is termed the translational shift since it is caused by interactions between translationally equivalent molecules.

While $L^{f}_{I\,II}(\underset{\sim}{0})$ can be evaluated from the Davydov splitting, no experimental evaluation of the site shift Δ or the translational shift $L^{f}(\underset{\sim}{0})$ in naphthalene has been available. The entire exciton band structure[5] and the perturbation shifts of guest levels observed in isotopic mixed crystals discussed in this paper permit such an evaluation. Consequently the intermolecular interactions between translationally equivalent and interchange equivalent molecules can be compared. These experimental data (the total exciton band structure, the site shift, the translational shift, and the transition energies of isotopic guests) serve as stringent new criteria with which to evaluate theoretical descriptions of the $^{1}B_{2u}$ exciton band in crystalline naphthalene. This paper will show that none of the past theoretical calculations[3] of the intermolecular exciton interactions is in sufficient agreement with the experimental data to establish confidence in the model upon which it is based.

B. Energy Levels of Mixed Molecular Crystals

The use of isotopic mixed crystals has long been recognized as a powerful technique for the evaluation of intermolecular interactions or force fields in crystals.[6] A fundamental theory of the energy states of crystal defects has been described by Koster and

Slater[7] and explicitly summarized by Rice and Jortner.[8] The application of this Green's function formalism to the general molecular crystal already has been considered by Merrifield[9] and Takeno.[10] An independent approach has been developed by Rashba and Broude,[11] and by Rashba.[12] These general conclusions have been illustrated further by Craig and Philpott,[3c] and by Body and Ross,[3d] who applied the Green's function formalism to isotopic mixed crystals of benzene and naphthalene. The application of this theory, however, requires that the dispersion relation or density-of-states function for the exciton band be known. Thus, the key to the description of the energy levels in benzene and naphthalene mixed crystals is the density-of-states function.[5]

The theoretical formalism used for the understanding of excited states of mixed crystals in terms of the band structure is now summarized. The general Hamiltonian of a mixed molecular crystal can be written as

$$\mathcal{H} = \sum_p H_p + \sum_i h_i + \sum_{p>m} \sum V_{pm} + \sum_p \sum_i v_{pi} + \sum_{i>j} \sum \nu_{ij} \qquad (3)$$

where H_p = the Hamiltonian of the host molecule at site $\underline{p}$.

h_i = the Hamiltonian of the guest molecule at site $\underline{i}$.

V_{pm} = the intermolecular potential between host molecules at sites $\underline{p}$ and $\underline{m}$.

v_{pi} = the intermolecular potential between the host molecule at site $\underline{p}$ and the guest molecule at site $\underline{i}$.

ν_{ij} = the intermolecular potential between guest molecules at sites $\underline{i}$ and $\underline{j}$.

Note that $\underline{p}$, $\underline{m}$ and $\underline{i}$, $\underline{j}$ run over mutually exclusive sets, i.e., $\underline{p}$ and $\underline{m}$ only run over the sites occupied by host molecules, and $\underline{i}$ and $\underline{j}$ only run over the sites occupied by guest molecules.

Experimental conditions often can be chosen to simplify this equation. For example, for isotopic mixed crystals, the intermolecular terms might be assumed to be equal, i.e., $V_{pm} = v_{pi} = \nu_{ij}$. By using very dilute mixed crystals, a Hamiltonian involving only one guest may be applicable. Under these experimental conditions the Hamiltonian becomes

$$\mathcal{H} = \mathcal{H}^0 + \mathcal{H}' = \sum_{p \neq i} H_p + \sum_{p>m} \sum V_{pm} + h_i , \qquad (4)$$

where the summations are now over $\underline{\text{all}}$ crystal sites; $\mathcal{H}^0$ is the Hamiltonian of the pure crystal; and $\mathcal{H}'$ is the perturbation, $h_i - H_i$.

The basic problem is to find the eigenvalues and eigenvectors of $\mathcal{H}$ in a representation[3c] based on either localized excitation wavefunctions or the one-site exciton functions. It is only from the approximate Hamiltonian in Eq. (4) that the simple Green's function,

$$V = \left\{ \sum_i \frac{D(E_i)}{E' - E_i} \right\}^{-1} , \qquad (5)$$

is obtained. Eq. (5), which results from the simultaneous homogeneous equations, expresses the relationship between the energy

V of a dilute isotopic guest in an ideal mixed crystal to its energy E′ in the real mixed crystal. The normalized density-of-states function $D(E_i)$ is given by $N^{-1}\rho(E_i)\Delta E_i$, where $\rho(E_i)$ is the absolute density-of-states function that gives the number of exciton states in the band in the unit interval ΔE_i at E_i, and N is the total number of states in the band. The zero of energy for this equation is the ideal mixed crystal level of the host.

The denominator of Eq. (5) can be expanded in a power series provided $|E'| > |E_i|$. The numerators in this expansion are just the successive moments of the density-of-states function. Consequently Eq. (5) becomes

$$V = \left\{ \frac{1}{E'} \sum_{n=0}^{\infty} \frac{S_n}{E'^n} \right\}^{-1}, \tag{5a}$$

where the n^{th} moment $S_n = \sum_i D(E_i)E_i^n$. The second moment of the density-of-states function is a measure of the individual excitation exchange interactions since $S_2 = \sum_j \mathscr{M}_{ij}^2$. This relationship was pointed out by Body and Ross[3d] and is valid whether the series expansion converges rapidly or not.

When $|E'| \gg |E_i|$, the series expansion does converge rapidly and can be truncated after the second moment. By substituting $V + \delta$ for E′ and using the binomial theorem, the second-order perturbation formula of Nieman and Robinson[6c] is obtained[3d]

provided $|V| \gg |\delta|$. Alternatively, it is required by perturbation theory that the off-diagonal matrix elements be much smaller than the energy denominator. In this approximation the quasiresonance shift δ of the guest level is given by

$$\delta \approx \frac{S^2}{V} \equiv \frac{4\beta^2}{V} . \tag{6}$$

Consequently β, a measure of the excitation exchange interactions, can be evaluated by varying the energy denominator and experimentally determining δ in each case. Since the transition energy E of a guest, referred to the ground vibronic state of the crystal, is

$$E = \bar{\epsilon} + \Delta + \delta , \tag{7}$$

where the quantities all refer to the guest molecule, $4\beta^2$ can be calculated from the guest transition energies for any two guest-host systems:

$$4\beta^2 = \frac{(E_2 - E_1) - (\bar{\epsilon}_2 - \bar{\epsilon}_1)}{V_2^{-1} - V_1^{-1}} . \tag{8}$$

This approach is not expected to be a good approximation for isotopic mixed crystals of naphthalene because the criteria ($|E'| \gg |E_i|$ and $|V| \gg |\delta|$) for rapid convergence of the series expansions are not met. The relationship between the energy parameters E', E, V, δ and the ideal mixed crystal level of the host $\bar{\epsilon} + \Delta$ is shown in Fig. 1.

Equation (5) in its most general form can be used for naphthalene to relate the total density of states and the ideal mixed crystal level of the guest to the actual transition energy of the guest, providing of course the $D(E_i)$ is known. Figures 2-5 illustrate this relationship for some different density functions. The summation

in Eq. (5) was carried out in 1 cm^{-1} intervals over the entire exciton band. The determination of the density functions is discussed in Ref. 5.

Figure 2 illustrates the trivial case where $L^{f\alpha}(\underset{\sim}{k}) = w(\underset{\sim}{k}) = 0$. The density of states is a delta function at the ideal mixed crystal level. All moments except the zeroth vanish, and E' always equals V.

The density of states shown in Fig. 3 arises when the excitation exchange interactions between translationally equivalent molecules are small. The resulting E' vs V curve (solid line) deviates from the 45° line of Fig. 1, but approaches it asymptotically. For $-40 < V < 55$ cm^{-1}, no guest bound state arises; that is, the guest state lies inside the host band and increasingly is mixed with the host exciton states as V approaches zero. The data points are experimental values (see Sec. IV. D.).

The corresponding plots for the case of transition octopole-octopole coupling are shown in Fig. 4. This Figure is analogous to Figs. 1 and 5 of Ref. 3c, pp. 605, 611, except that our Fig. 4 is based on the 95 °K, rather than the room temperature crystal structure. Exciton band levels for both temperatures are given in Table I of Ref. 3c. When the room temperature crystal structure is used, better agreement between experiment and theory is obtained for $V > 0$ but not for $V < 0$.

The density-of-states function obtained from band-to-band transitions[5] is shown in Fig. 5 along with the guest energies obtained from this function.

C. Relationship to Experimental Data

It is apparent from Figs. 2-5 that discussions of the exciton band structure of mixed molecular crystals can be conveniently classified as (1) very shallow guests ($V \lesssim \frac{1}{2}$ bandwidth), (2) shallow guests ($V \gtrsim \frac{1}{2}$ bandwidth), and (3) deep guests ($V \gg \frac{1}{2}$ bandwidth). The subclassifications (a) isolated guests and (b) aggregated guests must be considered for finite guest concentrations.

The present paper presents experimental data only for the case 2a, applicable for dilute mixed crystals where V is sufficiently large to produce a bound state separated from the band of energy levels. These data can be related to the crystal band structure by the above theoretical formalism. Some experimental data for this classification are already present in the literature, but tabulations of these data contain many errors, e.g., around half the entries and references for Table X.1, p. 472 of Ref. 8 are incorrect. Conceptual errors involve the determination of V, the energy denominator in the perturbation problem. This problem is discussed in Sec. IV.C. The available data are re-tabulated in Tables I and II with the correct energy denominators along with new data obtained in our own laboratory on other isotopic mixed crystals of naphthalene. These new data were obtained to compare shifts of guest

levels lying both above and below the exciton band of the host. This comparison provides an excellent evaluation of the asymmetry in the density function (compare the examples in Figs. 2-5) and of configuration interaction with higher crystal states, e.g., charge transfer states (Sec. IV. G.).[13] Additional experimental data have also been obtained for classifications (1a), (1b), (2b)[14] and (3b)[15] and will be the subject of future papers.

An interesting theoretical and experimental question concerns the nature of the exciton band in the presence of small perturbations [small V, classification (1)]. As the perturbation V approaches zero the crystal energy levels must approach those of the pure crystal. Consequently for small values of V there should be little difference between the electronic states and spectra of the mixed and pure crystals. This point has been discussed by Craig and Philpott.[3c] For some intermediate values of V, virtual bound states of the exciton may be found that are reminiscent of the virtual bound states of electrons in alloys.[16]

III. EXPERIMENTAL

All spectra were obtained photographically using a 150 W Xe arc lamp and the third order of a 600 line/mm Bausch and Lomb grating (212 × 157 mm) blazed at 17°27′ in a 2-m Czerny-Turner mount. Eastman recrystallized naphthalene and Merck, Sharp and Dohme deuteronaphthalenes were purified by zone-refining and potassium fusion.[17] This technique reduces the concentration of

spectroscopically active impurities to less than one part in 10^7. The isotopic purity of the deuteronaphthalenes is 98%. In general, to avoid contact with oxygen after purification, the crystals were grown in quartz cells with optically flat windows 10-20μ apart. Thermal contact with the liquid helium bath during the spectroscopic experiment was assured either by introducing an atmosphere of helium gas or by breaking the cell open under the liquid helium.

The $^1B_{2u} \leftarrow {}^1A_{1g}$ absorption was observed in the following crystals: $C_{10}H_8$; α-$DC_{10}H_7$; β-$DC_{10}H_7$; $C_{10}D_8$; 0.0001%, 0.1% and 1% $C_{10}H_8$ in $C_{10}D_8$; 0.1% and 1% α-$DC_{10}H_7$ in $C_{10}D_8$; 0.1% and 1% β-$DC_{10}H_7$ in $C_{10}D_8$; 3% $C_{10}D_8$ in $C_{10}H_8$; 1% and 10% $C_{10}D_8$ in α-$DC_{10}H_7$; and 1% and 10% $C_{10}D_8$ in β-$DC_{10}H_7$. Corresponding data for $C_{10}H_8$ in β-$D_4C_{10}H_4$, $C_{10}H_8$ in α-$D_4C_{10}H_4$, and β-$D_4C_{10}H_4$ in $C_{10}H_8$ are available in the literature.[18] The measured transition energies are tabulated in Tables I and II. Sharp lines (the ac Davydov components and guest transitions below the band) could easily be measured with a precision comparator (Fred C. Hensen Co., Pasadena, California) to the cited precision in all crystals. In the thinnest crystals of the highest quality, the b-Davydov components could be measured reproducibly to this same precision. Generally, however, the uncertainty in the latter measurement was 5-10 cm^{-1} due to the large linewidth. These broad lines could

be measured most accurately from a highly magnified (50×) microdensitometer (Joyce-Loebel Model E12 MK III) tracing of the absorption with a superimposed iron arc standard. The limited accuracy in systems containing β-$DC_{10}H_7$ arises because of atypical amounts of chemical impurities present in this isotope. These impurities produce a general broadening of the β-$DC_{10}H_7$ Davydov components. Reproducibility was evaluated for the mixed and neat crystals of $C_{10}H_8$ and $C_{10}D_8$ by growing crystals (1) of various thicknesses in quartz cells and between compressed quartz discs, (2) from hexane solution on water, and (3) by sublimation. Consequently, the accuracy for these systems is somewhat higher than for the others. The Davydov splittings in $C_{10}H_8$ and $C_{10}D_8$ generally agree, within the uncertainty of the measurements, with values reported in the literature.[19] The sharpest lines were observed in crystals grown by sublimation in an inert atmosphere and mounted between thin, flexible Teflon washers. Supporting pressure was applied to the Teflon and not directly to the crystal.

IV. RESULTS AND DISCUSSION

In this Section the approximations that lead to Eq. (5) are examined, the dependence of guest levels on the variation in energy denominator is considered, and the magnitude of the translational shift and site shift is obtained. In view of the new experimental data, configuration interaction with ion-pair states, the multipole expansion of the intersite potential, the second moment approximation, and the origin of the exciton interactions are discussed.

A. Isotope Effects on the Intermolecular Interactions

In pure molecular crystals the obvious feature of the exciton band is the Davydov splitting or factor group splitting between $\underset{\sim}{k} = \underset{\sim}{0}$ components. As shown in Table I, the constancy of the Davydov splitting in all the deuterium isotopes indicates that any deuterium effect on the exciton interaction lies within the experimental uncertainty. Since the Davydov splitting equals $2L^{f}_{I\,II}(\underset{\sim}{0}) = 8M_{I\,II}(\underset{\sim}{0})$ where $M_{I\,II}(\underset{\sim}{0})$ is the sum of excitation exchange integrals over all the different interchange equivalent molecules, $M_{I\,II}(\underset{\sim}{0}) = +19.75 \pm 0.38\ cm^{-1}$ for naphthalene and $+20.38 \pm 0.63\ cm^{-1}$ for deuteronaphthalene. The sign of $M_{I\,II}$ is determined within the $\underset{\sim}{C}_2$ interchange convention.[1,2] In view of the above discussion, $L^{f}(\underset{\sim}{0}) = 2[M_a(\underset{\sim}{0}) + M_b(\underset{\sim}{0}) + M_c(\underset{\sim}{0})]$ is assumed also to be independent of isotopic substitution ($M_a(\underset{\sim}{0})$ is the sum of excitation exchange integrals over all translationally equivalent molecules along the $\underset{\sim}{a}$ crystallographic axis). The conclusion that resonance excitation exchange interactions are independent of deuteration is significant and underlies the conclusions formed in the following Sections.

The observed gas-to-crystal shift in the pure electronic transitions of molecular crystals such as naphthalene is the sum of a site shift and a translational shift. The absence of a deuterium effect on the site shift is important if isotopic guest-host systems are to be used in determining the magnitude of the exciton interactions. Since the excitation exchange interactions are independent of deuteration to within approximately 5%, the energy separation

$\Delta E^{f\alpha}(\underset{\sim}{k})$ for the corresponding $\underset{\sim}{k}$ levels in all the isotopes should be just equal to the difference in the gas-phase energies plus the difference in the site shift terms. $\Delta E^{f\alpha}(\underset{\sim}{k})$ is determined from the mean values of the Davydov components for $C_{10}H_8$ and $C_{10}D_8$ to be $115 \pm 4\ cm^{-1}$. The possible 5% isotope effect on the Davydov splitting cancels when the mean values are used in this evaluation, since this isotope effect shifts the Davydov components in opposite directions. Craig, et al.,[20] give the gas phase energy difference as $118.0\ cm^{-1}$; hence the difference in the site shift terms is $3 \pm 4\ cm^{-1}$. The isotope effect on the site shift is therefore negligible within experimental accuracy.

It should be noted that the dependence of the site shift on isotopic substitution in mixed crystals of benzene[21] was detected by the anomalous behavior of guest levels lying above the host exciton band relative to those lying below the band. This fact is especially clear for the case of m-$C_6D_4H_2$ as a guest in C_6D_6 and C_6H_6. If the site shift were independent of isotopic substitution, then the guest transition energy E (m-$C_6D_4H_2$ in C_6H_6) should be greater than E (m-$C_6D_4H_2$ in C_6D_6) because of the relative directions of the perturbation shift by the host exciton band, but the converse was found experimentally. For the present case of naphthalene no such anomalous behavior was detected. In fact, the experimental results

are just those predicted from the experimentally determined[5] density-of-states function. The conclusion then is that within experimental accuracy both the dynamic excitation exchange interactions and the static "site shift" interactions are independent of isotopic substitution in neat and isotopically mixed crystals of naphthalene.

B. Validity of the Single Guest Hamiltonian

The applicability of Eq. (5) also depends upon the assumption that the energy levels of a dilute mixed crystal (ca. 1% guest) can be described by a Hamiltonian for an infinitely dilute mixed crystal (only one guest). The validity of this assumption is not obvious for crystals with a guest-to-host ratio of 1:100, but fortunately this assumption can be tested by observing the guest transition over a range of concentrations. The pertinent data are given in Table IV.

The principal effect of guest-guest interactions at these low concentrations is line broadening. The apparent slight shift in transition energies as shown by $C_{10}H_8$ in $C_{10}D_8$, where a ratio of $1/10^6$ is assumed to be infinitely dilute, is taken to be within the experimental accuracy of the data. Both a shift and a broadening are predicted by the theoretical work of Craig and Philpott,[3c] who show in effect that the guest states in the crystal comprise a very narrow energy band. The width and energy of this band is concentration dependent. It should be noted that concentration dependent broadening and apparent shifts in line position also may arise from inhomogeneous sources.

For the guest-host systems where the guest level is at a higher energy than the host exciton band, a guest concentration of 1% to 10% is necessary to observe the guest transition. This apparent loss of intensity by the guest has been called the Rashba effect[6b] and generally indicates that $\underset{\sim}{k} \neq \underset{\sim}{0}$ states extend beyond the $\underset{\sim}{k} = \underset{\sim}{0}$ state. However, for "above the band" guests, intensity changes due to mixing with phonon states also should be considered.

C. Determination of the Energy Denominator

In using Eq. (5) or the second-order perturbation formula[6c] Eq. (6) to relate guest levels to the exciton band structure it is necessary to know the value of the energy denominator V. The correct value corresponds to the energy difference between the ideal mixed crystal levels of the guest and host. Unfortunately the experimental values given for some isotopic mixed crystals of naphthalene in the literature are not correct due to a poor choice in the method of determining the ideal mixed crystal levels. This method due to Broude[22a] consists of first locating the center of a vibronic band and then subtracting the vibrational quantum. The approach has been widely accepted[22b] in spite of the fact it was criticized some time ago in its application to benzene.[6c] Even though the method is valid in principle when used critically, it is questionable for both naphthalene and benzene because of (1) uncertainties in the assignment of the components of the vibronic exciton band, (2) the

existence of quasi-resonance effects from multi-exciton states,[23] and (3) uncertainties in the appropriate value of the vibrational quantum. In fact, quasi-resonance shifts in the vibronic levels of isotopic guest-host naphthalene systems are very apparent from the quoted data in Ref. 18b. When applied to $C_{10}H_8$[3e] Broude's method locates the ideal mixed crystal level at 31, 520 cm^{-1}. If this value were correct, the quasi-resonance shift for a $C_{10}H_8$ guest in $C_{10}D_8$ would be in the wrong direction (the guest shifted 23 cm^{-1} towards the host). In addition, the energy denominator (97 cm^{-1}) given in Table II of Ref. 18b for the naphthalene-deuteronaphthalene system differs from the value of 87 cm^{-1} obtained from the difference between 31, 629 and 31, 542 cm^{-1} due apparently to a typographical or arithmetic error. It should be noted that recently Broude, Rashba, and Sheka[24] have revised the above analysis and now correctly locate the ideal mixed crystal level near the mean of the Davydov components (Sec. IV. E.).

Because of the invariance in naphthalene of the excitation exchange interactions to isotopic substitution, the correct energy denominators can be obtained from differences in the mean values of the Davydov components as previously discussed. These data are given in Table II. Because of the invariance of the site shift these energy differences are identical within experimental accuracy to the differences in the gas phase transition energies.

D. Guest Energies and Quasiresonance

Introducing a defect into the crystal, even by isotopic substitution, destroys the translational and interchange symmetry. Near-resonance interactions are still expected, and their magnitude depends upon the magnitudes of the resonance interactions relative to the energy denominator.[25] The concomitant energy shift has been called[6c] the quasi-resonance shift δ. That the second-order perturbation formula [Eq. (6)] for δ is not a good approximation for the $^1B_{2u}$ state of crystalline naphthalene can be seen by comparing the values of $4\beta^2$ obtained from Eq. (8) for the guest-host systems given in Table II. The second-order calculation predicts values of $4\beta^2$ ranging from 1200 cm^{-2} to 2600 cm^{-2} for the isotopic mixed crystals given in Table II. The value of β, which is supposed to be constant, therefore ranges from 17-26 cm^{-1} using this approximate theory.

To improve upon this approximation, Body and Ross[3d] derived an approximate expression for the energy levels of guests that depends upon both the second moment and extrema of the exciton band. Their calculated energies compared unfavorably with experimental results because the incorrect energy denominators were used. When the correct energy denominators are used, the translational shift, exciton band maximum, and guest energies derived from their Eq. (33) are in better agreement with the experimental data.

Alternatively, the Green's function formalism can be used. Guest energies calculated from Eq. (5) for guests of varying energy denominators are given in Figs. 2-5 for the different density-of-states functions. The zero of energy in these Figures is the ideal mixed crystal level of the host, i.e. where E′ of Eq. (5) is zero. To plot the experimental transition energies using this zero of energy, the guest transition energy is measured relative to the lower Davydov component (ac-polarized) of the host. Call this energy λ. Since the lower Davydov component is known to be the lowest level of the exciton band,[3d, 5] the determination of λ fixes the experimental guest level in Figs. 3-5. Values for E_{ac}, E, V, and λ are given in Table III. Guest transition energies predicted from the theoretical curves (E′ vs V) in Figs. 3-5 also are given in Table III. The predicted transition energy E for a particular value of V is obtained by combining the theoretical value of λ and the experimental transition energy of the ac Davydov component.

By comparing the experimental points with the computed curves in Figs. 3-5 or the experimental with the calculated transition energies in Table III, it is found that the experimental guest levels for the several isotopic mixed crystals of naphthalene agree reasonably well with the levels predicted from the experimental density-of-states function (Fig. 5) but disagree by comparison with the levels predicted from the density-of-states function for the octopole model (Fig. 4). The deviations between experiment and theory in Fig. 5 are probably due to uncertainties in the experimental

function caused by phonon contributions to the band ⟷ band transitions.[5] Note that the density function derived when the translationally equivalent interactions are approximately zero (Fig. 3) also gives a reasonable fit to the experimental data, especially for guest levels below the band. Of all the density functions considered, however, only the band structure of Fig. 5 correctly predicts no bound state for the case of $C_{10}H_8$ in β-$D_4C_{10}H_4$.

E. Translational Shift

The density-of-states function determined from the band-band transition has been independently verified by the experiments reported here. Assuming that this experimental function is accurate, the ideal mixed crystal level lies 81 cm^{-1} above the ac-polarized Davydov component, e.g. it occurs at 31, 556 cm^{-1} for $C_{10}H_8$. Since the mean of the Davydov components is 31, 554 ± 2 cm^{-1}, the translational shift $L^f(\underset{\sim}{0})$ is -2 ± 2 cm^{-1}. An uncertainty of ~10 cm^{-1} should be introduced in $L^f(\underset{\sim}{0})$ to account for errors in the density-of-states function. Even though $L^f(\underset{\sim}{0}) \equiv M_a + M_b + M_c \approx 0$, the components M_a, M_b and M_c individually must not be very small since this leads to a density function like that shown in Fig. 3. This function disagrees with the experimental observation of the density function, being too strongly

peaked in the middle. It is therefore concluded that the excitation exchange integrals between translationally equivalent molecules are fairly large ($\lesssim 10$ cm^{-1}) but of differing sign such that their sum $L^f(\underset{\sim}{0})$ is approximately zero.

The symmetrical positions of guest levels lying above and below the exciton band of the host provide evidence, independent of the density-of-states function, that $L^f(\underset{\sim}{0}) \approx 0$. Table V gives the energy levels of the $C_{10}H_8$-$C_{10}D_8$ mixed crystals. The $C_{10}H_8$ guest level is as far (45.2 cm^{-1}) from the lower $C_{10}D_8$ Davydov component as the $C_{10}D_8$ guest level is (46 cm^{-1}) from the upper $C_{10}H_8$ Davydov component. This symmetry is also found in the other isotopic mixed crystals and would not arise if $L^f(\underset{\sim}{0})$ were large and the exciton band were highly asymmetric.

F. Site Shift

Since the ideal mixed crystal level is at 31,556 ± 10 cm^{-1} for $C_{10}H_8$, the site shift (Δ) can now be evaluated.

$$\bar{\epsilon} + \Delta = 31,556 \pm 10 \text{ cm}^{-1}$$

$$\bar{\epsilon} = 32,020 \text{ cm}^{-1} \text{ (Ref. 20)}$$

$$\Delta = -464 \pm 10 \text{ cm}^{-1}.$$

The sublimation energy[26] for crystalline naphthalene is 5354 cm^{-1}, so the crystal binding energy is approximately 9% larger in the excited state than in the ground state. These values can be compared with the corresponding values of $\Delta = -248$ cm^{-1}, a sublimation energy of 3800 cm^{-1}, and an increase in binding of 6% for benzene.[2]

G. Configuration Interaction with Charge Transfer States

In a paper on the electronic states of crystalline naphthalene by Silbey, Jortner, Vala, and Rice,[3b] it is claimed that dipole-dipole, octopole-octopole, and exchange interactions including crystal-field mixing and three-center integrals do not account for the observed exciton spectra. These authors therefore suggest that mixing with charge transfer states is responsible for the observed Davydov structure. To explain the Davydov splitting in the $^1B_{2u}$ state solely in terms of the charge transfer perturbation, the lowest charge transfer state is located by these authors at 300 to 500 cm^{-1} above the neutral exciton state in both[27] naphthalene and deutero-naphthalene.

The perturbation of isotopic guest levels now is considered in view of this charge transfer model. In order to explain the quasi-resonance shifts in isotopic mixed crystals of naphthalene, the perturbing state must be lower in energy than the "above the band" guests, and higher than the "below the band" guests. This conclusion is based on the fact that for corresponding guest-host systems, e.g. $C_{10}H_8$ in $C_{10}D_8$ and $C_{10}D_8$ in $C_{10}H_8$, the guest levels are further apart in energy in the crystal than in the gas phase. Thus the most effective perturbing state must lie between the two guests. Since the behavior of all the mixed crystal systems is consistent with this conclusion, the phenomenon seems to demand a coincidence

of the perturbing state and the neutral exciton state in all the isotopic crystals studied. This extreme requirement indicates that the perturbing state is the neutral exciton state and not the charge-transfer states. If the charge transfer states, as presented in Ref. 3b, were the source of the perturbation, the transition energies of such guests should be closer together in the crystal than in the gas phase.[13] In fact, there is other experimental evidence[28] that the charge-transfer states are at much higher energies than used in Ref. 3b and probably are not the source of the Davydov splitting or quasi-resonance shifts.

In the above discussion, it is assumed that if the charge-transfer state is the sole origin of the Davydov splitting, it is also the sole origin of quasi-resonance shifts. It should be emphasized that this discussion is qualitative and involves the difference between predicted and actual directions of second-order energy shifts and does not involve the magnitude of these shifts. It should be noted that the higher-order perturbation of the guest level by the charge-transfer state acting through the neutral exciton state has been neglected. A preliminary estimate of this term shows that it does not affect the conclusions of the preceding paragraph. However, a thorough calculation of the charge-transfer perturbation in isotopic mixed crystals would be of interest in this regard.

In principle a density-of-states function is obtainable from a given charge-transfer model for the exciton band. However, it cannot be extracted from Ref. 3b since no matrix elements involving charge transfer between translationally equivalent molecules were calculated. Therefore no comparison can be made between this model and the observed density function, although such a comparison would be of tremendous value.

H. Accuracy of the Multipole Expansion

Craig and Philpott[3c] recently extended the work of Craig and Walmsley[3a] by calculating the structure of the entire exciton band using empirically derived transition octopole moments as parameters. They also discuss the energy levels of isotopic mixed crystals of naphthalene in terms of this calculated band structure. Rice and coworkers,[3b] however, have shown from ab initio calculations that the actual transition octopole moments for the $^1B_{2u}$ state of naphthalene are much smaller than the empirical ones needed to fit the Davydov splitting. It is therefore of interest to examine experimentally Craig and Philpott's calculated band structure. Criteria now available for the evaluation of the theoretical model are the density-of-states function, the energies of guest levels, and the translational shift.

As discussed in Sec. IV. D., the experimental density function and guest energies disagree with the predictions of the octopole model. From Table I of Ref. 3c for the 95°K crystal structure, a

translational shift of -33 cm^{-1} can be derived. The calculated Davydov splitting for this crystal structure is 206 cm^{-1}. The translational shift may be scaled by the factor (160/206) that brings the calculated and observed pure electronic Davydov splittings into agreement. The scaled theoretical value of -26 cm^{-1} should be compared with the experimental value of -2 ± 10 cm^{-1}. These discrepancies in the density function, guest energies, and translational shift most likely reflect the inadequacy of the octopole model. This inadequacy probably arises from the fact that the molecular size is comparable to the intermolecular separation in crystalline naphthalene; consequently, the multipole expansion should converge only slowly.

J. Nature of the Intermolecular Exciton Interactions

We have seen that in its present form neither the charge-transfer model nor the transition-octopole model is capable of explaining the wide variety of experimental data now available on the lowest singlet exciton of crystalline naphthalene. Several possible approaches are available for removing this dilemma. The charge-transfer or octopole theories may be re-parameterized possibly to give better fit with the extended experimental data. Higher terms in the multipole expansion may be included. Alternatively the charge distribution in each molecule may be approximated by a number of point charges or point multipoles.[29] The charge-transfer perturbation also can be combined[30] with

the multipole expansion, and, as briefly discussed in Ref. 5, exciton-phonon coupling may be included. The latter approaches have the advantage (or disadvantage) of introducing additional parameters. It should be emphasized in this regard that future theoretical descriptions of these crystal states must be consistent not only with the Davydov splitting ($\underset{\sim}{k} = \underset{\sim}{0}$) and intensities but also with the location of all $\underset{\sim}{k}$ states and the energy levels of isotopic mixed crystals.

On the other hand, a new approach may be suggested by the result reported here, which indicates that the sum of the pair-wise interactions between translationally equivalent molecules is small even though the individual terms are fairly large. This fact implies, although it does not require, the presence of two different "types" of interactions, of opposite sign, whose importance depends upon relative molecular orientations in the crystal. This idea is supported by the naphthalene crystal structure. For some sets of molecules, the molecular planes are perpendicular to the intermolecular axis. For these molecules one would expect π-electron terms to dominate the intermolecular interactions. For other sets, the molecular planes are parallel to the intermolecular axis. For these molecules, carbon-hydrogen and hydrogen-hydrogen intermolecular distances are only 2 or 3 Å. It therefore seems that sigma electrons could play a more substantial role than previously imagined.[31] Intramolecular σ-π mixing has received considerable attention,[32] and may well be important for these exciton interactions.[13]

V. SUMMARY

The general and specific goals of this work as well as the experimental results are summarized below.

1. These experiments are part of a general study of the properties of molecular aggregates. In particular they focus on the nature of the energy states and the distance and orientation dependence of the individual intermolecular interactions in aromatic molecular crystals such as benzene and naphthalene.
2. The exciton splitting in the lowest excited singlet state of crystalline naphthalene has been explained by two different theories: one involving coupling through transition octopole moments, the other involving interaction with low-lying charge-transfer states. Additional experimental data are provided here to compare with the predictions of these theories. Neither is in complete agreement with the new experimental results. It is proposed that the electron density on hydrogen atoms should be considered explicitly in describing the intermolecular exciton interactions.
3. These experiments also served to evaluate the suitability of the Green's function technique for describing the states of mixed molecular crystals. The results for naphthalene isotopic mixed molecular crystals are consistent with the assumptions underlying the simple Green's function formulation. In particular, the invariance of the intermolecular interactions to isotopic

substitution and the realization of the dilute mixed crystal limit are of central importance.

4. An independent test of the experimentally determined density-of-states function is provided. The present results are consistent with that band structure.

5. The following values were found for the gas-to-crystal shifts and splittings described in the theoretical section.

   a. Site shift $\Delta = -464 \pm 10\ cm^{-1}$.

   b. Translational shift $L^{f}(\underset{\sim}{0}) = -2 \pm 10\ cm^{-1}$.

   c. Interchange splitting $L^{f}_{I\,II}(\underset{\sim}{0}) = +80 \pm 4\ cm^{-1}$.

   These quantities along with the density-of-states function and the transition energies of isotopic guests are stringent criteria with which to evaluate theoretical descriptions of the excited electronic states of molecular crystals.

ACKNOWLEDGMENT

A manuscript that discusses the energy levels of isotopic mixed crystals of naphthalene and benzene in terms of our then-unpublished experimental density-of-states functions was received from B. Sommer and J. Jortner during the final writing of this paper.

REFERENCES

1. R. Kopleman, J. Chem. Phys. 47, 2631 (1967).
2. E.R. Bernstein, S.D. Colson, R. Kopelman, and G.W. Robinson, J. Chem. Phys. 00, 0000 (1968), "Electronic and Vibrational Exciton Structure in Crystalline Benzene."
3. (a) D.P. Craig and S.H. Walmsley, Mol. Phys. 4, 113 (1961); (b) R. Silbey, J. Jortner, M.T. Vala, and S.A. Rice, J. Chem. Phys. 42, 2948 (1965); (c) D.P. Craig and M.R. Philpott, Proc. Roy. Soc. (London) 290A, 583 (1966); ibid. 290A, 602 (1966); ibid. 293A, 213 (1966); (d) R.G. Body and I.G. Ross, Aust. J. Chem. 19, 1 (1966).
4. S.D. Colson, R. Kopelman, and G.W. Robinson, J. Chem. Phys. 47, 27 (1967); 47, 5462 (1967).
5. S.D. Colson, D.M. Hanson, R. Kopelman, and G.W. Robinson, J. Chem. Phys. 48, 2215 (1968).
6. (a) G.L. Hiebert and D.F. Hornig, J. Chem. Phys. 20, 918 (1952); (b) E.I. Rashba, Opt. Spektrosk. 2, 568 (1957); (c) G.C. Nieman and G.W. Robinson, J. Chem. Phys. 39, 1298 (1963); (d) D.P. Craig, Advances in Chemical Physics, I. Prigogine, Ed. (Interscience Publishers, Inc., New York, 1964), Vol. VIII., p. 27.
7. G.F. Koster and J.C. Slater, Phys. Rev. 95, 1167 (1954); ibid. 96, 1208 (1954).
8. S.A. Rice and J. Jortner, Physics and Chemistry of the Organic Solid State, D. Fox, M.M. Labes, and A. Weissberger,

Eds. (Interscience Publishers, Inc., New York, 1967), Vol. III., Chap. 4.

9. R.E. Merrifield, J. Chem. Phys. 38, 920 (1963).

10. S. Takeno, J. Chem. Phys. 44, 853 (1966).

11. V.L. Broude and E.I. Rashba, Sov. Phys.—Solid State 3, 1415 (1962).

12. E.I. Rashba, Sov. Phys.—Solid State 4, 2417 (1963).

13. These experimental data and conclusions were discussed at the Twentieth Symposium on Molecular Structure and Spectroscopy (The Ohio State University, Columbus, Ohio, 1966), Abstract W2.

14. D.M. Hanson and G.W. Robinson, unpublished results.

15. R. Kopelman, unpublished results.

16. C. Kittel, Quantum Theory of Solids (John Wiley and Sons, Inc., New York, 1963), Chap. 18.

17. D.M. Hanson and G.W. Robinson, J. Chem. Phys. 43, 4174 (1965).

18. (a) E.F. Sheka, Opt. Spectrosc. 10, 360 (1961); (b) V.L. Broude, E.I. Rashba, and E.F. Sheka, Sov. Phys.—Dokl. 6, 718 (1962); (c) E.F. Sheka, Akad. Nauk SSR Isvestiia Ser. Fiz. 27, 503 (1963); α-$D_4C_{10}H_4$ = 1, 4, 5, 8-tetradeuteronaphthalene; β-$D_4C_{10}H_4$ = 2, 3, 6, 7-tetradeuteronaphthalene.

19. (a) D.S. McClure and O. Schnepp, J. Chem. Phys. 23, 1575 (1955); (b) A. Zmerli, J. Chim. Phys. 56, 387 (1959); (c) Ref. 18; (d) D.P. Craig, L.E. Lyons, and J.R. Walsh, Mol. Phys. 4, 97 (1961); (e) V.L. Broude, Opt. Spectrosc.,

Suppl. II, 25 (1963); (f) E.F. Sheka, Opt. Spectrosc. 17, 25 (1964); (g) P. Sarti-Fantoni, Mol. Cryst. 1, 457 (1966).

20. (a) D.P. Craig, J.M. Hollas, M.F. Redies, and S.C. Wait, Phil. Trans. Roy. Soc. (London) A253, 543 (1962); (b). D.P. Craig and J.M. Hollas, ibid. p. 569.

21. S.D. Colson, J. Chem. Phys. 48, 3324 (1968).

22. (a) V.L. Broude, Sov. Phys.—Usp. 74, 577 (1961); (b) Refs. 3d; 8, p. 472; 18b; 19e; and 19f.

23. (a) R. Kopelman, J. Chem. Phys. 44, 3547 (1966); (b) J. Jortner and S.A. Rice, J. Chem. Phys. 44, 3364 (1966).

24. V.L. Broude, E.I. Rashba, and E.F. Sheka, Phys. Stat. Sol. 19, 395 (1967).

25. (a) Ref. 6c; (b) D.P. Craig and T. Thirunamachandran, Proc. Roy. Soc. A271, 207 (1963).

26. K.L. Wolf and H.Weghofer, Z. Physik Chem. 39, 194 (1938).

27. R. Silbey, J. Jortner, M. Vala, and S.A. Rice, Mol.Cryst. 2, 385 (1967).

28. M. Pope and J. Burgos, Mol. Cryst. 1, 395 (1966).

29. (a) F. London, J. Phys. Chem. 46, 305 (1942); (b) E.F. Haugh and J.O. Hirschfelder, J. Chem. Phys. 23, 1778 (1955).

30. W.L. Greer, S.A. Rice, and J. Jortner, "A Reexamination of the Theoretical Interpretations of the Spectra of Crystalline Benzene and Naphthalene," unpublished manuscript.

31. (a) Ref. 3b; (b) R. Silbey, J. Jortner, and S.A. Rice, J. Chem. Phys. 42, 1515 (1965).

32. (a) H.M. McConnell, J. Chem. Phys. 24, 764 (1956); (b) A.D. McLachlan, H.H. Dearman, and R. Lefebvre, J. Chem. Phys. 33, 65 (1960); (c) J.M. Schulman and J.W. Moskowitz, J. Chem. Phys. 43, 3287 (1965).

TABLE I. Pure electronic energies in cm^{-1} for the $^1B_{2u}$ states of neat crystalline naphthalene and some deuteronaphthalenes.

Crystal	$E_{\underset{\sim}{ac}}$	$E_{\underset{\wedge}{b}}$	ΔE_D	$\overline{E}$	$\Delta\overline{E}$
$C_{10}H_8$	31,475.2 ± 0.3	31,633 ± 3	158 ± 3	31,554.1 ± 1.7	0
α-$DC_{10}H_7$	31,486 ± 1	31,651 ± 5	165 ± 6	31,568.5 ± 3	14 ± 5
β-$DC_{10}H_7$	31,500 ± 5	31,660 ± 10	160 ± 15	31,580 ± 7	26 ± 9
α-$D_4C_{10}H_4$[a]	31,526 ± 2	31,684 ± 2	158 ± 4	31,605 ± 2	51 ± 4
β-$D_4C_{10}H_4$[a]	31,549 ± 2	31,707 ± 2	158 ± 4	31,628 ± 2	74 ± 4
$C_{10}D_8$	31,587.7 ± 0.3	31,751 ± 5	163 ± 5	31,669.4 ± 2.7	115.3 ± 4.4

[a] V.L. Broude, E.I. Rashba, and E.F. Sheka, Sov. Phys.--Dokl. 6, 718 (1962).

$E_{\underset{\sim}{ac}}$ and $E_{\underset{\wedge}{b}}$, the transition energies of the Davydov components.

$\Delta E_D = E_{\underset{\wedge}{b}} - E_{\underset{\sim}{ac}}$, the Davydov splitting.

$\overline{E} = \frac{1}{2}(E_{\underset{\wedge}{b}} + E_{\underset{\sim}{ac}})$, the mean of the Davydov components.

$\Delta\overline{E} = \overline{E}_j - \overline{E}_{H_8}$, the isotope shift relative to $C_{10}H_8$.

TABLE II. Guest states in isotopic mixed crystals of naphthalene.

Guest	Host	V	E
$C_{10}H_8$	$C_{10}D_8$	-115 ± 4	31,542.5 ± 0.2
$C_{10}D_8$	$C_{10}H_8$	+115 ± 4	31,679 ± 2
α-$DC_{10}H_7$	$C_{10}D_8$	-101 ± 6	31,550.7 ± 0.5
$C_{10}D_8$	α-$DC_{10}H_7$	+101 ± 6	31,687 ± 2
β-$DC_{10}H_7$	$C_{10}D_8$	- 89 ± 10	31,555.7 ± 0.5
$C_{10}D_8$	β-$DC_{10}H_7$	+ 89 ± 10	31,694 ± 8
$C_{10}H_8$	β-$D_4C_{10}H_4$	- 74 ± 4	31,530 ± 2[a]
β-$D_4C_{10}H_4$	$C_{10}H_8$	+ 74 ± 4	not observed[b]
$C_{10}H_8$	α-$D_4C_{10}H_4$	- 51 ± 4	31,519 ± 2[a]

[a] V.L. Broude, E.I. Rashba, and E.F. Sheka, Sov.Phys.--Dokl. 6, 718 (1962).

[b] E.F. Sheka, Akad. Nauk SSR Isvestiia Ser.Fiz. 27, 503 (1963).

V = zero-order energy difference ($\overline{E}_{guest} - \overline{E}_{host}$, see Sec.IV.C.).

E = transition energy of the crystal state that correlates with the guest.

TABLE III. Comparison of experimental and calculated guest energies. [a]

Host	E_{ac} [b]	Guest	V	Experimental		Fig. 2 Band Structure		Octopole Band Structure		Experimental Band Structure	
				E [c]	λ [d]	E [e]	λ [f]	E [e]	λ [f]	E [e]	λ [f]
$C_{10}D_8$	31,587.7 ± 0.3	$C_{10}H_8$	-115 ± 4	31,542.5 ± 0.2	- 45.2 ± 0.5	31,541	- 47	31,555	- 33	31,542	- 46
$C_{10}D_8$	31,587.7 ± 0.3	α-$DC_{10}H_7$	-101 ± 6	31,550.7 ± 0.5	- 37.0 ± 0.8	31,552	- 36	31,566	- 22	31,552	- 35
$C_{10}D_8$	31,587.7 ± 0.3	β-$DC_{10}H_7$	- 89 ± 10	31,555.7 ± 0.5	- 32.0 ± 0.8	31,556	- 32	31,573	- 15	31,563	- 25
β-$D_1C_{10}H_1$	31,549 ± 2	$C_{10}H_8$	- 74 ± 4	31,530 ± 2	- 19 ± 4	31,530	- 16	31,542	- 7	31,536	- 13
α-$D_1C_{10}H_1$	31,526 ± 2	$C_{10}H_8$	- 51 ± 4	31,519 ± 2	- 7 ± 4	31,521	- 5	no bound state		31,525	- 1
$C_{10}H_8$	31,475.2 ± 0.3	$C_{10}D_8$	+115 ± 4	31,679 ± 2	+203.8 ± 2.3	31,693	+218	31,719	+235	31,687	+212
α-$DC_{10}H_7$	31,486 ± 1	$C_{10}D_8$	+101 ± 6	31,687 ± 2	+201 ± 3	31,692	+206	31,709	+223	31,687	+201
β-$DC_{10}H_7$	31,500 ± 5	$C_{10}D_8$	+ 89 ± 10	31,694 ± 8	+194 ± 13	31,698	+198	31,713	+213	31,693	+193
$C_{10}H_8$	31,475.2 ± 0.3	β-$D_1C_{10}H_1$	+ 74 ± 4	not observed	—	31,663	+188	31,677	+202	no bound state	

[a] Energies are in cm^{-1}.

[b] Coincident with the bottom edge of the band.

Values taken from Table I.

[c] Values taken from Table II.

[d] λ(experimental) = E (experimental) - E_{ac}.

[e] E (calculated) = E_{ac} + λ(calculated).

[f] λ (calculated), see Sec. IV. D.

V = zero order guest-host energy difference (see Sec. IV.C.).

E = transition energy of the guest.

E_{ac} = transition energy of the lower Davydov component.

λ = E - E_{ac}.

TABLE IV. The effect of concentration on guest levels.

Guest	Host	Guest:Host	Optical Path	Transition Energy	Linewidth
$C_{10}H_8$	$C_{10}D_8$	$1:10^2$	$\sim 10\mu$	$31,542.5 \pm 0.2\ cm^{-1}$	$3.5\ cm^{-1}$
		$1:10^6$	2 cm	$31,541.6 \pm 0.5\ cm^{-1}$	$<1.0\ cm^{-1}$
α-$DC_{10}H_7$	$C_{10}D_8$	$1:10^2$	$\sim 10\mu$	$31,550.7 \pm 0.2\ cm^{-1}$	$3.5\ cm^{-1}$
		$1:10^3$	$\sim 10\mu$	$31,550.2 \pm 0.5\ cm^{-1}$	$2.5\ cm^{-1}$
β-$DC_{10}H_7$	$C_{10}D_8$	$1:10^2$	$\sim 10\mu$	$31,555.7 \pm 0.5\ cm^{-1}$	$3.5\ cm^{-1}$
		$1:10^3$	$\sim 10\mu$	$31,555.5 \pm 0.5\ cm^{-1}$	$2.5\ cm^{-1}$

TABLE V. Guest and host energy levels (in cm^{-1}) for the $C_{10}H_8$-$C_{10}D_8$ mixed crystals.

System	E	$E_{\underset{\sim}{ac}}$	$E_{\underset{\wedge}{b}}$	$E - \begin{cases} E_{\underset{\sim}{ac}} \\ E_{\underset{\wedge}{b}} \end{cases}$
$C_{10}H_8$ in $C_{10}D_8$	31,542.5 ± 0.5	31,587.7 ± 0.3	31,751 ± 5	-45.2 ± 0.8
$C_{10}D_8$ in $C_{10}H_8$	31,679 ± 2	31,475.2 ± 0.3	31,633 ± 3	46 ± 5

FIG. 1. The relationship between the energy parameters E', E, V, δ and $\overline{\epsilon} + \Delta$. Note that the distances are not drawn to scale.

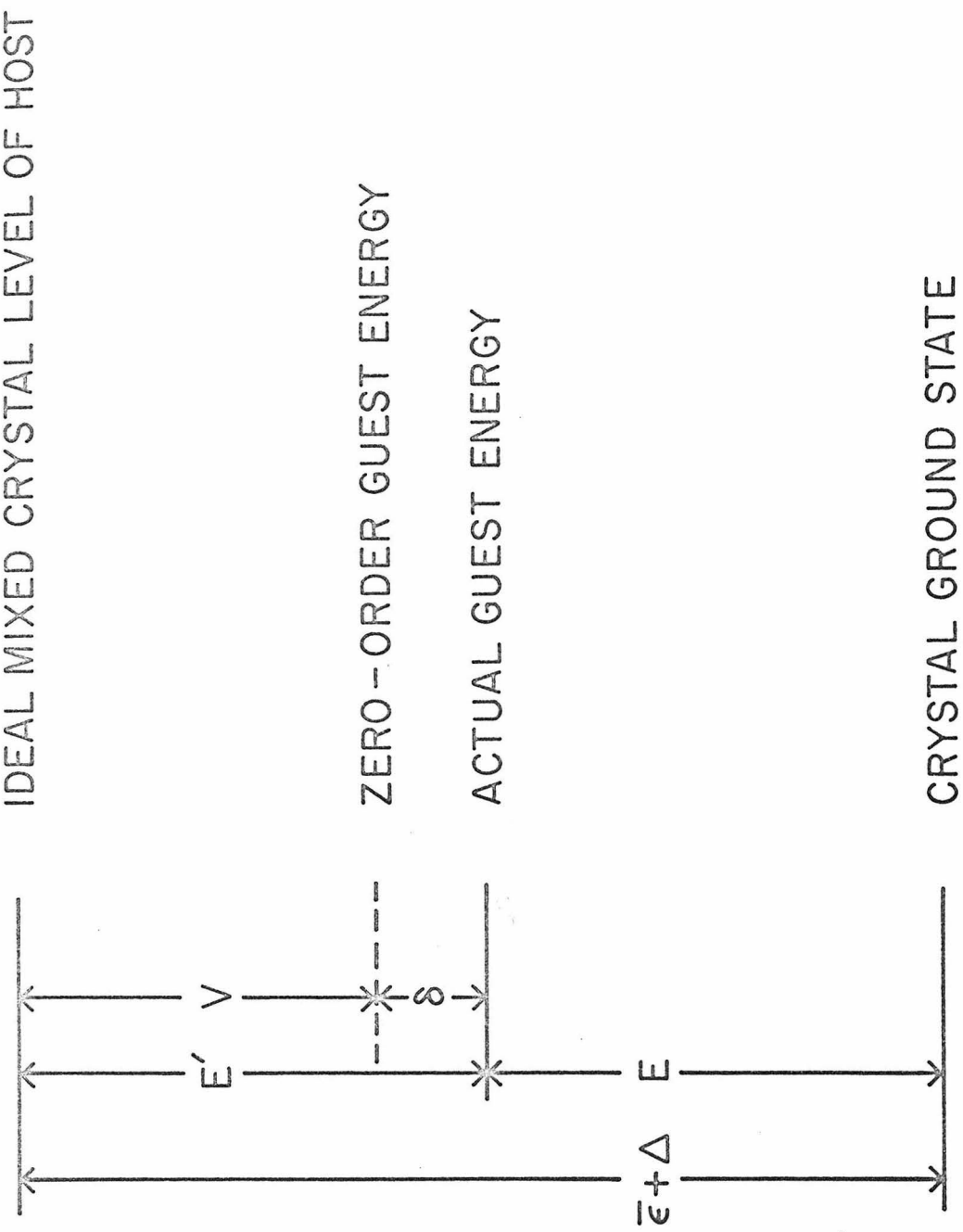
IDEAL MIXED CRYSTAL LEVEL OF HOST
ZERO-ORDER GUEST ENERGY
ACTUAL GUEST ENERGY
CRYSTAL GROUND STATE
V
δ
E'
E
ε̄+Δ

FIG. 2. The normalized density function $D(E_i)$ and the dependence of the guest energy E' on the zero-order guest-host energy difference V when the intermolecular exciton interactions are identically zero. Note that the vertical scale applies to both parts of these figures.

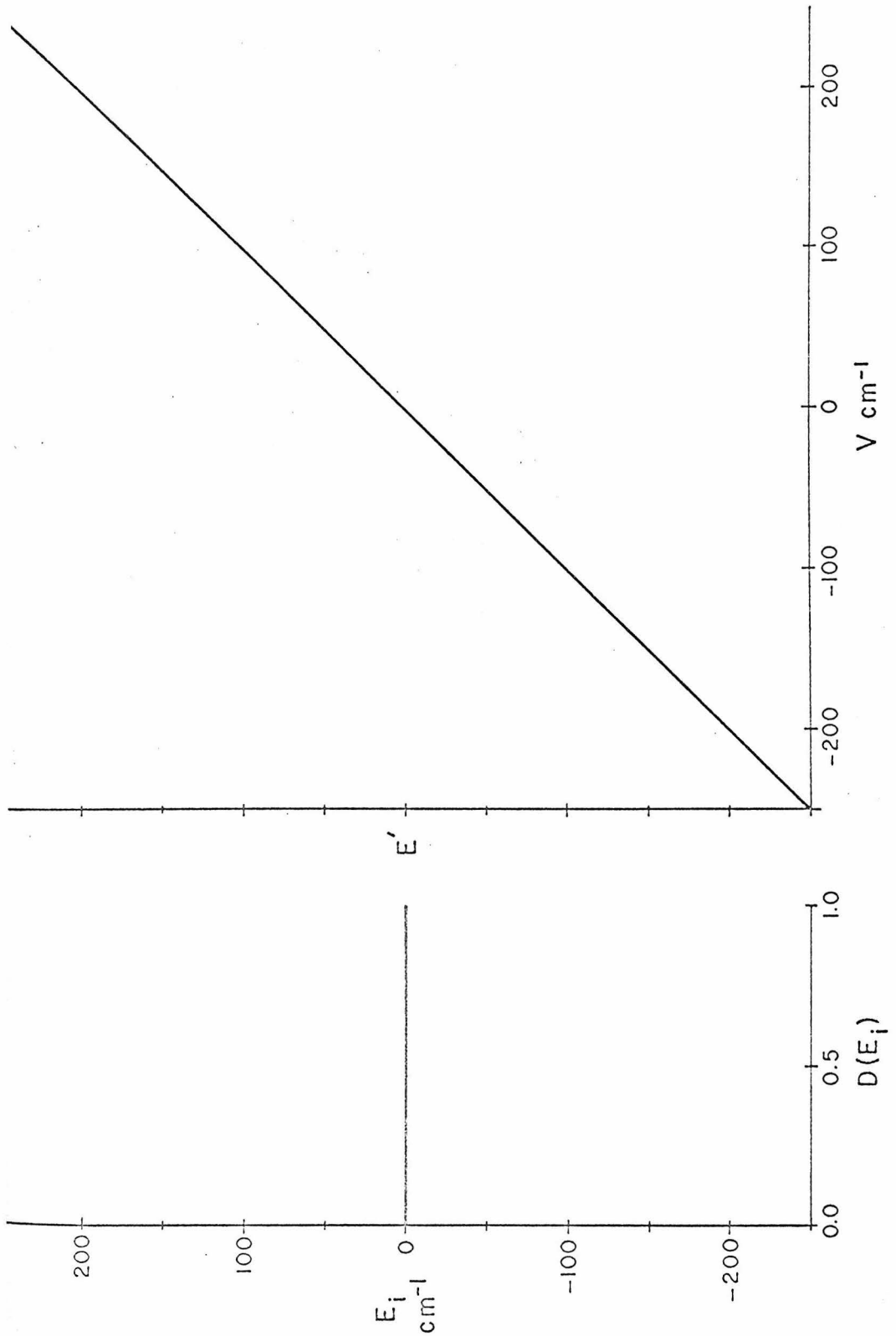
200
100
0
-100
-200
E_i cm^{-1}
0.0
0.5
1.0
$D(E_i)$
E'
200
100
0
-100
-200
V cm^{-1}

FIG. 3. The normalized density function $D(E_i)$ and the dependence of the guest energy E' on the zero-order guest-host energy difference V for the following excitation exchange integrals $\mathscr{M}_a = 2$, $\mathscr{M}_b = -1$, $\mathscr{M}_c = -1$, $M_{I\,II} = 22$, and $\mathscr{M}_{I\,II'} = -2\ cm^{-1}$, except that levels below the lower Davydov component are omitted since this component is known to lie at the bottom of the band.[3d, 5] The $\mathscr{M}$'s could be varied to give this result, but the overall change in the density function would be small.

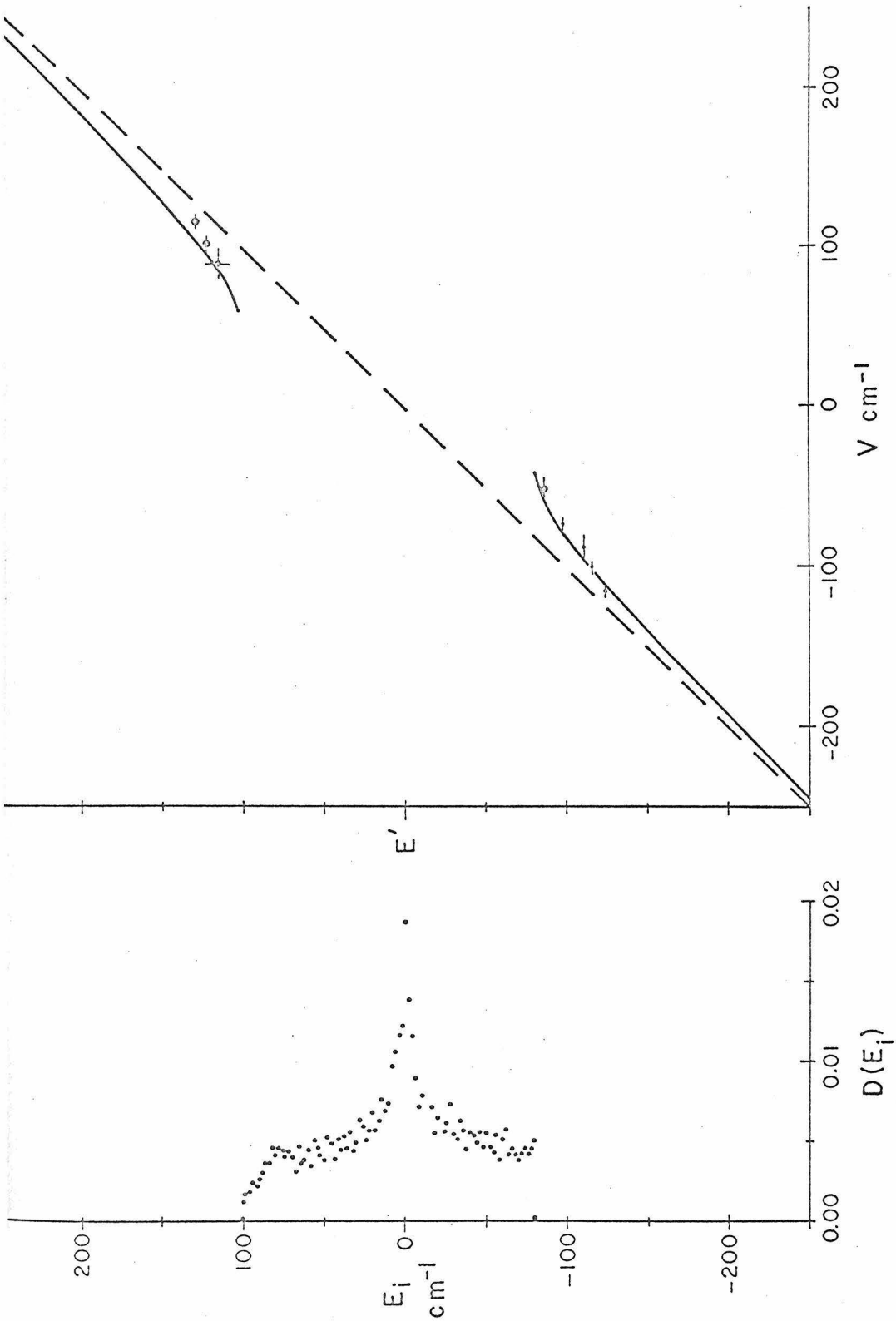
E'
V cm⁻¹
200
100
0
-100
-200
Eᵢ cm⁻¹
D(Eᵢ)
0.00
0.01
0.02

FIG. 4. The normalized density function $D(E_i)$ and the dependence of the guest energy E' on the zero-order guest-host energy difference V for a transition octopole interaction. The apparent shift of the experimental points in this figure relative to those in Fig. 3 is a result of the fact that the zero of energy ($E' = 0$) relative to the lowest Davydov component is different in the two instances.

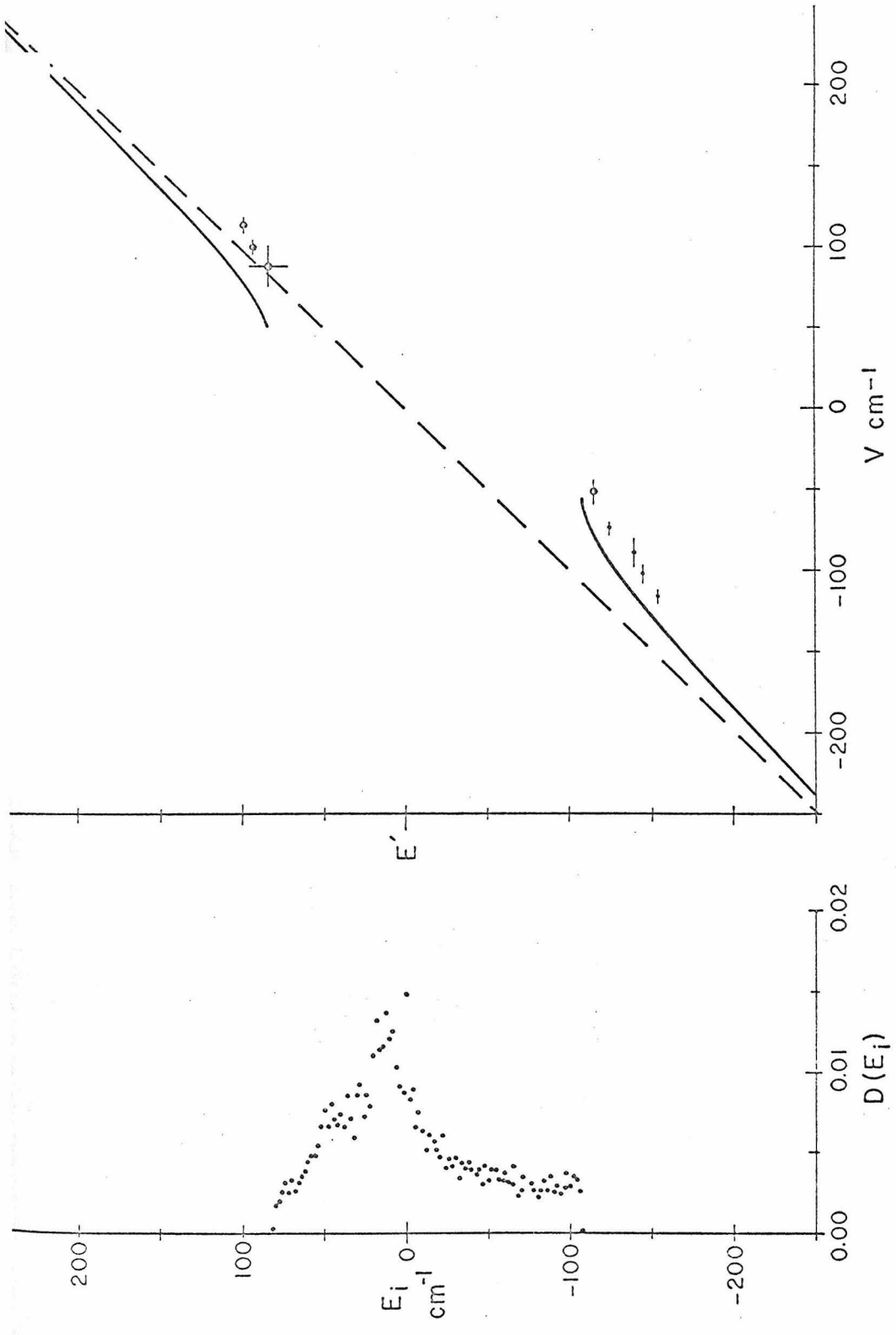
E´
V cm⁻¹
200
100
0
-100
-200
Eᵢ cm⁻¹
0.00
0.01
0.02
D(Eᵢ)

FIG. 5. The normalized density function $D(E_i)$ and the dependence of the guest energy E' on the zero-order guest-host energy difference V for the density-of-states function derived from the band ⟷ band transition spectra.

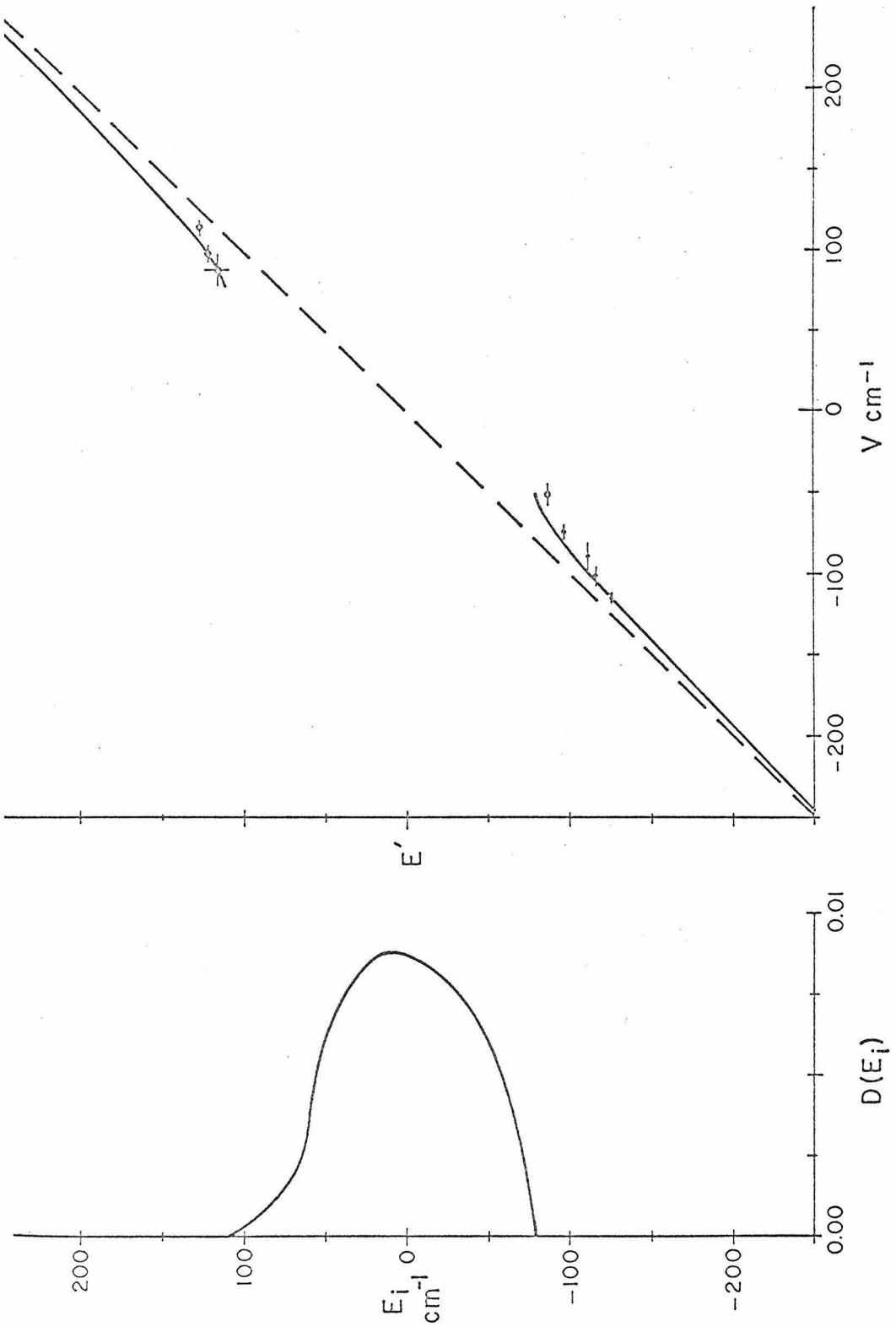
E'
V cm⁻¹
200
100
0
-100
-200
E_i cm⁻¹
D(E_i)
0.00
0.01

PART III

Resonance Pair Spectra of Crystalline Naphthalene

I. INTRODUCTION

Theoretical descriptions of the energy states of ideal crystals are quite common. Ideal crystals vary considerably but generally are restricted in dimension, composed of simple units, and void of lattice motion and defects including chemical and isotopic impurities, vacancies, interstitials, and similar structural faults. In spite of these obvious approximations the grosser properties of ideal crystals often are discovered in experimental investigations because the basic feature of a crystal, the coulombic force between electrons and nuclei, is represented accurately in the simple model. Much research effort is expended, however, to discover and explain the finer properties of solids, and matter in general, that deviate from the predictions of the idealized model.

For the lowest excited vibrational and electronic states of molecular crystals, the basic spectral features and details of the energy band structure are understood in terms of the Frenkel tight-binding model[1, 2] in which molecular states are the progenitors of crystal states. Even energy levels introduced by the presence of an isotopic impurity are described by an extension[3] of the Frenkel theory. In principle, this extension also can be used to describe the states of chemical impurities, structural defects, and associated concentration effects. However, electron-phonon coupling generally is neglected in the Frenkel theory even though the effect is considerable[4] above 77 °K.

The present paper extends the earlier research[3, 4] and reports the experimental observation of energy states produced by the aggregation of isotopic guests in naphthalene mixed crystals. The object of this research, besides providing information fundamental to knowledge of the organic solid state, is to evolve, by the close juxtaposition of experiment and theory, a good understanding of the properties of molecular aggregates. This knowledge is basic to understanding the liquid and biological states and may in the future be of significant technological importance.

The fundamental quantities in Frenkel exciton theory are the intermolecular excitation transfer matrix elements. These pairwise intermolecular interactions are responsible[1] for exciton mobilities and Davydov splittings as well as for the full exciton band structures of both neat[4] and mixed[3] molecular crystals. Such excitation exchange interactions also may contribute significantly to energy transfer in the gas and liquid phases.

The experiments reported here were designed to determine directly both the magnitudes and relative signs of these important quantities. Very high resolution spectra at 4.2 °K reveal fine structure in the electronic transitions of naphthalene mixed crystals.[5] Some of this structure corresponds to the resonance splitting of pairs of guest molecules in the host lattice. The individual positions of the molecules are assumed to be completely determined by the crystal structure in the excited as well as in the ground state. For the case of isotopic mixed crystals these positions are precisely

those of the pure crystal[6] provided the intermolecular interactions are independent of isotopic substitution.

The electronic transitions of such a resonance pair are expected to consist of doublets nearly symmetrically displaced around the corresponding transition of the "monomer" guest. The resonance interaction energy is just one-half the doublet splitting; the relative intensities of the doublet components are determined by the orientation in the crystal of the transition dipoles in the molecules that comprise the pair. For a pair of translationally equivalent guests, only a single absorption line would be observed since the out-of-phase transition moments cancel exactly. The allowed transition should have the same polarization properties as that for the isolated guest. Generally, for a pair of interchange equivalent[2, 7] guests, both transitions are allowed but with different polarization properties. For example, in naphthalene with space group $\underset{\sim}{C}^5_{2h}$, one line is polarized parallel to and the other perpendicular to the $\underset{\sim}{b}$ crystallographic axis. This polarization is the same as the polarization of the pure crystal Davydov components. Indeed, in an isotopic mixed crystal, the nearest-neighbor interchange equivalent resonance pair, neglecting quasiresonance effects, can be considered as an isolated naphthalene unit cell (Fig. 1).

In the Frenkel exciton model the Davydov splitting in crystalline naphthalene is $8\mathcal{M}_{12} + 8\mathcal{M}_{12'} + 8\mathcal{M}_{12''} + \cdots$, where $\mathcal{M}_{12}$ is the excitation exchange integral for the nearest-neighbor interchange equivalent molecules, $\mathcal{M}_{12'}$ is that for the next-nearest interchange

equivalent molecules, etc. Obviously in the ideal mixed crystal limit,[2] the corresponding resonance pair doublets will be split by $2\mathcal{M}_{12}$, $2\mathcal{M}_{12'}$, etc., the splittings decreasing as the separation between interchange equivalent molecules increases. The validity of the ideal mixed crystal limit of the Frenkel exciton model recently has been discussed for the isotopic mixed crystals of naphthalene.[3] For short-range interactions only the first few splittings are observable while an upper limit can be established for the rest. Similarly the $\mathcal{M}_a$, $\mathcal{M}_b$, $\mathcal{M}_c$, etc., terms that correspond to translationally equivalent pairs can be observed. These terms give the translational shift[2, 3] of the exciton band. The band structure therefore can be deduced completely from the resonance pair spectra, provided a large number of small terms do not dominate. The additional detailed information that this technique provides can be compared and contrasted with the indirect information on the intermolecular interactions derived from the Davydov splitting and experimental band structure of neat crystals, and from the quasi-resonance shifts of isotopic mixed crystals.

Some success in the study of resonance pair spectra has already been reported in a very preliminary way.[5, 8, 9] The results reported in this paper are for the lowest singlet and triplet state of $C_{10}H_8$ molecules in a $C_{10}D_8$ host. Non-isotopic mixed systems such as naphthalene in durene[8] deviate from the ideal mixed crystal limit. However, the spectra of resonance pairs in these systems are of interest because the guest-host energy interval is large thereby

decreasing quasiresonance effects and also revealing higher vibronic transitions of the resonance pairs. Measurements utilizing a series of host crystals and uniaxial stresses would permit the evaluation of the resonance interactions as a function of intermolecular separation and orientation. Such an investigation should clarify the quantum mechanical origin of these interactions. So far, neither transition dipole interactions, transition octopole interactions,[10] nor perturbations by charge transfer states[11] appear to account for all the existing experimental data.[3,4]

II. EXPERIMENTAL TECHNIQUES

A. Instrumentation

Two different series of experiments were carried out to characterize the spectral absorptions appearing in the region of the 0, 0 guest transition in dilute isotopic mixed crystals of naphthalene. The moderate resolution experiments employed a 2-m f/12 Czerny-Turner spectrograph equipped with a 600 line/mm Bausch and Lomb grating No. 33-53-27-52 (212 × 157 mm) blazed at 17°27'. As used in the third order, the resolving power and plate factor of this instrument are 50,000 and 2.4 Å/mm. The high resolution experiments employed a 3.4-m f/38 Jarrell-Ash Ebert spectrograph equipped with a 300 line/mm grating No. 35-00-90-78 (190 × 63 mm) blazed at 58.05°. As used in the eighteenth order, the theoretical resolving power and plate factor are 1,000,000 and 0.27 Å/mm. Generally a slit width of 30μ was used with the 2-m instrument and 50 to 100μ with the 3.4-m instrument.

In both series of experiments, absorption spectra were taken using a 200 W high pressure Xe arc lamp and Eastman Kodak type 103a-0 spectroscopic plates. In the moderate resolution experiments, the light was filtered with an aqueous cobalt chloride filter and a Corning 9863 glass filter to eliminate overlapping orders. In the high resolution experiments, the light was predispersed with a Bausch and Lomb 0.25-m high intensity monochromator and filtered with a Corning 9863 filter, a pyrex glass filter, and an

aqueous solution of H_2SO_4, $NiSO_4$, and $CoSO_4$ to give a total band pass of 70 Å.

Polarization measurements were made by placing one Glan-Thompson polarizing prism above another, with orientations differing by 90°, in front of the spectrograph slit. In this configuration light polarized parallel to the $\underset{\sim}{b}$-crystallographic axis of the sample only passed through the upper half of the slit, while light polarized perpendicular to the $\underset{\sim}{b}$-crystallographic axis only passed through the lower half of the slit.

The emission from an iron-neon hollow cathode standard[12] was photographed between these two spectra and served to calibrate the plate. Spectral line positions were measured with a precision comparator made by the Fred C. Hensen Company. Vacuum wavenumbers corresponding to the calculated wavelengths were obtained from the National Bureau of Standards' "Table of Wavenumbers."[13] Tracings of the photographic plates were made with a Jarrell-Ash Model 23-500 microphotometer.

High resolution phosphorescence spectra were photographed using the Jarrell-Ash instrument in the twelfth order. Front surface excitation of the crystal was provided by two 200 W high pressure Xe arc lamps filtered by dilute cobalt chloride solutions and Corning 9863 glass filters. A Corning 3387 filter was placed before the spectrograph slit to eliminate scattered light from the source. The best spectrum was obtained by exposing an Eastman Kodak 103a-0 plate for six h with the sample (1.4% $C_{10}H_8$ in $C_{10}D_8$) immersed in liquid helium.

B. Sample Preparation

Isotopic mixed crystals were prepared from Eastman recrystallized naphthalene and Merck, Sharp and Dohme deutero-naphthalene. Both isotopes had been extensively purified by potassium fusion and zone-refining.[14] Each isotope was purified separately because proton exchange occurs[15] during the fusion process. Different concentrations of $C_{10}H_8$ in $C_{10}D_8$ were obtained by weighing the amount of each isotope added to a pyrex tube suspended from an analytical balance. Different concentrations for any one set of experiments were obtained by successive dilution. The tube was attached to a high vacuum system with a $\frac{1}{2}$-in. Swagelok-Teflon ferrule fitting. After the sample was degassed and the system pumped down to 10^{-6} Torr, the sample tube was sealed and pulled from the vacuum manifold. Homogeneous samples were obtained by agitating the sample for 30-60 min in an oven held at 90 °C, ten degrees above the naphthalene melting point. The sample tubes were reattached to the vacuum system, and the naphthalene was sublimed through a break seal to the appropriate crystal growing cell.

Crystals were grown from the melt by slowly (0.05 in./h) lowering the cell through a temperature gradient into a dewar filled with either liquid nitrogen or 50 °C water. Two types of crystal growing cells were used. One consisted of quartz windows placed a specified distance apart; the other consisted of a 10-mm o.d. pyrex tube with a seeding tip. The crystals were removed from the pyrex crystal growing tubes, cleaved, oriented conoscopically,

and mounted for the spectroscopic experiment.
Crystals a few microns thick were grown by sublimation in an inert atmosphere and likewise mounted between thin Teflon washers in a brass ring. Supporting pressure was applied to the Teflon and not directly to the crystal. The samples were masked to assure that all transmitted light had passed through the crystal. During the spectroscopic experiment the samples were immersed in liquid helium in a conventional pyrex double dewar with a quartz tip.

The following series of crystals were examined in the moderate resolution experiments: sublimation crystals a few microns thick of 1.2%, 1.8%, 3.3%, and 5.0% $C_{10}H_8$; and crystals in 20μm, 100μm, 1 mm, 1 mm, 2 mm, and 1 cm thick optical cells at respective $C_{10}H_8$ concentrations of 1.2%, 1.2%, 1.2%, 0.10%, 0.50%, and 0.10%.

The following series of crystals were examined in the high resolution experiments: 1.2% and 0.10% $C_{10}H_8$ crystals in 1-mm thick optical cells; and 0.007%, 0.013%, 0.050%, 0.12%, 0.65%, and 1.40% $C_{10}H_8$ crystals that had been cleaved. The thicknesses of these crystals were 1.2 ± 0.2, 1.0 ± 0.1, 1.5 ± 0.1, 2.0 ± 0.3, 1.0 ± 0.1, and 1.6 ± 0.2 mm, respectively.

III. EXPERIMENTAL RESULTS

The experimental results are summarized in Fig. 2 and Tables I and II. For the simple system of dilute isotopic mixed crystals of naphthalene in deuteronaphthalene, 23 different absorption lines were observed where most naively only one due to the 0, 0 transition in the $C_{10}H_8$ guest is expected. In this section explanations for the fine structure are considered, and experiments that lead to an assignment of these spectral lines are discussed.

From the known intensity of the $C_{10}H_8$ transition, an estimate can be made of the concentration and path length needed (0.1%, 1 mm) to observe pairs of neighboring guest molecules in the host lattice. From this fact, the nonlinear concentration dependence, and the unique polarization characteristics as discussed earlier, the transitions due to such resonance pairs are readily identified.

In addition to the resonance pair transitions, transitions due to isotopic impurities are expected to be observed. The various partially deuterated naphthalenes present in $C_{10}D_8$ can be identified from the known 0, 0 transition energies. About 11% of the naphthalene contains one ^{13}C atom. The 0, 0 transition in $^{13}CC_9H_8$ is expected to lie at a slightly higher energy from the $C_{10}H_8$ transition and to be roughly an order of magnitude less intense.

Other spectral lines and splittings or apparent splittings may arise since any crystal is by no means perfect and homogeneous. Surface effects or surface states should be recognized by observations made on crystals of various thicknesses. Impurities or lattice

defects associated with impurities should be recognized from spectra of $C_{10}D_8$ crystals or mixed crystals as a function of purification. Strains, crystal twinning, and related effects should not give consistent results from one crystal to another, especially when the crystals vary in size, and method of growth and mounting.

A. Moderate Resolution Experiments

The absorption lines observed in the moderate resolution experiments are listed in Table I. No data on the concentration dependence of the intensity are available for some of the lines because these lines are unresolved, at the higher concentrations, from the broad intense absorption due to the monomer transition. The line designated in Table I as weak is only present in the more concentrated crystals and is not assigned. Although an accurate determination of intensities was not possible due to the poor resolution of these lines, it is clear that the intensity of the lines marked nonlinear decreases more rapidly than the intensity of the monomer line as the concentration is lowered.

The frequencies of the two monodeuteronaphthalene isotopes are assigned in agreement with earlier investigations.[3] The intensities of these lines varied with the sample due to the proton exchange reaction mentioned earlier. The transition at 31, 544.5 cm^{-1} is assigned to $^{13}CC_9H_8$ because of the expected 2 cm^{-1} shift from $C_{10}H_8$ and the fact that at low concentrations only these two transitions are present, the high energy line being about one-tenth as intense as the other.

Some of the lines are assigned to resonance pairs on the basis of their polarization and intensity behavior. The following experiment clearly shows the nonlinear intensity variation in the lines at 31, 526.7 and 31, 533.8 cm^{-1} relative to the line at 31, 519.5 cm^{-1}. Spectra of a 1-cm crystal containing 0.1% $C_{10}H_8$ and a 0.1-cm crystal containing 1.0% $C_{10}H_8$ were photographed. Monomer intensities should be constant in the two spectra; pair intensities and surface states involving $C_{10}H_8$ molecules should decrease by 1/10; and trimer intensities should decrease by 1/100. The spectra are shown in Fig. 3. It is found that the lines at 31, 526.7 and 31, 533.8 cm^{-1} are weaker in the 1-cm crystal while the line at 31, 519.5 cm^{-1} is unchanged. In fact in the 1.0-cm crystal all lines are about the same intensity while in the 0.1-cm crystal the higher energy pair is about a factor of 10 more intense than the lower energy line. From this experiment it is concluded that the two lines correspond to resonance pairs while the low energy line is neither a $C_{10}H_8$ surface state nor a $C_{10}H_8$ trimer, but most likely is a bulk lattice defect associated with $C_{10}H_8$ molecules. The line is not present in a 2-cm crystal of pure $C_{10}D_8$.

B. High Resolution Experiments

Representative high resolution spectra are shown in Fig. 1 and the spectral data given in Table II. The second column in Table II indicates the concentration at which an absorption was first observed in the ~1-mm crystals and is a rough measure of the intensity of that absorption. The observations here support the conclusions drawn from the moderate resolution spectra.

At the lowest concentration only the transitions due to $C_{10}H_8$ and $^{13}CC_9H_8$ are observed. The figure clearly shows the $^{13}CC_9H_8$ transition at the expected energy and intensity. Although three ^{13}C isomers are present, the corresponding transitions are unresolved. In the ac polarized spectrum of the 1.4% crystal in Fig. 1, the α- and β-deuteronaphthalene transitions are as intense as the $^{13}CC_9H_8$ transition in the 0.007% crystal. At these $C_{10}H_8$ concentrations, the naturally occurring isotopes are present in the same amount, i.e. in 0.007% $C_{10}H_8$ the concentration of $^{13}CC_9H_8$ is 8×10^{-4}% and in 1.4% $C_{10}H_8$ the concentration of $C_{10}H_7D$ is 9×10^{-4}%. This result supports the assignment of the $^{13}CC_9H_8$ transition, and the data leading to it are summarized[16] in Table III.

In the 0.12% crystal the transitions assigned as resonance pairs in the moderate resolution experiments begin to appear. Fig. 1 also shows that the $^{13}CC_9H_8$ absorption is no longer resolved at this concentration and that a diffuse b polarized absorption is developing in the region between the guest and host transitions.

In the 0.65% crystal both the monomer linewidth and the diffuse absorption increase. New lines appear at 31, 537.6, 31, 534.9, and 31, 531.4 cm^{-1}. The first two can reasonably be assigned to resonance pairs containing one $^{13}CC_9H_8$ molecule as this species is expected to appear at this concentration (3 times that for the ^{12}C-^{12}C pairs) and energy ($\frac{1}{2}$ the monomer ^{13}C shift). Experiments on ^{13}C enriched naphthalene should verify this assignment. The line at 31, 531.4 cm^{-1} is not well characterized; it may arise from trimers, also expected at this concentration, or lattice defects of some sort. The monodeuteronaphthalenes also are observed in the 0.65% crystal.

At 1.4% the lattice defect at 31, 519.5 cm^{-1} in the moderate resolution spectra appears and is split into three components, probably corresponding to a ^{13}C isotope and site splitting. Also appearing in the 1.4% crystal is a transition in another $^{13}CC_9H_8$-$C_{10}H_8$ pair; this transition is weaker than that in the other such pairs because it corresponds to the ac component of the interchange pair. Mixed C-isotope pairs correlating with the lines at 31, 545.5 and 31, 538.5 cm^{-1} are unresolved from the broad absorption associated with the monomer transition.

C. Doublet Splittings

In some of the spectra, lines that are expected to be singlets actually split into doublets. This effect was observed and is indicated in Table II for the lowest energy resonance pair. Another example is shown in Fig. 4, and the corresponding spectral data

are given in Table IV. Here transitions due to $C_{10}H_8$, α-$DC_{10}H_7$, and β-$DC_{10}H_7$ are observed in a 0.1% $C_{10}H_8$ 1-mm crystal. Each is split into a doublet and except for β-$DC_{10}H_7$, is accompanied by the transition in the ^{13}C species. The concentration of β-$DC_{10}H_7$ is too low for the $^{13}CC_9H_7D$ transition to appear. Although several isomers containing one ^{13}C atom and one deuterium atom are possible, the corresponding spectral lines are not resolved. In addition to the lines listed in Table IV, transitions due to other resonance pairs and partially deuterated naphthalenes were indicated faintly on the photographic plate.

Observations leading to an explanation of the doublet splitting are summarized below. It appears that the doublet components for β-$DC_{10}H_7$ are not equally intense. The occurrence of the doublets is concentration dependent since only single lines appear for the resonance pairs, ^{13}C species, and higher deuterated isotopes, these being present in lower concentrations. The intensities of the two components for $C_{10}H_8$ and α-$DC_{10}H_7$ appear equal only because of their high optical density. The fact that the doublet splitting in Table IV is larger for β-$DC_{10}H_7$ is due to the difficulty in measuring the position of the very weak component. Visually the splitting appears the same for the three doublets.

In the 1.2-mm, 0.007% crystal, only the $\underset{\sim}{b}$ component of the 0, 0 $C_{10}H_8$ absorption appears split into a doublet. The second component of the $\underset{\sim}{ac}$ line probably is too weak to be observed since the observed $\underset{\sim}{ac}$ line occurs at the same energy as one of the $\underset{\sim}{b}$ lines.

Alternatively, the presence and absence of splitting in the two polarizations may arise from different parts of the sample being used to record the two polarizations with the stigmatic optics. In two different crystals having about the same concentration and thickness, the splitting is present in one but absent in the other. The differences in thickness and concentration are not sufficient to account for this effect.

From these experimental results, it is concluded that the splitting arises from some crystal inhomogeneity, e.g. regions with a slightly different crystal structure leading to a small change in the intermolecular interactions. In many of the crystals a $1\,cm^{-1}$ variation in the transition energy across the crystal appeared as a change in the line position on the photographic plate again due to the stigmatic optics. This observation supports the proposed origin of the doublet. It should be noted that the $1\ cm^{-1}$ splitting or shift is only 0.2% of the total gas-to-crystal shift in naphthalene.

Other explanations can be eliminated by these experiments. For example, some directional stress that makes the two interchange equivalent molecules in the unit cell inequivalent, should produce doublets of equal intensity. The possibility that the doublet arises from the formation of a guest exciton band at high concentrations is eliminated by the splitting in the 0.007% crystal.

An orientation effect[9] may occur for the monodeuteronaphthalenes but not for naphthalene. The observed doublet for naphthalene does not arise from such an effect. Assuming that the splittings in

the monodeuteronaphthalenes also are not due to an orientation effect means that the orientation effect for these molecules is less than half the 1.1 cm^{-1} linewidth. In monodeuterobenzene the orientational effect is 1.2 cm^{-1} for the $^1B_{2u} \leftarrow {}^1A_g$ transition. As discussed by Nieman and Tinti, [17] the orientational effect in the $^3B_{1u} \leftarrow {}^1A_g$ transition is about five times larger.

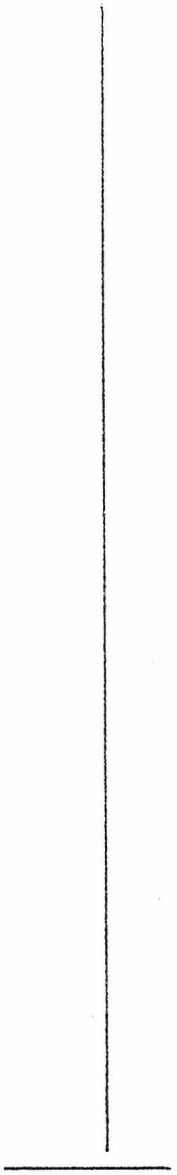

At first the smaller orientation effect in naphthalene is surprising because the intermolecular interactions, as manifested in the gas-to-crystal shift and exciton splittings, are larger in naphthalene than in benzene. However, the observation of an orientational effect depends upon two factors. The crystal field must affect the zero-point energies of the ground and excited states to a different extent, and this influence must change for the different orientations of the molecule in the crystal site. Consequently, the fact that the orientation effect is smaller and the intermolecular interactions larger in naphthalene implies either that the effect on the two states is nearly the same in any one orientation or that the intermolecular interactions are more isotropic in naphthalene.

It is indeed possible that the doublet appears by a different mechanism under different conditions. In which case, many of the preceding arguments are no longer valid.

D. Phosphorescence Spectra

High resolution phosphorescence spectra ($^3B_{1u} \rightarrow {}^1A_g$) of 1.4% $C_{10}H_8$ in $C_{10}D_8$ reveal three satellite lines near the intense 0,0 transition of the monomer guest as shown in Fig. 5. The two lines at +1.3 and -1.2 cm^{-1} relative to the monomer transition tentatively are assigned to the resonance splitting of the nearest interchange equivalent pair since precisely this splitting is anticipated from the Davydov splitting for the triplet state found in the pure crystal.[14]

A third line is expected due to the 11% natural abundance of $^{13}CC_9H_8$ and is observed at +3 cm^{-1}. The latter assignment is reasonable since the corresponding ^{13}C-isotope shift for the singlet state is +2.0 cm^{-1}. These isotope effects are in qualitative agreement with the isotope effects found for the benzene molecule.[9] If the assignments are correct, the translationally equivalent exciton interactions are not twice the interchange equivalent interactions for the lowest triplet state of crystalline naphthalene as predicted theoretically[18] and suspected to be true for anthracene.[19]

The dependence of the intensity on concentration was not determined because of the long exposure times (6 h) required even for this high concentration and the uncertain influence of energy transfer processes that would affect the accuracy of such a study. Polarization measurements would have required increasing exposure times by a factor of four and are better undertaken with other experimental techniques.

It is of interest that the resonance pair and Davydov splittings give a value of 1.25 ± 0.25 cm^{-1} for the excitation exchange matrix element while exchange narrowing of the magnetic resonance line[20] gives a value of 5.0 ± 0.7 cm^{-1} for the exchange integral. This discrepancy probably arises from the assumptions inherent in the analysis of the magnetic resonance linewidth.[21]

IV. DISCUSSION AND CONCLUSIONS

The effect of guest aggregation on the energy states of naphthalene isotopic mixed crystals ($C_{10}H_8$ as a guest in $C_{10}D_8$) has been observed by high resolution optical spectroscopy at 4.2°K. In the concentration range studied (< 5%), transitions involving the lowest singlet and triplet states of guest pairs are observed. A diffuse concentration dependent absorption also is observed below the host exciton band. This absorption is due to the ^1A_u component of the interchange equivalent resonance pair and to naturally occurring isotopic impurities. The fact that these transitions are diffuse is explained qualitatively[22] by the mixing of these states with levels in the exciton band. This interaction causes levels to move out of the band producing the diffuse absorption.

The data on the resonance pair absorptions are summarized in Table V. These transitions were assigned on the basis of three independent observations: (1) the concentration at which they first appeared, (2) the nonlinear dependence of intensity on concentration, and (3) their polarization. The excitation exchange matrix elements in Frenkel theory are just one-half the resonance pair splitting. The signs of these intermolecular matrix elements are meaningful within a specified interchange convention[7] and are derived from the observed polarization and energy of the spectral lines from a given pair. Since the lower energy component of the interchange pair is polarized in the ac plane ($\underset{\sim}{B}$ representation of C_2), and the higher energy component is polarized along the b axis ($\underset{\sim}{A}$ representation

of $\underset{\sim}{C}_2$), the sign of $\mathcal{M}_{12}$ is positive. For the translation pairs the sign is determined by the energy of the optically allowed component. The experimentally derived matrix elements and signs are summarized and compared, in Table VI, with values derived from a transition octopole model[23] for the interaction. Figure 6 shows the naphthalene crystal structure and the relative positions of the resonance pairs.

The first column in Table VI specifies the lattice vector between the centers of $C_{10}H_8$ molecules. The length of this vector is in the second column. The magnitude and sign of the pairwise excitation exchange integrals calculated from the transition octopole model for the intermolecular interaction are in the last column. The values of these integrals determined from the resonance pair data are in the column titled Exp. These values were obtained by neglecting quasiresonance effects and assuming the components of each pair split symmetrically about the monomer line. The assignments of lines to specific resonance pairs is somewhat arbitrary. Certainly the largest interchange equivalent interaction corresponds to the nearest interchange equivalent pair separated by $\frac{1}{2}(\underset{\sim}{a} + \underset{\sim}{b})$. The translation pairs are assigned to agree, as closely as possible, with the octopole model. An experimental assignment can be made from uniaxial stress experiments. The agreement between the octopole and resonance pair data is only fair. The disagreement in sign between the experimental and octopole data may be due only to the use of a different phase convention. All other interactions, including

next-nearest interchange equivalent molecules, are assumed to be less than half the linewidth ($\frac{1}{2} \times 6$ cm^{-1}) of the central guest absorption at the expected intensity of these transitions. If the additional absorptions could be resolved and assigned, one would have a direct measure of the intermolecular interactions throughout the crystal. One should remember that these additional terms may have positive or negative signs.

Since the Davydov splitting equals[2,3] $8M_{I\,II}(\underset{\sim}{0})$ where $M_{I\,II}(\underset{\sim}{0})$ is the sum of excitation exchange integrals over all the different interchange equivalent molecules, the fact that $M_{I\,II}(\underset{\sim}{0}) = +15.3$ cm^{-1} + 3 cm^{-1} = 18 cm^{-1} is in good agreement with the 160 cm^{-1} Davydov splitting and indicates that only nearest and next-nearest interchange equivalent interactions are required to give essentially the total Davydov splitting. It should be noted that quasiresonance effects, interactions with more distant molecules, and the experimental accuracy in column 3 of Table VI readily explain the difference between the 144 cm^{-1} obtained for $8M_{I\,II}(\underset{\sim}{0})$ from the resonance pair data and the 160 cm^{-1} Davydov splitting.

The normalized density function calculated using the resonance pair matrix elements in the dispersion relation is shown in Fig. 7. In this calculation the matrix elements were assigned to specific pairs of molecules to give the best agreement with the earlier experimental data[3,4] on the density of states. This assignment supports the idea of the presence of two different "types" of interactions.[3] Only one translationally equivalent interaction is

positive in sign, and only one neighboring pair of translationally equivalent molecules has the molecular planes perpendicular to the intermolecular axis. The remaining translationally equivalent interactions are negative in sign, and the remaining translationally equivalent molecules have the molecular planes parallel to the intermolecular axis, see Fig. 6.

The conclusion then is that several independent experimental results[3,4] indicate that the lowest excited singlet state of crystalline naphthalene is an isolated Frenkel exciton state, and in spite of several theoretical investigations, the quantum mechanical origin of the exciton interactions remains uncertain. New theoretical[3] and experimental investigations have been suggested. A general theoretical expression giving the spectral lineshape of a mixed crystal system as a function of the concentration of the compounds over all concentration ranges also must be developed. Such an expression should explain quantitatively the diffuse absorption observed between 31,550 and 31,580 cm^{-1}, and may better relate the resonance pair splittings to the band structure by accounting for the asymmetry in the splitting about the monomer line.

ACKNOWLEDGMENTS

Helpful discussions with G. W. Robinson, R. Kopelman, E. R. Bernstein, S. D. Colson, and D. S. Tinti were very much appreciated. Special thanks are due Professors Robinson and Kopelman for help in preparing parts of the manuscript, and E. W. Siegel and L. Minghetti for designing and making the optical cells.

REFERENCES

1. (a) J. Frenkel, Phys. Rev. 37, 17, 1276 (1931); (b) A.S. Davydov, Theory of Molecular Excitons (McGraw-Hill Book Co., Inc., New York, 1962); (c) A.S. Davydov, Sov. Phys.--Usp. 7, 145 (1964).
2. E.R. Bernstein, S.D. Colson, R. Kopelman, and G.W. Robinson, J. Chem. Phys. 00, 0000 (1968), "Electronic and Vibrational Exciton Structure in Crystalline Benzene."
3. D.M. Hanson, R. Kopelman, and G.W. Robinson, "The Exciton Band Structure of the $^1B_{2u}$ State of Crystalline Naphthalene by the Variation of Energy Denominators Method Using Isotopic Substitution," unpublished results.
4. S.D. Colson, D.M. Hanson, R. Kopelman, and G.W. Robinson, J. Chem. Phys. 48, 2215 (1968).
5. Preliminary results were reported at the Symposium on Molecular Structure and Spectroscopy (The Ohio State University, Columbus, Ohio, 1966).
6. S.C. Abrahams, J.M. Robertson, and J.G. White, Acta Cryst. 2, 233, 238 (1949).
7. R. Kopelman, J. Chem. Phys. 47, 2631 (1967).
8. R. Kopelman, Symposium on Molecular Structure and Spectroscopy (The Ohio State University, Columbus, Ohio, 1967), Abstract R7.
9. E.R. Bernstein, S.D. Colson, D.S. Tinti, and G.W. Robinson, J. Chem. Phys. 00, 0000 (1968), "Static Crystal Effects on the

Vibronic Structure of the Phosphorescence, Fluorescence, and Absorption Spectra of Benzene Isotopic Mixed Crystals."

10. D.P. Craig and S.H. Walmsley, Mol. Phys. 4, 113 (1961).

11. S.A. Rice and J. Jortner, Physics and Chemistry of the Organic Solid State, D. Fox, M.M. Labes, and A. Weissberger, Eds. (Interscience Publishers, Inc., New York, 1967), Vol. III, Chap. 4.

12. H.M. Crosswhite, The Spectrum of Iron I, Johns Hopkins Spectroscopic Report No. 13, The Johns Hopkins University, Department of Physics, Baltimore, Maryland, 1958.

13. C.D. Coleman, W.R. Bozman, and W.F. Meggers, Table of Wavenumbers, National Bureau of Standards Monograph 3, U.S. Government Printing Office, Washington, D.C., 1960.

14. D.M. Hanson and G.W. Robinson, J. Chem. Phys. 43, 4174 (1965).

15. Roughly half the $C_{10}H_8$ in a sample initially containing 0.1% $C_{10}H_8$ in $C_{10}D_8$ reacts to form partially deuterated naphthalenes when fused with potassium for 40 h at 90-100 °C.

16. C.D. Hodgman, Ed., Handbook of Chemistry and Physics (Chemical Rubber Company, Cleveland, Ohio, 1960).

17. G.C. Nieman and D.S. Tinti, J. Chem. Phys. 46, 1432 (1967).

18. J. Jortner, S.A. Rice, and J.L. Katz, J. Chem. Phys. 42, 309 (1965).

19. M. Levine, J. Jortner, and A. Szöke, J. Chem. Phys. 45, 1591 (1966).

20. M. Schwoerer and H.C. Wolf, Molecular Crystals 3, 177 (1967).

21. (a) P.W. Anderson and P.R. Weiss, Rev. Mod. Phys. 25, 269 (1953); (b) P.W. Anderson, J. Phys. Soc. Japan 9, 316 (1954).

22. D.P. Craig and M.R. Philpott, Proc. Roy. Soc. (London) 290A, 583 (1966).

23. (a) R.G. Body, private communication; (b) R.G. Body and I.G. Ross, Australian J. Chem. 19, 1 (1966); (c) D.P. Craig and M.R. Philpott, Proc. Roy. Soc. (London) 290A, 602 (1966).

TABLE I. Moderate Resolution Spectral Data

$\bar{\nu}$ ($\pm$ 0.5 cm^{-1})	Polarization	Concentration Dependence	Assignment
31, 559.9	$\underset{\sim}{b} > \underset{\sim}{ac}$	irregular	β-$DC_{10}H_7$
31, 550.5	$\underset{\sim}{b} > \underset{\sim}{ac}$	irregular	α-$DC_{10}H_7$
31, 544.5	$\underset{\sim}{b} > \underset{\sim}{ac}$		$^{13}CC_9H_8$
31, 542.5	$\underset{\sim}{b} > \underset{\sim}{ac}$	linear	$C_{10}H_8$
31, 538.2	$\underset{\sim}{b} > \underset{\sim}{ac}$		
31, 536.8	$\underset{\sim}{b} > \underset{\sim}{ac}$		
31, 533.8	$\underset{\sim}{b} > \underset{\sim}{ac}$	nonlinear	translation pair
31, 531.4	$\underset{\sim}{b} > \underset{\sim}{ac}$	weak	
31, 526.7	$\underset{\sim}{ac}$	nonlinear	interchange pair
31, 519.5		linear	lattice defect

TABLE II. High Resolution Spectral Data

$\bar{\nu}$ [a] cm^{-1}	Minimum Concentration	Concentration Dependence	Polarization	Assignment
31,580 to 31,550			$\underset{\wedge}{b}$	see b
31,556.4	0.65		$\underset{\wedge}{b} > \underset{\sim}{ac}$	β-$DC_{10}H_7$
31,550.7	0.65		$\underset{\wedge}{b} > \underset{\sim}{ac}$	α-$DC_{10}H_7$
31,545.5	0.05	nonlinear	$\underset{\wedge}{b} > \underset{\sim}{ac}$	translation pair
31,543.6	0.007		$\underset{\wedge}{b} > \underset{\sim}{ac}$	$^{13}CC_9H_8$
31,541.8	0.007	linear	$\underset{\wedge}{b} > \underset{\sim}{ac}$	$C_{10}H_8$
31,538.5	0.12	nonlinear	$\underset{\wedge}{b} > \underset{\sim}{ac}$	translation pair
31,537.6	0.65			$^{13}CC_9H_8$-$C_{10}H_8$ pair
31,536.7	0.12	nonlinear	$\underset{\wedge}{b} > \underset{\sim}{ac}$	translation pair
31,535.0	0.65			$^{13}CC_9H_8$-$C_{10}H_8$ pair
31,533.9	0.12	nonlinear	$\underset{\wedge}{b} > \underset{\sim}{ac}$	translation pair

TABLE II. (continued)

$\bar{\nu}$ [a] cm^{-1}	Minimum Concentration	Concentration Dependence	Polarization	Assignment
31,531.4	0.65		$\underset{\sim}{b} > \underset{\sim}{ac}$	
31,529.3	1.14		$\underset{\sim}{b} \approx \underset{\sim}{ac}$	
31,528.1	1.14		$\underset{\sim}{ac}$	$^{13}CC_9H_8$-$C_{10}H_8$ pair
31,527.4	0.12 - 1.14	nonlinear	$\underset{\sim}{ac}$	interchange pair
31,526.5			$\underset{\sim}{ac}$	
31,524.8	1.14		$\underset{\sim}{b} \approx \underset{\sim}{ac}$	
31,520.9	1.14		$\underset{\sim}{ac} \gtrsim \underset{\sim}{b}$	lattice defect
31,519.7	1.14		$\underset{\sim}{ac} \gtrsim \underset{\sim}{b}$	
31,518.2	1.14		$\underset{\sim}{ac} \gtrsim \underset{\sim}{b}$	

[a] The accuracy is ± 0.2 cm^{-1} and, where the last figure is underlined, 0.5 cm^{-1}.

[b] Diffuse absorption due to isotopic molecules and the ^1A_u component of the interchange pair.

TABLE III. Natural Concentrations of Isotopic Species

Atom	Abundance	Molecule	Abundance
C-13	1.1%	$^{13}CC_9H_8$	11%
D	1.6×10^{-2}%	$C_{10}H_7D$	6.4×10^{-2}%

TABLE IV. Doublet Splittings

$\bar{\nu}$ [a] cm^{-1}	I	Assignment	Splitting	^{13}C Shift
31,558.1	w	β-$DC_{10}H_7$	1.7	
31,556.4	vw			
31,552.5	w	α-$D^{13}CC_9H_7$		1.8
31,550.7	s	α-$DC_{10}H_7$	1.0	
31,549.7	s			
31,545.6	vw	translation pair		
31,543.8	m	$^{13}CC_9H_8$		1.8
31,542.0	vs	$C_{10}H_8$	1.0	
31.541.0	vs			

[a] Accuracy is ± 0.2 cm^{-1}, linewidths are 1.1 cm^{-1}, slitwidth is 0.3 cm^{-1}.

TABLE V. Principal Lines of the Pure Electronic Transition of $C_{10}H_8$ in $C_{10}D_8$

$\bar{\nu}$ (± 0.5 cm^{-1})	Polarization	Intensity	Assignment
31, 550 to 31, 580	$\underset{\sim}{b}$	Diffuse absorption due to other isotopic species and the ^1A_u component of the interchange pair.	
31, 545.5	$\underset{\sim}{b} > \underset{\sim}{ac}$	nonlinear	translation pair
31, 541.8	$\underset{\sim}{b} > \underset{\sim}{ac}$	linear	$C_{10}H_8$ monomer
31, 538.5	$\underset{\sim}{b} > \underset{\sim}{ac}$	nonlinear	translation pair
31, 536.7	$\underset{\sim}{b} > \underset{\sim}{ac}$	nonlinear	translation pair
31, 533.9	$\underset{\sim}{b} > \underset{\sim}{ac}$	nonlinear	translation pair
31, 527.0	$\underset{\sim}{ac}$	nonlinear	interchange pair

TABLE VI. Pairwise Intermolecular Interactions in the $^1B_{2u}$ State of Crystalline Naphthalene

Position	Å	Interaction in cm^{-1}	
		Exp (cm^{-1})	Octopole[a]
$\frac{1}{2}(\underset{\wedge}{a} + \underset{\wedge}{b})$	5.10	+15.3	-21.1
$\underset{\wedge}{b}$	6.00	-5.1	-3.9
$\frac{1}{2}(\underset{\wedge}{a} + \underset{\wedge}{b}) + \underset{\wedge}{c}$	7.89	$\lesssim \lvert 3 \rvert$	+1.6
$\underset{\wedge}{a} + \underset{\wedge}{c}$	7.96	+3.7	-0.15
$\underset{\wedge}{a}$	8.24	-7.9	-4.3
$\underset{\wedge}{c}$	8.66	-3.3	-2.05

[a] R. G. Body, private communication.

FIG. 1. Resonance pairs, an isolated naphthalene unit cell.

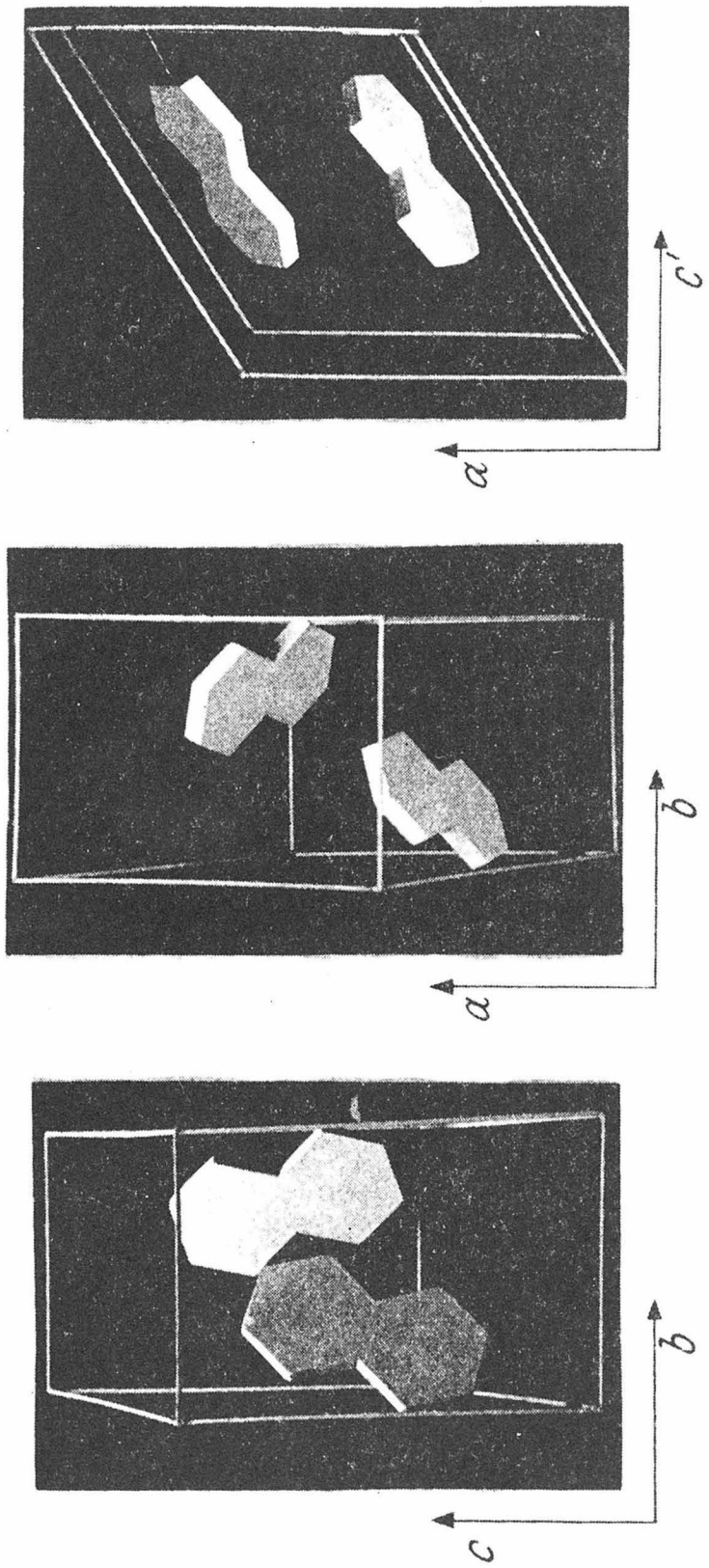
c'
a
b
a
b
c

FIG. 2. Polarized absorption spectra of naphthalene mixed crystals, $C_{10}H_8$ as a guest in $C_{10}D_8$, in the region of the $^1B_{2u} \leftarrow {}^1A_g$ guest transition. The intense absorption at high energy corresponds to the $^1B_{2u}$ exciton band of the host. The arrows indicate lines that are apparent on the photographic plate but lost in the microphotometer trace.

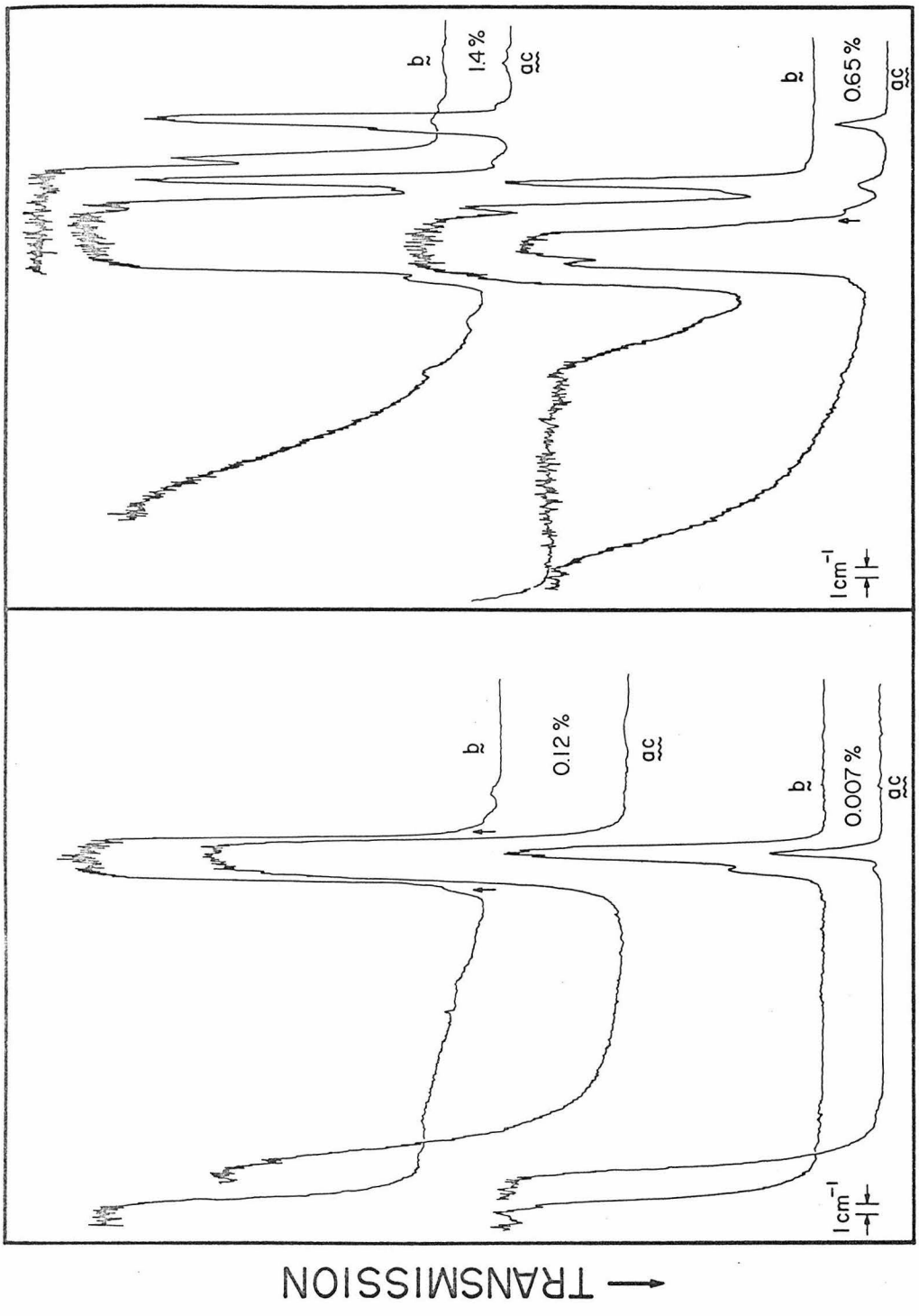
TRANSMISSION
ν (cm⁻¹)
b
ac
0.12 %
0.007 %
1.4 %
0.65 %
1 cm⁻¹

FIG. 3. Absorption spectra of (A) a 0.1-cm crystal of 1.0% $C_{10}H_8$ and (B) a 1.0-cm crystal of 0.1% $C_{10}H_8$ in $C_{10}D_8$. Note the intensity variation of the three lines that are marked next to the intense monomer absorption, and compare with the discussion in the text.

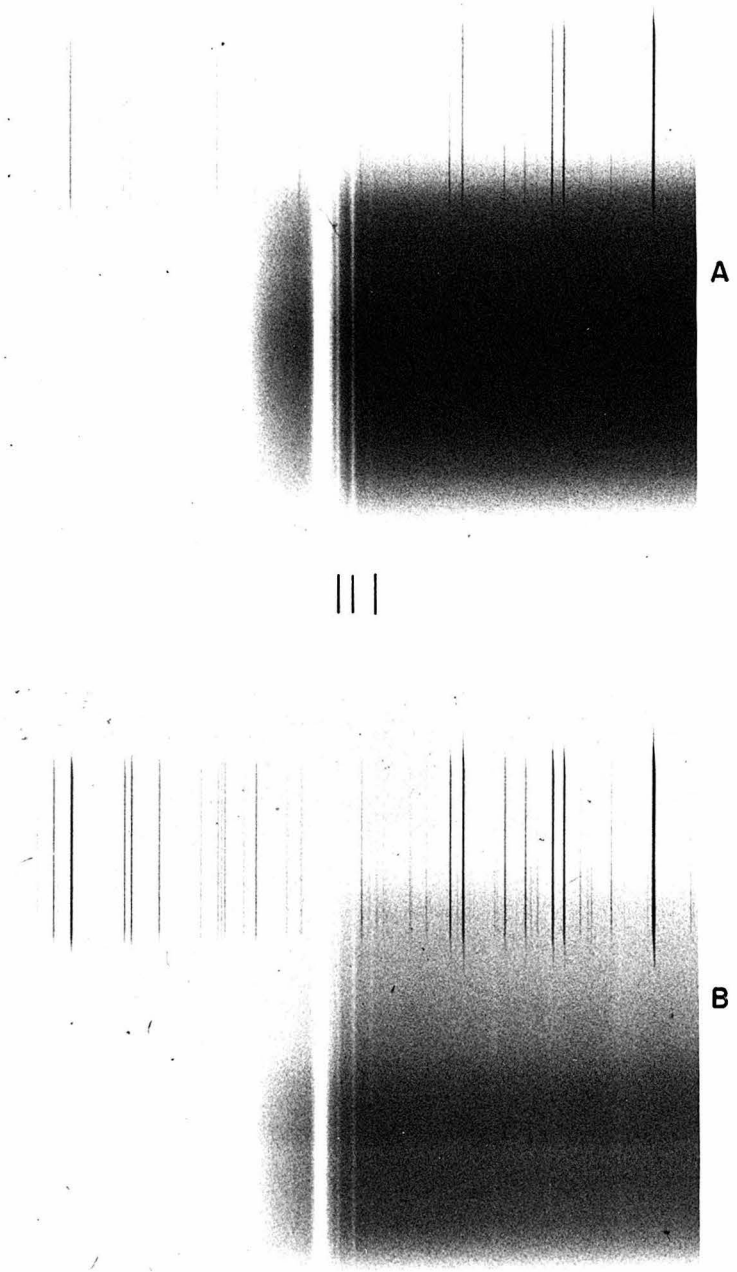
A
B

FIG. 4. Spectrum of a 1-mm crystal of 0.1% $C_{10}H_8$ in $C_{10}D_8$ that had been fused with potassium for 40 h. The doublets and ^{13}C transitions are marked. The high concentrations of α-$DC_{10}H_7$ and β-$DC_{10}H_7$ arise from the isotope exchange reaction mentioned in the text.

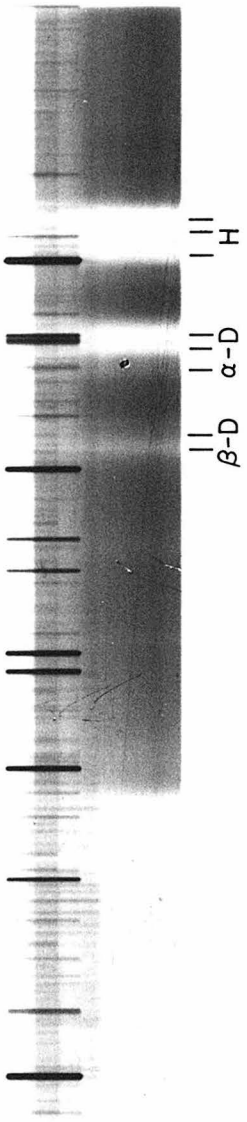
H
α-D
β-D

FIG. 5. The 0, 0 $^{3}B_{1u} \rightarrow {}^{1}A_{g}$ transition of $C_{10}H_{8}$ photographed at high resolution showing satellite lines probably due to $^{13}CC_{9}H_{8}$ and a resonance pair.

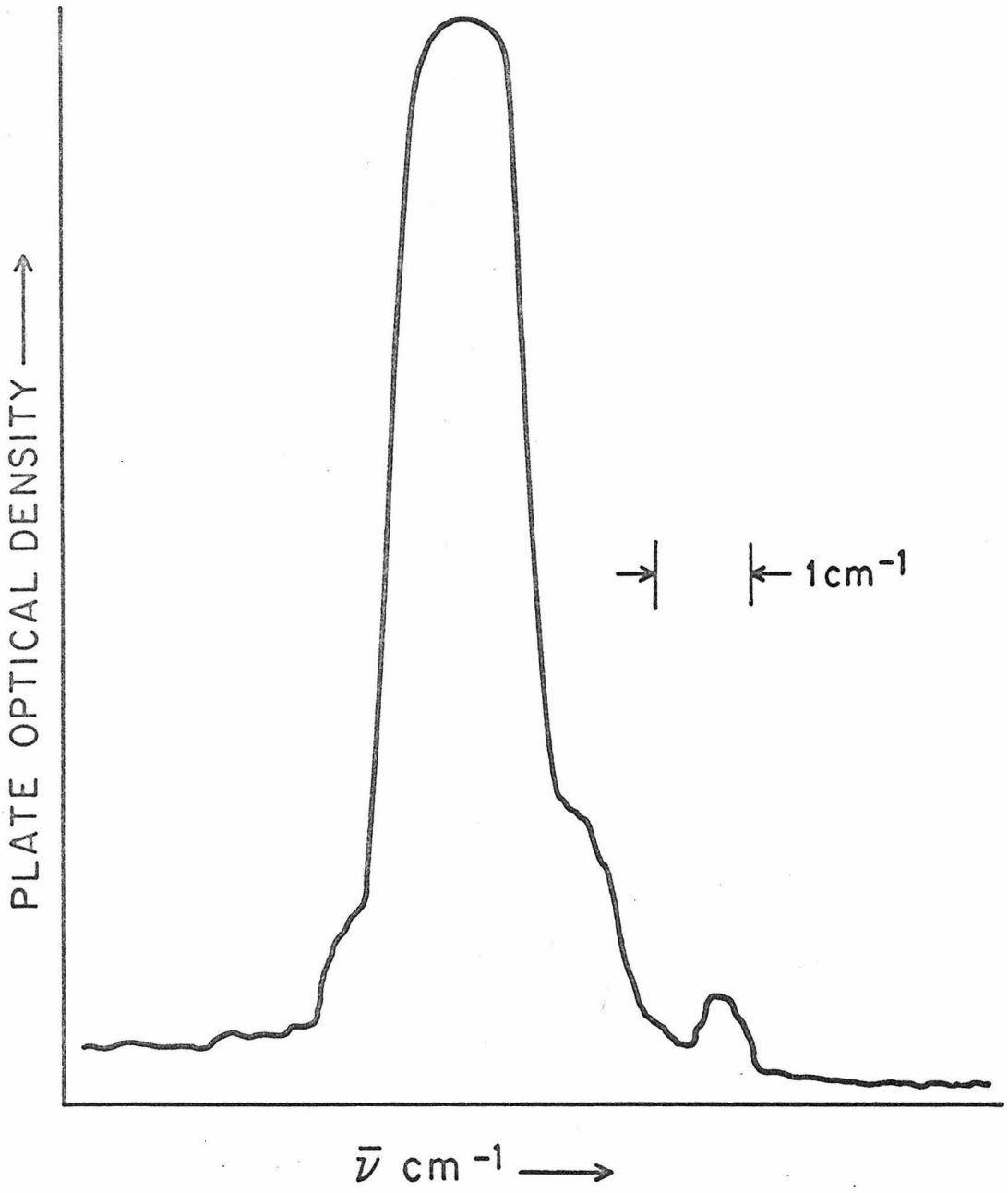
PLATE OPTICAL DENSITY
1cm⁻¹
ν̄ cm⁻¹

FIG. 6. The naphthalene unit cell showing the relative positions of the resonance pairs.

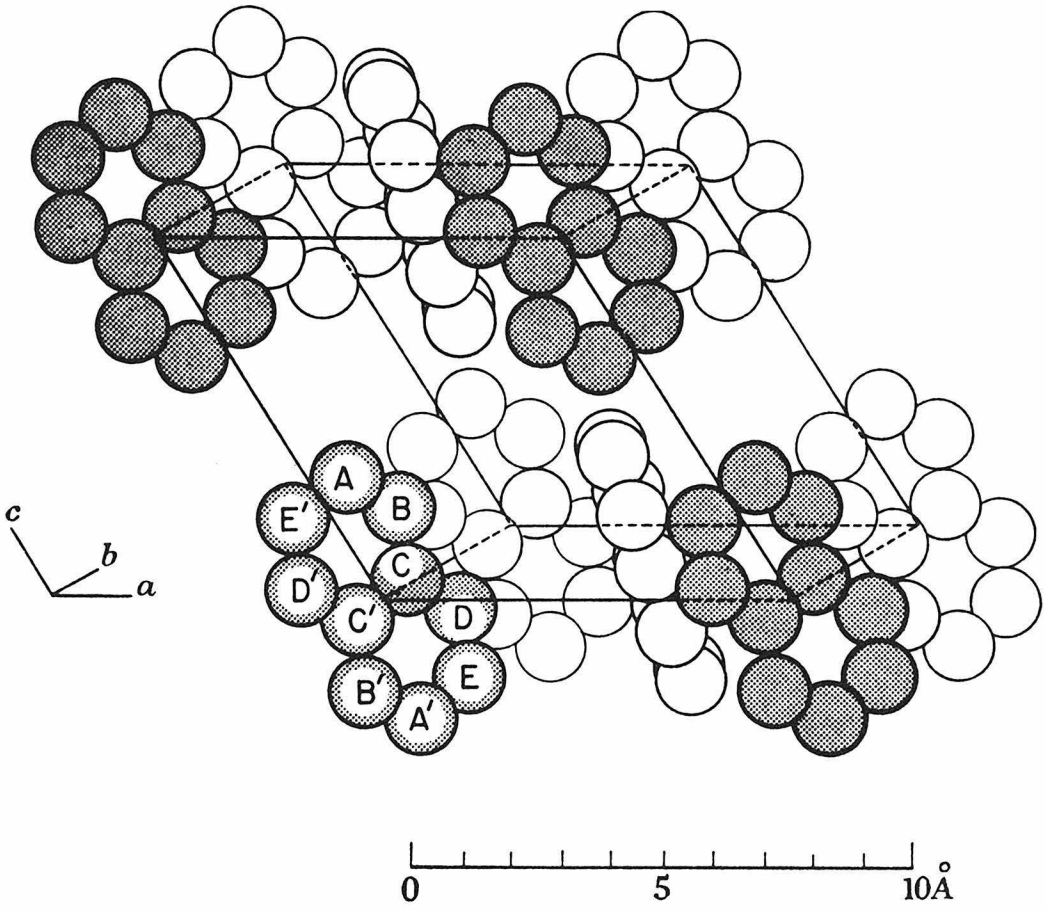
c
b
a
A
B
C
D
E
A′
B′
C′
D′
E′
0
5
10Å

FIG. 7. The normalized density function $D(E_i)$ calculated from the dispersion relation using matrix elements derived from the resonance pair splittings: $M(\underset{\sim}{a}) = +3.7\ cm^{-1}$, $M(\underset{\sim}{b}) = -7.9\ cm^{-1}$, $M(\underset{\sim}{c}) = -3.3\ cm^{-1}$, $M(\underset{\sim}{a}+\underset{\sim}{c}) = -5.1\ cm^{-1}$ $M(\frac{1}{2}\underset{\sim}{a}+\frac{1}{2}\underset{\sim}{b}) = +15.3\ cm^{-1}$, and $M(\frac{1}{2}\underset{\sim}{a}+\frac{1}{2}\underset{\sim}{b}+\underset{\sim}{c}) = +3\ cm^{-1}$. The lattice vector between the centers of the molecules forming the resonance pair is given in parentheses. This calculation gives the energies of the A_u and B_u factor group components as $+48\ cm^{-1}$ and $-98.4\ cm^{-1}$, respectively. The zero of energy is the ideal mixed crystal level. Note that the ordinate scale changes at 0.012.

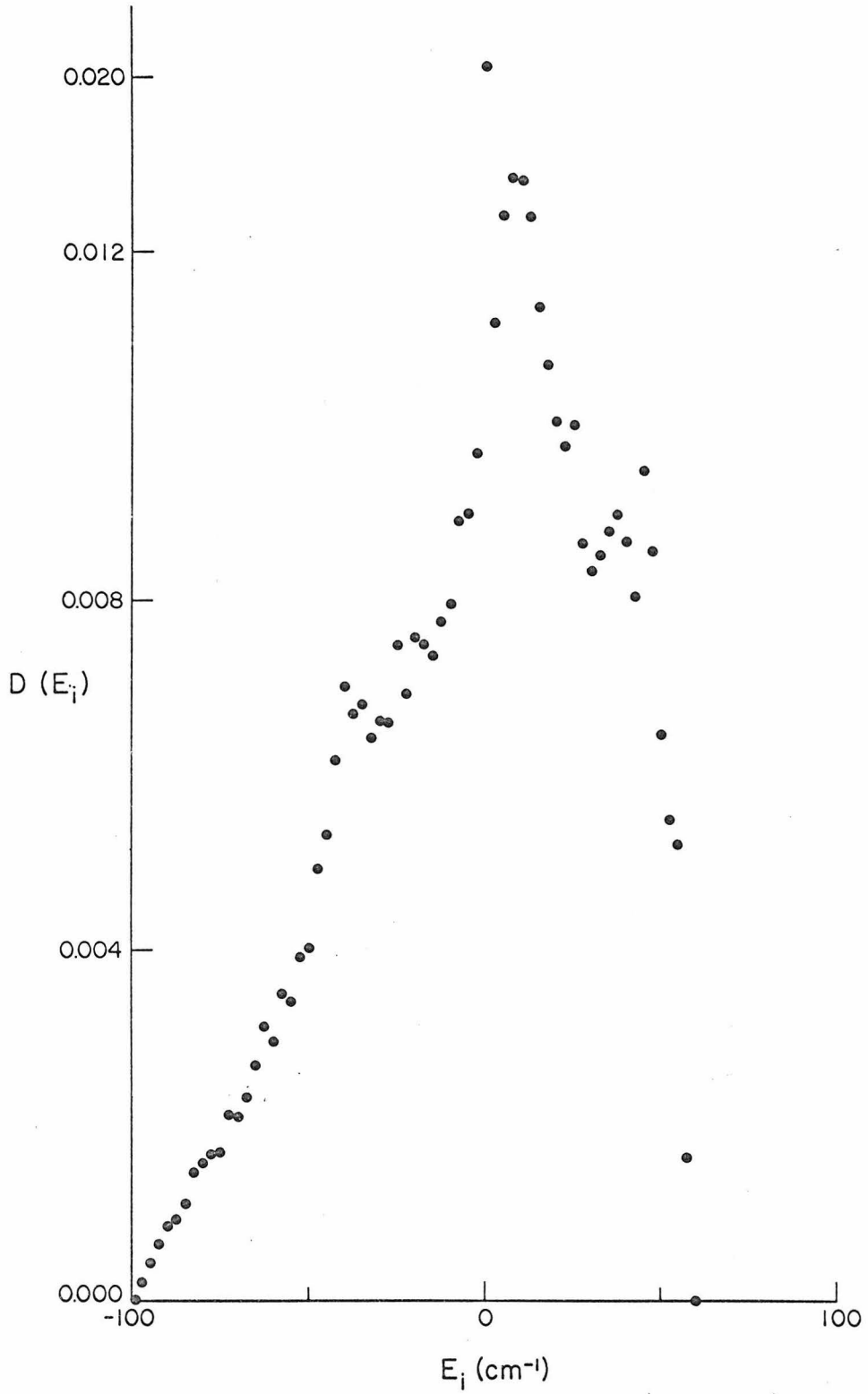
0.020
0.012
0.008
0.004
0.000
D (E_i)
-100
0
100
E_i (cm^-1)

PART IV

Optical Transitions in $^{13}CC_5H_6$ - C_6H_6 Mixed Crystals in the Region of the Factor Group Components of Crystalline Benzene.

Recent investigations of the energy levels in mixed crystal systems have been reported.[1-3] The exciton band structure has been classified[2] according to the concentration of the guest and the magnitude of the local perturbation. This scheme results in the following classifications and subclassifications: (1) very shallow guests, (2) shallow guests, (3) deep guests, and (a) isolated guests, (b) aggregated guests. Only for the cases 2(a) and 3(a) are the theoretical description and the experimental result shown to be in quantitative agreement.[2, 4] Some experimental data for case 2(b) have been reported and discussed qualitatively in terms of the exciton band structure.[5] No theoretical expression was presented, however, to predict the spectral lineshape as a function of concentration in the mixed crystal system. On the other hand, theoretical results[3] predict the appearance of virtual bound states or broad absorptions for classification 1, but no experimental results are available regarding this point.

The present paper reports spectral data for carbon-13 mixed crystals of benzene. This perturbation falls in classification 1. The $^{13}CC_5H_6$-C_6H_6 mixed crystals are of special interest because the theoretical estimates predict only a broadening of the exciton structure while experimental considerations[6, 7] indicate that the lines assigned as Davydov components in C_6H_6 or the other lines reported in this spectral region[8] might actually be due to the lowest singlet transition in $^{13}CC_5H_6$.

To clarify these points, spectra of Phillips' Research Grade benzene containing approximately 6%, 25%, and 50% $^{13}CC_5H_6$ were obtained and are shown in Figs. 1-2. The polycrystalline samples were grown in 14μ, 10μ, and 8μ quartz cells, respectively, after degassing in a vacuum system at 10^{-6} Torr. During the spectroscopic experiment the crystals were in contact with liquid helium. The 0, 0 absorptions were photographed with a 200 W Xe arc lamp and a 3.4 M Jarrell-Ash Ebert spectrograph using the twelfth order of a 300 lines/mm grating (190 mm × 80 mm) blazed at 18.3°. The theoretical resolution and reciprocal dispersion are 680, 000 and 0.72 Å/mm, respectively. A high intensity Bausch and Lomb 0.25 M monochromator was used to predisperse the light.

It is apparent from the figures that no pronounced changes in the relative line intensities are observed over the concentration range studied. In other words, none of these transitions are due to $^{13}CC_5H_6$; in fact, no transition due to $^{13}CC_5H_6$ is observed.

Theoretical conclusions following from Craig and Philpott's one-dimensional model[1] with a periodic impurity are consistent with this experimental result. The energy levels of such a mixed crystal are described by using the wavefunctions of the pure crystals as the basis functions. The presence of this shallow impurity manifests itself only as a slight shift in the energy of the host states and a broadening of the host transitions. The spectral broadening arises from the mixing of the dipole-allowed $\underset{\sim}{k} = \underset{\sim}{0}$ exciton states with other exciton states. For a periodic impurity this mixing is restricted by

a selection rule based on the translational symmetry. A random impurity distribution can be considered either as destroying all translational symmetry or as a superposition of all periodicities. Thus, mixing of all $\underset{\sim}{k}$ states is possible. The exact lineshape produced by this perturbation depends upon both the magnitude of the perturbation and the density-of-states function of the exciton band.[7] The observed shift of $+2\ cm^{-1}$ for the energy of the Davydov component in going from 6% to 50% $^{13}CC_5H_6$ as well as the $5\ cm^{-1}$ increase in linewidth is explained by such a model. In fact, rough estimates predict a $2\ cm^{-1}$ shift and an $8\ cm^{-1}$ increase in linewidth. It should be emphasized that the energy shift is predicted to be in the direction of the impurity, and indeed this is observed. Similar effects also have been observed in mixed crystals of naphthalene by employing deuterium substitution.[9]

The conclusions are (1) the lines appearing in the region of the C_6H_6 factor group structure are not attributable to naturally abundant $^{13}CC_5H_6$, (2) no absorptions due to the virtual bound states, predicted theoretically,[3] were observed even though concentrations of $^{13}C_2C_4H_6$ and $^{13}C_3C_3H_4$ should be in excess[10] of 2% and 0.03%, respectively, and (3) the extension of the Frenkel tight-binding model quite accurately describes the energy levels of mixed molecular crystals although a quantitative treatment of the concentration dependence has not been done.

ACKNOWLEDGMENT

About 20 mg of C_6H_6 containing approximately 50% $^{13}CC_5H_6$ were donated by Professor A. Kalantar, Department of Chemistry, The University of Alberta, Edmonton, Alberta, Canada.

REFERENCES

1. D. P. Craig and M. R. Philpott, Proc. Roy. Soc. (London) 290A, 583 (1966).
2. D. M. Hanson, R. Kopelman, and G. W. Robinson, "The Exciton Band Structure of the $^1B_{2u}$ State of Crystalline Naphthalene by the Variation of Energy Denominators Method Using Isotopic Substitution," unpublished results.
3. (a) B. Sommer and J. Jortner, "On the Electronic States of Mixed Molecular Crystals," unpublished manuscript; (b) B. Sommer and J. Jortner, "On the Electronic States of Mixed Molecular Crystals: Singlet Excited States of Isotopic Impurities in Crystalline Benzene and Naphthalene," unpublished manuscript.
4. D. P. Craig and T. Thirunamachandran, Proc. Roy. Soc. (London) A271, 207 (1963).
5. D. M. Hanson, "Energy States and Intermolecular Interactions in Molecular Aggregates--Resonance Pair Spectra of Crystalline Naphthalene," unpublished results.
6. In a C_6D_6 host the 0, 0 transition in $^{13}CC_5H_6$ is shifted by $+3.7\ cm^{-1}$ relative to the C_6H_6 transition. E. R. Bernstein, S. D. Colson, D. S. Tinti, and G. W. Robinson, J. Chem. Phys. 00, 0000 (1968), "Static Crystal Effects on the Vibronic Structure of the Phosphorescence, Fluorescence, and Absorption Spectra of Benzene Isotopic Mixed Crystals."

7. S. D. Colson, D. M. Hanson, R. Kopelman, and G. W. Robinson, J. Chem. Phys. 48, 2215 (1968).

8. Absorption lines at 37, 799 cm^{-1}, 37, 803 cm^{-1}, 37, 839 cm^{-1}, 37, 846 cm^{-1}, and 37, 847 cm^{-1} have been reported by V. L. Broude, V. S. Medvedev, and A. F. Prikhot'ko, Opt. Spektrosk. 2, 317 (1957) and V. L. Broude, Sov. Phys.--Usp. 4, 584 (1962).

9. D. M. Hanson, unpublished results.

10. Estimated by assuming the following probabilities for the crystal containing 50% $^{13}CC_5H_6$: $Pr[^{13}CC_5H_6] = 0.50$, $Pr[^{13}C_2C_4H_6] = 5 \times 0.01 \times 0.50$, and $Pr[^{13}C_3C_3H_6] = 7 \times (0.01)^2 \times 0.5$, based on the 1% natural abundance of ^{13}C.

11. S. D. Colson, J. Chem. Phys. 45, 4746 (1966).

FIG. 1. Photographs of the 0, 0 $^1B_{2u}$ benzene absorption in crystals containing $^{13}CC_5H_6$ at concentrations of (A) 6%, (B) 25%, and (C) 50%. (D) Absorption spectrum of an apparently strained crystal containing 50% $^{13}CC_5H_6$. The effects of strain generally vary across the length of the slit and thus can be distinguished from the effects of isotopic substitution.[5, 11] Broude's polarization results[8] are used to indicate the factor group components. The 2 cm^{-1} shift of the factor group components to higher energy in going from 6% to 50% $^{13}CC_5H_6$ is seen by careful comparison of the line positions with respect to the iron-neon standard.

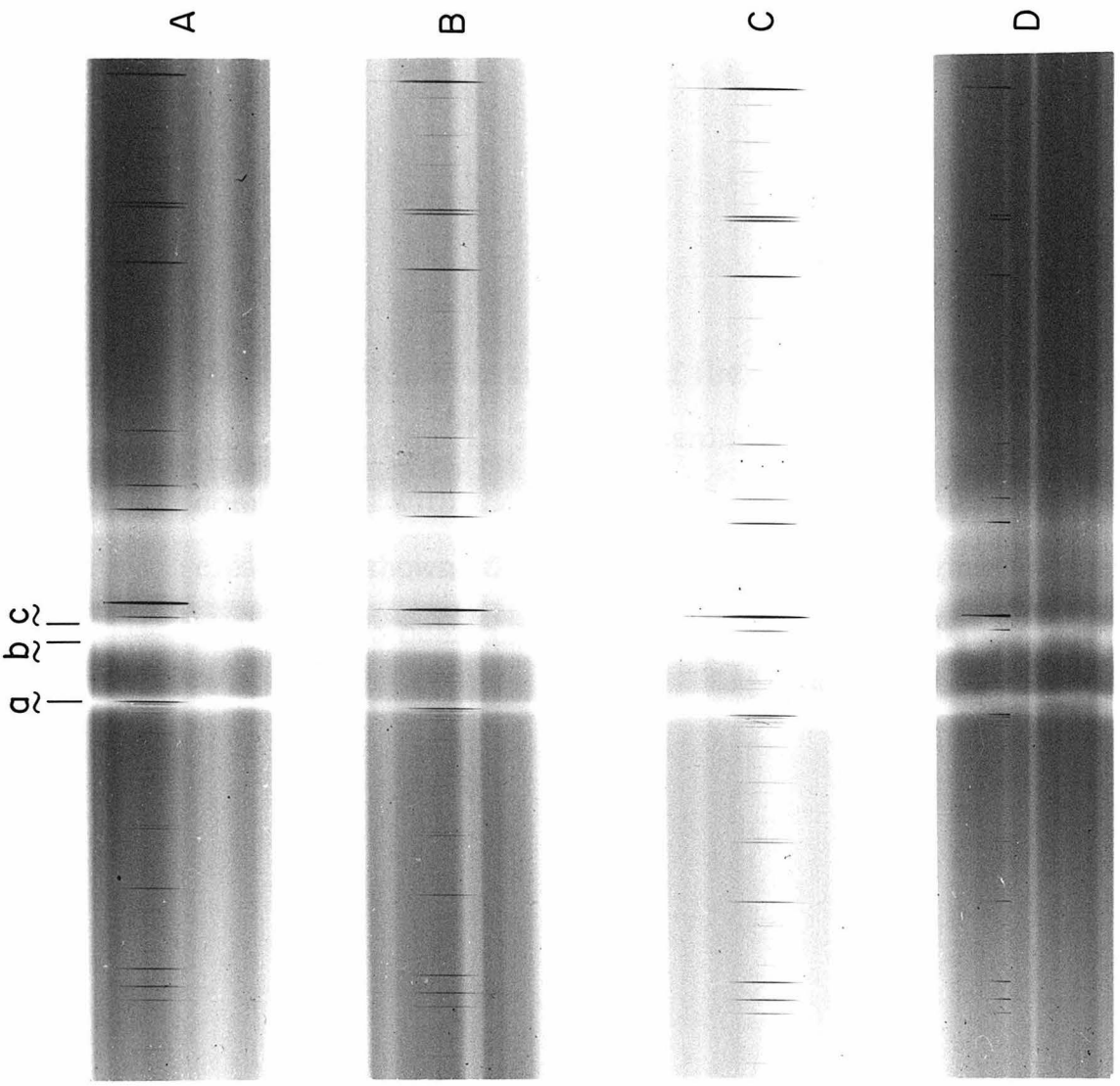
A
B
C
D
a
b
c

FIG. 2. Microdensitometer tracings of the absorption spectra pictured in Fig. 1. The broadening of the factor group components with increasing $^{13}CC_5H_6$ concentration clearly is shown. The broad absorptions at higher energy have been assigned as phonon addition bands.[7]

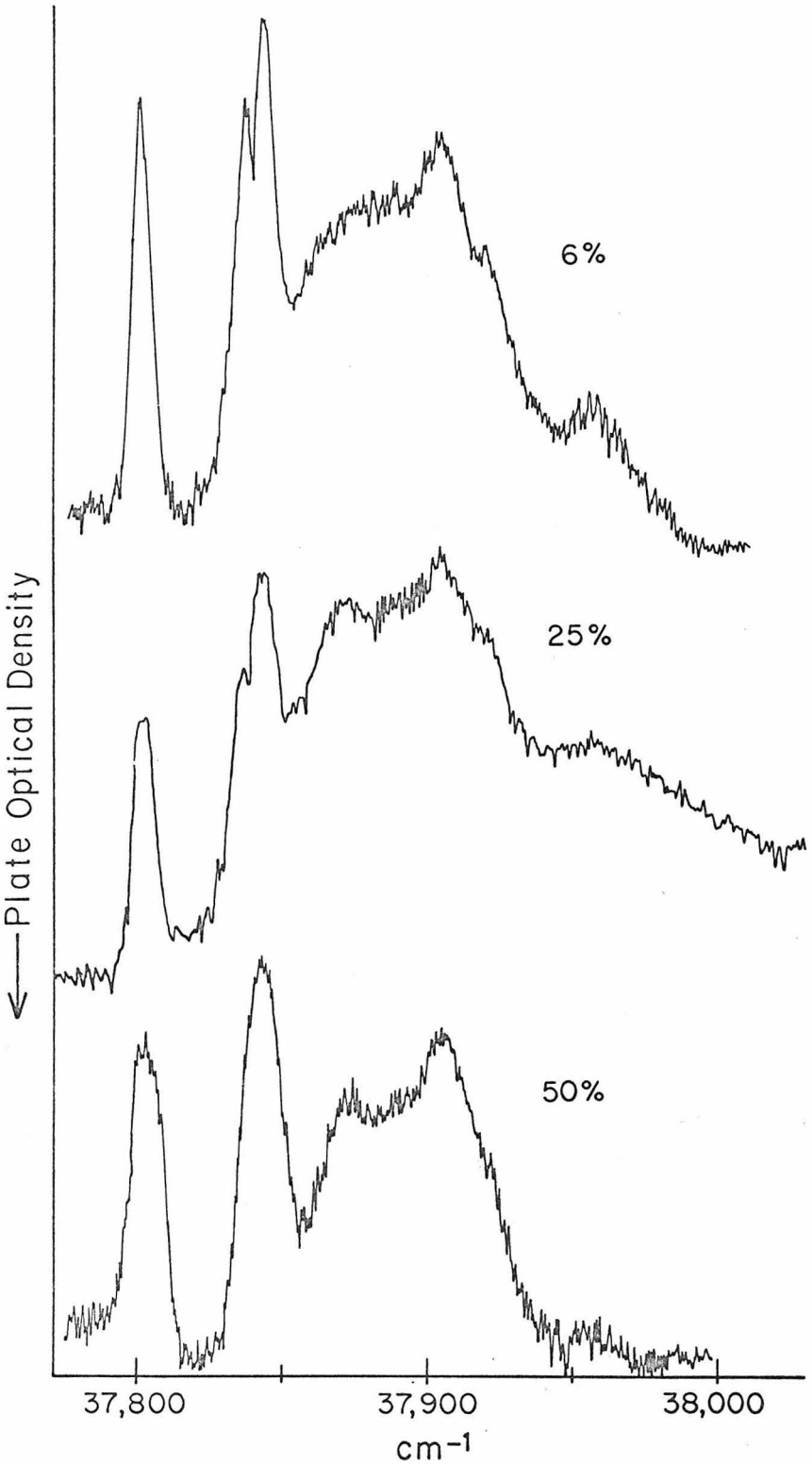
6%
25%
50%
Plate Optical Density
37,800
37,900
38,000
cm⁻¹

PART V

Exciton Structure in Two Triplet States of Crystalline Naphthalene

Reprinted from THE JOURNAL OF CHEMICAL PHYSICS, Vol. 43, No. 11, 4174–4175, 1 December 1965
Printed in U. S. A.

Exciton Structure in Two Triplet States of Crystalline Naphthalene*

DAVID M. HANSON AND G. WILSE ROBINSON

Gates and Crellin Laboratories of Chemistry,† California Institute of Technology, Pasadena, California

(Received 24 September 1965)

DURING the last few years much emphasis has been placed on excitation exchange interactions and the concomitant energy transfer in weakly absorbing systems.[1,2] This communication reports preliminary work on pure crystalline naphthalene ($C_{10}H_8$) and is intended to illustrate further the importance of excitation exchange interactions even when no strong transition dipoles are present. In addition, the position of a new triplet state of naphthalene is reported.

The naphthalene was purified in a manner similar to that used earlier.[3,4] The important parts of the purification process consist of preliminary zone refining, followed by a fusion with potassium at 100°C, and finally a further extensive zone-refining stage. The middle portion of the zone-refined ingot is sublimed into various sample cells for spectroscopic observation, the bottom, least pure, part being kept at −78°C during this process to prevent contamination. Contact with air is rigorously avoided during the entire process, all steps after the first zone refining being carried out in a grease-free, well-outgassed vacuum system. Crystals in the sample cells were grown from the melt by slowly lowering the cells through a sharp temperature gradient directly into a *liquid-nitrogen*-cooled chamber. Large, translucent crystals that did not have a tendency to crack when cooled to liquid-helium temperature could be made in this way. Since there is no added gas in the sample cell, thermal contact between the crystal and the cold bath is poor, and as much as 8-h submersion is required to reach thermal equilibrium at ~4°K. Decreases in temperature can be followed by the disappearance of "hot band" structure and the sharpening of spectral features.

The purity of the naphthalene was determined by examining the spectrum of the crystal at 4.2°K. As in earlier experiments,[3] no emission in the phosphorescence region could be detected visually or spectroscopically. Only the fluorescence spectrum of naphthalene itself was detected in the near-ultraviolet region. In addition, a 40-mm thickness of crystal at 4.2°K showed no detectable impurity absorption. Because of the sharpness (1–10 cm^{-1}) of absorption features of many impurities at very low temperatures, this sets an upper limit of such impurities at about 1 part in 10^7.[4] In particular, no trace of β-methylnaphthalene absorption or emission was found. On the contrary, an extensively zone-refined, 7-mm-thick sample, not treated with potassium, was found to exhibit fluorescence, weak phosphorescence, and complex absorption due to impurities. This finding is consistent with the experience of other workers[5,6] with zone-refined naphthalene, and indicates the inadequacy of zone refining alone as the method of obtaining *ultra*pure organic compounds. Thus, it is felt that the naphthalene used here is by far the purest that has yet been prepared, and that the usual artifacts in crystal spectroscopy and energy-transfer experiments associated with impurities are absent.

Exciton splittings for the first ($^3B_{2u}$) and third (?) triplet ($^3B_{3u}$)[7] states of naphthalene were observed directly in absorption in the 40-mm crystal cooled to 4.2°K. The two Davydov components (polarization unknown) for the (0–0) band of the first triplet are well resolved; they are found to lie at 21 203±1 cm^{-1} and 21 213±1 cm^{-1}. The absorption is barely detectable in the 40-mm crystal.[8] The center of gravity of these components is close, as expected, to the (0–0) band of the phosphorescence spectrum of $C_{10}H_8$ in $C_{10}D_8$, which lies at 21 208.7 cm^{-1}.[3] In addition to the (0–0) band, four other vibronic components have been observed, each having its own unique exciton splitting. The measured vibrational frequencies in the triplet state are 497, 955, 1345, and 1841 cm^{-1}, in excellent agreement with those reported by Avakian and Abramson[9] who used an indirect, low-resolution technique for observing the $^3B_{2u}\leftarrow{}^1A_{1g}$ absorption in the crystal. Davydov splittings of 10, 6, 8, 6, 6 cm^{-1}, respectively, appear to be roughly consistent with the relative intensities of the five vibronic components. Summing over these vibronic splittings and allowing for a residual

splitting of a few cm^{-1} from bands too weak to detect give a total splitting that lies extremely close to the theoretical value of $\sim$40 cm^{-1} obtained by Jortner, Rice, Katz, and Choi.[1] However, the center of gravity of the Davydov components, predicted by this same theory to be shifted substantially away from the zero of energy, is not in agreement with the position of the $C_{10}H_8$ in $C_{10}D_8$ phosphorescence origin which indicates little or no shift. This could mean either that the real value of K_3 (see Table III, p. 314 of Ref. 1) is around -1×10^{-4} eV or that some of the other constants K_2, K_4, $\cdots$, K_8 make contributions that cancel the effect of K_3.

An oscillator strength of $f=5\times10^{-10.0\pm0.5}$ can be estimated from the absorption intensity. This value is in good agreement with the oscillator strength calculated from the $\sim$10-sec radiative lifetime of the $^3B_{2u}$ state,[10–12] and constitutes the first evidence that oscillator strengths obtained from phosphorescence lifetime measurements, corrected for all presently known nonradiative effects,[12,13] are indeed reasonable.

As in benzene,[4] the second *ungerade* triplet state of naphthalene lies just below the first singlet. The Davydov components (polarization unknown) appear at 30 785$\pm$1 cm^{-1} and at 30 814$\pm$1 cm^{-1}, while the *a* and *b* components of the first singlet (our measurements) occur at 31 475$\pm$1 cm^{-1} and at 31 624$\pm$5 cm^{-1}, respectively. The absorption intensity to this new triplet, as in the case of benzene,[4] is a factor of 10–100 greater than that to the first triplet.

* Work supported in part by the U.S. Army Research Office.
[1]† Contribution No. 3309.

J. Jortner, S. A. Rice, J. L. Katz, and S.-I. Choi, J. Chem. Phys. **42**, 309 (1965); and extensive references cited there. This paper discusses triplet electronic excitons in organic crystals.

[2] E. R. Bernstein, S. D. Colson, R. Kopelman, and G. W. Robinson (to be published); this paper is concerned with vibrational excitons and the lowest singlet electronic exciton structure in crystalline benzene.

[3] M. A. El-Sayed, M. T. Wauk, and G. W. Robinson, Mol. Phys. **5**, 205 (1962).

[4] S. D. Colson and E. R. Bernstein, J. Chem. Phys. **43**, 2661 (1965).

[5] H. C. Wolf, Z. Naturforsch. **18a**, 724 (1963).

[6] F. Lipsett (private communication).

[7] R. Pariser, J. Chem. Phys. **24**, 250 (1956).

[8] This result emphasizes the advantage of using liquid helium, where the absorption lines are sharper. There would be little chance of observing this weak absorption at 77°K in the 40 mm crystal. The higher triplet was, however, observed not only at 4°K but also at 77°K bracketed by hot band structure from the singlet.

[9] P. Avakian and E. Abramson, J. Chem. Phys. **43**, 821 (1965).

[10] E. H. Gilmore, G. E. Gibson, and D. S. McClure, J. Chem. Phys. **20**, 829 (1952); **23**, 399 (1955).

[11] C. A. Hutchison Jr. and B. W. Mangum, J. Chem. Phys. **32**, 1261 (1960).

[12] G. W. Robinson, J. Mol. Spectry. **6**, 58 (1961).

[13] M. R. Wright, R. P. Frosch, and G. W. Robinson, J. Chem. Phys. **33**, 934 (1960).

PART VI

The Phosphorescence Spectrum, Vibronic Analysis, and Lattice Frequencies of the Naphthalene Molecule in a Deuteronaphthalene Crystal

I. INTRODUCTION

In studies of molecular properties, benzene undoubtedly is considered the prototype aromatic molecule. Naphthalene, however, complements this role in spectroscopic studies of intra- and intermolecular perturbations. Relative to benzene both the naphthalene molecule and crystal have lower symmetry; consequently spectroscopic transitions that are forbidden in benzene are allowed in naphthalene. Similarly, effects characteristic of benzene may be atypical of other aromatic molecules, e.g., crystal field perturbations,[1] vibronic and spin-orbit coupling mechanisms,[2] and some radiationless processes[3] including temperature, environment, and isotope effects.[4]

A detailed study of these phenomena in naphthalene is limited by ambiguities in the assignment of the fundamental vibrational frequencies. The uncertainties in the present assignments and the need for additional experimental work repeatedly have been cited in the literature[5] and become apparent when one attempts to compare the results of normal coordinate calculations with experimental data, to determine vibronic spin-orbit coupling mechanisms, and to identify the source of spectral absorption and emission in crystalline naphthalene.

The present paper reports the observation of many weak lines in the phosphorescence spectrum of the naphthalene molecule. It should be emphasized that these data only could be obtained

through the use of extremely pure naphthalene crystals. The phosphorescence spectrum shows absolutely no trace of β-methylnaphthalene emission. The 0, 0 transition of β-methylnaphthalene should be found[6] at 20, 909.1 ± 0.5 cm^{-1}. Similarly, none of the unidentified spectral lines reported in Table V of Ref. 6a are present in Fig. 1.

It is found that ambiguities in the vibrational assignments can be eliminated by comparing the phosphorescence spectrum with the fluorescence[7] and Raman[8] spectra. In particular, confident assignments of the b_{1g} and b_{2g} modes can be made, and the two nearly degenerate vibrations[5b] at 510 and 512 cm^{-1} are resolved and shown in Fig. 2. The assignments of the normal modes are discussed in greater detail in Ref. 8. The data also have been used to interpret[9] the phosphorescence and absorption spectra of pure crystalline naphthalene. In fact, the polarization[9b] of the $^3B_{1u} \leftarrow {}^1A_g$ vibronic transitions confirm the assignments here that are based on the Raman polarizations.[8] This confirmation is possible because the symmetry-based selection rules for spin-orbit coupling require that an a_g vibration introduce no M intensity, a b_{2g} vibration no N intensity, and a b_{3g} vibration no L intensity through either the first-order spin-orbit or spin vibronic perturbations or the second-order spin-orbit vibronic perturbation. M, N, and L represent the short molecular axis, the normal to the molecular plane, and the long molecular axis, respectively. Using the coordinate system recommended by Mullikan,[10] M transforms as B_{1u}, L transforms as B_{2u}, and N transforms as B_{3u}.

II. EXPERIMENTAL

The weak lines in the phosphorescence spectrum were observed by combining several special experimental techniques. These techniques involve intense excitation, long exposures using a fast, moderately high resolution spectrograph, liquid helium temperatures, and extremely pure isotopic mixed crystals.

Front surface excitation of the crystal was provided by an 800 W Xe arc lamp combined with a 5-cm focal length quartz lens, an aqueous $CoCl_2$ filter, and a Corning 9863 glass filter. The phosphorescence was collected with a 10-cm focal length lens, passed through a Corning 3389 filter, and imaged on the 20μ slits of the spectrograph. The spectrograph employs a 600 line/mm Bausch and Lomb grating (212 × 157 mm) blazed at 17°27' in a 2-m f/12 Czerny-Turner mount. The phosphorescence primarily is dispersed into the second-order spectrum of the grating where the plate factor and resolving power are 3.6 Å/mm and 50,000, respectively. The intensity from the grating sharply decreases between 4700 and 6000 Å. An Eastman-Kodak type 103a-F spectroscopic plate was exposed for two hours. This system, for the resolution obtained, is more sensitive than conventional photoelectric detection using dc amplification. A tracing of the photographic plate was obtained with a Jarrell-Ash Model 23-500 microphotometer.

A mixture of 1% Eastman recrystallized naphthalene and 99% Merck, Sharp and Dohme deuteronaphthalene was purified by zone-

refining and potassium fusion.[11] To avoid contact with oxygen after purification, the mixture was transferred, in a clean vacuum system, to a 2-mm thick quartz optical cell. The crystal in the cell was grown from the melt by lowering the cell through a sharp temperature gradient into liquid nitrogen. Thermal contact with the liquid helium bath during the spectroscopic experiment was provided by introducing an atmosphere of helium gas into the cell after the crystal was grown. The use of isotopic mixed crystals and liquid helium temperatures provides extremely sharp spectra. Many of the weaker lines and much of the fine structure would not be detected under conditions that yield broader spectra. An appreciable intensity enhancement also is obtained from the efficient host-guest excitation transfer that occurs[12] in these systems.

The spectral line positions were measured relative to the emission of an iron-neon hollow cathode standard[13] using a precision comparator made by the Fred C. Hensen Company, Pasadena, California. Wavelengths were calculated and checked using the IBM System/360 Model 50 computer. Corresponding vacuum wavenumbers were obtained from the National Bureau of Standards' "Table of Wavenumbers."[14] The precision for the transition energies listed in Table I is two units in the last significant figure. The spectral intensities were estimated visually and are designated by s = strong, m = medium, w = weak, vw = very weak.

A Cary 81 Raman Spectrophotometer was used to obtain the $C_{10}D_8$ phonon spectrum shown in Fig. 3.

III. RESULTS

A. Vibrational Assignments

The phosphorescence spectrum is shown in Fig. 1, and the transition energies and assignments are given in Table I. An attempt was made to verify the assignment of both the g and u fundamental frequencies by their activity in progressions. The IBM System/360 Model 50 computer was used to compare all possible combinations giving total g symmetry of roughly 80 frequencies with the phosphorescence spectrum. These frequencies had been assigned as fundamentals in earlier investigations[15] of the Raman and infrared spectra. Unfortunately this technique is practical only to the 0, 0-1000 cm^{-1}. Beyond that point, numerous combinations of both g and u modes are possible for each observed transition, and a detailed analysis cannot be made with confidence. A 4 cm^{-1} agreement between the combination and phosphorescence frequency was considered satisfactory. The transitions shifted from the 0, 0 by more than 1000 cm^{-1} are assigned either as fundamentals in agreement with the Raman data[8] or as the expected combinations involving ν_1, ν_5, ν_7, and ν_{17}. Some discussion of these assignments is given below.

Lines 1 and 2 in Table 1 are assigned as α- and β-deuteronaphthalenes to agree with the isotope effect on the $^1B_{2u} \leftarrow\!\!\!\rightarrow {}^1A_g$ transitions. Preliminary evidence[16] indicates, however, that this assignment may be reversed for the $^3B_{1u}$ state even though the magnitude of the shifts agree with that found for the singlet state.

It is reasonable to assign either Line 26 or Line 28 as ν_{16} and the other as 360 cm^{-1} (b_{1u}) + 618 cm^{-1} (b_{2u}). No other combination of gerade or ungerade fundamentals resulting in total g symmetry agrees with the energy of Line 26. Line 28 is favored as the fundamental because it is more intense and appears in combination with ν_1, ν_5, ν_7, and ν_{17} while Line 26 does not. Line 28 at 0, 0-982.8 cm^{-1} might also be assigned as 176 (b_{3u}) + 810 (b_{1u}), but recently it has been found[5d] that the 810 cm^{-1} infrared transition disappears at low temperatures.

Lines 29, 30, and 31 can be assigned from the following list: $2 \times \nu_{17}$ = 1020.0 cm^{-1} (a_g), $\nu_1 + \nu_{17}$ = 1022.0 cm^{-1} (b_{3g}), $2 \times \nu_1$ = 1024.0 cm^{-1} (a_g), and ν_3 (a_g). Since all four lines are resolved in the Raman spectra,[8] and only the 1022 cm^{-1} frequency appears in combination with ν_5 and ν_7, it is concluded that both ν_3 and $\nu_1 + \nu_{17}$ probably are present but unresolved in the phosphorescence spectrum.

Other than several u × u combinations, the assignments for Lines 32-36 may be chosen from the following list: ν_4 (a_g), $\nu_2 + \nu_{10}$ = 1153.2 (b_{1g}), $\nu_2 + \nu_{13}$ = 1157.4 (b_{2g}), $\nu_{10} + \nu_{15}$ = 1159.9 (b_{3g}), $\nu_{13} + \nu_{15}$ = 1164.1 (a_g), ν_{19} (b_{3g}), ν_{12} (b_{1g}), and ν_{16} (b_{2g}). The last two possibilities, however, contradict calculations[17] that show all b_{1g} and b_{2g} modes at less than 1100 cm^{-1}. Due to the lack of decisive criteria, none of these lines is assigned.

Table II summarizes the observed fundamentals. These assignments are consistent with, in fact supported by, the Raman scattering tensors[8] and $^3B_{1u} \leftarrow {}^1A_g$ polarized absorption.[9b] A few additional comments regarding the data in Table II should be made: Although ν_2 is very weak in the phosphorescence spectrum, its

appearance in the Raman and fluorescence spectra leads to a definitive assignment as a_g . No combination frequency agrees with 469.5 and 727.5 cm^{-1} thereby supporting the assignments of these as fundamentals. Other than ν_{12}, alternative assignments for 950.8 cm^{-1} are 210 (a_u) + 740 (a_u) and 2 × 475 (b_{3u}), but both of these possibilities are inconsistent with the Raman tensor for this mode that is characteristic of a b_{1g} vibration. Other than ν_{15}, the only assignment for 771.5 cm^{-1} is 210 (a_u) + 562 (b_{2u}), but the 210 cm^{-1} transition, predicted by calculations,[18] has never been observed.

Mixing of ν_1 and ν_{17}, allowed by the reduced symmetry of the molecule in the crystal field,[19] is evident from the form of the Raman scattering tensors and the appearance in phosphorescence of both combinations with ν_2, ν_5, ν_7, ν_{11}, ν_{13}, ν_{14}, and ν_{16}. The near degeneracy of ν_1 and ν_{17} was suspected first from gas-phase spectroscopic data.[20] Fluorescence spectra[21] of naphthalene dissolved in glass matrices tended to confirm this suspicion although the vibrational frequencies in the matrix were quite different from those observed in the vapor. Figure 2 shows ν_1 and ν_{17} clearly resolved in the mixed crystal phosphorescence spectrum at frequencies nearly identical to those observed for naphthalene vapor.

B. Lattice Vibrations

The transitions near the 0, 0 in the mixed crystal phosphorescence spectrum are assigned to lattice vibrations or phonons in the final state because of the small shift from the 0, 0 and the relatively large linewidth. The common distinction between lattice vibrations and molecular vibrations in molecular crystals is made. Line 5 in Table I displaced 8.2 cm^{-1} from the 0, 0 is left unassigned because both the shift and linewidth are too small to be convincingly interpreted in terms of lattice modes.

The remaining transitions near the 0, 0 are compared in Table III with the Raman active lattice modes of pure naphthalene and deuteronaphthalene crystals. The Raman spectrum of the deuteronaphthalene phonons at room temperature is shown in Fig. 3. The lack of agreement between the mixed crystal and pure crystal frequencies may indicate that the lattice vibrations of the isotopic guest are localized, to some extent, in the region of the guest. In a perturbation approach using the eigenfunctions of the pure crystal as a basis, one would expect the mixed crystal phonon spectrum, as observed in phosphorescence, to depend upon the density of states of the pure crystal as well as the energy of the $\underset{\sim}{k} = \underset{\sim}{0}$ levels. In view of this hypothesis and the observation of a transition at 0, 0-27 cm^{-1}, it is of interest that preliminary neutron diffraction data indicate[22] a peak in the naphthalene lattice spectrum (phonon density of states) between 20 and 30 cm^{-1}.

It is also apparent from Table III and the early polarization data of Kastler and Rousset[23] that the phonon $\underset{\wedge}{k} = \underset{\wedge}{0}$ components occur in symmetric and antisymmetric pairs split by 3 to 20 cm^{-1}. Such small splittings may imply that a rotational or librational Frenkel exciton model can be used to describe the lattice vibrations in molecular crystals as it has been used[24] to describe the molecular vibrations and electronic states. An effect to be explained by such a model is the coupling between the phonons and electronic transitions. For example, the phonon transitions in the 4.2 °K mixed crystal phosphorescence are weaker than the no-phonon transition by at least a factor of 100, in contrast to the fluorescence and phosphorescence of the pure crystal at 77 °K where the transition intensities[25] appear equal.

C. Spin-Orbit Coupling

Spin-orbit coupling generally is accepted[26] as the mechanism that explains interconversions between molecular singlet and triplet states. The polarizations of the vibronic transitions assist in evaluating the active spin-orbit routes provided the symmetry properties of the vibrational modes and electronic states are known. For the case of naphthalene, the 0, 0 and totally symmetric vibronic transitions are the most intense components of the $^3B_{1u} \leftrightarrow {}^1A_g$ spectra. This fact implies that the lowest triplet state is geometrically similar to the ground state and is primarily mixed with singlet states via the first-order spin-orbit term in the Hamiltonian.

An interesting and unrecognized feature of the naphthalene phosphorescence spectrum is the activity of a few non-totally symmetric vibrational modes. This spectral feature is significant to the intramolecular heavy-atom effect on the phosphorescence process since the phosphorescence of 1, 4- and 2, 3-dihalonaphthalenes consists[27] of two subspectra. One, as in naphthalene, is composed of the 0, 0 and totally symmetric vibronic transitions. The other (subspectrum II) requires a vibronic perturbation. As pointed out by El-Sayed,[28] the presence or absence of subspectrum II in naphthalene, the parent compound, depends upon the mechanism of the heavy-atom effect. It therefore is of interest to examine whether any of the non-totally symmetric vibronic transitions in naphthalene correlate with subspectrum II and the spin-

orbit coupling mechanism of the halonaphthalenes. The halonaphthalene subspectrum II primarily is polarized in the molecular plane, while the naphthalene vibronic transitions primarily are polarized[9b] perpendicular to the molecular plane. It therefore is concluded that the presence of a heavy atom, at least for this specific case, does not intensify mechanisms present in the parent compound but essentially introduces new spin-orbit routes which, according to El-Sayed,[28] may involve carbon-halogen vibrations or sigma electrons of the carbon-halogen or carbon-carbon bonds.

REFERENCES

1. (a) G.C. Nieman and D.S. Tinti, J. Chem. Phys. 46, 1432 (1967); (b) E.R. Bernstein, S.D. Colson, D.S. Tinti, and G.W. Robinson, J. Chem. Phys. 00, 0000 (1968), "Static Crystal Effects on the Vibronic Structure of the Phosphorescence, Fluorescence, and Absorption Spectra of Benzene Isotopic Mixed Crystals."
2. A.C. Albrecht, J. Chem. Phys. 33, 169 (1960); ibid. 38, 354 (1963).
3. G.W. Robinson, J. Chem. Phys. 47, 1967 (1967).
4. (a) A. Kalantar, private communication; (b) G.C. Nieman, private communication.
5. (a) J.M. Hollas, J. Mol. Spectry. 9, 138 (1962); (b) D.P. Craig and H.C. Wolf, J. Chem. Phys. 40, 2057 (1964); (c) N. Neto, M. Scrocco, and S. Califano, Spectrochim. Acta 22, 1981 (1966); (d) N. Rich, Ph.D. thesis, University of Southern California, 1968.
6. (a) F.R. Lipsett and G. Macpherson, Can. J. Phys. 44, 1485 (1966); (b) E.B. Priestley, unpublished results.
7. (a) Ref. 6a; (b) P.A. Pröpstl and H.C. Wolf, Z.Naturforsch. 189, 724 (1963); (c) D.M. Hanson, unpublished results.
8. A.R. Gee and D.M. Hanson, "Raman Scattering Tensors of Crystalline Naphthalene," to be submitted for publication in J. Chem. Phys.

9. (a) E.B. Priestley and A. Haug, J. Chem. Phys. 00, 0000 (1968), "Phosphorescence Spectrum of Pure Crystalline Naphthalene"; (b) G. Castro and G.W. Robinson, "Singlet-Triplet Absorption of Crystalline Naphthalene," to be submitted for publication in J. Chem. Phys.

10. R.S. Mullikan, J. Chem. Phys. 23, 1997 (1955).

11. D.M. Hanson and G.W. Robinson, J. Chem. Phys. 43, 4174 (1965).

12. M.A. El-Sayed, M.T. Wauk, and G.W. Robinson, Mol. Phys. 5, 205 (1962).

13. H.M. Crosswhite, The Spectrum of Iron I, Johns Hopkins Spectroscopic Report No. 13, The Johns Hopkins University, Department of Physics, Baltimore, Maryland (1958).

14. C.D. Coleman, W.R. Bozman, and W.F. Meggers, Table of Wavenumbers, National Bureau of Standards Monograph 3, U.S. Government Printing Office, Washington, D.C. (1960).

15. (a) W.B. Person, G.C. Pimentel, and O. Schnepp, J. Chem. Phys. 23, 230 (1955); (b) E.R. Lippincott and E.J. O'Reilly Jr., J.Chem. Phys. 23, 238 (1955); (c) A.L. McClellan and G.C. Pimentel, J. Chem. Phys. 23, 245 (1955); (d) H. Luther, K. Feldmann, and B. Hampel, Z. Elektrochem. 59, 1008 (1955); (e) H. Luther, G. Brandes, H. Günzler, and B. Hampel, Z. Elektrochem. 59, 1012 (1955); (f) J. Brandmüller and E. Schmid, Z. Physik 144, 428 (1956); (g) S.S. Mitra and H.J. Bernstein, Can. J. Chem. 37, 553 (1959);

(h) N.I. Zhirnov, Opt. Spektrosk. 9 , 734 (1960) [Opt. Spektrosc. 9, 385 (1960)]; (i) H. Luther and H.J. Drewitz, Z. Elektrochem. 63, 546 (1962); (j) A brief review of the above and other work is given in Ref. 5a.

16. G. Castro, unpublished results.

17. D.J. Evans and D.B. Scully, Spectrochim. Acta 20, 891 (1964).

18. D.B. Scully and D.H. Whiffen, Spectrochim. Acta 16, 1409 (1960).

19. (a) V.L. Strizhevsky, Opt. Spektrosk. 8 , 165 (1960) [Opt. Spektrosc. 8, 86 (1960)]; (b). E.R. Bernstein, "Site Effects in Isotopic Mixed Crystals--Site Shift, Site Splitting, Orientational Effect and Intermolecular Fermi Resonance in the Vibrational Spectrum of Benzene," to be submitted for publication in the J.Chem. Phys.

20. D.P. Craig, J.M. Hollas, M.F. Redies, and S.C. Wait Jr., Phil. Trans. Roy. Soc. London A253, 543 (1961).

21. T.N. Bolotnikova, Opt. Spektrosk. 7 , 138 (1959) [Opt. Spektrosc. 7, 24 (1959)].

22. S.H. Walmsley, private communication.

23. A. Kastler and A. Rousset, J. Phys. Radium 2, 49 (1941).

24. (a) J. Frenkel, Phys. Rev. 37, 17 (1931); ibid. 37, 1276 (1931); (b) A.S. Davydov, Theory of Molecular Excitons (McGraw-Hill Book Co., Inc., New York, 1962); (c) The possibility of describing the librational motions in molecular

crystals by the Frenkel exciton model arose through discussions with Professors G.W. Robinson and R. Kopelman.

25. (a) S.D. Colson, D.M. Hanson, R. Kopelman, and G.W. Robinson, J. Chem. Phys. 48, 2215 (1968); (b) Ref. 9a.

26. D.S. McClure, J. Chem. Phys. 17, 905 (1949); ibid. 20, 682 (1952).

27. T. Pavlopoulos and M.A. El-Sayed, J. Chem. Phys. 41, 1082 (1964).

28. M.A. El-Sayed, J. Chem. Phys. 43, 2864 (1965).

TABLE I. Phosphorescence Assignments

Line	$\bar{\nu}$ (cm^{-1})	$\Delta\bar{\nu}$ (cm^{-1})	Intensity	Assignment	Symmetry in D_{2h}	Predicted Value ($\pm 1\,cm^{-1}$)
1	21224.1	-15.9	vw	β-D, 0-0		
2	21216.1	-7.9	vw	α-D, 0-0		
3	21211.7	-3.5	m	^{13}C, 0-0		
4	21208.2	0.0	s	0-0		
5	21200.0	8.2	vw			
6	21181.2	27.0	vw	phonon		
7	21162.3	45.9	w	phonon		
8	21153.0	55.2	w	phonon		
9	21131.4	76.8	vw	phonon		
10	21117.3	90.9	vw	phonon		
11	20815.6	392.6	m	ν_{10}	b_{1g}	
12	20738.7	469.5	vw	ν_{14}	b_{2g}	
13	20704.8	503.4	vw	$^{13}C\ \nu_{17}$		
14	20702.7	505.5	w	$^{13}C\ \nu_{1}$		

TABLE I. (continued)

Line	$\bar{\nu}$ (cm^{-1})	$\Delta\bar{\nu}$ (cm^{-1})	Intensity	Assignment	Symmetry in D_{2h}	Predicted Value ($\pm 1\,cm^{-1}$)
15	20698.2	510.0	s	ν_{17}	b_{3g}	
16	20696.2	512.0	s	ν_1	a_g	
17	20653	556	vw	ν_1, ν_{17} + phonons		~557
18	20642	567	vw	ν_1, ν_{17} + phonons		~566
19	20480.7	727.5	vw	ν_{11}	b_{1g}	
20	20443.4	764.8	vw	ν_2	a_g	
21	20436.7	771.5	vw	ν_{15}	b_{2g}	
22	20422.3	785.9	vw	$2 \times \nu_{10}$	a_g	785.2
23	20306.1	902.1	vw	$\nu_{10} + \nu_{17}$	b_{2g}	902.6
24	20303.9	904.3	vw	$\nu_{10} + \nu_1$	b_{1g}	904.6
25	20257.4	950.8	vw	ν_{12}	b_{1g}	
26	20235	973	w			
27	20228.4	979.8	vw	$\nu_{14} + \nu_{17}$	b_{1g}	979.5
27a	20228	982	vw	$\nu_{14} + \nu_1$	b_{2g}	981.5

TABLE I. (continued)

Line	$\bar{\nu}$ (cm^{-1})	$\Delta\bar{\nu}$ (cm^{-1})	Intensity	Assignment	Symmetry in D_{2h}	Predicted Value ($\pm 1\,cm^{-1}$)
28	20225.4	982.8	m	ν_{16}	b_{2g}	
29	20187.7	1020.5	m	$2 \times \nu_{17}$	a_g	1020.0
30	20186.0	1022.2	m	ν_3, $\nu_1 + \nu_{17}$	a_g, b_{3g}	1022.0
31	20184.3	1023.9	w	$2 \times \nu_1$	a_g	1024.0
32	20060.8	1147.4	m			
33	20057.1	1151.1	vw			
34	20053.9	1154.3	m			
35	20048.8	1159.4	m			
36	20045.3	1162.9	w			
37	19971	1237	vw	$\nu_{17} + \nu_{11}$	b_{2g}	1237.5
38	19967.2	1241.0	vw	$\nu_1 + \nu_{11}$	b_{1g}	1239.5
39	19933.9	1274.3	vw	$\nu_{17} + \nu_2$	b_{3g}	1274.8
40	19929.7	1278.5	vw	$\nu_1 + \nu_2$	a_g	1276.8
41	19868.6	1339.6	vw			

TABLE I. (continued)

Line	$\bar{\nu}$ (cm^{-1})	$\Delta\bar{\nu}$ (cm^{-1})	Intensity	Assignment	Symmetry in D_{2h}	Predicted Value ($\pm 1 cm^{-1}$)
42	19857.3	1350.9	vw			
43	19840.7	1367.5	vw			
44	19833.9	1374.3	w	$\nu_{16} + \nu_{10}$	b_{3g}	1375.4
45	19832.0	1376.2	w	^{13}C ν_5		
46	19826.6	1381.6	s	ν_5	a_g	
47	19748.8	1459.4	vw			
48	19717.1	1491.1	vw	$\nu_{17} + \nu_{16}$	b_{1g}	1492.8
49	19714.5	1493.7	vw	$\nu_1 + \nu_{16}$	b_{2g}	1494.8
50	19681.8	1526.4	vw			
51	19641.8	1566.4	vw			
52	19639.0	1569.2	w	^{13}C ν_7		
53	19631.2	1577.0	s	ν_7	a_g	
54	19614.8	1593.4	vw			
55	19583.1	1625.1	vw			

TABLE I. (continued)

Line	$\bar{\nu}$ (cm^{-1})	$\Delta\bar{\nu}$ (cm^{-1})	Intensity	Assignment	Symmetry in D_{2h}	Predicted Value ($\pm 1\ cm^{-1}$)
56	19579.0	1629.2	m	ν_{22}	b_{3g}	
57	19549	1659	vw			
58	19539	1669	vw			
59	19533.1	1675.1	vw			
60	19432.6	1775.6	w	$\nu_5 + \nu_{10}$	b_{1g}	1774.2
61	19315.5	1892.7	m	$\nu_5 + \nu_{17}$	b_{3g}	1891.6
62	19312.5	1895.7	s	$\nu_5 + \nu_1$	a_g	1893.6
63	19238.9	1969.3	vw	$\nu_7 + \nu_{10}$	b_{1g}	1969.6
64	19121.5	2086.7	m	$\nu_7 + \nu_{17}$	b_{3g}	2087.0
65	19119.7	2088.5	m	$\nu_7 + \nu_1$	a_g	2089.0
66	19070.4	2137.8	vw			
67	18921.4	2286.8	vw			
68	18873.5	2334.7	vw	$\nu_5 + \nu_{12}$	b_{1g}	2332.4
69	18841.8	2366.4	vw	$\nu_5 + \nu_{16}$	b_{2g}	2364.4

TABLE I. (continued)

Line	$\bar{\nu}$ (cm^{-1})	$\Delta\bar{\nu}$ (cm^{-1})	Intensity	Assignment	Symmetry in D_{2h}	Predicted Value ($\pm 1\,cm^{-1}$)
70	18804.7	2403.5	vw	$\nu_5 + \nu_3$	a_g	2401.4
71	18801.6	2406.6	w			
72	18678.0	2530.2	vw	$\nu_7 + \nu_{12}$	b_{1g}	2527.8
73	18670.6	2537.6	vw			
74	18667.2	2541.0	vw			
75	18662.2	2546.0	w			
76	18658.5	2549.7	vw			
77	18651.5	2556.7	m	$\nu_7 + \nu_{16}$	b_{2g}	2559.8
78	18607.8	2600.4	vw	$\nu_7 + \nu_3$	a_g	2596.8
79	18484.0	2724.2	vw	$\nu_7 + \nu_4$	a_g	2724.4
80	18469.5	2738.7	w			
81	18443.5	2764.7	s	$2 \times \nu_5$	a_g	2763.2
82	18365.0	2843.2	vw			
83	18331	2877	vw			

TABLE I. (continued)

Line	$\bar{\nu}$ (cm^{-1})	$\Delta\bar{\nu}$ (cm^{-1})	Intensity	Assignment	Symmetry in D_{2h}	Predicted Value ($\pm 1\ cm^{-1}$)
84	18302	2906	vw			
85	18254.2	2954.0	s	$\nu_7 + \nu_5$	a_g	2958.6
86	18197.2	3011.0	w	$\nu_5 + \nu_{22}$	b_{3g}	3010.8
87	18054.9	3153.3	w	$2 \times \nu_7$	a_g	3154.0
88	18002.4	3205.8	vw	$\nu_7 + \nu_{22}$	b_{3g}	3206.2
89	17932.7	3275.5	m	$2 \times \nu_5 + \nu_1$	a_g	3275.2
90	17743.1	3465.1	m	$\nu_7 + \nu_5 + \nu_1$	a_g	3470.6
91	19544	3664	vw	$2 \times \nu_7 + \nu_1$	a_g	3666.0
92	17066.4	4141.8	vw	$3 \times \nu_5$	a_g	4144.8
93	16880.2	4328.0	w			

TABLE II. The gerade fundamentals appearing in the $C_{10}H_8$ phosphorescence spectrum.

D_{2h} Symmetry	Number	Frequency (cm^{-1})
a_g	ν_1	512.0
	ν_2	764.8
	ν_5	1381.6
	ν_7	1577.0
b_{1g}	ν_{10}	392.6
	ν_{11}	727.5
	ν_{12}	950.8
b_{2g}	ν_{14}	469.5
	ν_{15}	771.5
	ν_{16}	982.8
b_{3g}	ν_{17}	510.0
	ν_{22}	1629.2

TABLE III. Comparison of phonon frequencies (cm^{-1}) in mixed and pure naphthalene crystals.

$C_{10}H_8$ in $C_{10}D_8$[a] 4.2°K	$C_{10}H_8$[b] 4.2°K	$C_{10}D_8$[c] 4.2°K	$C_{10}H_8$[b] 293°K	$C_{10}D_8$[a] 293°K
27				
46				
55	56	52	46	42
	69	64	51	46
77	81	76	71	68
	88	82	74	
99	120	110	109	99
	141	128	125	112

[a]Present work.

[b]M. Suzuki, T. Yokoyama, and M. Ito, Tech. Report ISSP, Series A, No. 284 (1967).

[c]Estimated from the 293°K data for $C_{10}D_8$ and the temperature dependence of the $C_{10}H_8$ frequencies.

FIG. 1. The phosphorescence spectrum of $C_{10}H_8$ in a $C_{10}D_8$ host crystal. Although transition energies are marked, the abscissa is linear in wavelength. The ordinate gives the percent transmission of the photographic plate. The last four lines in Table I are not shown here. The arrow designates the position of the 0, 0 transition of β-methylnaphthalene.

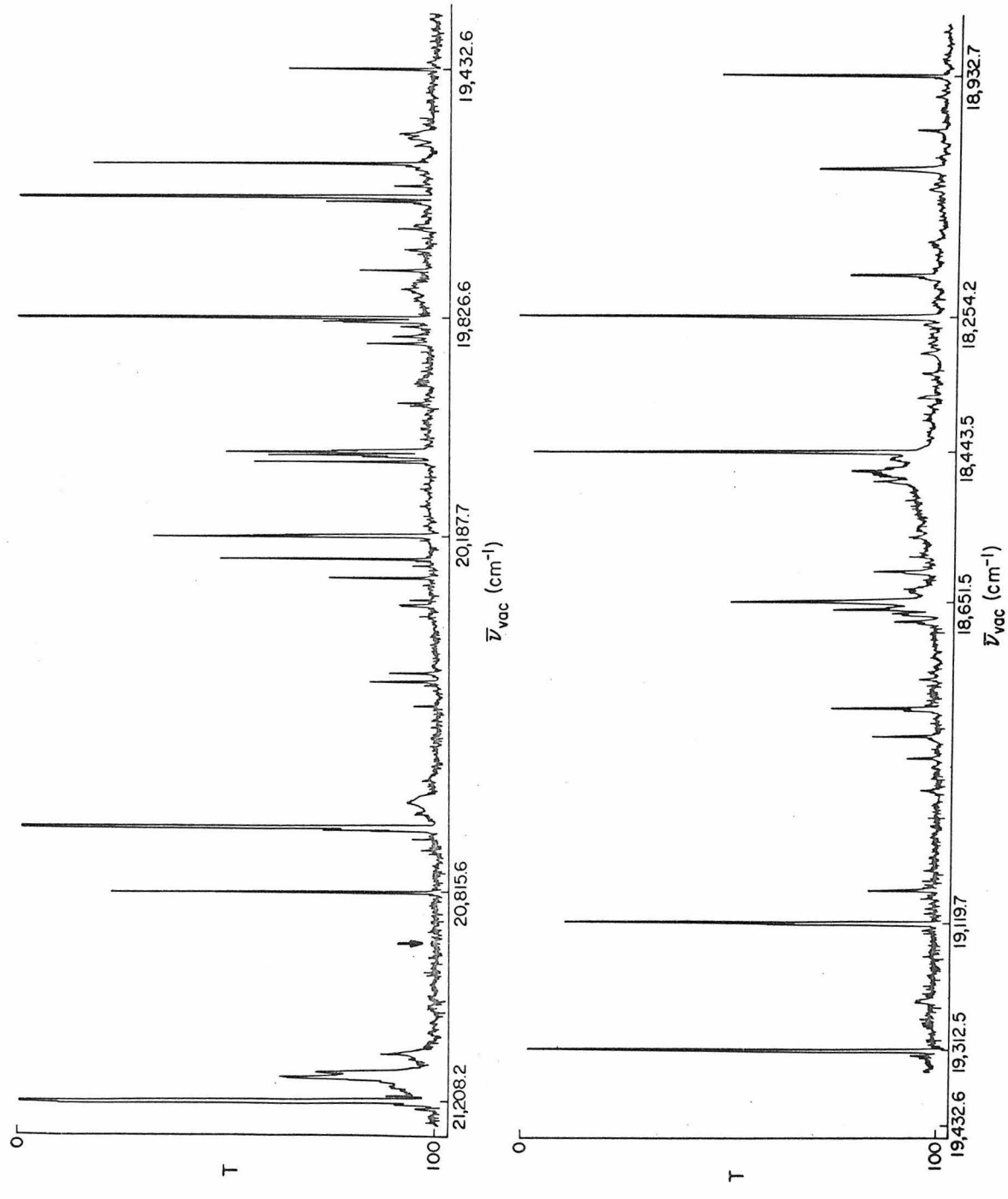
0
T
100
21,208.2
20,815.6
20,187.7
19,826.6
19,432.6
$\bar{\nu}_{vac}$ (cm^{-1})
0
T
100
19,432.6
19,312.5
19,119.7
18,651.5
18,443.5
18,254.2
18,932.7
$\bar{\nu}_{vac}$ (cm^{-1})

FIG. 2. The nearly degenerate fundamentals ν_1 and ν_{17}.

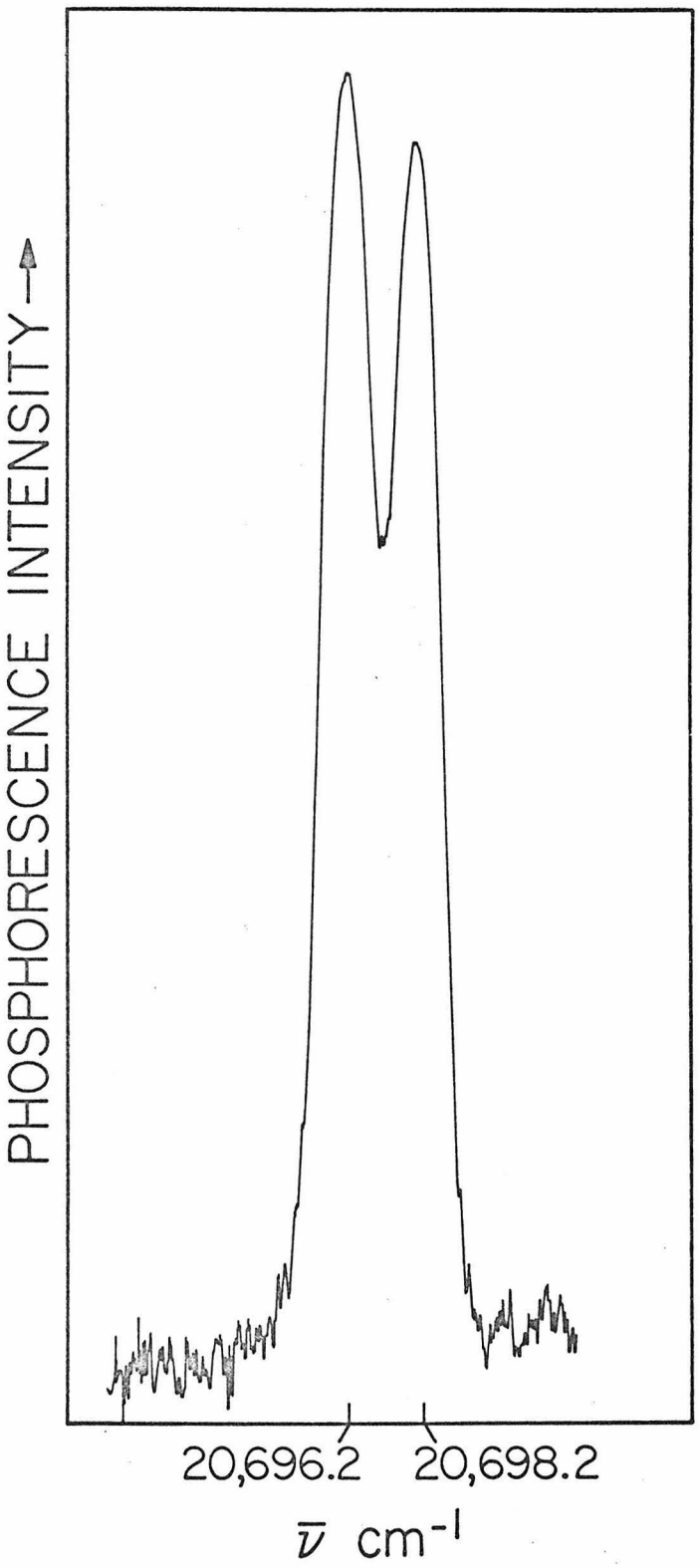
PHOSPHORESCENCE INTENSITY →
20,696.2
20,698.2
$\bar{\nu}$ cm^{-1}

FIG. 3. Room temperature Raman spectrum of the deuteronaphthalene lattice vibrations.

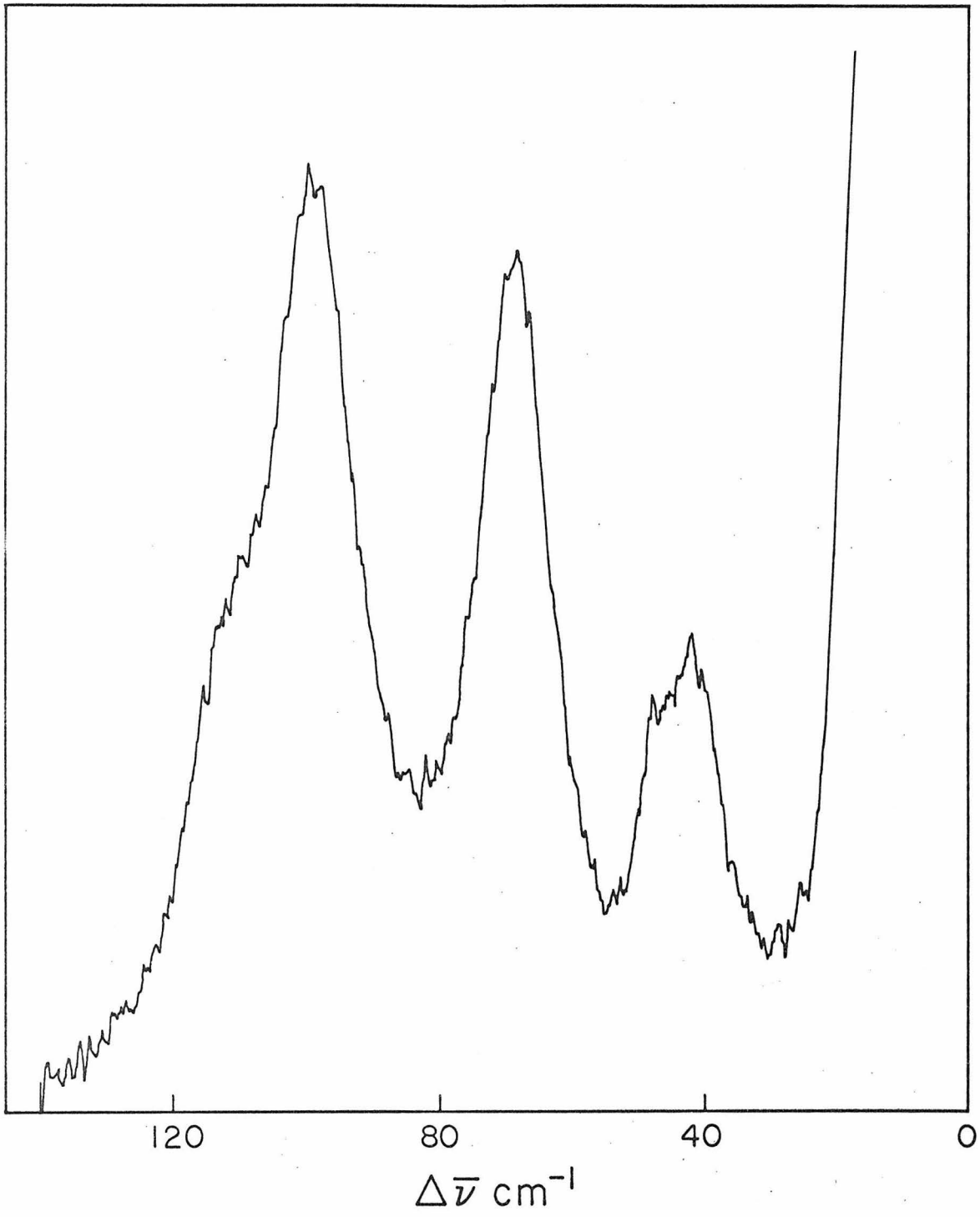
120
80
40
0
Δν̄ cm⁻¹

PART VII

Raman Scattering Tensors for Single Crystals of Naphthalene

I. INTRODUCTION

The effect of the crystalline state upon molecular spectra has been studied extensively, [1] but relatively little attention has been given to Raman scattering by molecular crystals. The observation of polarized Raman scattering from oriented single crystals allows the scattering tensor for each vibrational mode to be determined. Such experimental data allow unambiguous vibrational assignments to be made and provide a measure of the intermolecular interactions in the crystal.

Generally the zero-order description of a molecular crystal is based on the oriented gas model. In this approximation spectral intensities, polarizations, and frequencies are identical to those of the molecule in the gas phase. Each state other than the ground state is at least n-fold degenerate where n is the number of molecules in the crystal. The intermolecular interactions in the crystal remove these degeneracies producing spectral splittings, frequency shifts, and intensity changes.

The experimental data[2] reported in this paper on the polarized Raman spectra of crystalline naphthalene serve to clarify ambiguities[3] in the assignment of normal frequencies, and to test intramolecular[4] and intermolecular[5] potentials. In addition, the data should complement and be compared with results of recent experimental[6] and theoretical[7] investigations of the effect of intramolecular interactions in crystalline benzene.

II. EXPERIMENTAL

Eastman recrystallized naphthalene was purified by zone-refining and potassium fusion.[8] Single crystals were grown by slowly lowering (0.05 in./h) evacuated pyrex tubes (13 mm i.d.) of naphthalene from 100 °C through a sharp temperature gradient to 60 °C. The transparent crystals were cooled slowly to room temperature. After removing the crystals from the tube, the cleavage plane (001) was found; the crystallographic axes were identified; and the crystal was cut along the principal axes of the refractive index ellipsoid. The crystal birefringence, the extinction directions, the conoscopic isogyres, and a Laue X-ray diffraction pattern were used to identify[9, 10] the crystal axes. Agreement among these independent determinations verified that the (001) plane had been found in the first step because naphthalene, like anthracene, also cleaves along the (100) plane. The crystal was cut with precision commensurate with the optical experiment by using a jig having faces cut at the appropriate angles. The accuracy of the polarization measurements is limited by the collection of Raman scattered light by f/12 optics. This accuracy is sufficient for the present purposes because only qualitative measurements are needed as the light scattering is very anisotropic.

Raman spectra of the crystals obtained at room temperature and 77 °K are shown in Fig. 1. For the room temperature experiment, crystals polished with a clean chamois were placed on a microscope slide in the optical train shown in Fig. 2. For the low temperature

experiment, the polished crystal was placed in a cell, shown in Fig. 3, supported at the end of a stainless steel rod in a double pyrex Dewar.[6a] By threading the rod into different faces of the cell, the crystal could be rotated while immersed in liquid nitrogen. A few cracks developed in the crystal while being cooled to 77 °K, but by judicious positioning of the crystal, scattering from the cracks was avoided. Only a few spectra were photographed at 77 °K since only one doublet (ν_{17}) was resolved.

The data obtained from these experiments is given in Table I. Line positions were measured with a precision comparator relative to the emission of an iron-neon hollow cathode standard[11] recorded between the polarized Raman spectra. Wavelengths were calculated and checked using the IBM System/360 Model 50 computer. Corresponding vacuum wavenumbers were obtained from the National Bureau of Standards' "Table of Wavenumbers."[12] The frequency shifts given in Table I are accurate to ± 2 cm^{-1}, and where tenths are specified, to $\pm$ 0.5 cm^{-1}.

The relative magnitudes of pairs of elements in the Raman scattering tensor is determined in these experiments. The procedure used has been described previously.[13] Briefly, light scattered by virtue of a diagonal component is separated from that scattered by an off-diagonal component by placing one Glan-Thompson polarizing prism above another, with orientations differing by 90°, in front of the spectrograph slit. In this configuration light polarized parallel to that of the source passes through half the slit while light polarized

perpendicular to this passes through the other half. Visual estimates of the intensities on the photographic plates also are given in Table I and designated by S = strong, M = medium, W = weak, and F = faint in order of decreasing intensity.

A Raytheon LG12, 1 W argon ion laser was used to excite the Raman spectrum. Spectra were recorded with a f/12 2-m Czerny-Turner spectrograph equipped with a 600 line/mm Bausch and Lomb grating (212 × 157 mm) blazed at 17°27'. The plate factor in second order is 3.6 Å/mm, and the actual resolving power is approximately 50,000. The very excellent grating combined with a pre-slit interference filter provides spectra almost entirely free of ghosts and scattered light. Kodak 103a-F plates were used generally with exposure time of 2 h, although the more intense lines could be photographed in 10 min.

The number of lines observed in the naphthalene Raman spectrum often has been used as a criterion of instrument sensitivity.[14] It therefore is of interest that 58 lines are recorded in Table I, although some lines reported in other investigations[15] were not observed, presumably due to the higher purity[8] of our samples.

The IBM System/360 Model 50 computer was used to compare all sum and difference combinations of roughly 80 possible fundamentals[16] looking for 4 cm^{-1} agreement with the Raman data. Unfortunately a confident detailed analysis cannot be made because several assignments are possible for each line; consequently, only

the fundamentals are assigned in Table I. The reader should be assured that more than one reasonable assignment exists for the remaining frequencies.

III. RESULTS AND DISCUSSION

A. Raman Scattering Tensors

The Raman scattering of light by molecular vibrations is described by a symmetric tensor.[17] In an oriented gas approximation, the crystal tensor is determined by molecular properties, and the total intensity of the light scattered by the crystal is just the sum of the light scattered by the individual molecules. The Raman scattering tensor of the crystal must be measured in a coordinate system conforming with the symmetry and optical properties of the crystal. For polarization measurements the coordinate axes must coincide with the principal axes of the refractive index ellipsoid,[18] X, Y, and Z respectively referring to the acute bisectrix, the principal optic axis, and the obtuse bisectrix. These axes are shown on the model of the naphthalene crystal pictured in Fig. 4. The use of the crystallographic axes $\underset{\sim}{a}$, $\underset{\sim}{b}$, and $\underset{\wedge}{c}$ or $\underset{\sim}{a}$, $\underset{\sim}{b}$, and $\underset{\wedge}{c}'$, where $\underset{\wedge}{c}'$ is perpendicular to $\underset{\sim}{a}$ and $\underset{\sim}{b}$, is not suitable for this experiment since light propagating along $\underset{\sim}{b}$ is not polarized along $\underset{\wedge}{a}$ and $\underset{\wedge}{c}$ but along X and Z.

The relative magnitudes of the elements in the crystal tensor can be obtained from the molecular tensor by a similarity transformation relating the molecular coordinate system to the crystal

coordinate system. The direction cosines in the transformation are well known.[19] The polarized light scattered by the crystal is proportional to the square of the appropriate tensor element. The intensities, i.e. tensor elements squared, are given in tensor form in Fig. 5. These data are rearranged in Table II to facilitate a comparison with Table I. The notation M, L, and N is used to designate the short molecular axis, the long molecular axis, and the normal to the molecular plane. In the coordinate system recommended by Mullikan,[20] M transforms as B_{1u}, L as B_{2u}, and N as B_{3u}.

Each element in the molecular tensor for a totally-symmetric vibration is unique, although symmetry does require that the tensor be diagonal. The relative magnitudes of the three diagonal elements depend upon the specific vibration. The following approximation, however, allows a relative estimate of the tensor elements to be made. It is assumed that the element in the Raman scattering tensor for an a_g mode is independent of the vibration and proportional to the corresponding element in the optical polarizability tensor. This essentially assumes that the change in polarizability due to the molecular vibration is proportional to the polarizability. The a_g intensities given in Fig. 5 and Table II are derived from this assumption and the fact[21] that the normal, long, and short axis optical polarizabilities are in the ratio of 1.0 to 4.2 to 3.3. Note that the data in Fig. 5 and Table II do not make any predictions about absolute intensities or relative intensities of different modes.

It is quite obvious from Table II that the scattered light is sufficiently anisotropic to distinguish the vibrational modes of different symmetry. If the intermolecular interactions are sufficiently large, the n-fold degeneracy of each molecular mode will be removed, and the two $\underset{\wedge}{k} = \underset{\wedge}{0}$ factor group components should be observed. The tensor for the a_g factor group component consists of the diagonal and xz elements while that for the b_g component consists of xy and yz. The magnitudes of these elements may still be related to those of the oriented gas model but this relationship is not necessary nor expected. The main conclusions of the above discussion are that in the limit of weak intermolecular interactions no exciton splitting is expected and the Raman intensities should conform to the predictions of the oriented gas model. Within these conditions, polarization measurements identify the normal modes and allow the magnitudes of the intermolecular interactions to be evaluated.

In spite of their obvious value such measurements are not very common. Some time ago Nedungadi[22] reported gerade vibrational exciton splitting in crystalline naphthalene that was assigned on the basis of polarization experiments. Under improved resolution, Raman intensity, and decreased scattered light, it is found that these lines actually arise from nearly degenerate molecular vibrations (vide infra). Polarization spectra of the naphthalene lattice modes were reported by Kastler and Rousset.[23] The real utility of Raman polarization work awaited the development of the cw-laser.

This advance quickly was popularized by S.P.S. Porto and co-workers.[13] Laser Raman spectroscopy recently has been used with crystals of naphthalene, anthracene and some halobenzenes by Ito, Suzuki, and Yokoyama.[24] Unfortunately the polarization measurements were made in the abc′ crystal axis system which, as discussed above, may give misleading results.

B. Assignment of the Fundamental Frequencies

The assignment of the fundamental vibrational frequencies of molecular naphthalene has not been made with certainty. This fact often has been mentioned in the literature.[25] For the gerade modes the problem arises because all fundamentals are not Raman active and some are nearly degenerate. In addition, criteria used in making assignments have not been very restrictive, e.g. criteria based on the Teller product rule, sum rules, thermodynamic data, and isotope effects have the disadvantage that one incorrect assignment can be compensated by a second. Normal coordinate calculations are significantly helpful but not entirely conclusive, especially for large polyatomic molecules with many nearly degenerate fundamental and combination tones.

Ideally one would like to make assignments by using a high resolution experimental technique that is capable of observing and characterizing by symmetry each fundamental tone. Polarized Raman spectroscopy of oriented single crystals approaches this idealization for the gerade modes. Each symmetry species is readily

identified from its characteristic scattering tensor. By using high resolution, sensitive detection, and the conclusions drawn from electronic spectra, a confident assignment of the gerade modes can be made. In particular, the Raman tensors readily distinguish between the b_{1g} and b_{2g} modes where no experimental identification[3] had been available. Especially significant to the assignment of these two symmetry species is the fact that in the present work no vibrational transitions in the Raman or phosphorescence spectra were observed below 388 cm^{-1}. The two nearly degenerate vibrations[3] at 510 and 514 cm^{-1} also are resolved.

The fundamental gerade frequencies summarized in Table III are assigned primarily on the basis of empirical considerations. It is assumed that each fundamental will be active in the Raman, phosphorescence, or fluorescence spectra. The vibrational analysis of the phosphorescence[26] and fluorescence[27] is available elsewhere. Very weak Raman transitions, i.e. those appearing with only one or two tensor elements, are not considered fundamentals. The remaining frequencies are sorted according to the form of the Raman scattering tensor, and their assignments are considered below. The comments in Ref. 26 regarding the fundamentals are applicable here also. The only uncertain assignments in view of this work are ν_4 and some H-stretching modes. The conclusion is that the gerade modes of a large polyatomic molecule only can be assigned after considering Raman and electronic spectra, and theoretical calculations. The complex theoretical problem can be

simplified experimentally by the use of liquid helium temperatures, polarization data, high resolution, extremely pure crystals, lasers, double monochromators, and sensitive photoelectric detection techniques.

The assignment of the normal modes is especially significant in understanding vibronic activity and singlet-triplet coupling mechanisms and in identifying the emitting and absorbing species in crystal spectra. A complete and accurate experimental analysis also serves to evaluate computational procedures and intramolecular potentials.

1. The a_g Modes

The totally symmetric vibrations are expected to have strong diagonal tensor elements: zz > yy > xx. The observed and oriented gas intensities are given in Tables I and II, respectively. The lines at 514, 763, 1022, 1382, 1464, 1577, and 3057 cm^{-1} have quite unambiguous a_g tensors. The remaining two a_g fundamentals can not be so unambiguously assigned. Another hydrogen stretching mode must be present as well as a "mid-range" frequency. There really are no empirical criteria for choosing the former but the fluorescence spectra of crystals[27] indicate that the latter is 1146 ± 2 cm^{-1}.

Empirically the presence of a fundamental near 1020 cm^{-1} only could be suspected due to the combinations $2 \times \nu_1$, $\nu_1 + \nu_{17}$, and $2\nu_{17}$, appearing near 1020 cm^{-1}. The Raman intensity indicates

a fundamental present, and in our spectra all four transitions are resolved, although the possibility of factor group splitting introduces a further ambiguity.

The remaining frequencies with a_g tensors (737, 1019, 1162, 1369, 1378) can be assigned as sum or difference bands appear by mixing with intense fundamentals.

2. The b_{1g} Modes

These vibrations are expected to have intense xz and weak xx and zz tensor elements. The only possible frequencies are 388, 392, 723, 725, 950, 1146, and 1524 cm^{-1}. The fundamentals are assigned as 392, 725, and 950 cm^{-1}.

The low frequency vibrations at 388 and 392 cm^{-1} are either b_{1g} or b_{2g} modes. The N polarization of the $^3B_{1u} \leftarrow {}^1A_g$ absorption indicates that the 392 cm^{-1} line is <u>not</u> a b_{2g} mode while the intense xz Raman polarization indicates that it <u>is</u> a b_{1g} mode. The 725 cm^{-1} frequency is chosen over 723 cm^{-1} because it is more intense and also appears in phosphorescence.[26] The 1146 and 1524 cm^{-1} frequencies most likely are not b_{1g} modes in view of the calculations of Scully and Whiffen[28] and Evans and Scully.[29] The calculations show that all b_{1g} and b_{2g} modes must have frequencies less than 1100 cm^{-1}.

3. The b_{2g} Modes

These vibrations are expected to have a weak zz tensor element and intense xx and yy elements. The only possibilities are 388, 773, and 783 cm^{-1}. Since it is unlikely that two fundamentals of the same symmetry have such close eigenvalues, a better choice is the 983 cm^{-1} frequency observed in phosphorescence. The 773 cm^{-1} frequency is chosen as the fundamental over 783 cm^{-1} because no zz element appears, and a 773 cm^{-1} mode appears in the phosphorescence spectrum. The computer search for agreement between Raman lines and combination tones reveals seven reasonable alternative assignments for 783 cm^{-1}. The remaining b_{2g} mode also is assigned from the phosphorescence spectrum as 469.5 even though it is only weakly Raman active. Lines at 191 and 285 cm^{-1} that had been assigned as b_{2g} modes[30] were not observed, probably due to the higher purity of our crystals.

4. The b_{3g} Modes

The b_{3g} modes are expected to have intense yz and weak xx tensor elements. The possibilities are 510, 1168, 1244, 1443, 1458, 1627 cm^{-1}, and the frequencies in the H-stretching region. As for the a_g modes, the two b_{3g} H-stretching modes cannot be chosen on empirical arguments. The 1442 cm^{-1} frequency is chosen over 1458 cm^{-1} because it is more intense, and the 1458 cm^{-1} line likely appears by mixing with ν_6. The $^1B_{2u} \leftarrow {}^1A_g$ electronic spectra[27, 31, 32] show that 938 cm^{-1} also is a b_{3g} fundamental. Freeman and Hollas[32]

have assigned ν_{19} as 1099 cm^{-1} from the gas-phase fluorescence. However, it is difficult to see why this frequency does not appear in the crystal fluorescence[27] if it is intrinsic to naphthalene.

5. Comparison with Calculations

The data for this comparison are given in Table IV. The experimental values are derived from the fluorescence, phosphorescence, and Raman spectra from the empirical considerations discussed above. The calculated values for the a_g and b_{3g} modes are taken from Table 4 of the paper[4] by Neto, Scrocco, and Califano. While recent calculations[4, 33] favor Freeman and Ross'[34] assignment of 1099 cm^{-1} as ν_{19}, both the absence of this frequency in crystal fluorescence and the b_{3g} Raman tensor of the 1168 cm^{-1} line support Scully and Whiffen's[28b] assignment of 1168 cm^{-1} as ν_{19}.

The calculated b_{1g} and b_{2g} frequencies are taken from the papers of Scully and Whiffen,[28] and Evans and Scully.[29] In general the agreement is poorer than for the in-plane vibrations. The only real disagreement arises because we observe no gerade mode near 880 cm^{-1}. Consequently the fourth b_{2g} is assigned as 388 cm^{-1} rather than[28a] 881 cm^{-1}.

C. Intermolecular Interactions

The differences in gas phase and crystal spectra are related to the magnitude and nature of the intermolecular forces in the crystal. These differences are observed as gas-to-crystal frequency shifts, exciton splittings and shifts, site and orientational splittings, intensity changes, and temperature-dependent linewidths and lineshapes. The appearance of these effects in benzene spectra has been discussed[35] extensively with respect to both experiment and theory. Relatively little attention, however, has been given to the case of naphthalene. Except for site and orientational splittings, which are absent in $C_{10}H_8$, the importance of such effects for the gerade modes of crystalline naphthalene is discussed below. This work complements both past[36] and current research[5] that primarily has been concerned with the ungerade modes.

1. Gas-to-Crystal Frequency Shifts

Gas phase gerade vibrational frequencies of the naphthalene molecule are available only from fluorescence spectra.[32, 37] The available data are given in Table III and indicate that the shifts are 2-4 cm^{-1}. This fact is consistent with the behavior of the ungerade modes,[36] but the shifts for benzene often are much larger.[7]

2. Exciton Splitting and Shifts

Exciton structure in the gerade vibrations of crystalline naphthalene has been reported, but these splittings actually are transitions to nearly degenerate molecular vibrations. The observed exciton splitting, polarization data, and mixed crystal frequencies indicate that the factor group splitting in crystalline naphthalene is less than 1 cm^{-1}. The only resolved factor group splitting (ν_{17}) measures 0.7 cm^{-1} with the a_g component at higher energy. Figures 6 and 7 are a photograph and microphotometer trace showing the polarization and splitting of ν_{17}. Figure 6 includes a photograph of the ν_7 Raman transition; the doublet there does not correspond to factor group splitting since one of the lines is unpolarized. The unique polarization of the ν_{17} components indicates this splitting is indeed factor group structure and not, for example, due to $^{13}CC_9H_8$. Both the polarization data and the close coincidence of the mixed crystal frequencies with the pure crystal frequencies, as shown in Table III, contradict the possibility that the factor group splitting is large but only one of the two components is observed in the Raman spectra.

A comparison of the mixed crystal phosphorescence and pure crystal Raman frequencies in Table III shows that within experimental accuracy the ideal mixed crystal levels are coincident with the pure crystal vibrational exciton band. Consequently the interactions between both interchange equivalent and translationally equivalent

molecules must be very small ($\lesssim 0.5\ cm^{-1}$). This fact contrasts with the reported exciton splittings for the ungerade modes[5, 39] being generally larger than 1 cm^{-1} with some as large as 10-15 cm^{-1}.

Theoretical calculations of the naphthalene intermolecular interactions based on atom-atom potentials[5] predict splittings larger than 1 cm^{-1} for half the gerade modes while in the experiments reported here all splittings are less than 1 cm^{-1}. For example, the calculated splitting for ν_{17} is $+3.2\ cm^{-1}$ compared to the experimental value of $-0.7\ cm^{-1}$, the sign from $E(b_g) - E(a_g)$. In contrast, the calculated splittings for the ungerade modes are generally too small. Quantitatively the calculations only differ from experiment by factors of 2 to 4, but the qualitative difference between the results for gerade and ungerade vibrations may indicate that some finer features of the intermolecular interactions are not well represented by the atom-atom potential model even though some macroscopic features[38] are described quite well.

3. Intensity Effects

A comparison of the data in Tables I and II shows that the intermolecular forces enhance the intensity of the light scattered through the weak tensor elements while the strong elements are just those predicted by the oriented gas model. Intensity changes occur because the intermolecular forces and symmetry alter the intramolecular forces and symmetry. This change can be described by a mixing of the normal molecular modes. Strizhevsky[39] has

discussed crystal induced mixing or Fermi resonance while Bernstein[6b] has documented the effect in benzene infrared spectra. An unambiguous example involving ν_1 and ν_{17} arises in naphthalene crystal spectra. In the vapor[31, 32] the activity of these modes is quite different: ν_{17} appears as an intense fundamental while ν_1 appears only as weak combinations. In both the Raman and phosphorexcence[26] of the crystal, the activity of the two modes is nearly identical: both appear with equal intensity and as combinations with other modes.

Since the Raman spectrum is characterized by groups of lines while electronic spectra are characterized by progressions, mixing with a fundamental appears to be a necessary criterion for Raman activity. An especially clear example of this effect arises in $C_{10}D_8$ where, at 2272 cm^{-1}, the intense fundamental ν_9 is nearly degenerate with many combination bands and overtones. Figure 8 shows that many combinations gain intensity by mixing with ν_9; their intensity decreasing with increasing energy denominator. Away from this fundamental and in $C_{10}H_8$, the Raman transitions in this region are extremely weak.

4. Linewidth and Shape

The intermolecular interactions also affect the temperature dependence of the width and shape of the Raman lines as summarized below. The frequencies of 763, 1378, 1464, and 3057 cm^{-1} are especially diffuse at room temperature. The frequency shifts,

documented in Table I, that appear for many of the modes between room temperature and 77°K are more correctly considered asymmetric sharpenings of the lines, e.g. see index numbers 27 and 28 in Table I. The hydrogen-stretch ν_9 is roughly 4 cm^{-1} wide at room temperature where the width of most other modes is 1 cm^{-1}. At 77°K all linewidths are an instrument limited 0.5 cm^{-1}. The bottom spectrum in Fig. 1 was taken at 77°K while the others were taken at room temperature.

Although the mechanism of the observed effects is uncertain, theoretical developments could proceed along the lines of phonon coupling, intermolecular induced anharmonicities, thermally induced inhomogeneities in the lattice, or some general formalization of which these three are a part. In addition to the thermal effects, preliminary data indicate that the intensity of combinations in $C_{10}D_8$ is less than in $C_{10}H_8$. This decrease may arise from a change in the vibronic coupling or anharmonicities in the deuterated compound.

Interestingly enough, both temperature, environment, and "anomalous" isotope effects also have been observed in the relaxation rates in benzene and naphthalene.[40] Such effects may be explained in terms of changes in Franck-Condon factors;[41] consequently, a theory that explains the effects in the Raman or infrared spectra might contain significant implications concerning energy relaxation processes, especially since the temperature dependence of the Raman lineshape in both benzene[6a] and naphthalene is most severe for the hydrogen-stretching modes, and these play a key role in the relaxation process.[42]

IV. SUMMARY

A comparison of the phosphorescence,[26] fluorescence,[27] and polarized Raman spectra of naphthalene crystals enables the fundamental gerade vibrational frequencies of the naphthalene molecule to be assigned empirically. The empirical assignments generally agree with those Freeman and Ross,[34] and Scully and Whiffen[28b] made on the basis of valence force field calculations. Although more refined calculations[4, 33] favor the assignment of 1099 cm^{-1} rather than 1168 cm^{-1} as ν_{19}, a 1099 cm^{-1} frequency is not present in the crystal spectra while the Raman scattering tensor definitely indicates that the 1168 cm^{-1} transition corresponds to a b_{3g} species. The Raman spectra also show no transitions near 880 cm^{-1} or below 380 cm^{-1}, except for the lattice modes. This result disagrees with the computations[28, 29] and earlier experiments[15] that indicate a b_{2g} mode near 880 cm^{-1} and gerade vibrations at 191 and 285 cm^{-1}. This negative result is quite significant since we use higher purity samples and still report more Raman transitions than the previous investigators. In addition, the nearly degenerate fundamentals at 510 and 512 cm^{-1} are resolved as well as their combination bands, overtones, and the fundamental near 1020 cm^{-1}.

Information concerning the intermolecular interactions in the crystal also is obtained from the Raman spectra. It is found that the gas-to-crystal frequency shifts are only 2-4 cm^{-1}, the exciton splittings and shifts are less than 1 cm^{-1}, and the Raman intensities qualitatively correspond to the predictions of the oriented gas model

although cases of Fermi resonance are clearly evident, e.g. ν_1 and ν_{17}, and Fig. 8. Using an atom-atom potential model,[38] calculations[5] of the exciton splittings in the naphthalene vibrations generally underestimate the splittings in the ungerade modes while the splittings in the gerade modes are overestimated. This qualitative difference may indicate that some finer feature of the intermolecular potential is not accurately represented by the atom-atom potential model. However, for the one observed factor group splitting ν_{17}, the calculation did not predict correctly the ordering of the components.

The temperature dependence of the shape and width of the Raman line is documented. Since the largest effect arises from the carbon-hydrogen modes, the suggestion is made that a theory explaining this effect might also contribute to the theory of energy relaxation processes.

REFERENCES

1. E.R. Bernstein, S.D. Colson, R. Kopelman, and G.W. Robinson, J. Chem. Phys. 00, 0000 (1968), "Electronic and Vibrational Exciton Structure in Crystalline Benzene" and cited references.
2. A.R. Gee and D.M. Hanson, Twenty-second Symposium on Molecular Structure and Spectroscopy (The Ohio State University, Columbus, Ohio, 1967), Abstract B12.
3. (a) J.M. Hollas, J. Mol. Spectry. 9, 138 (1962); (b) D.P. Craig and H.C. Wolf, J. Chem. Phys. 40, 2057 (1964).
4. N. Neto, M. Scrocco, and S. Califano, Spectrochim. Acta 22, 1981 (1966) and cited references.
5. (a) D.A. Dows, S. Hayashi, and N. Rich, Twenty-second Symposium on Molecular Structure and Spectroscopy (The Ohio State University, Columbus, Ohio, 1967), Abstract N3; (b) N. Rich, Ph.D. thesis, University of Southern California, 1968.
6. (a) A.R. Gee and G.W. Robinson, J. Chem. Phys. 46, 4847 (1956); (b) E.R. Bernstein, "Site Effects in Isotopic Mixed Crystals--Site Shift, Site Splitting, Orientational Effect and Intermolecular Fermi Resonance in the Vibrational Spectrum of Benzene", unpublished results; (c) E.R. Bernstein and G.W. Robinson, "Vibrational Exciton Structure in Crystals of Isotopic Benzenes", unpublished results.

7. E.R. Bernstein, "Calculation of Ground State Vibrational Structure and Phonons of the Isotopic Benzene Crystals," unpublished results.

8. D.M. Hanson and G.W. Robinson, J. Chem. Phys. 43, 4174 (1965).

9. A.N. Winchell, The Optical Properties of Organic Compounds (University of Wisconsin Press, Madison, Wisconsin, 1943), pp. 62, 313.

10. (a) E.E. Wahlstrom, Optical Crystallography (John Wiley and Sons, Inc., New York, 1960); (b) N.H. Hartshorne and A. Stuart, Crystals and the Polarizing Microscope (Edward Arnold, Publishers, London, 1960).

11. H.M. Crosswhite, The Spectrum of Iron I, Johns Hopkins Spectroscopic Report No. 13, The Johns Hopkins University, Department of Physics, Baltimore, Maryland, 1958.

12. C.D. Coleman, W.R. Bozman, and W.F. Meggers, Table of Wavenumbers, National Bureau of Standards Monograph No. 3, U.S. Government Printing Office, Washington, D.C., 1960.

13. T.C. Damen, S.P.S. Porto, and B. Tell, Phys. Rev. 142, 570 (1966).

14. (a) C.E. Hathaway, Spectrochim. Acta 23a, 881 (1967); (b) D.C. Nelson and W.N. Mitchell, Anal. Chem. 36, 555 (1964); (c) J.R. Ferraro, J. S. Ziomek, and G. Mack, Spectrochim. Acta 20, 901 (1964); H. Moser and D. Stieler, Z. Angew. Phys. 12, 280 (1960).

15. (a) W.B. Person, G.C. Pimentel, and O. Schnepp, J. Chem. Phys. 23, 230 (1955); (b) E.R. Lippincott and E.J. O'Reilly Jr., J. Chem. Phys. 23, 238 (1955); (c) A.L. McClellan and G.C. Pimentel, J. Chem. Phys. 23, 245 (1955); (d) H. Luther, K. Feldman, and B. Hampel, Z. Elektrochem. 59, 1008 (1955); (e) H. Luther, G. Brandes, H. Günzler, and B. Hampel, Z. Elektrochem. 59, 1012 (1955); (f) J. Brandmüller and E. Schmid, Z. Physik 144, 428 (1956); (g) S.S. Mitra and H.J. Bernstein, Can. J. Chem. 37, 553 (1959); (h) N.I. Zhirnov, Opt. Spektrosk. 9, 734 (1960) [Opt. Spektrosc. 9, 385 (1960)]; (i) H. Luther and H.J. Drewitz, Z. Elektrochem. 63, 546 (1962).

16. Although the naphthalene molecule has only 48 normal vibrational frequencies, roughly twice that many frequencies had been assigned as fundamentals in Ref. 15. A brief review of that work is given in Ref. 3a.

17. (a) G. Placzek in Handbuch der Radiologie, E. Marx, Ed. (Akademische Verlagsgesellschaft, Leipzig, 1934), Bd. VI, Teil II, p. 209 [translated by Ann Werbin, UCRL Trans. No. 526 (L)]; (b) J. A. Koningstein, Chem. Phys. Letters 2, 31 (1968).

18. See Refs. 9 and 10. The principal optic axis coincides with the b crystallographic axis; the obtuse and acute bisectrices lie 23°25' from the a and c′ crystallographic axes, respectively.

19. The angles between the molecular axes and the crystallographic axes are given by S.C. Abrahams, J.M. Robertson, and

J.G. White, Acta Cryst. 2, 233, 238 (1949). The angles between the crystallographic axes and the principal refractive index axes are given in Ref. 18.

20. R.S. Mullikan, J. Chem. Phys. 23, 1997 (1955).

21. M. Ramanadham, Proc. Indian Acad. Sci. 1A, 425 (1935).

22. T.M.K. Nedungadi, Proc. Indian Acad. Sci. 15A, 376 (1942).

23. A. Kastler and A. Rousset, J. Phys. Radium 2, 49 (1941).

24. (a) M. Ito, M. Suzuki, and T. Yokoyama, Bull. Chem. Soc. Japan 40, 2461 (1967); (b) M. Suzuki, T. Yokoyama, and M. Ito, Tech. Rept. ISSP A284 (1967).

25. Refs. 3-5.

26. D.M. Hanson, "The Phosphorescence Spectrum, Vibronic Analysis, and Lattice Frequencies of the Naphthalene Molecule in a Deuteronaphthalene Crystal," unpublished results.

27. (a) A. Pröpstl and H.C. Wolf, Z. Naturforsch. 18a, 724 (1963); (b) F.R. Lipsett and G. Macpherson, Can. J. Phys. 44, 1485 (1966); (c) D.M. Hanson, unpublished results.

28. (a) D.B. Scully and D.H. Whiffen, J. Mol. Spectry. 1, 257 (1957); (b) D.B. Scully and D.H. Whiffen, Spectrochim. Acta 16, 1409 (1960).

29. D.J. Evans and D.B. Scully, Spectrochim. Acta 20, 891 (1964).

30. Refs. 15 and 3a.

31. D.P. Craig, J.M. Hollas, M.R. Redies, and S.C. Wait Jr., Phil. Trans. Roy. Soc. London A253, 543 (1961).

32. (a) D.E. Freeman, J. Mol. Spectry. 6, 305 (1961); (b) J.M. Hollas, J. Mol. Spectry. 9, 138 (1962).

33. J.R. Scherer, J. Chem. Phys. 36, 3308 (1962).

34. D.E. Freeman and I.G. Ross, Spectrochim. Acta 16, 1393 (1960).

35. Refs. 1, 6-7, and cited references.

36. G.C. Pimentel, A.L. McClellan, W.B. Person, and O. Schnepp, J. Chem. Phys. 23, 234 (1955).

37. O. Schnepp and D.S. McClure, J. Chem. Phys. 20, 1375 (1952).

38. (a) A.I. Kitaigorodskii, Acta Cryst. 18, 585 (1965); (b) A.I. Kitaigorodskii and K.V. Mirskaya, Kristallografiya 9, 174 (1964) [Sov. Phys.--Crystallogr. 9, 137 (1964)]; (c) D.E. Williams, Science 147, 605 (1965); (d) D.E. Williams, J. Chem. Phys. 45, 3770 (1966).

39. V.L. Strizhevsky, Opt. Spektrosk. 8, 165 (1960) [Opt. Spektrosc. 8, 86 (1960)].

40. (a) A. Kalantar, private communication; (b) G.C. Nieman, private communication; (c) R.J. Watts and S.J. Strickler, "Deuterium Isotope Effects on the Lifetime of the Phosphorescence Triplet State of Naphthalene," unpublished manuscript; (d) N. Hirota and C.A. Hutchison, J. Chem. Phys. 46, 1561 (1967).

41. This point arose during discussions with D.M. Burland.

42. (a) G.W. Robinson, J. Mol. Spectry. 6, 58 (1961); (b) G.W. Robinson and R.P. Frosch, J. Chem. Phys. 37, 1962 (1962); (c) G.R. Hunt, E.F. McCoy, and I.G. Ross,

Australian J. Chem. 15, 591 (1962); (d) G.W. Robinson and R.P. Frosch, J. Chem. Phys. 38, 1187 (1963).

TABLE I. Raman Assignments

Index	$\Delta\bar{\nu}$ (cm^{-1}) RT	77°	Intensities xx	xz	zz	zy	yy	xy	Mode	D_{2h}
1	388	388.4		F	F	F	F		ν_{10}	b_{1g}
2	392		F	W	F			F	ν_{13}	b_{2g}
3	466						W		ν_{14}	b_{2g}
4	510	508.9				M		W	ν_{17}	b_{3g}
		509.6	W	W	M		W			
5	514	512.9	W	M	S	M	W	W	ν_1	a_g
6	723			W						
7	725	726.0			F	W	F		ν_{11}	b_{1g}
8	737				F		F	F		
9	758				F		F			
10	763[a]	765.0	S	M	S	M	S	M	ν_2	a_g
11	773		F				F	W	ν_{15}	b_{2g}
12	783[b]		F		W		M	F		

TABLE I. (continued)

Index	$\Delta\bar{\nu}$ (cm^{-1})		Intensities						Mode	D_{2h}
	RT	77°	xx	xz	zz	zy	yy	xy		
13	950			F		F			ν_{12}	b_{1g}
14	1019	1018.0	W	F	M	F	M	F	$2\times\nu_{17}$	a_g
15	1022	1019.8 1021.6	M	W	S	W	S	M	ν_3 $\nu_1+\nu_{17}$	a_g
16	1027				F				$2\times\nu_1$	a_g
17	1146	1145.6	F	M	W		W	W		
18	1147	1148.0				M				
19	1162			F	W		F			
20	1168	1168.4		F	W	M	W	F	ν_{19}	b_{3g}
21	1244[b]	1243.8		W	W	M	W	F	ν_{20}	b_{3g}
22	1274				F					
23	1335				F		F			
24	1338				F		F			
25	1347				F					

TABLE I. (continued)

Index	$\Delta\bar{\nu}$ (cm^{-1})		Intensities						Mode	D_{2h}
	RT	77°	xx	xz	zz	zy	yy	xy		
26	1357				F					
27	1369	1370.5			W	F	W	F		
28	1378[a]	1379.5			S	W	M	W		
29	1382[a]	1383.0	M	M	S	M	S	M	ν_5	a_g
30	1389				F					
31	1443[a]	1445.2		F	M	F	F		ν_{21}	b_{3g}
32	1458[a]	1458.0		F	W	F				
33	1464[a]	1464.4	F	W	S	M	W	F	ν_6	a_g
34	1524						W	F		
35	1569						F			
36	1573				F		W			
37	1576	1576.4	M	F	M		S		ν_7	a_g
38	1578	1578.6				M		M		

TABLE I. (continued)

Index	$\Delta\bar{\nu}$ (cm^{-1})		Intensities						Mode	D_{2h}
	RT	77°	xx	xz	zz	zy	yy	xy		
39	1591						F			
40	1596				F		F			
41	1627	1628.7		F	M	F	F		ν_{22}	b_{3g}
42	2487				F					
43	2499				F					
44	2565				F					
45	2827					F				
46	2851					F				
47	2952				F					
48	2974				W		F			
49	3004				W					
50	3006	3006.7			M	F	W			
51	3012				F					

TABLE I. (continued)

Index	$\Delta\bar{\nu}$ (cm^{-1}) RT	77°	Intensities xx	xz	zz	zy	yy	xy	Mode	D_{2h}
52	3021	3018			W					
53	3031				F		W			
54	3051	3049.9			M	F				
55	3057	3057.2	M	F	S	F	M	F	ν_9	a_g
56	3071				F					
57	3086				F					
58	3103				F					

[a] Highly asymmetric.

[b] May be a doublet.

TABLE II. Oriented Gas Intensities

Mode	Relative Intensities					
	xx	xz	zz	zy	yy	xy
a_g	10	<1	83	<1	42	4
b_{1g}	1	76	1	18	4	3
b_{2g}	61	3	<1	2	61	34
b_{3g}	<1	18	17	64	14	2

TABLE III. The gerade Frequencies and Frequency Shifts

Mode		Frequency in cm^{-1}				M.C.-P.C. cm^{-1}	Crystal-Vapor cm^{-1}
		Vapor[a]	MCP[b]	PCR[c]	CF[d]		
a_g	ν_1	514, 516	512.0	512.9		-0.9 ± 1.0	-2.5
	ν_2	761	764.8	765.0	765	-0.2 ± 1.0	+4
	ν_3	1020, 1025		1019.8	1021		0, -5
	ν_4				1148		
	ν_5	1380	1381.6	1383.0	1383	-1.4 ± 1.0	+2
	ν_6			1464.4			
	ν_7		1577.0	1576.4	1578	-0.5 ± 1.0	
	ν_8						
	ν_9			3057.2			
b_{1g}	ν_{10}		392.6	392		+0.6 ± 2.5	
	ν_{11}		727.5	726.0		+1.5 ± 1.0	
	ν_{12}		950.8	950		+0.8 ± 2.5	

TABLE III. (continued)

Mode		Frequency in cm^{-1}				M.C.-P.C. Crystal-Vapor	
		Vapor[a]	MCP[b]	PCR[c]	CF[d]	cm^{-1}	cm^{-1}
b_{2g}	ν_{13}			388.4			
	ν_{14}		469.5	466		+3.5 ± 2.5	
	ν_{15}		771.5	773		-1.5 ± 2.5	
	ν_{16}		982.8				
b_{3g}	ν_{17}	506	510.0	508.9 509.6	510	+0.75 ± 1.0	+4
	ν_{18}	936			938		+2
	ν_{19}			1168.4			
	ν_{20}	1240		1243.8			+4
	ν_{21}			1445.2			
	ν_{22}		1629.2	1628.7	1628	+0.5 ± 1.0	
	ν_{23}						
	ν_{24}						

TABLE III. (continued)

[a] Refs. 32 and 37.

[b] Mixed crystal phosphorescence, accuracy is ± 0.5 cm^{-1}.

[c] Pure crystal Raman, accuracy is ± 2 cm^{-1}; ± 0.5 cm^{-1} where tenths are specified.

[d] Crystal fluorescence, Ref. 27ab.

TABLE IV. Comparison of Experimental and Calculated Vibrational Frequencies

Mode		Exp. (cm^{-1})	Calc.[a] (cm^{-1})	$\Delta\nu$ (cm^{-1})
a_g	ν_1	512	511	-1
	ν_2	765	771	+6
	ν_3	1020	1014	-6
	ν_4	1146	1170	+24
	ν_5	1382	1373	-9
	ν_6	1464	1445	-19
	ν_7	1577	1584	+7
	ν_8		3014	
	ν_9	3057	3069	+12
b_{1g}	ν_{10}	392	365	-27
	ν_{11}	727	704	-23
	ν_{12}	950	920	-30
b_{2g}	ν_{13}	388	881	
	ν_{14}	468	485	+17
	ν_{15}	772	770	-2
	ν_{16}	983	971	-12
b_{3g}	ν_{17}	510	495	-15
	ν_{18}	938	939	+1

TABLE IV. (continued)

Mode	Exp. (cm^{-1})	Calc.[a] (cm^{-1})	$\Delta\nu$ (cm^{-1})
ν_{19}	1168	1114	-54
ν_{20}	1244	1254	+10
ν_{21}	1445	1436	-9
ν_{22}	1629	1612	-17
ν_{23}		3015	
ν_{24}		3066	

[a] Refs. 4, 28, and 29.

FIG. 1. Photographs of the $C_{10}H_8$ polarized Raman spectra designated by the elements of the scattering tensor. Although the abscissa is linear in wavelength, the frequency shifts of the most intense transitions are specified. Two lines originating from the laser are labeled by L. The zz-zy spectrum on the bottom was taken at 77 °K; the others were taken at room temperature. Slit widths are 2 cm^{-1}, 0.9 cm^{-1}, and 0.45 cm^{-1} for the first four, the fifth, and the sixth bands, respectively.

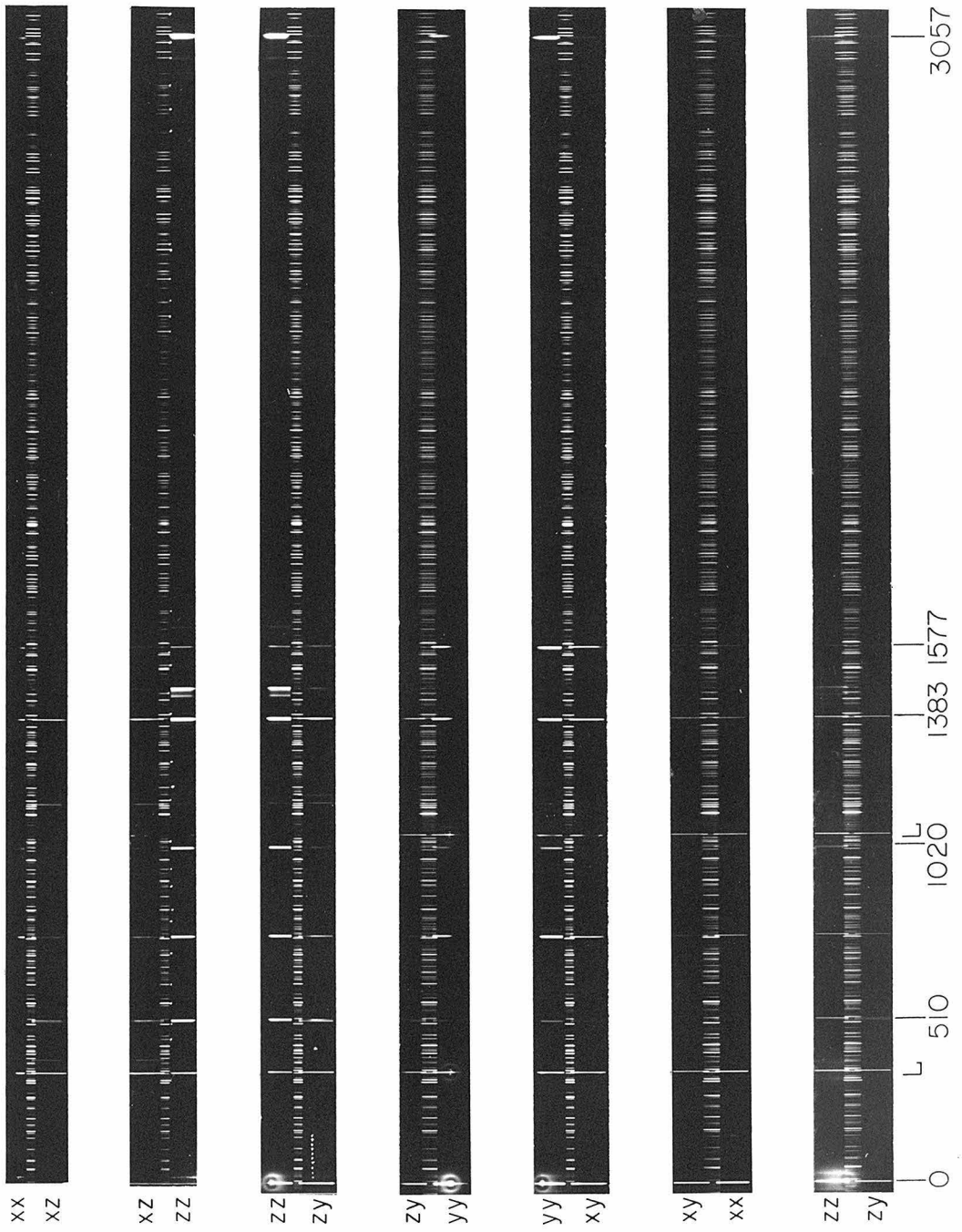
xx
xz
xz
zz
zz
zy
zy
yy
yy
xy
xy
xx
zz
zy
0
510
1020
1383
1577
3057
Δν̄ cm⁻¹

FIG. 2. A diagram of the apparatus. The laser wavelengths are selected by a dense flint prism P and the aperture A. L_1 and L_2 are lenses that focus the light in the crystal C and on the spectrograph slit S. A mirror M reflects the light through the crystal. The scattered light passes through the interference filter I, the polarizing prisms N, and is imaged in the focal plane F of the spectrograph.

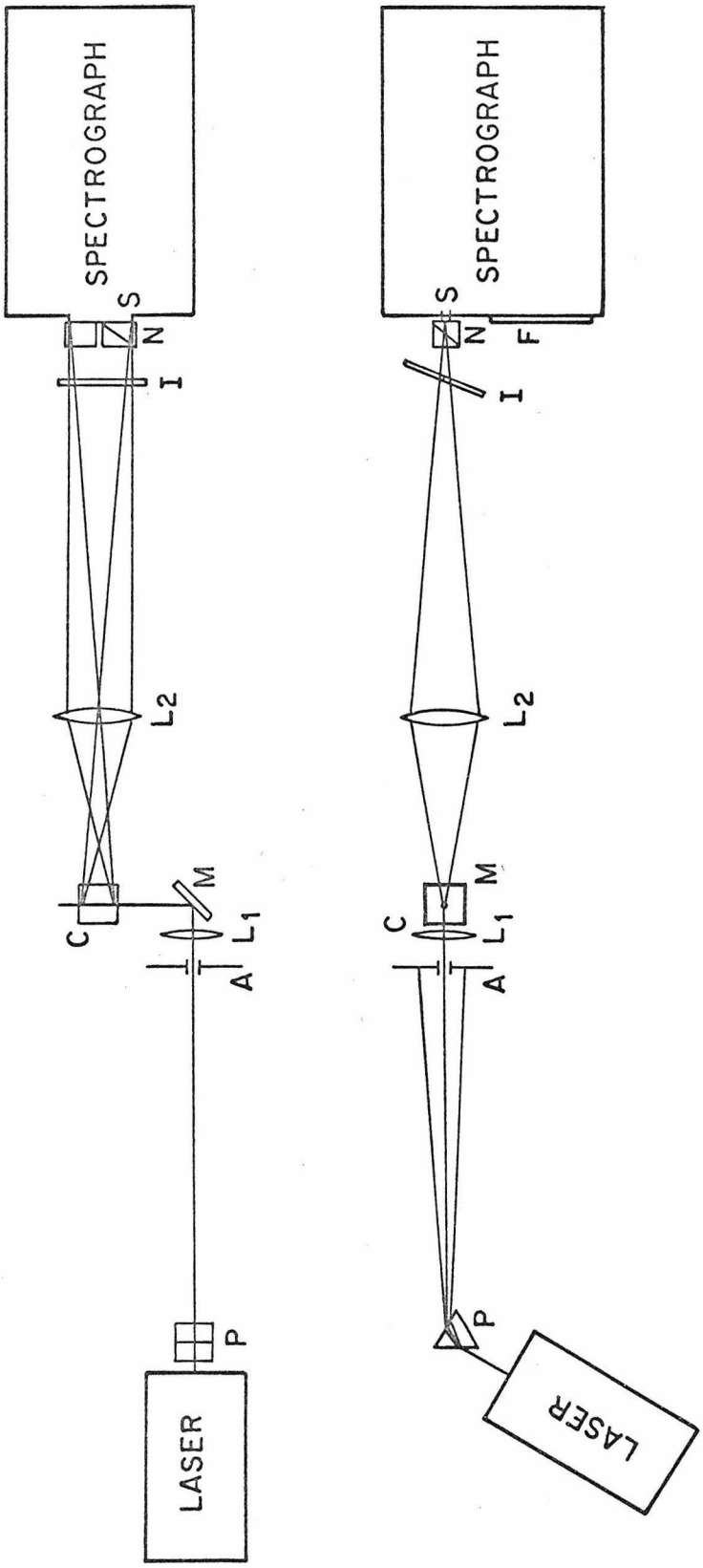
SPECTROGRAPH
S
N
I
L2
M
C
L1
A
P
LASER
SPECTROGRAPH
S
N
F
I
L2
M
C
L1
A
P
LASER

FIG. 3. A photograph of the low temperature crystal cell that facilitates rotating the crystal at 77°K.

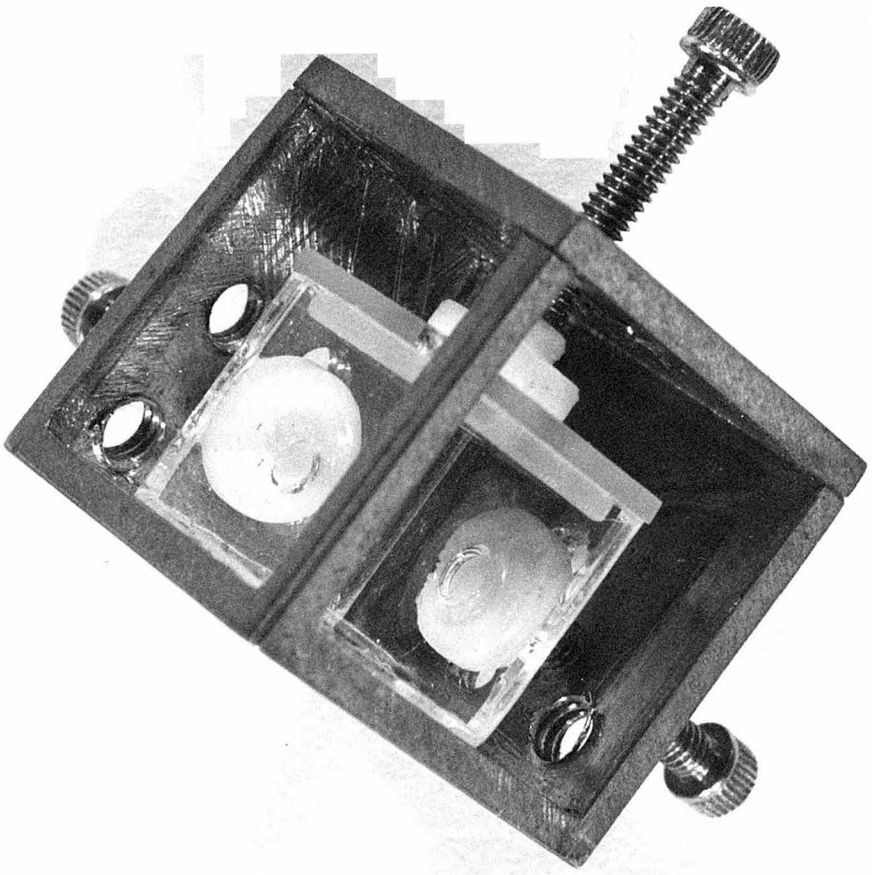

FIG. 4. The naphthalene crystal exhibiting the xyz axis system. y is perpendicular to the page; x is close to the $\hat{a}$ crystallographic axis, which is horizontal.

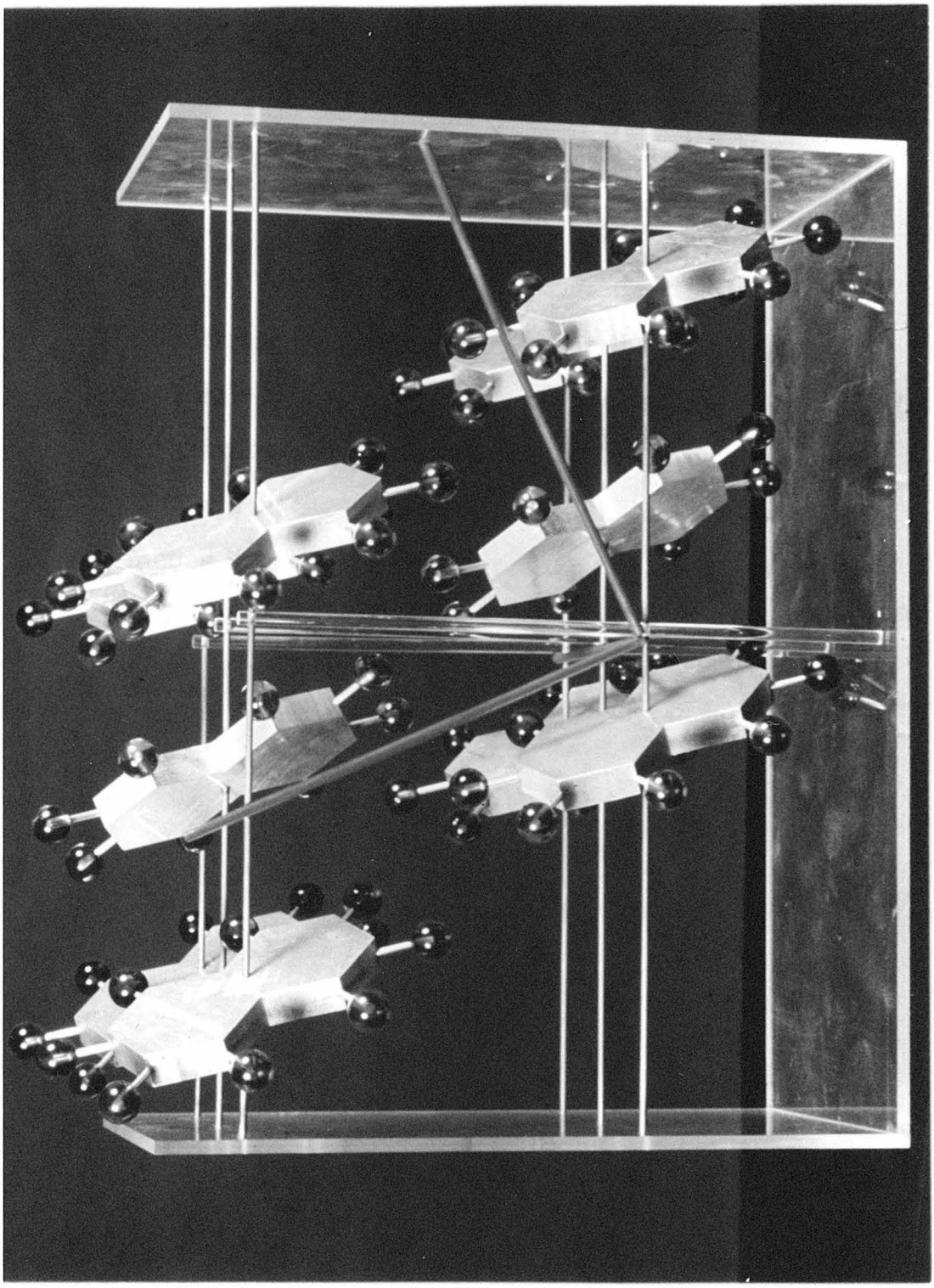

FIG. 5. The Raman scattering tensors for the naphthalene molecule and crystal. The tensor elements are squared to indicate the relative intensities. The crystal tensor is based on the oriented gas model, and for the a_g modes it is assumed that $\alpha_N : \alpha_L : \alpha_M = 1.0$ to 4.2 to 3.3; see text.

Mode Symmetry	Molecule NLM	Crystal XYZ
a_g	$\begin{pmatrix} \alpha_N^2 & 0 & 0 \\ 0 & \alpha_L^2 & 0 \\ 0 & 0 & \alpha_M^2 \end{pmatrix}$	$\alpha^2\begin{pmatrix} 10 & 4 & <1 \\ 4 & 42 & <1 \\ <1 & <1 & 83 \end{pmatrix}$
b_{1g}	$\alpha_1^2\begin{pmatrix} 0 & 1 & 0 \\ 1 & 0 & 0 \\ 0 & 0 & 0 \end{pmatrix}$	$\alpha_1^2\begin{pmatrix} 1 & 3 & 76 \\ 3 & 4 & 18 \\ 76 & 18 & 1 \end{pmatrix}$
b_{2g}	$\alpha_2^2\begin{pmatrix} 0 & 0 & 1 \\ 0 & 0 & 0 \\ 1 & 0 & 0 \end{pmatrix}$	$\alpha_2^2\begin{pmatrix} 61 & 34 & 3 \\ 34 & 61 & 2 \\ 3 & 2 & <1 \end{pmatrix}$
b_{3g}	$\alpha_3^2\begin{pmatrix} 0 & 0 & 0 \\ 0 & 0 & 1 \\ 0 & 1 & 0 \end{pmatrix}$	$\alpha_3^2\begin{pmatrix} <1 & 2 & 18 \\ 2 & 14 & 64 \\ 18 & 64 & 17 \end{pmatrix}$

FIG. 6. Photographs of ν_{17} and ν_1 on the left and ν_7 on the right taken with the sample at 77 °K and a slitwidth of 0.45 cm^{-1}. Close examination of ν_{17} shows that the component above the standard (zy) is superimposed on one of the standard lines while the component below (zz) lies to the right of this line. The complete polarization of these two factor group components demonstrates the excellent quality of the polarization data. The doublet appearing for ν_7 is not factor group structure since one of the lines is unpolarized.

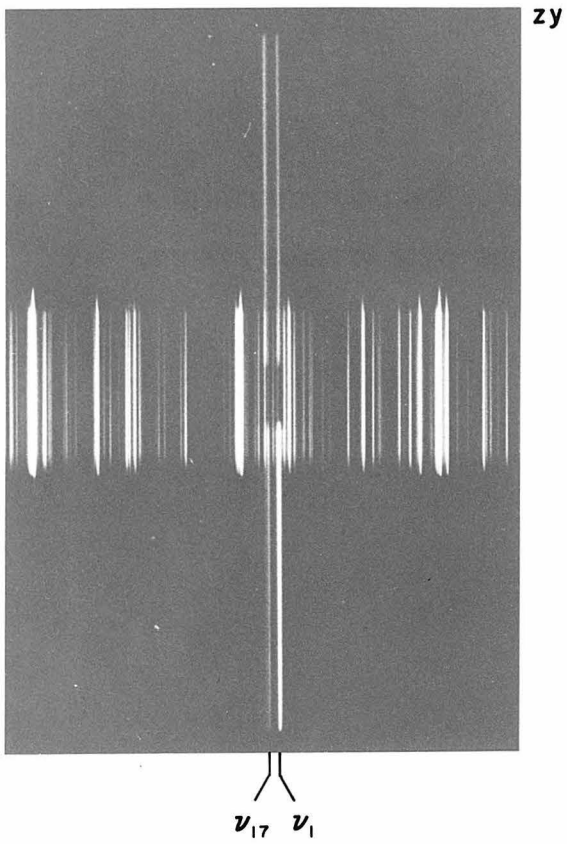
zy
ν_{17}
ν_1

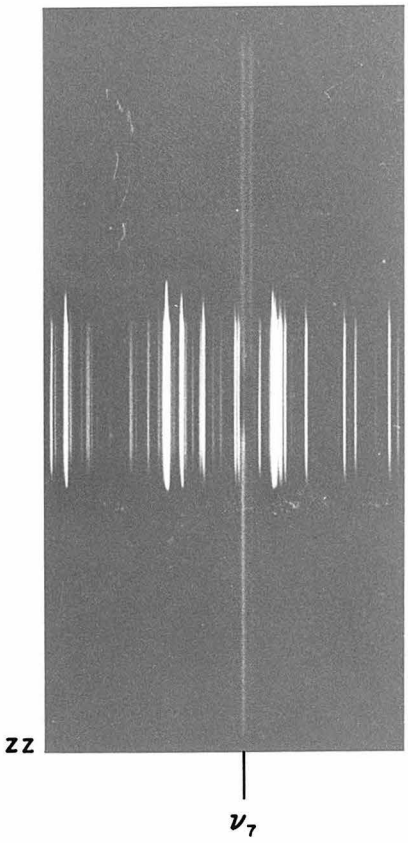
zz
ν_7

FIG. 7. A microphotometer tracing of ν_1 and ν_{17} in an unoriented crystal clearly showing the factor group structure.

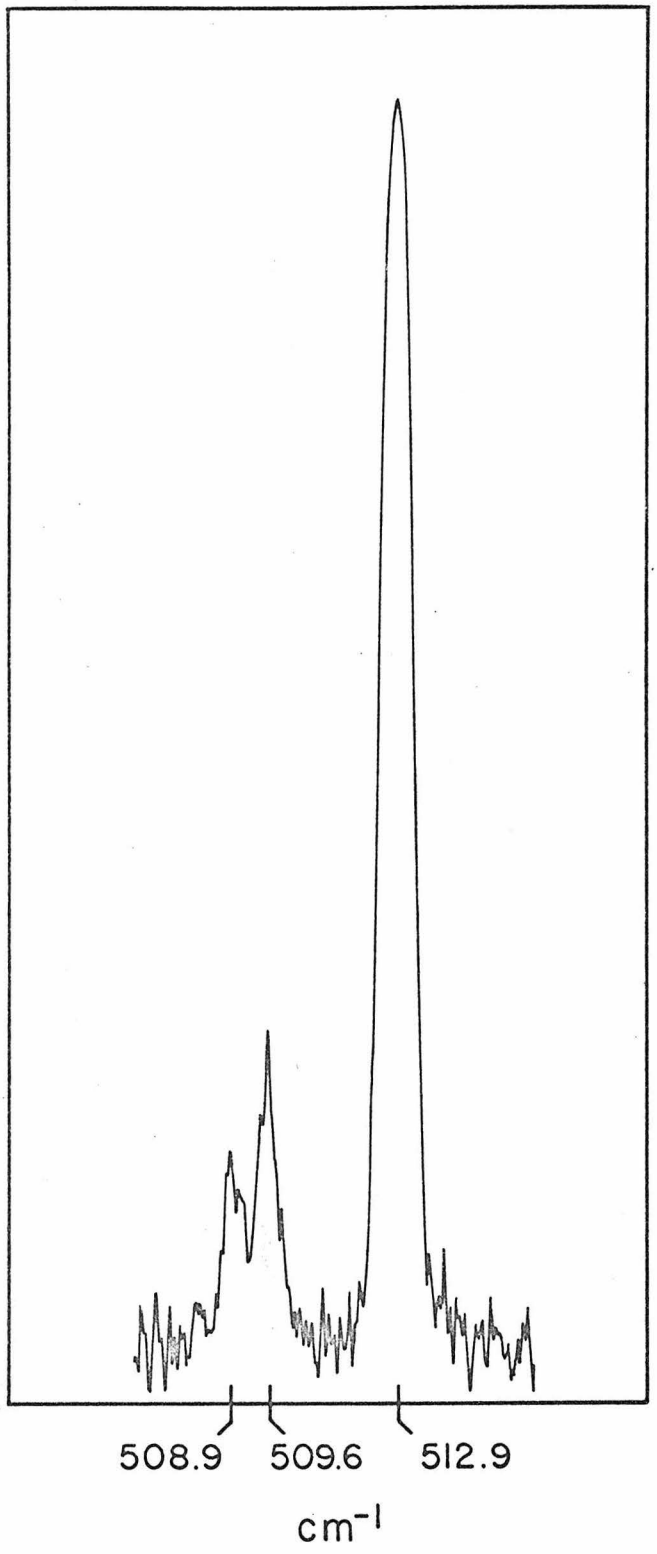
508.9
509.6
512.9
cm⁻¹

FIG. 8. A microphotometer tracing of ν_9 in $C_{10}D_8$ illustrating what should be a classic example of Fermi resonance.

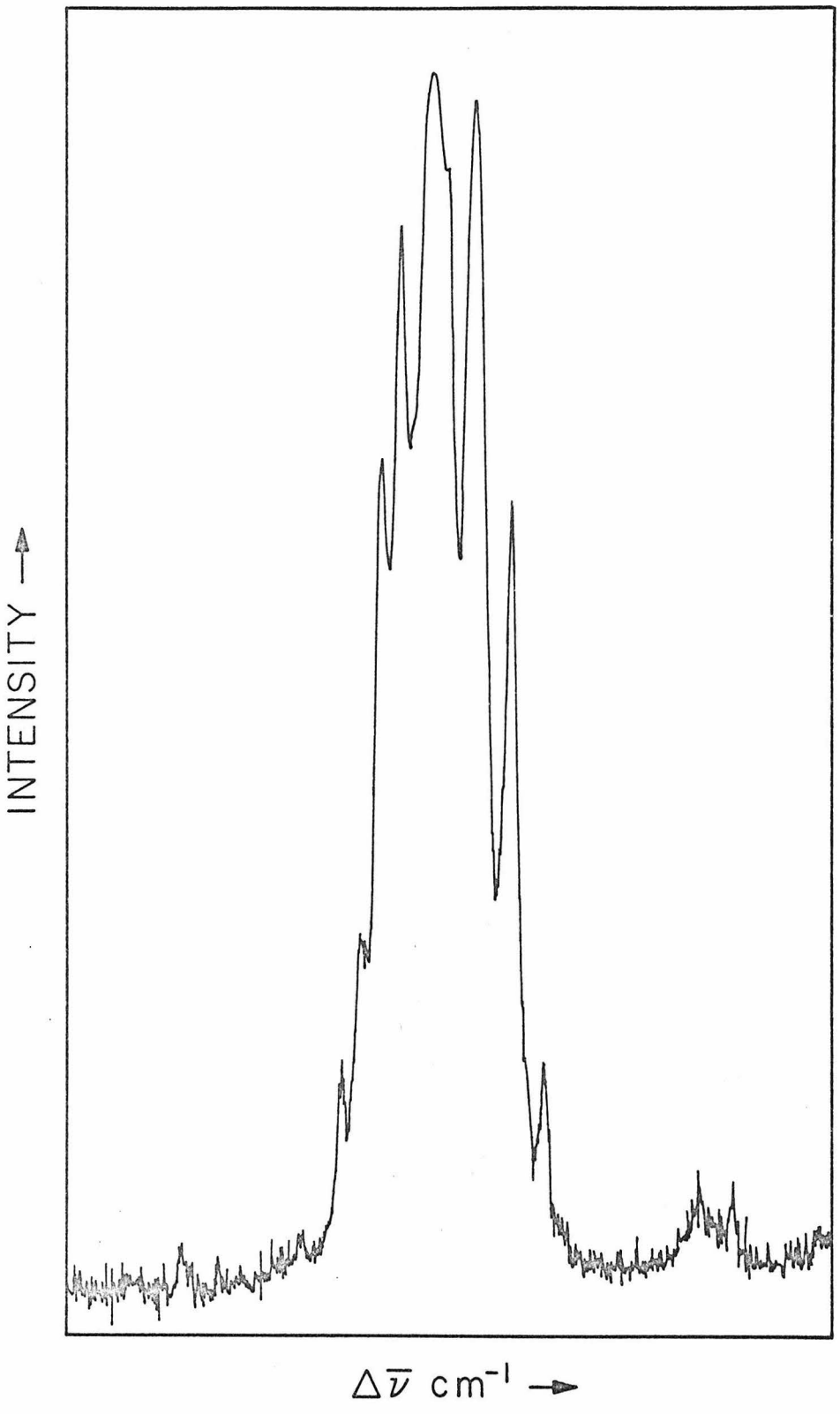
INTENSITY →
Δν̄ cm⁻¹ →

PART VIII

Propositions

ABSTRACTS OF PROPOSITIONS

David M. Hanson

Proposition I. Stark modulated absorption spectroscopy is to be used to detect and characterize some higher energy states of molecular crystals. This technique makes it possible to observe these transitions even though more intense transitions to Frenkel exciton states lie at the same energy. Information will be obtained about the dipole moments, symmetries, and the interactions of these states that are important in the processes of relaxation and the mechanisms of charge generation and transport.

Proposition II. A technique using photon angular momentum is proposed to measure the second-order spin magnetic dipole transition probability between singlet and triplet states in molecules. The experimental results will determine the importance of this radiative mechanism, test theoretical estimates of this process relative to the spin-orbit coupling mechanism, and allow some intrinsic properties of triplet states to be measured.

Proposition III. The physical and chemical dynamics of molecular solids represents an area of chemistry in which relatively little research of a fundamental nature has been done. This proposition discusses in some detail potential research on photochemical oxidation-reduction reactions and electron transfer processes in solids. While these studies are of general chemical interest, the conclusions should be significant to the study of similar processes in biological systems. Preliminary suggestions also are made for research in the areas of photochromism and phase transitions in solids.

Proposition IV. The identification and assignment of the factor group components in the spectra of molecular crystals is fundamental to understanding the spectra in terms of the intermolecular interactions. For the $^1B_{2u}$ state of benzene, the prototype aromatic molecular crystal, the assignment always has been somewhat ambiguous. The reasons for this ambiguity are summarized, and an experimental approach is proposed for avoiding the difficulties faced in earlier investigations.

Proposition V. The relationship between magnetism and chemical bonding is discussed. It is proposed to use optical, gamma resonance and electron magnetic resonance spectroscopy to investigate systems of weakly interacting electrons. Some interesting, novel, and basic systems are suggested. Interpretation of the experimental data will lead to better understanding of chemical bonding, especially the coupling between the sigma and pi electrons in planar aromatic molecules, and the exchange interactions that determine the balance between ferromagnetism and antiferromagnetism in weakly interacting systems.

PROPOSITION I

The electronic states generally characterize solids as insulators, semiconductors, or metals.[1] In some respects molecular crystals are an exception to this scheme. For these solids the concepts of a valence band and a conduction band are ambiguous because the electrons are highly localized. The ground and lowest excited electronic states are better described by the Frenkel tight-binding method in which molecular states are the progenitors of crystal states.[2] At higher energies, however, crystal states not present in the free molecule should be found. Such states may be similar to the Wannier and conducting states of insulators, semiconductors, and metals or may be unique to the molecular solid, e.g. states in which both an electron and hole are localized on neighboring lattice sites.

Experimental investigations of the higher energy states have resulted from interest in the electrical conductivity[3] of molecular solids. Some highly excited states have been observed indirectly through the photoconductivity of photoionization action spectrum. The observable in these experiments is the end result of a complicated series of processes; consequently, the conclusions derived from the experiments are somewhat controversial.[4]

The chain of processes resulting in photoconductivity or photoionization could be better understood if the properties and presence of higher crystal states were elucidated using a more

direct technique. Direct absorption spectroscopy, even utilizing optical pumping or multiphoton phenomena, is not suitable because the spectral absorption is dominated by transitions to Frenkel exciton states, i.e. states that are also present in the free molecule. A spectroscopic technique must be used that is sensitive to the purely crystal states but insensitive to the Frenkel states.

It is proposed that Stark modulated absorption spectroscopy is just this technique. By using phase sensitive detection at $n\omega$ where n is some integer and ω is the Stark modulation frequency, only the n^{th} order Stark spectrum is recorded. For $n = 1$ only the crystal states should appear since these have a larger dipole moment than the Frenkel states. For example, the dipole moment for an electron and hole localized on neighboring molecules is five Debye; the dipole moment for the lowest excited states of benzene, naphthalene, anthracene, etc., is zero.

A series of Stark spectra of various molecular crystals will serve to locate and characterize some of the more highly excited electronic states of molecular crystals. Information will be obtained about dipole moments, symmetry properties, and the mixing of states in the presence and absence of the electric field. Besides characterizing electronic states that may be unique in solid state physics, this information will be useful in understanding relaxation processes, and the mechanisms of charge generation and transport in molecular crystals.

REFERENCES

1. J.M. Ziman, Principles of the Theory of Solids (Cambridge University Press, Cambridge, 1964).
2. J. Frenkel, Phys. Rev. 37, 17 (1931); ibid. 37, 1276 (1931).
3. (a) F. Gutman and L.E. Lyons, Organic Semiconductors (John Wiley and Sons, Inc., New York, 1967); (b) D. Fox, M.M. Labes, and A. Weissberger, Eds., Physics and Chemistry of the Organic Solid State (Interscience Publishers, Inc., New York, 1967) Vol. III.
4. (a) G. Castro and J.F. Hornig, J. Chem. Phys. 42, 1459 (1965); (b) M. Pope, H. Kallmann, and J. Giachino, J. Chem. Phys. 42, 2540 (1965); (c) M. Sano, M. Pope, and H. Kallmann, J. Chem. Phys. 43, 2920 (1965); (d) M. Pope, J. Burgos, and J. Giachino, J. Chem. Phys. 43, 3367 (1965); (e) N. Geacintov, M. Pope, and H. Kallmann, J. Chem. Phys. 45, 2639 (1966); (f) N. Geacintov and M. Pope, J. Chem. Phys. 45, 3884 (1966); (g) R.F. Chaiken and D.R. Kearns, J. Chem. Phys. 45, 3966 (1966); (h) M. Pope and J. Burgos, Mol. Cryst. 1, 395 (1966); ibid. 3, 215 (1967); (i) M. Silver and R. Sharma, J. Chem. Phys. 46, 692 (1967); (j) N. Geacintov and M. Pope, J. Chem. Phys. 47, 1194 (1967); (k) M. Pope, J. Chem. Phys. 47, 2197 (1967); (l) G.T. Pott, Bull. Am. Phys. Soc. 13, 478 (1968).

PROPOSITION II

The conservation of angular momentum in the exchange of energy between atoms and the radiation field has been researched thoroughly.[1] Similar consideration has not been given to the problem involving molecules because angular momentum does not commute with the molecular Hamiltonian. The polarization effects, observed in the atomic case, will appear for molecules under special conditions. In some molecules the electronic spin is little affected by molecular symmetry, spin angular momentum then approximately commutes with the Hamiltonian. Effects of angular momentum conservation in the absorption and emission process involving changes in the electronic spin might then appear, e.g. in triplet $\rightleftharpoons$ singlet transitions. Even in the absence of spin-orbit coupling these transitions occur through the interaction of the spin magnetic moment with the radiation field. The first-order term causes transitions within a spin manifold while the second-order term causes transitions between spin manifolds.[2] The radiation emitted by this mechanism should be left circularly polarized ($+\hbar$), right circularly polarized ($-\hbar$), or linearly polarized (0) as determined by the conservation of angular momentum. In a molecular triplet state, the spin-spin interaction mixed the T_+ and T_- states; therefore, the circular polarizations will only appear in a sufficiently high magnetic field.

Spin-orbit coupling is presumed, however, to be the dominant mechanism allowing transitions between singlet and triplet states[3]

and is neglected in the above discussion. Phosphorescence produced through the spin-orbit mechanism is linearly polarized because the transition matrix element involves only singlet states. The fraction of circularly polarized light in phosphorescence is a direct measure, then, of the importance of the second-order spin magnetic dipole mechanism.

Theoretical estimates of this quantity have been made.[4-7] It is found that the direct mechanism may contribute 1% to 20% of the total phosphorescence intensity in aromatic hydrocarbons where the spin-orbit interaction is weak.

Experiments have been proposed[7, 8] to measure the magnitude of this effect. The experiments require careful measurements of the angular dependence of the intensity and polarization of the phosphorescence or use of the interference technique proposed by Selenyi.[9] In these techniques both transition mechanisms contribute to the observation. It is doubtful whether the experimental conditions can be defined sufficiently well to distinguish the small magnetic dipole contribution from experimental artifacts, e.g. scattered light, poorly oriented molecules in poorly oriented samples, and optical anisotropy in the sample.[10]

A better technique for this measurement was developed by R.A. Beth[11] to measure the angular momentum of light. The torque exerted by the incident light on a doubly refracting plate is measured. This torque is due to the conservation of angular momentum at the surface of the plate. Linearly polarized light from the spin-orbit

mechanism exerts no torque while the circularly polarized light from the direct mechanism does. The advantage of this technique over the others is that only the light produced by the direct transition is observed, and that intensity easily can be compared with the total phosphorescence intensity.

These experimental results will determine the importance of the second-order spin magnetic dipole mechanism in causing "spin-forbidden" transitions, test the theoretical calculations of spin-orbit coupling and the radiative process in molecules, and measure the intrinsic properties of triplet states such as vibronic coupling as it would be in the absence of spin-orbit mixing with singlet states.

REFERENCES

1. For example, A. Kastler, Ann. Phys. (Paris) 6, 663 (1936), translated by D.M. Hanson, unpublished.
2. This mechanism is called, most descriptively, "second-order spin magnetic dipole radiation." Second order refers to the expansion of $\exp(i\underset{\sim}{k}\cdot\underset{\sim}{r})$.
3. D.S. McClure, J. Chem. Phys. 17, 905 (1949); ibid. 20, 682 (1952).
4. D. Bohm, Quantum Theory (Prentice-Hall, Inc., New York, 1951), p. 446.
5. H.F. Hameka, J. Chem. Phys. 37, 328 (1962); ibid. 37, 1085 (1962).
6. M. Mizushima, Phys. Rev. 124, A 883 (1964).

7. M. Sharnoff, The Triplet State, A. B. Zahlan, Ed. (Cambridge University Press, London, 1967), p. 165.

8. Ying-Nan Chiu, J. Chem. Phys. 46, 772 (1967).

9. (a) P. Selenyi, Phys. Rev. 56, 477 (1939); (b) S. I. Weissman and D. Lipkin, J. Am. Chem. Soc. 66, 2100 (1944).

10. Most crystals will not transmit circularly polarized light.

11. R. A. Beth, Phys. Rev. 50, 115 (1936).

PROPOSITION III

The physical and chemical dynamics of molecular solids represents an area of chemistry in which relatively little research of a fundamental nature has been done. This subject covers a wide range of phenomena, and although represented by a series of books with a very general title, [1] the chapters in the books primarily treat the mechanisms of charge generation and transport, and energy dissipation, multiplication, transfer, and trapping. Other areas in this field are discussed descriptively rather than in a detailed mechanistic sense. This proposition discusses photochemical oxidation-reduction reactions and electron transfer processes in solids. While the research is of general chemical interest, the conclusions should be significant in the study of similar processes in biological systems. Preliminary suggestions are also made for research on photochromism and phase transitions in solids.

Only the results of a few investigations of solid state photochemistry have been reported. It is readily seen that this research is not very extensive. Most recently, the photoreduction of solid ferric oxalate has been observed by gamma resonance spectroscopy but no mechanism for this reaction was discussed. [2] In a recent communication[3] it was reported that Eu^{+3} in a CdF_2 host is photoreduced to Eu^{+2}. A simple kinetic scheme supported the hypothesis that two different types of Eu^{+3} ions are reduced. The two ions

arise from two types of charge compensation: interstitial fluoride ions and trapped electrons. In this research the wavelength dependence of the quantum yield was not even measured. That determination would have provided a good test for the two-ion hypothesis.

The most complete study has been that of Heidrich and Mössbauer.[4] Although photochemical oxidation-reduction was observed in several systems, the results primarily are for solid ferric citrate. The reaction here, as for ferric oxalate, involves the reduction of the ferric ion and the oxidation of the ligand, eliminating carbon dioxide. The ferric citrate data are consistent with a charge transfer transition as the primary process in the absorption. Although this possibility is consistent with the solution photochemistry, the quantum yield in solution is constant above some threshold value, whereas in the solid, the quantum yield runs through a maximum at 5500 Å. Due to the low absorption coefficient here, it is suggested that the primary process involves photodissociation of the ligand; the chemical intermediates then react to reduce the metal ion. This possibility can be tested by determining the time interval between the absorption and the production of ferrous iron.

The photochemical reduction most readily occurs in the presence of an easily and, to some extent, irreversibly oxidized ligand. Presumably in systems containing anions such as iodide, the reaction easily and rapidly reverses, i.e. the excited charge-transfer state rapidly decays back to the initial state. These decay processes also are candidates for research.

It is proposed to study further photochemical oxidation-reduction reactions in solids using ferric oxalate as a model system because the molecular structure is relatively simple, the cation is easily reduced and observations made by a variety of techniques, and the solution photochemistry of oxalates[5] is relatively well understood. Finally, iron is quite fundamental to both chemistry and biology.

The chemical stoichiometry in solution is[6]

$$2\,Fe^{+3}(C_2O_4)_3^{-6} \xrightarrow{h\nu} 2\,M^{+2}(C_2O_4)^{-2} + 3\,C_2O_4 + 2\,CO_2\,.$$

A tentative mechanism[7] involves at least one, perhaps two, intermediate excited states. One ferric ion is reduced in the charge transfer transition; the other is reduced by an intermediate oxalate radical ion.

The experimental approach to elucidating a similar reaction in the solid state seems clear. The products and quantum yields can be determined from the evolution of carbon dioxide and the ferric-ferrous gamma resonance spectrum. The metastable electronic and chemical intermediates can be detected by optical or magnetic resonance spectroscopy. At very low temperatures the intermediates should be quite long-lived. Flash techniques, now on the nano- and picosecond time scale, can be used to determine the kinetics of the electron transfer processes.

Photochromism is a word used to classify diverse chemical reactions by the observable effect, a color change upon exposure

to light, even though specific mechanisms may differ, involving isomerization, dissociation, oxidation-reduction, or electron trapping. Solids exhibiting this effect are becoming technologically useful for the storage, transmission, and display of information and for the control of light intensity. Consequently, the results of basic research in this area are of interest. Several review articles have been published[8] but are primarily descriptive in content.

The problems encountered in investigations of molecular photochromic activity are apparent in the recent work on salicylideneaniline.[9] The molecular electronic states must first be characterized, and then the principal effects responsible for photochromism can be identified. In return for this effort information is obtained about the mechanism of the color change, inter- and intramolecular rearrangements, hydrogen-transfer reactions, and radiationless transitions.[9]

The review articles contain sufficient examples for years of research making it necessary to choose research topics carefully. A case that complements McClure's salicylideneaniline work is salicylidene-m-toluidine. The latter molecule, unlike the former, is photochromic only in the crystal.[8] In view of the similarity between these two molecules and the extensive ground work carried out by McClure, a spectroscopic investigation of the intermolecular photochromism should proceed relatively efficiently.

Phase transitions in solids are an example of the inseparability of structure and dynamics. Although there are three aspects to research on phase transitions, the thermodynamics and statistical mechanics of the problem receive the major emphasis. The prime consideration is evaluating the intermolecular interactions that determine the stable phase, structure, at any particular temperature and formulating this many-body problem in a general statistical-mechanical way. The dynamical aspect, the mechanism by which the structural changes occur, has received little attention.

It has been suggested[10] that phase transitions in ferroelectric crystals occur because a lattice vibration approaches zero frequency at the transition temperature. The motion of the nuclei in this vibrational mode is just that required to transform one structure into the other. It is proposed that this mechanism is the general mechanism for structural phase transitions in solids. This hypothesis can be tested by observing the temperature dependence of the Raman and infrared spectra and neutron diffraction data on the lattice vibrations of a variety of crystals having phase transitions. It is only because of recent technological advances in the Raman and far-infrared that the lattice vibrations in the 0 to 200 cm^{-1} region of the spectrum have been accessible to observation.

REFERENCES

1. D. Fox, M.M. Labes, and A. Weissberger, Eds., Physics and Chemistry of the Organic Solid State (Interscience Publishers, Inc., New York), Vol. I (1963), Vol. II (1965), Vol. III (1967).
2. N. Saito, H. Sano, T. Tominaga, and F. Ambe, Bull. Chem. Soc. Japan 38, 681 (1965).
3. M.J. Vrabel and H.A. Atwater, J. Chem. Phys. 48, 946 (1968).
4. W. Heidrich and R.L. Mössbauer, "Isomer Shifts Induced by Light Irradiation," unpublished manuscript.
5. E.L. Wehry, Quart. Rev. 21, 213 (1967).
6. T.B. Copestake and N. Uri, Proc. Roy. Soc. (London) 228A, 252 (1955).
7. C.A. Parker and C.G. Hatchard, J. Phys. Chem. 63, 22 (1959).
8. (a) G.H. Brown and W.G. Shaw, Rev. Pure Appl. Chem. 11, 2 (1961); (b) R. Dessauer and J.P. Paris, Adv. Photochem. 1, 275 (1963); (c) P. Douzou and C. Wippler, J. Chim. Phys. 60, 1409 (1963); (d) R. Exelby and R. Grinter, Chem. Rev. 65, 247 (1965).
9. M. Ottolenghi and D.S. McClure, J. Chem. Phys. 46, 4613 (1967); ibid. 46, 4620 (1967).
10. W. Cochran, Adv. Phys. 9, 387 (1960).

PROPOSITION IV

One effect of the crystalline state upon the electronic spectra of molecules such as benzene is the splitting of the molecular transitions into multiplets. These multiplets are the $\underset{\sim}{k} = \underset{\sim}{0}$ components[1] of the electronic exciton bands and commonly are called Davydov components[2] or factor group components.[3] The identification and assignment of these components is fundamental to understanding the crystal spectra in terms of the intermolecular interactions.[4] The Davydov components can be identified readily from the spectra of isotopic mixed crystals studied over a large concentration range[5, 6] or from their characteristic polarization.[2] Polarization measurements also serve to assign the Davydov components to the appropriate representation of the factor group.

For the $^1B_{2u}$ state of benzene, this assignment always has been somewhat ambiguous. The earliest experimental work[7] showed a doublet in the crystal spectrum corresponding to the 0, 0 transition in the molecule. This observation was consistent with the predictions of Davydov[8] but not with the group theoretical predictions of Winston.[9] This discrepancy has been discussed by Fox and Schnepp,[10] and recently by Kopelman,[3] and Bernstein, et al.[4] It is now well known that there are four exciton states at $\underset{\sim}{k} = \underset{\sim}{0}$, but an optical transition from the crystal ground state to one of these is forbidden by symmetry. One thus expects to observe three components, and

indeed three spectral lines have been observed[11, 12] (37, 803 cm^{-1}, 37, 839 cm^{-1}, and 37, 846 cm^{-1}).[11] These lines are assigned as Davydov components primarily because three components are expected. One might also expect, however, to observe an additional line due to the 0, 0 transition in $^{13}CC_5H_6$ which is present at a concentration of 6.6% as a natural isotopic impurity. This transition is shifted[13] by +3.7 cm^{-1} relative to the C_6H_6 transition in a C_6D_6 host. In fact in some papers,[11, 14] five lines have been reported (37, 799 cm^{-1}, 37, 803 cm^{-1}, 37, 839 cm^{-1}, 37, 846 cm^{-1}, and 37, 847 cm^{-1}).

Unfortunately the isotopic mixed crystal technique[5, 6] cannot be used to identify which lines are Davydov components because in such experiments, only a doublet is resolved due to the inhomogeneous composition of the crystals. Alternatively the three Davydov components could be identified with a high degree of confidence if three and only three lines were observed to be totally polarized along the appropriate crystal axes. A series of such polarization experiments has been reported by Broude.[14] This and related work have been summarized recently in Sec. V of a paper by Colson, Hanson, Kopelman, and Robinson.[15]

There are two main problems associated with the polarization experiments. Suitable single crystals must be obtained and their crystallographic axes determined. Once this is done, the spectra must be sufficiently sharp, the resolution sufficiently high, and the polarization sufficiently complete to determine whether the lines are polarized uniquely along the respective crystallographic axes.

In regard to the first problem, because of the transition intensity, thin ($\sim 5\mu$) benzene crystals exhibiting at least two crystal faces are needed. The faces and axes in them must then be identified. Both optical and X-ray identification techniques are more easily applied to thick crystals. Furthermore, the optical method requires that the relationship of the optical axes to the crystallographic axes be known. If one uses X-ray techniques, one is faced with the difficulty of handling these thin crystals. Growing the crystals in quartz cells is unsatisfactory because the scattering cross section for the quartz is much larger than that for the thin hydrocarbon crystal.

Broude's latest results[14] are based on the X-ray and refractive index measurements of Guy and Lemanceau.[16] Although these data are probably correct, an element of uncertainty in the assignment of the $\underset{\wedge}{a}$ and $\underset{\wedge}{c}$ polarized Davydov components is introduced because Broude was unable to measure the refractive indices in the same crystals that were used for the spectroscopic studies. Furthermore, no refractive index measurements were made on crystal faces exhibiting the $\underset{\wedge}{b}$ axis. The $\underset{\wedge}{b}$ axis was identified tentatively on the basis of the spectral line intensities. It should be remembered that the actual purpose of the experiment was to learn about the spectral line intensities <u>after</u> assigning the axes.

In regard to the second problem, one cannot claim with any certainty that each line that Broude reports[14] is uniquely polarized along a crystallographic axis. Even Broude does not make this

claim for the $\underset{\wedge}{b}$ component. In his Fig. 10, the three levels near 37,843 cm^{-1} are not clearly resolved. This is also true of another reproduction of these spectra.[17] Furthermore, the $\underset{\wedge}{a}$-polarized line also appears in the $\underset{\wedge}{b}$-polarized spectra. Consequently the $\underset{\wedge}{b}$-polarized line may actually be unpolarized, appearing with finite intensity along each axis. The intrinsic poor quality of spectra obtained from thin crystals is a well-known fact.[18]

Further ambiguity regarding Broude's assignments arises when the presence of phonon addition bands that may mask other lines and the relative intensities of the three Davydov components are considered. In the spectra taken by Colson[12], the weakest line is the middle component and not the high energy component as Broude reports. This discrepancy may be due to changes in the linewidth or to a preferential orientation of the polycrystals. The results are, however, entirely reproducible for several different samples. Also, one would expect the $\underset{\sim}{ac}$ face to be favored in the polycrystalline samples, thus decreasing rather than increasing the relative intensity of the $\underset{\wedge}{b}$-polarized component.

Because the correlation of transition energies with polarization is a criterion for evaluating theoretical models[19] that explain the Davydov splittings as well as for determining the sign and assignment[4, 15] of the individual intermolecular interactions, the verification of Broude's results is a problem of considerable importance. This fact often has been mentioned in the literature,[20] and several different research groups have made attempts in this direction.[21]

What is needed for this verification are good polarization measurements at high resolution using well-oriented crystals of excellent quality with correctly assigned axes. With these data one could prove or disprove the unique polarizations of these lines and the ordering of the components as $\underset{\sim}{a}$, $\underset{\sim}{c}$, and $\underset{\sim}{b}$.

The difficulties and uncertainties faced by other workers can be averted by using a farily large crystal (~ 1 cm^3) in the polarization work. Such a crystal is easily prepared in an unstrained state. All axes are available for study in the same crystal and are readily identified by X-ray or neutron diffraction techniques. This crystal is also easily mounted and, most important, precisely oriented in the optical path.

The problem of using such a large crystal is that the absorption spectrum is virtually a continuum. This difficulty can be circumvented by observing the 0, 0 fluorescence rather than the absorption. At temperatures where the upper Davydov components are populated, each component will fluoresce with its characteristic polarization. Presumably the temperature should be kept below 20 °K or resolution will be lost through the thermal broadening of these transitions.[15] Since this emission is expected to be very weak,[15] and since it is necessary to collect the fluorescence only over a small aperture, one of several techniques for the detection of very low light levels must be used.

REFERENCES

1. Actually $\underset{\sim}{k} = \underset{\sim}{q}$ where $\underset{\sim}{q}$ is the radiation wave vector.
2. A.S. Davydov, Theory of Molecular Excitons (McGraw-Hill Book Co., Inc., New York, 1962).
3. R. Kopelman, J. Chem. Phys., 47, 2631 (1967). This paper clarifies and generalizes the use of group theory in molecular crystal spectroscopy.
4. E.R. Bernstein, S.D. Colson, R. Kopelman, and G.W. Robinson, J.Chem. Phys., 00, 0000 (1968), "Electronic and Vibrational Exciton Structure in Crystalline Benzene."
5. V.L. Broude and M.I. Onoprienko, Opt. i Spektroskopiya 10, 635 (1961) [English transl.: Opt. Spectry. (USSR) 10, 333 (1961)].
6. E.F. Sheka, Opt. i Spektroskopiya 10, 684 (1961) [English transl.: Opt. Spectry. (USSR) 10, 360 (1961)].
7. V.L. Broude, V.S. Medvedev, and A.F. Prikhot'ko, Zh. Eksp. Teor. Fiz. 21, 665 (1951).
8. A.S. Davydov, Zh. Eksp. Teor. Fiz. 21, 673 (1951).
9. H. Winston, J. Chem. Phys. 19, 156 (1951).
10. D. Fox and O. Schnepp, J. Chem. Phys. 23, 767 (1955).
11. V.L. Broude, V.S. Medvedev, and A.F. Prikhot'ko, Opt. i Spektroskopiya 2, 317 (1957).
12. S.D. Colson, J. Chem. Phys. 48, 3324 (1968).

13. E.R. Bernstein, S.D. Colson, D.S. Tinti, and G.W. Robinson, J. Chem. Phys. 00, 0000 (1968), "Static Crystal Effects on the Vibronic Structure of the Phosphorescence, Fluorescence, and Absorption Spectra of Benzene Isotopic Mixed Crystals."

14. V.L. Broude, Usp. Fiz. Nauk 74, 577 (1961) [English transl.: Sov. Phys.--Usp. 4, 584 (1962)].

15. S.D. Colson, D.M. Hanson, R. Kopelman, and G.W. Robinson, J. Chem. Phys. 48, 2215 (1968).

16. R. Guy and B. Lemanceau, Cahiers Phys. 38, 23 (1956).

17. V.L. Broude, G.V. Klimusheva, A.L. Liberman, M.I. Onoprienko, A.F. Prikhot'ko, and A.I. Shatenstein, Absorption Spectra of Molecular Crystals (Academy of Sciences of Ukrain S.S.R., Physics Institute, Kiev, 1965), p. 59.

18. S.D. Colson, J. Chem. Phys. 45, 4746 (1966).

19. (a) Ref. 10; (b) T.A. Claxton, Ph.D. thesis, University of London, 1961; (c) T. Thirunamachandran, Ph.D. thesis, University of London, 1961; (d) R. Silbey, S.A. Rice, and J. Jortner, J. Chem. Phys. 43, 3336 (1965).

20. (a) G.C. Nieman and G.W. Robinson, J. Chem. Phys. 39, 1298 (1963); (b) O. Schnepp, Ann. Rev. Phys. Chem. 14, 35 (1963); (c) Ref. 15; (d) S.A. Rice and J. Jortner, Physics

and Chemistry of the Organic Solid State, D. Fox, M.M. Labes, and A. Weissberger, Eds. (Interscience Publishers, Inc., New York, 1967), Vol. III, Chap. 4, p. 446.

21. (a) Ref. 18(b); (b) O. Schnepp, private communication; (c) S.D. Colson, unpublished results.

PROPOSITION V

The magnetic properties of matter arise from the same physical effects as chemical bonding. In fact, the Heitler-London description[1] of the chemical bond is fundamental to the Heisenberg-Dirac theory[2] of magnetism. The Heisenberg Hamiltonian has been quite successful in phenomenologically explaining and correlating the magnetic properties of systems characterized by weak interactions, e.g. rare earth and transition metal salts, organo-metallic crystals,[3] and radical-ion salts.[4] In spite of the success of this empirical approach, the basic form as well as the approximations in the Heisenberg formula recently have been criticized quite severely.[5] It seems clear that in specific applications, the physics represented by the simple Hamiltonian is not well understood.[6]

It is proposed, after a brief discussion of the Heisenberg-Dirac theory and its relationship to the Heitler-London description of chemical bonding, to use gamma resonance spectroscopy to study the pressure dependence of chemical bonding and the magnetic properties in a selected series of rare earth compounds. Spectroscopic studies of some new "magnetic" molecules are mentioned also. This experimental approach should lead to a more complete understanding of magnetism in weakly interacting systems.

The Heisenberg Hamiltonian as formulated by Van Vleck[7] is

$$H = -2 \sum_{i>j} J'_{ij} \underset{\sim}{S}_i \cdot \underset{\sim}{S}_j \qquad (1)$$

$$J'_{ij} = J_{ij} - 2 S_{ij} V_{ij} \qquad (2)$$

The sums are over the appropriate electrons in the system; the indices represent, somewhat symbolically, both the electrons and the electronic wavefunctions. J' is the effective electron exchange integral consisting of the actual integral and a term depending upon the overlap of the wavefunctions and an attractive potential. The potential term is equivalent to the exchange integral β appearing in molecular orbital theory. Ferro- and antiferromagnetism thus arise from an electrostatic coupling of the electron spins. For positive J' the lowest energy state is ferromagnetic; for negative J' the lowest state is antiferromagnetic. If J and V are positive quantities,[3,8] the sign of J' depends upon the magnitude of the overlap integral. Most molecular systems are antiferromagnetic, i.e. have singlet ground states, due to the electronic overlap.

A chemically interesting case in which to study the balance between ferromagnetism and antiferromagnetism is benzyne.[9] The magnetic system consists of two neighboring sigma electrons that, by rough theoretical estimates, form a singlet ground state.[10] Triplet ground states may occur, however, for meta- and para-benzyne.[11] Good calculations of the electronic structure of these molecules should be tractable and when combined with experimental studies, will lead to a better understanding of chemical bonding especially the coupling between sigma and pi electrons in planar aromatic molecules.

The radical-ion salts generally are antiferromagnetic.[4] Eq. 2 predicts these crystals would become ferromagnetic if the overlap were decreased. This decrease might be brought about by adding large alkyl substituents. The alkyl groups would increase the lattice parameters without affecting the magnetic electron interactions in

other ways. In additional experiments, resonance pairs of magnetic electrons can be generated in host crystals by photochemical bond dissociation reactions.[12] The above research might lead to a molecular magnet, either a radical-ion salt or a hydrocarbon polymer with sites of oriented spin. Even if the molecular magnet proves to be a technological dream, studies of such systems by optical or magnetic resonance spectroscopy will provide empirical data on chemical bonding and electron exchange interactions. The intermolecular distances and consequently the electronic overlap can be changed by using different crystals or, more desirably, by applying uniaxial pressure.

Finally, it is proposed that gamma resonance spectroscopy be used to study chemical bonding and magnetism in the europium chalcogenides as a function of temperature and pressure. Gamma resonance spectroscopy is well-suited for such an investigation because information can be derived from three sources. The isomer shift and quadrupole splitting are determined by the s electron density and electric field gradient at the nucleus, respectively, and consequently depend upon the nature of the chemical bonds. The magnetic hyperfine structure measures the internal magnetic field at the nuclear site. For work at high pressures and low temperatures gamma resonance is better than magnetic resonance spectroscopy because a tuned cavity is not required.

Both experimentally and theoretically, the europium chalcogenides form an excellent series of compounds for this study. The nuclear transition energy in europium is low[13] resulting in a large recoil-free fraction. The magnetic properties vary in the series,

EuO being ferromagnetic and EuTe antiferromagnetic.[14] Calculations are tractable because the Eu^{+2} ion is an S state ion in a cubic lattice.[15] In addition, related compounds have interesting variations in their magnetic properties, e.g. Eu metal and EuF_2 are antiferromagnetic while EuH_2 and EuI_2 are ferromagnetic.

The uniaxial pressure experiments should prove extremely useful in elucidating the nature of the interatomic interactions, the significance of electron overlap, and the fine balance between ferromagnetism and antiferromagnetism.

REFERENCES

1. W. Heitler and F. London, Z. Physik 44, 455 (1927).
2. (a) W. Heisenberg, Z. Physik 49, 619 (1928);
   (b) P. A. M. Dirac, Proc. Roy. Soc. A123, 714 (1929).
3. P. W. Anderson, Solid State Physics, F. Seitz and D. Turnbull, Eds. (Academic Press, New York, 1963) Vol. 14, p. 99.
4. P. L. Nordio, Z. G. Soos, and H. M. McConnell, Annual Review of Physical Chemistry, H. Eyring, Ed. (Annual Reviews, Inc., Palo Alto, 1966) Vol. 17, p. 237.
5. C. Herring, Magnetism, G. T. Rado and H. Suhl, Eds. (Academic Press, New York, 1966) Vol IIB, Chapt. 1.
6. For example see M. T. Hutchings, R. J. Birgeneau, and W. P. Wolf, Phys. Rev. 168, 1026 (1968) where Gd^{+3} pair interactions are measured in a $LaCl_3$ host crystal, and the conclusion is "that the nearest-neighbor exchange is relatively weak and antiferromagnetic while the next-nearest neighbor exchange is four times stronger and ferromagnetic.... The values of the parameters have been discussed in Sec. 6, but we have not been able to find any fundamental explanation for their magnitudes nor even their signs."
7. J. H. Van Vleck, Theory of Electric and Magnetic Susceptibilities (Oxford University Press, London, 1932) Chapt. XI.
8. C. C. J. Roothaan, Rev. Mod. Phys. 23, 69 (1951).
9. An investigation of the electronic structure of this interesting and fundamental molecule was first proposed as part of the candidacy requirements, David M. Hanson, March 14, 1966.

Electron paramagnetic resonance studies of triplet ground state molecules frequently have appeared in the literature beginning with R. W. Brandon, G. L. Closs, and C. A. Hutchison Jr., J. Chem. Phys. 37, 1878 (1962). These investigations primarily are concerned, however, with magnetic dipole interactions and not with the ordering of the singlet and triplet states.

10. R. S. Berry, G. N. Spokes, and M. Stiles, J. Am. Chem. Soc. 84, 3570 (1962).

11. Ortho-, meta-, and para- are used here to specify the relative positions of the two sigma electrons. The synthesis of the meta and para species alone represents an interesting chemical challenge.

12. Photochemical cleavage of the central bond in R—O—O—R, R—S—S—R, R_2—N—N—R_2, and R_2—P—P—R_2 molecules is well-documented, J. G. Calvert and J. N. Pitts, Photochemistry (John Wiley and Sons, New York, 1967). These molecules also comprise interesting series for study.

13. A. H. Muir Jr., K. J. Ando, and H. M. Coogan, Mössbauer Effect Data Index 1958-1965 (Interscience, New York, 1966).

14. (a) B. T. Matthias, R. M. Boyarth, and J. H. Van Vleck, Phys. Rev. Letters 7, 160 (1961);
(b) T. R. McGuire, B. E. Argyle, M. W. Shafer, and J. S. Smart, J. Appl. Phys. 34, 1345 (1963).

15. S. J. Cho, Phys. Rev. 157, 632 (1967).

16. (a) R. L. Yanowick and W. E. Wallace, Phys. Rev. 126, 537 (1962); (b) T.R. McGuire and M.W. Shafer, J. Appl. Phys. 35, 984 (1964).